

# Seismic Imaging with the Elliptic Radon Transform in 3D: Analytical and Numerical Aspects

Zur Erlangung des akademischen Grades eines

DOKTORS DER NATURWISSENSCHAFTEN

von der KIT-Fakultät für Mathematik des  
Karlsruher Instituts für Technologie (KIT)  
genehmigte

DISSERTATION

von

Christine Grathwohl

Tag der mündlichen Prüfung: 6. November 2019

Referent: Prof. Dr. Andreas Rieder

Korreferent: Apl. Prof. PD Dr. Peer Christian Kunstmann

Korreferent: Prof. Dr. Roland Schnaubelt



This document is licensed under a Creative Commons  
Attribution-ShareAlike 4.0 International License (CC BY-SA 4.0):  
<https://creativecommons.org/licenses/by-sa/4.0/deed.en>

*„...offen gesagt ist dieser Tag nicht gerade geeignet für Plutimikation.“*

Pippi Langstrumpf



---

# Contents

---

<b>Introduction</b>	<b>1</b>
<b>1 Derivation of a problem in seismic imaging</b>	<b>7</b>
1.1 Notations . . . . .	7
1.2 The considered problem . . . . .	8
1.2.1 Prolate spheroidal coordinates . . . . .	13
1.2.2 The operator $F$ expressed using prolate spheroidal coordinates . . . . .	15
1.2.3 A note concerning a non-constant background velocity $c$ . . . . .	18
<b>2 Preliminaries</b>	<b>21</b>
2.1 Basics of microlocal analysis . . . . .	21
2.1.1 Basic definitions and results . . . . .	22
2.1.2 Singularities and their propagation . . . . .	30
2.2 The generalised Radon transform in terms of defining measures . . . . .	39
<b>3 Theoretical results concerning the operator <math>F</math></b>	<b>45</b>
3.1 The operator $F$ – A generalised Radon transform . . . . .	45
3.2 Properties of $F$ . . . . .	56
3.2.1 $F$ as Fourier integral operator . . . . .	57
3.2.2 The normal operator and its wave front set . . . . .	59
3.3 The reconstruction operator $\Lambda$ . . . . .	65
3.3.1 The choice of $\Lambda$ . . . . .	66
3.3.2 Microlocal properties of $\Lambda$ . . . . .	81
3.3.3 Modification of the reconstruction operator $\Lambda$ . . . . .	87
<b>4 Numerical realisation</b>	<b>95</b>
4.1 Approximation of $\Lambda_n$ by the concept of approximate inverse . . . . .	95
4.2 The operator $F$ applied to a function supported in a closed ball . . . . .	96
4.2.1 Change of the considered coordinate system . . . . .	96
4.2.2 Some geometrical considerations . . . . .	99
4.2.3 Calculation of the required angles . . . . .	101
4.2.4 Determination of the limits for the travel time . . . . .	105
4.3 The operator $F$ applied to the characteristic function of a half-space . . . . .	108
<b>5 Numerical experiments</b>	<b>111</b>
5.1 Different reconstruction kernels . . . . .	111
5.1.1 The reconstruction kernel for $\Lambda$ . . . . .	111
5.1.2 The reconstruction kernels for the modified operators . . . . .	116

5.2	Preparations for numerical experiments . . . . .	118
5.2.1	The considered data . . . . .	120
5.2.2	Implementation . . . . .	122
5.3	Numerical results . . . . .	126
5.3.1	Reconstructions with the reconstruction operator $\Lambda$ . . . . .	127
5.3.2	Experiments concerning the offset $\alpha$ . . . . .	131
5.3.3	Comparison of the different reconstruction operators . . . . .	137
5.3.4	Reconstructions of different planes . . . . .	141
5.3.5	Reconstructions using data from the wave equation . . . . .	144
<b>A</b>	<b>Various calculations</b>	<b>151</b>
A.1	The explicit expression of the Beylkin determinant $B$ . . . . .	151
A.2	The proof of Lemma 3.22 . . . . .	153
A.3	Calculations of limits associated with the top order symbol $\sigma(\Lambda)$ . . . . .	154
A.4	The transformation theorem and the $\delta$ -distribution . . . . .	156
	<b>Danksagung</b>	<b>159</b>
	<b>Bibliography</b>	<b>163</b>

---

## Introduction

---

In many situations it is important to know what is beneath the earth's or the ocean's surface. The reasons why this knowledge is worthwhile are wide-ranging. One common reason is for fundamental research in order to get an impression how the subsurface is composed. Extensive studies of the underground are also needed to decide what kind of buildings and tunnels can be constructed on or below the surface. Another use case, this knowledge is necessary for, is the investigation of the extent and danger of contaminated areas.

In contrast to these examples, there is a large application field, where the interest lies in the subsurface itself. Information about the surface is crucial for the prospection and exploration of mineral resources, like ground or mineral water, construction materials (sand, clay, grit), oil and gas.

An obvious method to obtain information about the underground is to carry out drillings. However, these are expensive and it is often not beneficial to use such invasive methods for reasons of stability. In case of the exploration of mineral resources it is in advance not clear whether a proper location was chosen or the desired mineral resources will not be found at all.

*Seismic imaging* is a method to obtain information about the spatial structure of a medium in a non-invasive way. The idea behind this approach is that a wave contains information about the varying structure of a material after it has travelled through it.

The arrangement that is used to receive this information is the following. At the surface, one places sources which excite waves. These waves travel through the different material layers of the subsurface. Depending on which material they go through, the speed of sound of the waves changes. During this procedure the waves are reflected on part of the propagation medium and the occurring reflections are recorded by receivers. These receivers are located at the surface, too.

For this experimental setup there are different possibilities to arrange sources and receivers like for example the common midpoint and the common source geometry. In the common midpoint geometry the midpoint of each source and the associated receiver pair plays a decisive role. As the name suggests, each pair shares its midpoint with all of the other pairs. The setting of the common source geometry is determined by one single source and receivers lying on the same line with an arbitrary distance to the source. In this thesis, we consider the so called common offset geometry. This means that the distance from a source to its receiver is always the same.

In practice, raw seismic data is often recorded by using one source and a fixed number of receivers located in a line, i.e. in the common source geometry. This arrangement is called a "shot". A survey of an area consists of many shots. In order to obtain recordings on a whole area, the arrangement described above is shifted. In theory, the data which relates to the considered acquisition geometry is picked out of these recordings. In marine seismology typically an airgun is used as source and hydrophones as receivers (see also [Sym09]).

Experiments on shore work with hammer blows as sources and geophones as receivers, for example.

The aim of seismic imaging is to deduce material parameters from the recordings of the receivers. This means that we have observations and want to reconstruct the factors which caused them, i.e. we consider an inverse problem. The corresponding direct problem is given when we know the material the waves go through but are interested in how it changes the speed of sound of the wave. An obvious approach is to search for a direct inversion formula. In many cases this is not possible and in applications we only have limited data available. Hence, even if a direct inversion formula exists, it might be useless in practice. In this thesis, we present an approach to obtain information about the cause from observations in the situation of seismic imaging with the common offset acquisition geometry.

In 1921 John Clarence Karcher first used the reflection seismic method for petroleum exploration (see [Bro99]). His notes are the oldest remaining documents concerning the usage of seismic imaging. In May 1929 Karcher applied for a patent of the method he used, which was accepted in February 1932 [Kar29]. Since that time, many people have improved his methods to obtain information about the earth's or ocean's subsurface by seismic imaging. The progress of this technique starts with the pioneering work of Bleistein and Cohen published in [BC77] and [BC79]. The book [BCS01] they wrote together with Stockwell additionally yields a broad overview of the developments in seismic imaging. A more detailed historical outline is given in the topical review [Sym09] by Symes. He also illustrates how mathematics influenced practical application.

In the presented approach we simplify the elastic wave equation by some physical restrictions. We assume that no shear waves appear and the medium has constant mass density. Further, we consider a constant background velocity  $c$  and interpret the speed of sound  $\nu$  of the excited waves as the background velocity plus an additional perturbation. More precisely, we take

$$\frac{1}{\nu^2(x)} = \frac{1 + n(x)}{c^2}$$

for  $x \in \mathbb{R}^3$ . The quantity  $n$  thereby contains the same singularities as  $\nu$ , which occur when the material of the subsurface changes. Henceforth, we are searching for  $n$  instead of the actual speed of sound  $\nu$ . The last simplification we make is to assume the absence of multiple scattering. This assumption is very common. According to the topical review [Sym09] it causes only small errors in case of our choices for  $c$  and  $n$ . These already small errors can be minimised according to the authors of [BDM18]. Therein they invent a model to map measured seismic data to data which contains virtually no effects caused by multiple scattering. After adapting measured data by this model, the data concerning multiple reflections is filtered out. Every method, which does not regard multiple scattering, is suitable for the filtered data. However, we take the small errors into account and do not manipulate the data.

After some computations, we approximate  $n$  by the solution of the equation

$$Fn = y. \tag{1}$$

Here, the right-hand side, given by  $y$ , represents the measured data and the operator  $F$  is defined by

$$Fn(s, t) := \int_{E(s, t)} n(x) d\sigma(x)$$

for  $(s, t) \in S_0 \times (2\alpha, \infty)$  with an open, bounded and connected subset  $S_0 \subseteq \mathbb{R}^2$  and a weighted surface measure  $\sigma$  on  $E(s, t)$ . The parameter  $s \in S_0$  determines the location of the source  $\mathbf{x}_s(s) = (s_1, s_2 - \alpha, 0)^\top$  and the receiver  $\mathbf{x}_r(s) = (s_1, s_2 + \alpha, 0)^\top$ , which have a constant distance  $2\alpha$  with offset  $\alpha > 0$ . Further, we have

$$E(s, t) := \{x \in \mathbb{R}_+^3 \mid |\mathbf{x}_s(s) - x| + |x - \mathbf{x}_r(s)| = t\}$$

for  $(s, t) \in S_0 \times (2\alpha, \infty)$  with  $\mathbb{R}_+^3 := \{y = (y_1, y_2, y_3)^\top \in \mathbb{R}^3 \mid y_3 > 0\}$ . Hence, we integrate along open half-ellipsoids with the two foci  $\mathbf{x}_s(s)$  and  $\mathbf{x}_r(s)$  and the travel time  $t$ .

The representation of the operator  $F$  raises the question whether a function can be determined by knowing certain means of this function. This problem has already been studied by Johann Radon. In 1917 his report “Über die Bestimmung von Funktionen durch ihre Integralwerte längs gewisser Mannigfaltigkeiten” was published (see [Ra17]). Therein, Radon approached the determination of functions from their integral values along certain manifolds. He answered the question in case of sufficiently smooth functions depending on two variables and their line integral over all lines in the plane, where the functions are defined on. In this case, he also proved an inversion formula. Both formulas are named after him, the Radon transform and the inverse Radon transform.

As the German title of Radon’s publication suggests, integration along certain manifolds and not only along lines is not far to seek. Under certain conditions such integral representations are called generalised Radon transforms. We introduce them according to Quinto in [Quin80] by their defining measures. Then, we verify that the operator  $F$  satisfies the required conditions to be a generalised Radon transform. Since we integrate over open half-ellipsoids, the operator  $F$  is often called the *elliptic Radon transform*.

To the best of our knowledge there is no inversion formula for  $F$  if we have the full data over all open half-ellipsoids. However, in the application we only have data limited by the numbers of sources and receivers determined by  $S_0$  and a certain interval of travel times  $t$ . Thus, even if there exists an inversion formula for  $F$  in case of full data, it does not apply in practice.

For this reason, we choose a different approach to obtain information about  $n$ . By our ansatz,  $n$  is a kind of perturbation in addition to a constant background velocity. The quantity  $n$  has the same singularities as the speed of sound, which occur when the material changes.

In order to describe singularities of a function or even a distribution, there is the notion of the wave front set. It contains the locations of the singularities and, roughly speaking, in which direction the functions are not smooth.

The name wave front set is derived by the fact that for a fixed time  $t$  the singularities of the solution to the wave equation are located at all points with travel time  $t$ . In case of constant velocity, these points are precisely the ones with the same distance to the source, which excited the wave. The directions related to the singularities point in the direction of the movement of the wave. By this means, the wave front set describes the evolution of a wave front in the physical sense.

For the determination of the wave front set of  $n$  we apply a result of microlocal analysis, a field that goes back to Hörmander and Sato. They started independently of each other to consider local properties of distributions and certain functions. The groundbreaking work of Hörmander for pseudodifferential and Fourier integral operators with smooth symbols is still widely used today. At the beginning and throughout Chapter 2 we give some more details concerning his work.

The approach for the determination of the wave front set of  $n$  is to consider the wave front set of  $\Lambda n$  where  $\Lambda$  is a so called reconstruction operator. For this reason, we have to find an operator  $\Lambda$  which adds no singularities and preserves as many as possible.

One of the aforementioned results from microlocal analysis is that applying a pseudodifferential operator to a function or a certain kind of distribution does not add any singularities. If the pseudodifferential operator is additionally elliptic, it even preserves the wave front set. However, ellipticity on the whole domain of the operator is a strong assumption, but a weaker generalisation suffices. Provided that  $\Lambda$  is a pseudodifferential operator, which is microlocally elliptic at certain points, the singularities and their directions related to these points are preserved.

In this thesis, we take advantage of a result in [GS77]. Since we are able to verify that  $F$  is a generalised Radon transform and satisfies another condition provided in [FKNQ16], we obtain that the operator  $F^*\psi F$  is a pseudodifferential operator, where  $\psi$  is a smooth cut-off function. Further, we present a more elementary approach to verify that  $F^*\psi F$  is a sum of a pseudodifferential operator and a smoothing operator, i.e. an operator without singularities. For this purpose, we rewrite  $F^*\psi F$  and finally obtain an explicit expression of the top order symbol of  $F^*\psi F$ .

A pseudodifferential operator with positive order emphasises the preserved singularities. We thus augment the operator  $F^*\psi F$  with differential operators in order to get a reconstruction operator  $\Lambda$  of positive order. Then, we determine at which points the operator  $\Lambda$  is microlocally elliptic and at which it is smoothing.

In a further step, we analyse the asymptotic behaviour of the top order symbol of  $\Lambda$ . Using these results, we modify  $\Lambda$  in different ways. We also investigate the microlocal properties of the modified operators.

Now, the question is posed how we deduce the value of  $\Lambda n$  at a point in the subsurface from the measured data  $y$ . At this point the structure of  $\Lambda$  helps to proceed.

The reconstruction operator  $\Lambda$  contains the composition  $F^*\psi F$ . Thus, by applying  $\Lambda$  to  $n$  the term  $F n$  appears, which is according to identity (1) equal to the given data  $y$ . Using this observation, we calculate  $\Lambda n$  evaluated at points  $p$  in the subsurface numerically and obtain reconstruction images presenting an approximation of  $\Lambda n$ .

In these reconstruction images we see the qualitative behaviour of  $n$ . The jumps we notice therein are the singularities which occur between different material layers. By this means, we obtain an impression how the underground is composed and what is beneath the surface. We recall that  $\Lambda n$  and  $n$  are only connected by their singularities and we do not get quantitative results.

Beside the mentioned analytical investigations of the operator  $F$  and the reconstruction operator  $\Lambda$ , the second major part of this thesis is the implementation of the approximation of  $\Lambda n$  at a certain point.

In order to efficiently compute  $\Lambda n$  we use geometrical considerations to simplify the calculation of  $F$  applied to certain functions. We test our implementation for synthetic data and different choices of parameters. Here, we also regard the modified reconstruction operators and compare them with  $\Lambda$ . Finally, we show that our implementation yields good results in an experiment with data generated from the wave equation.

In the joint work [GKQR18a] with Kunstmann, Quinto and Rieder we analyse the same setting in two space dimensions. In this case, the operator  $F$  does not integrate along open half-ellipsoids but along open half-ellipses in  $\mathbb{R}_+^2$ . Different from this thesis, the operator  $F$

therein is approximated to simplify calculations. The numerical examples performed there are comparable to the ones in this thesis.

Again, jointly with Kunstmann, Quinto and Rieder we show in [GKQR18b] some microlocal properties of the operator  $F$  in two space dimensions and present numerical experiments with different reconstruction operators as a continuation of [GKQR18a]. Therein, we determine the top order symbol of  $F^*\psi F$  in two and three space dimensions. Here, we greatly benefit from the publication [Quin80]. We state the three dimensional result in this thesis again and argue why the mentioned theorem in [Quin80] is applicable. However, we do not repeat the calculations already given in this publication.

Another closely related work is [QRS11] by Quinto, Rieder and Schuster. The authors consider a different acquisition geometry in three space dimensions, which corresponds to choosing  $\alpha = 0$  in our approach, i.e. source and receiver location coincide. This fact simplifies many of the appearing computations. Since they also assume the background velocity to be constant, this leads to an operator which integrates along open half-spheres. The reconstruction operator used there contains additional differential operators. However, they derived its representation motivated by an existing inversion formula in their setting.

The microlocal properties of operators  $R$  integrating along manifolds and the associated normal operators  $R^*R$  have been studied in various publications. At this point, we mention a few, which are connected to the content of this thesis.

The publication [KLQ12] is about the microlocal properties of the normal operators in two different acquisition geometries. The geometries are given in two space dimensions and one of them is the common offset geometry.

In [FKNQ16] the authors analyse the microlocal properties of the normal operator in the common offset and common midpoint geometry. We benefit from their result that the Bolker condition is satisfied in case of the common offset geometry. According to this publication, the Bolker condition does not hold in the common midpoint setting. Hence, our approach would not work in this geometry.

The publication [FQ15] deals with the artifacts in numerical reconstructions caused by limited data. The results the authors present therein are visible in our numerical experiments.

Microlocal properties of similar operators and the associated normal operators have also been studied in [FG10], [KQ11], [NS97], [Quin93] and many more.

In Chapter 1 of this thesis we derive our setting from the acoustic wave equation. Further, we introduce the prolate spheroidal coordinates we use many times throughout this thesis. Finally, we remark which changes appear if we consider a non-constant background velocity.

Background information concerning microlocal analysis is provided in Chapter 2. Moreover, we introduce generalised Radon transforms.

Chapter 3 attends to all theoretical investigations in conjunction with the operator  $F$ . In Section 3.1 we prove that the operator  $F$  is a generalised Radon transform by verifying the required conditions stated in [Quin80].

The representation of  $F$  as a Fourier integral operator is derived in the first subsection of Section 3.2. Afterwards, we consider the normal operator  $F^*\psi F$  where  $\psi$  is a smooth cut-off function. According to [FKNQ16], the operator  $F$  satisfies the Bolker condition. For this reason, a result in [GS77] yields that since  $F$  is a generalised Radon transform, the operator  $F^*\psi F$  is a pseudodifferential operator. In order to analyse which singularities of certain distributions  $n$  are preserved by the operator  $F^*\psi F$  we calculate the wave front set of  $F^*\psi F n$ . The proof is similar to the one in [KLQ12] where the authors consider the full

space  $\mathbb{R}^3$ . Based on this result, in Section 3.3 we define a reconstruction operator  $\Lambda$  and explain our choice. Further, we state the top order symbol of  $\Lambda$  and refer to Section 5.2 in [GKQR18b] for the calculation. The explicit expression therein is a result obtained by applying Theorem 2.1 in [Quin80]. However, this approach is not easily accessible. For this reason, we present a more straightforward way taking advantage of the structure of  $F^*\psi F$ . Using the obtained representation of the top order symbol, we analyse in which points the operator  $\Lambda$  is microlocally elliptic. As a consequence, we draw conclusions which of the singularities of  $n$  are preserved or even emphasised by applying  $\Lambda$ . Moreover, we show that  $\Lambda$  is smoothing off the closure of the set in which it is microlocally elliptic. In the last subsection we modify the operator  $\Lambda$ . For this purpose, we analyse the behaviour of the top order symbol depending on the offset  $\alpha$ . Based on these results, we define modified reconstruction operators. Finally, we deduce the microlocal properties of the modified operators from those of  $\Lambda$ .

In Chapter 4 we explain how we obtain an approximation of  $\Lambda n$  evaluated at a fixed point. A description how to apply the method of the approximate inverse in order to obtain the searched approximation is given in Section 4.1.

In the numerical experiments we present later on we choose a sum of characteristic functions of balls and one half-space as  $n$ . In order to generate synthetic data of  $n$ , we reformulate  $F$  applied to the characteristic function of a ball and a half-space. This is presented in Section 4.2 and Section 4.3, respectively. The first reformulation is also helpful for the reconstruction kernel appearing in the method of the approximate inverse.

The last chapter of this thesis focuses on numerical experiments. Except for the data, the reconstruction kernel is the second essential part we need to obtain an approximation of  $\Lambda n$ . In Section 5.1 we calculate the different reconstruction kernels associated to the reconstruction operator  $\Lambda$  as well as to the modified ones.

Further preparations are made in Section 5.2. We explain the expectations we have of the reconstructions based on the considered data and take a closer look at the implementation in the coding language Python.

In the very last section of this thesis we present the results obtained by different numerical experiments. First, we illustrate experiments using the reconstruction operator  $\Lambda$  and discuss the choices of certain parameters in the implementation. Afterwards, we observe what happens if we simulate errors in the positioning of sources and receivers. In a second experiment we see what changes if the distance between source and receiver used for recording data is different than their distance in the reconstruction procedure. In the next subsection of Section 5.3 additional reconstructions obtained by using the modified reconstruction operators introduced in Subsection 3.3.3 are presented. We compare the reconstructions obtained by the different reconstruction operators and note the improvements achieved by the modifications. The section concludes with the presentation of results we received using data from the wave equation. Here, we evaluate solutions of the wave equations (see Section 1.2) at the receiver points.

---

## Derivation of a problem in seismic imaging

---

We start this first chapter with a detailed list of the notions we use throughout this thesis. Subsequently, we derive the statement of the problem in seismic imaging we consider. A special kind of coordinates will be constantly recurring throughout this thesis. We state these coordinates and show how we apply them to reformulate the operator we obtained from the problem. Last, we remark the differences which arise by assuming a non-constant background velocity.

### 1.1. Notations

In this thesis, we use  $\mathbb{N}$  to denote the set of strictly positive integers. Now, let  $d \in \mathbb{N}$ . For  $u = (u_1, \dots, u_d)$  and  $\tilde{u} = (\tilde{u}_1, \dots, \tilde{u}_d)$  in  $\mathbb{R}^d$  we write  $u \cdot \tilde{u}$  for the Euclidean scalar product defined by  $u \cdot \tilde{u} := \sum_{i=1}^d u_i \tilde{u}_i$ . Further,  $|\cdot|$  is the corresponding norm. We also denote the multiplication of an element  $u \in \mathbb{R}^d$  with  $\lambda \in \mathbb{R}$  by  $\lambda \cdot u = (\lambda u_1, \dots, \lambda u_d)$  if it makes understanding easier. The space  $\mathbb{R}_+^3$  is the open half-space in  $\mathbb{R}^3$  given by  $\mathbb{R}_+^3 := \{x = (x_1, x_2, x_3)^\top \in \mathbb{R}^3 \mid x_3 > 0\}$ .

For a multi-index  $\alpha \in \mathbb{N}_0^d$  the differential operator  $D_x^\alpha$  means  $D_x^\alpha = \partial_{x_1}^{\alpha_1} \dots \partial_{x_d}^{\alpha_d}$ .

We denote by  $C_c^\infty(\mathbb{R}^d)$  the space of infinitely differentiable functions with compact support. Further,  $\mathcal{S}(\mathbb{R}^d)$  is the Schwartz space or the space of rapidly decreasing functions. These functions are infinitely differentiable and they and their derivatives go to zero as  $x \rightarrow \pm\infty$  faster than any inverse power of  $x \in \mathbb{R}^d$ .

We use the following form of the Fourier transform. For  $u \in \mathcal{S}(\mathbb{R}^d)$  the Fourier transform is given by

$$(\mathcal{F}f) := \hat{f}(x) := \frac{1}{(2\pi)^{\frac{d}{2}}} \int_{\mathbb{R}^d} f(\xi) e^{-ix \cdot \xi} d\xi$$

and its inverse is

$$(\mathcal{F}^{-1}g) := \frac{1}{(2\pi)^{\frac{d}{2}}} \int_{\mathbb{R}^d} g(\xi) e^{ix \cdot \xi} d\xi.$$

For Banach spaces  $X$  and  $Y$  we denote by  $\mathcal{L}(X, Y)$  the set of linear continuous operators from  $X$  to  $Y$ . The dual space  $\mathcal{L}(X, \mathbb{R})$  of  $X$  is called  $X^*$ . We also define for  $T \in \mathcal{L}(X, Y)$  the dual operator  $T^* : Y^* \rightarrow X^*$  by  $\langle Tx, y^* \rangle = \langle x, T^*y^* \rangle$  for all  $x \in Y$  and  $y^* \in Y^*$ . Here  $\langle \cdot, \cdot \rangle$  is the dual pairing, consequently we have  $x^*(x) := \langle x, x^* \rangle$  for  $x \in X$  and  $x^* \in X^*$ .

If we denote by  $\mathcal{E}(\mathbb{R}^d)$  the space of smooth functions with a suitable topology, the dual space is given by the space of distributions with compact support named  $\mathcal{E}'(\mathbb{R}^d)$ . The dual space of  $\mathcal{S}(\mathbb{R}^d)$  is the space of tempered distributions  $\mathcal{S}'(\mathbb{R}^d)$ . Last, we equip the space  $C_c^\infty(\mathbb{R}^d)$

with its usual topology and write therefore  $\mathcal{D}(\mathbb{R}^d)$ . Then, the dual space is  $\mathcal{D}'(\mathbb{R}^d)$ , the space of distributions.

We introduce the Sobolev space  $H^r(\mathbb{R}^d)$  for  $r \in \mathbb{R}$  given by

$$H^r(\mathbb{R}^d) := \{f \in \mathcal{S}'(\mathbb{R}^d) \mid (1 + |\cdot|^2)^{\frac{r}{2}} \mathcal{F}f \in L^2(\mathbb{R}^d)\},$$

i.e. we have  $H^r(\mathbb{R}^d) \subseteq L^2(\mathbb{R}^d)$  for  $r \geq 0$ . In addition, for an open subset  $\Omega \subseteq \mathbb{R}^d$  we define

$$H_{\text{loc}}^r(\Omega) := \{u \in \mathcal{D}'(\Omega) \mid \phi u \in H^r(\Omega) \text{ for each } \phi \in C_c^\infty(\Omega)\}.$$

For a given set  $A \subseteq \mathbb{R}^d$  the characteristic function  $\chi_A$  is defined by

$$\chi_A(x) = \begin{cases} 1, & \text{if } x \in A, \\ 0, & \text{if } x \notin A, \end{cases}$$

for  $x \in \mathbb{R}^d$ . By  $\partial A$  we denote the boundary of the set  $A$ . We write  $B_r(p) := \{x \in \mathbb{R}^d \mid |x-p| < r\}$  for an open ball and  $\overline{B_r(p)} := \{x \in \mathbb{R}^d \mid |x-p| \leq r\}$  for a closed ball in  $\mathbb{R}^d$  with midpoint  $p \in \mathbb{R}^d$  and radius  $r > 0$ . With  $S^{d-1} = \{x \in \mathbb{R}^d \mid |x| = 1\}$  we denote the unit sphere in  $\mathbb{R}^d$ , the boundary of the ball with radius one and midpoint zero.

Furthermore,  $C_a$  denotes a constant with  $C_a > 0$  that depends on the parameter  $a$ .

Finally, we use  $\text{Id}$  to denote the identity on a set which becomes clear by the context.

## 1.2. The considered problem

We consider an inverse problem of seismic imaging. This means we have a source  $\mathbf{x}_s$  which excites a wave at time  $t = 0$ . The excited wave propagates through different material layers and has a different speed of sound depending on which material layer it goes through. In the meantime, this wave is reflected and its reflections are recorded by a receiver  $\mathbf{x}_r$ .

We want to reconstruct the speed of sound in order to distinguish between the different material layers and to obtain their locations. Actually, this is modelled by the elastic wave equation. However, we simplify the model by assuming that no shear waves appear and that the medium has constant mass density. Then, the propagation of waves excited at the source point  $\mathbf{x}_s$  with speed of sound  $\nu$  is described by the acoustic wave equation

$$\frac{1}{\nu^2(x)} \partial_t^2 u(t, x; \mathbf{x}_s) - \Delta u(t, x; \mathbf{x}_s) = \delta(x - \mathbf{x}_s) \delta(t) \quad (1.1)$$

for time  $t \geq 0$  and at location  $x \in \mathbb{R}^3$ , where  $\mathbf{x}_s$  is the source point. As initial conditions we take

$$u(0, \cdot; \mathbf{x}_s) = \partial_t u(0, \cdot; \mathbf{x}_s) = 0 \quad (1.2)$$

since we assume the environment to be at rest before the wave is excited. The task is to reconstruct the speed of sound  $\nu$  from the backscattered field  $u(t, \mathbf{x}_r; \mathbf{x}_s)$  observed at a receiver point  $\mathbf{x}_r$  for  $(t, \mathbf{x}_r; \mathbf{x}_s) \in [0, T_{\text{max}}] \times \mathcal{R} \times \mathcal{S}$ , where  $T_{\text{max}}$  is the recording time and  $\mathcal{R}$  and  $\mathcal{S}$  are the sets of receiver and source positions, respectively.

In this thesis, we consider a special scanning geometry with constant distance from source to receiver. This geometry, the so called common offset geometry, is realised by  $\mathbf{x}_s = \mathbf{x}_s(s) = (s_1, s_2 - \alpha, 0)^\top$  and  $\mathbf{x}_r = \mathbf{x}_r(s) = (s_1, s_2 + \alpha, 0)^\top$  for fixed offset  $\alpha > 0$  and  $(s_1, s_2) \in S_0 \subseteq \mathbb{R}^2$ , which is a non-empty open, bounded and connected subset of  $\mathbb{R}^2$ . We remark that in the considered coordinate system the third space direction points downwards, i.e. source and receiver are at the surface. An illustration is given in Figure 1.1.

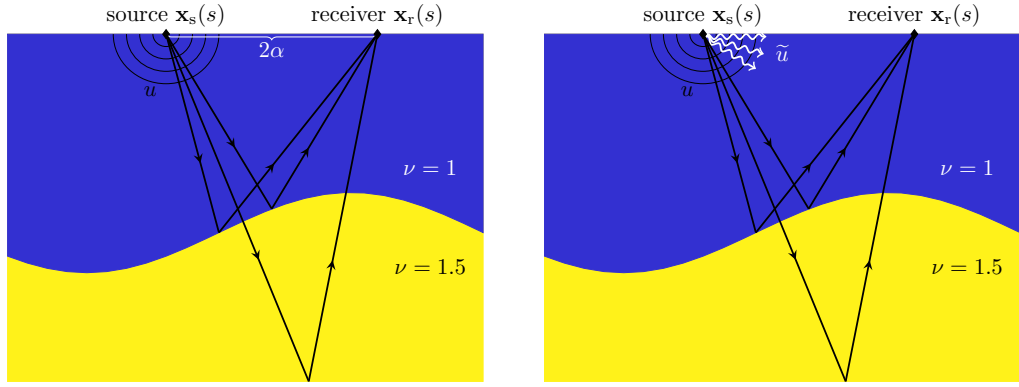


**Figure 1.1:** An illustration of the setting for fixed  $s \in S_0$ . Here, we have two different material layers with speed of sound  $\nu = 1$  in the blue area and  $\nu = 1.5$  in the yellow one.

In order to solve the mentioned problem, we make the ansatz

$$\frac{1}{\nu^2(x)} = \frac{1 + n(x)}{c^2} \quad (1.3)$$

for  $x \in \mathbb{R}^3$  with a smooth and a priori known background velocity  $c$ , which we assume to be constant, and a function  $n$  with  $\text{supp}(n) \subseteq \mathbb{R}_+^3$ . We recall that  $\mathbb{R}_+^3 = \{x = (x_1, x_2, x_3)^\top \in \mathbb{R}^3 \mid x_3 > 0\}$ .

For simplicity, we choose  $c = 1$ . The corresponding reference solution  $\tilde{u}$  satisfies (1.1) with speed of sound  $c = 1$  instead of  $\nu$ , i.e.

$$\partial_t^2 \tilde{u}(t, x; \mathbf{x}_s(s)) - \Delta \tilde{u}(t, x; \mathbf{x}_s(s)) = \delta(x - \mathbf{x}_s(s)) \delta(t) \quad (1.4)$$

for time  $t \geq 0$  and  $x \in \mathbb{R}^3$ .

By this ansatz, we are searching for  $n$  instead of  $\nu$ . Physically the quantity  $n$  can be interpreted as kind of reflectivity which includes the high frequency variations of  $\nu$  (see Section 3.2.1 in [BCS01]). For the further procedure we follow the lines of [BC79] and [Sym98]. We insert ansatz (1.3) in the acoustic wave equation (1.1). Afterwards, we subtract equation (1.4) and end up with

$$\partial_t^2 (u - \tilde{u})(t, x; \mathbf{x}_s(s)) - \Delta (u - \tilde{u})(t, x; \mathbf{x}_s(s)) = -n \partial_t^2 u(t, x; \mathbf{x}_s(s))$$

for  $t \geq 0$  and  $x \in \mathbb{R}^3$ . By Duhamel's principle a solution of this equation is given by

$$(u - \tilde{u})(t, y, \mathbf{x}_s(s)) = - \int_0^t \int_{\mathbb{R}_+^3} n(x) \partial_1^2 u(r, x; \mathbf{x}_s(s)) \tilde{u}(t - r, y, x) dx dr \quad (1.5)$$

for  $t \geq 0$  and  $y \in \mathbb{R}^3$ . Here,  $\tilde{u}$  is the fundamental solution since it solves equation (1.4). From now on, we write  $\partial_1$  for the derivative with respect to the first variable, i.e. with respect to time, to avoid confusion.

We do not have any further information about  $u$ , so we have to approximate the right hand-side. For this reason, we define formally the operator  $B$  by

$$Bu(t, y; \mathbf{x}_s(s)) = - \int_0^t \int_{\mathbb{R}_+^3} n(x) \partial_1^2 u(r, x; \mathbf{x}_s(s)) \tilde{u}(t - r, y, x) dx dr$$

for  $t \geq 0$  and  $y \in \mathbb{R}^3$ . Using this definition, equation (1.5) simplifies to  $u - \tilde{u} = Bu$  which we formally rewrite as

$$u = (\text{Id} - B)^{-1} \tilde{u}.$$

We write the operator  $(\text{Id} - B)^{-1}$  as a formal Neumann series. According to [Dem15], this is valid for small  $n$ . We have

$$u = \tilde{u} + B\tilde{u} + B^2\tilde{u} + \sum_{k=3}^{\infty} B^k\tilde{u}.$$

Inserting the definition of  $B$  yields

$$\begin{aligned} u(t, y; \mathbf{x}_s(s)) &= \tilde{u}(t, y; \mathbf{x}_s(s)) - \int_0^t \int_{\mathbb{R}_+^3} n(x) \partial_1^2 \tilde{u}(r, x; \mathbf{x}_s(s)) \tilde{u}(t-r, y, x) dx dr \\ &\quad + \int_0^t \int_{\mathbb{R}_+^3} \partial_1^2 \left[ \int_0^{r_1} \int_{\mathbb{R}_+^3} n(z) \partial_1^2 \tilde{u}(r_2, z; \mathbf{x}_s(s)) dz dr_2 \right] dz dr_1 + \dots \end{aligned}$$

for  $t \geq 0$  and  $y \in \mathbb{R}^3$ . Physically the first term  $\tilde{u}$  is the incident wave. If we approximate  $u$  up to the first order, we consider single scattering. By taking also the second order, we describe double scattering and so on. In this thesis, we do not regard multiple scattering. Thus, we approximate

$$u(t, y; \mathbf{x}_s(s)) \approx \tilde{u}(t, y; \mathbf{x}_s(s)) - \int_0^t \int_{\mathbb{R}_+^3} n(x) \partial_1^2 \tilde{u}(r, x; \mathbf{x}_s(s)) \tilde{u}(t-r, y, x) dx dr$$

with the terms up to the first order and so

$$u(t, y; \mathbf{x}_s(s)) - \tilde{u}(t, y; \mathbf{x}_s(s)) \approx - \int_0^t \int_{\mathbb{R}_+^3} n(x) \partial_1^2 \tilde{u}(r, x; \mathbf{x}_s(s)) \tilde{u}(t-r, y, x) dx dr$$

for  $t \geq 0$  and  $y \in \mathbb{R}_+^3$ . In the literature, the term linearisation often appears in context with this procedure since we only take the terms up to first order of the formal Neumann series.

Now, we evaluate at the receiver point  $\mathbf{x}_r(s)$  and deduce the linearised problem

$$u(t, \mathbf{x}_r(s); \mathbf{x}_s(s)) - \tilde{u}(t, \mathbf{x}_r(s); \mathbf{x}_s(s)) = Ln(t, \mathbf{x}_r(s); \mathbf{x}_s(s)) \quad (1.6)$$

with

$$\begin{aligned} Ln(t, \mathbf{x}_r(s); \mathbf{x}_s(s)) &:= - \int_0^t \int_{\mathbb{R}_+^3} n(x) \partial_1^2 \tilde{u}(r, x; \mathbf{x}_s(s)) \tilde{u}(t-r, \mathbf{x}_r(s); x) dx dr \\ &= - \int_0^t \int_{\mathbb{R}_+^3} n(x) \partial_1^2 \tilde{u}(t-r, x; \mathbf{x}_s(s)) \tilde{u}(r, \mathbf{x}_r(s); x) dx dr \end{aligned}$$

for  $t \geq 0$ . Moreover, we calculate

$$\begin{aligned}
& -\partial_t^2 \int_0^t \int_{\mathbb{R}_+^3} n(x) \tilde{u}(t-r, x; \mathbf{x}_s(s)) \tilde{u}(r, \mathbf{x}_r(s); x) \, dx \, dr \\
&= -\partial_t \left( \int_0^t \int_{\mathbb{R}_+^3} n(x) \partial_1 \tilde{u}(t-r, x; \mathbf{x}_s(s)) \tilde{u}(r, \mathbf{x}_r(s); x) \, dx \, dr \right. \\
&\quad \left. + \int_{\mathbb{R}_+^3} n(x) \tilde{u}(0, x; \mathbf{x}_s(s)) \tilde{u}(t, \mathbf{x}_r(s); x) \, dx \right) \\
&= -\int_0^t \int_{\mathbb{R}_+^3} n(x) \partial_1^2 \tilde{u}(t-r, x; \mathbf{x}_s(s)) \tilde{u}(r, \mathbf{x}_r(s); x) \, dx \, dr \\
&\quad + \int_{\mathbb{R}_+^3} n(x) \partial_1 \tilde{u}(0, x; \mathbf{x}_s(s)) \tilde{u}(t, \mathbf{x}_r(s); x) \, dx + \int_{\mathbb{R}_+^3} n(x) \tilde{u}(0, x; \mathbf{x}_s(s)) \partial_1 \tilde{u}(t, \mathbf{x}_r(s); x) \, dx \\
&= -\int_0^t \int_{\mathbb{R}_+^3} n(x) \partial_1^2 \tilde{u}(t-r, x; \mathbf{x}_s(s)) \tilde{u}(r, \mathbf{x}_r(s); x) \, dx \, dr,
\end{aligned}$$

where we used the initial conditions (1.2) in the last step. This yields

$$u_{\text{data}}(t, \mathbf{x}_r(s); \mathbf{x}_s(s)) = -\partial_t^2 \int_0^t \int_{\mathbb{R}_+^3} n(x) \tilde{u}(t-r, x; \mathbf{x}_s(s)) \tilde{u}(r, \mathbf{x}_r(s); x) \, dx \, dr \quad (1.7)$$

for  $t \geq 0$  with  $u_{\text{data}} = u - \tilde{u}$  out of equation (1.6).

Since we assume  $c = 1$ , the fundamental solution  $\tilde{u}$  is given by

$$\tilde{u}(t, x; \mathbf{x}_s(s)) = a_{\mathbf{x}_s(s)}(x) \delta(t - \tau_{\mathbf{x}_s(s)}(x)) \quad (1.8)$$

for  $t \geq 0$  and  $x \in \mathbb{R}^3$  with

$$a_y(x) = \frac{1}{4\pi|x-y|} \quad \text{and} \quad \tau_y(x) = |x-y|$$

for  $x \in \mathbb{R}_+^3$  and fixed  $y \in \mathbb{R}^3$ . Thus, we have

$$\tilde{u}(t, x; \mathbf{x}_s) = \frac{1}{4\pi|\mathbf{x}_s(s)-x|} \delta(t - |\mathbf{x}_s(s)-x|)$$

for  $t \geq 0$  and  $x \in \mathbb{R}^3$ . Inserting this in representation (1.7) yields

$$\begin{aligned}
& u_{\text{data}}(t, \mathbf{x}_r(s); \mathbf{x}_s(s)) \\
&= -\partial_t^2 \int_0^t \int_{\mathbb{R}_+^3} n(x) a_{\mathbf{x}_s(s)}(x) \delta(t-r - \tau_{\mathbf{x}_s(s)}(x)) a_{\mathbf{x}_r(s)}(x) \delta(r - \tau_{\mathbf{x}_r(s)}(x)) \, dx \, dr
\end{aligned}$$

for  $t \geq 0$ . The multiplication of the two  $\delta$ -distributions in the integrand is well defined as we will show in the following remark. For this reason, we anticipate some notions of microlocal analysis we introduce in Chapter 2. However, the next lines are not necessary for understanding. It is possible to skip the remark and go on with equation (1.10) by taking only the information that the appearing product is well defined.

**1.1 Remark.** We consider

$$f(r, x) := \delta(r - \tau_{\mathbf{x}_s(s)}(x)) \quad \text{and} \quad g(r, x) := \delta(t - r - \tau_{\mathbf{x}_r(s)}(x))$$

for  $r \in (0, t)$  and  $x \in \mathbb{R}^3$  and take a look at their wave front sets. A definition of this notion is given in (2.9). In order to determine them, we follow an example in [BDH14]. Related to  $f$  and  $g$  we define

$$\tilde{\phi}(r, x, v) := (r - \tau_{\mathbf{x}_s(s)}(x))v \quad \text{and} \quad \hat{\phi}(r, x, v) := (t - r - \tau_{\mathbf{x}_r(s)}(x))v$$

for  $r \in (0, t)$ ,  $x \in \mathbb{R}^3$  and  $v \in \mathbb{R}$ . Then, we deduce

$$\nabla_{r,x} \tilde{\phi}(r, x, v) = v \begin{pmatrix} 1 \\ -\nabla_x \tau_{\mathbf{x}_s(s)}(x) \end{pmatrix} \quad \text{and} \quad \nabla_{r,x} \hat{\phi}(r, x, v) = v \begin{pmatrix} -1 \\ -\nabla_x \tau_{\mathbf{x}_r(s)}(x) \end{pmatrix}$$

for  $r \in (0, t)$ ,  $x \in \mathbb{R}^3$  and  $v \in \mathbb{R}$ . According to Example 23 in [BDH14], this yields

$$\begin{aligned} \text{WF}(f) &= \{((r, x)^\top, -\nabla_{r,x} \tilde{\phi}(r, x, v)) \mid r \in (0, t), x \in \mathbb{R}_+^3, v \in \mathbb{R}\} \\ &= \{((r, x)^\top, v(-1, \nabla_x \tau_{\mathbf{x}_s(s)}(x))^\top) \mid r \in (0, t), x \in \mathbb{R}_+^3, v \in \mathbb{R}\} \end{aligned}$$

and

$$\begin{aligned} \text{WF}(g) &= \{((r, x)^\top, -\nabla_{r,x} \hat{\phi}(r, x, v)) \mid r \in (0, t), x \in \mathbb{R}_+^3, v \in \mathbb{R}\} \\ &= \{((r, x)^\top, v(1, \nabla_x \tau_{\mathbf{x}_r(s)}(x))^\top) \mid r \in (0, t), x \in \mathbb{R}_+^3, v \in \mathbb{R}\}. \end{aligned}$$

The product of the two distributions is well defined if there is no point  $(p, w) \in \text{WF}(f)$  such that  $(p, -w) \in \text{WF}(g)$  holds. In Chapter 2 right after Lemma 2.13 we go further into details on this assertion. The needed condition is satisfied if

$$\lambda \begin{pmatrix} -1 \\ \nabla_x \tau_{\mathbf{x}_s(s)}(x) \end{pmatrix} \neq - \begin{pmatrix} 1 \\ \nabla_x \tau_{\mathbf{x}_r(s)}(x) \end{pmatrix} \quad (1.9)$$

holds for all  $\lambda \in \mathbb{R}$ . We have

$$\nabla_x \tau_{\mathbf{x}_s(s)}(x) = \frac{x - \mathbf{x}_s(s)}{|\mathbf{x}_s(s) - x|} \quad \text{and} \quad \nabla_x \tau_{\mathbf{x}_r(s)}(x) = \frac{x - \mathbf{x}_r(s)}{|x - \mathbf{x}_r(s)|}$$

for  $x \in \mathbb{R}^3$  and thus  $|\nabla_x \tau_{\mathbf{x}_s(s)}(x)| = |\nabla_x \tau_{\mathbf{x}_r(s)}(x)| = 1$  for  $x \in \mathbb{R}^3$ . As a consequence, the only way to obtain equality in (1.9) is in case of

$$\nabla_x \tau_{\mathbf{x}_s(s)}(x) = -\nabla_x \tau_{\mathbf{x}_r(s)}(x).$$

is satisfied for  $x \in \mathbb{R}^3$ . However, this is not possible. The third component of both gradients is given by  $x_3$  divided by a strictly positive distance. Since  $x_3$  is strictly positive by assumption, these values are not negative and the condition needed for the multiplication of  $f$  and  $g$  is satisfied. Thus, the given integral is well defined without restrictions on  $\tau_y$  for fixed  $y \in \mathbb{R}_+^3$  and we obtain

$$\begin{aligned} &u_{\text{data}}(t, \mathbf{x}_r(s); \mathbf{x}_s(s)) \\ &= -\partial_t^2 \int_0^t \int_{\mathbb{R}_+^3} n(x) a_{\mathbf{x}_s(s)}(x) \delta(t - r - \tau_{\mathbf{x}_s(s)}(x)) a_{\mathbf{x}_r(s)}(x) \delta(r - \tau_{\mathbf{x}_r(s)}(x)) dx dr \\ &= -\partial_t^2 \int_{\mathbb{R}_+^3} \int_0^t n(x) a_{\mathbf{x}_s(s)}(x) \delta(t - r - \tau_{\mathbf{x}_s(s)}(x)) a_{\mathbf{x}_r(s)}(x) \delta(r - \tau_{\mathbf{x}_r(s)}(x)) dr dx \\ &= -\partial_t^2 \int_{\mathbb{R}_+^3} a_{\mathbf{x}_s(s)}(x) a_{\mathbf{x}_r(s)}(x) n(x) \delta(t - \tau_{\mathbf{x}_s(s)}(x) - \tau_{\mathbf{x}_r(s)}(x)) dx \end{aligned}$$

for  $t \geq 0$ .

By the considerations in the remark before we end up with

$$u_{\text{data}}(t, \mathbf{x}_r(s); \mathbf{x}_s(s)) = -\partial_t^2 \int_{\mathbb{R}_+^3} a_{\mathbf{x}_s(s)}(x) a_{\mathbf{x}_r(s)}(x) n(x) \delta(t - \tau_{\mathbf{x}_s(s)}(x) - \tau_{\mathbf{x}_r(s)}(x)) dx \quad (1.10)$$

for  $t \geq 0$ .

Last, we define

$$A(s, x) := 16\pi^2 a_{\mathbf{x}_s(s)}(x) a_{\mathbf{x}_r(s)}(x) = \frac{1}{|\mathbf{x}_s(s) - x| |x - \mathbf{x}_r(s)|} \quad (1.11)$$

and

$$\varphi(s, x) := \tau_{\mathbf{x}_s(s)}(x) + \tau_{\mathbf{x}_r(s)}(x) = |\mathbf{x}_s(s) - x| + |x - \mathbf{x}_r(s)|$$

for  $s \in S_0$  and  $x \in \mathbb{R}_+^3$  and therewith the operator

$$Fn(s, t) := \int_{\mathbb{R}_+^3} n(x) A(s, x) \delta(t - \varphi(s, x)) dx \quad (1.12)$$

for  $(s, t) \in S_0 \times (2\alpha, \infty)$ . Then, after integrating equation (1.10) two times with respect to  $t$  we end up with

$$Fn(s, t) = y(s, t) \quad (1.13)$$

for  $(s, t) \in S_0 \times (2\alpha, \infty)$  with

$$\begin{aligned} y(s, t) &= -16\pi^2 \int_0^t (t-r) u_{\text{data}}(r, \mathbf{x}_r(s); \mathbf{x}_s(s)) dr \\ &= -16\pi^2 \int_0^t (t-r) (u - \tilde{u})(r, \mathbf{x}_r(s); \mathbf{x}_s(s)) dr \end{aligned}$$

for  $(s, t) \in S_0 \times (2\alpha, \infty)$ .

In the next subsection, we introduce a special kind of coordinates suitable to the representation of the operator  $F$ . Using these, we rewrite the expression for the operator  $F$  in Subsection 1.2.2. The achievements therein convey an illustrative impression of the operator  $F$ . We shall use these in Chapter 4 to rewrite  $F$ .

### 1.2.1. Prolate spheroidal coordinates

There are numerous of situations in which the Cartesian coordinates are not the most suitable ones. Also in our setting we are able to simplify many calculations by using other coordinates, the *prolate spheroidal coordinates*. Their name derives from prolate spheroids which are a special kind of ellipsoids. More precisely, they arise by rotating an ellipse about the axis through its two foci. These two foci characterise the prolate spheroidal coordinates, which are related to prolate spheroids in the way spherical coordinates are related to spheres. But before we describe them in detail, we choose the two foci which characterise the prolate spheroidal coordinates in our case. Appropriate to the half-ellipsoids showing up in our situation we choose for fixed  $s \in S_0$  the two foci  $\mathbf{x}_s(s) = (s_1, s_2 - \alpha, 0)^\top$  and  $\mathbf{x}_r(s) = (s_1, s_2 + \alpha, 0)^\top$ . Since in our case the offset  $\alpha$  is fixed, we characterise this choice by the midpoint  $(s_1, s_2, 0)^\top$  of the two foci. For this reason, we obtain the prolate spheroidal coordinates on  $\mathbb{R}^3$  with respect to  $(s_1, s_2, 0)^\top$  given by

$$\begin{aligned} x_1 &= s_1 + \alpha \sinh(\rho) \sin(\phi) \cos(\theta), \\ x_2 &= s_2 + \alpha \cosh(\rho) \cos(\phi), \\ x_3 &= \alpha \sinh(\rho) \sin(\phi) \sin(\theta) \end{aligned} \quad (1.14)$$

for  $\rho > 0$ ,  $\phi \in [0, \pi)$  and  $\theta \in [0, 2\pi)$ .

In order to illustrate these coordinates, we take a look on how the values of the two angles run in this coordinate system. For illustration we also consider  $\phi \in [0, 2\pi)$ . However, it is sufficient to choose  $\phi \in [0, \pi)$  in order to obtain the whole space  $\mathbb{R}^3$ . First, we consider what we observe at the plane given by  $x_2 = s_2$  fixed to clarify the location of the different values of  $\theta$ . In this case, the definition of  $x_2$  yields that  $\phi = \frac{1}{2}\pi$  or  $\phi = \frac{3}{2}\pi$  is satisfied. Further, for a fixed value of  $\rho$  we get a concentric circle by taking the two mentioned values of  $\phi$  and  $\theta \in [0, 2\pi)$ . For different values of  $\rho$  we obtain different concentric circles which are illustrated in Figure 1.2. The different values of  $\theta$  are arranged radially around the point  $(s_1, 0)$ .

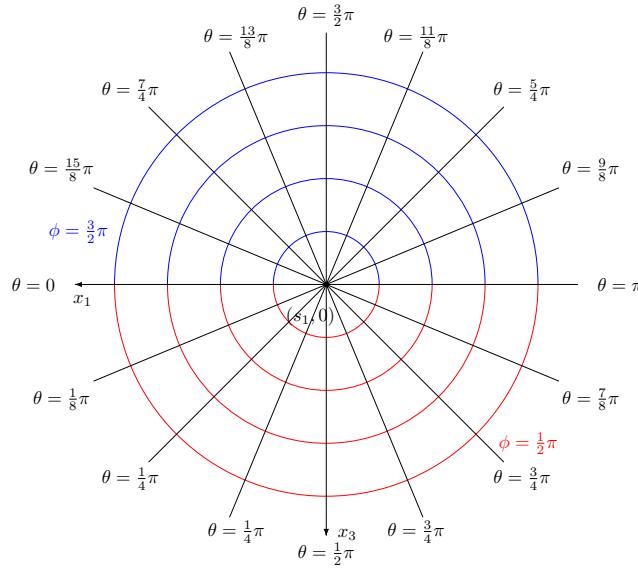


**Figure 1.2:** Cross section at  $x_2 = s_2$  for  $\theta \in [0, 2\pi)$ ,  $\phi \in \{\frac{1}{2}\pi, \frac{3}{2}\pi\}$  and four choices of  $\rho$ . The point in the middle is given by  $(s_1, 0)$ .

For a visualisation of the angle  $\phi$  we consider the plane given by  $x_1 = s_1$ . According to the definition of  $x_1$  we then have  $\theta = \frac{1}{2}\pi$  or  $\theta = \frac{3}{2}\pi$ . Moreover, for a fixed value of  $\rho$ , the two mentioned angles of  $\theta$  and  $\phi \in [0, 2\pi)$  yield an ellipse with the two foci  $(s_2 - \alpha, 0)^\top$  and  $(s_2 + \alpha, 0)^\top$ . In contrast to  $\theta$  the angle  $\phi$  is not arranged concentric. The four multiples of  $\frac{\pi}{4}$  are positioned orthogonal in a cross and the others in between are located in hyperbolic orbits. This is illustrated in Figure 1.3.

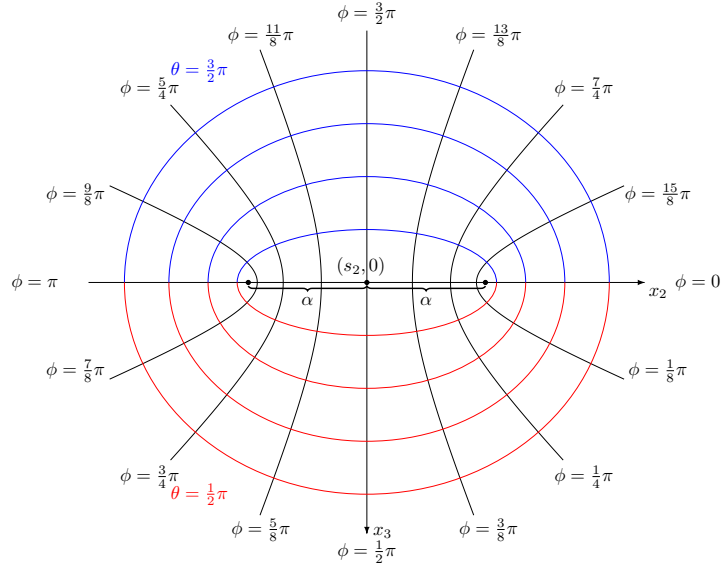


**Figure 1.3:** Cross section at  $x_1 = s_1$  for  $\phi \in [0, 2\pi)$ ,  $\theta \in \{\frac{1}{2}\pi, \frac{3}{2}\pi\}$  and four choices of  $\rho$ . The point in the middle is given by  $(s_2, 0)$ , the two other points are the two foci.

In our setting we consider values of  $x$  in  $\mathbb{R}_+^3$ , so we have  $x \in \mathbb{R}^3$  with  $x_3 > 0$ . This yields the limitations  $\theta \in (0, \pi)$  and  $\phi \in (0, \pi)$  on  $\theta$  and  $\phi$  since we do not need all values of  $\theta$  and  $\phi$  in  $[0, 2\pi)$  to describe the half-space  $\mathbb{R}_+^3$ . Beside the restrictions on the angles, we reformulate the coordinates stated in (1.14) once again. For fixed  $\rho > 0$  and  $\phi, \theta \in (0, \pi)$  we obtain an open half-ellipsoid by the coordinates given in (1.14). For each point of the open half-ellipsoid the sum of the two distances from this point to the two foci is constant. This sum is the travel time  $T$  of the open half-ellipsoid. For fixed  $\rho > 0$  the value of  $T$  is constant and given by  $T = 2\alpha \cosh(\rho)$ . Using this relation, we reformulate the coordinates with respect to  $(s_1, s_2, 0)^\top$  stated in (1.14) to

$$\begin{aligned} x_1 &= s_1 + \sqrt{\frac{1}{4}T^2 - \alpha^2} \sin(\phi) \cos(\theta), \\ x_2 &= s_2 + \frac{1}{2}T \cos(\phi), \\ x_3 &= \sqrt{\frac{1}{4}T^2 - \alpha^2} \sin(\phi) \sin(\theta) \end{aligned} \quad (1.15)$$

for  $T > 2\alpha$ ,  $\phi \in (0, \pi)$  and  $\theta \in (0, \pi)$ . Given a fixed travel time  $T$  this reformulation yields for  $\theta$  and  $\phi$  in  $(0, \pi)$  the associated open half-ellipsoid.

### 1.2.2. The operator $F$ expressed using prolate spheroidal coordinates

In order to get a deeper understanding of  $F$ , we rewrite the representation

$$Fn(s, t) = \int_{\mathbb{R}_+^3} n(x) A(s, x) \delta(t - \varphi(s, x)) dx$$

for  $(s, t) \in S_0 \times (2\alpha, \infty)$  in case of  $n \in C_c^\infty(\mathbb{R}_+^3)$  by using the prolate spheroidal coordinates introduced in (1.15). According to the second point of Section XI.3.1.2 in [Ste95], we understand the measure  $\mu = \delta(t - \varphi(s, x)) dx$  as an associated measure to a hypersurface  $S$ . Since

$$\nabla_x \varphi(s, x) = \left( \frac{x_1 - s_1}{|\mathbf{x}_s(s) - x|} + \frac{x_1 - s_1}{|x - \mathbf{x}_r(s)|}, \frac{x_2 - s_2 + \alpha}{|\mathbf{x}_s(s) - x|} + \frac{x_2 - s_2 - \alpha}{|x - \mathbf{x}_r(s)|}, \frac{x_3}{|\mathbf{x}_s(s) - x|} + \frac{x_3}{|x - \mathbf{x}_r(s)|} \right)^\top \quad (1.16)$$

does not vanish on  $\mathbb{R}_+^3$  due to the fact that  $x_3 > 0$  holds, this associated hypersurface is defined by  $\Phi$  with  $\Phi(s, t, x) = t - \varphi(s, x)$  for  $x \in \mathbb{R}_+^3$  and fixed  $(s, t) \in S_0 \times (2\alpha, \infty)$ , i.e.  $S = \{x \in \mathbb{R}_+^3 \mid \varphi(s, x) = t\}$ . In Lemma 3.1 we will see that the hypersurface  $S$  is an open half-ellipsoid in  $\mathbb{R}_+^3$ .

By the definition of Dirac measures related to hypersurfaces, we deduce

$$\begin{aligned} Fn(s, t) &= \int_{\mathbb{R}_+^3} n(x)A(s, x)\delta(t - \varphi(s, x)) \, dx \\ &= \lim_{\varepsilon \rightarrow 0} \frac{1}{2\varepsilon} \int_{\{x \in \mathbb{R}_+^3 \mid -\varepsilon < \Phi(s, t, x) < \varepsilon\}} n(x)A(s, x) \, dx \\ &= \lim_{\varepsilon \rightarrow 0} \frac{1}{2\varepsilon} \int_{\{x \in \mathbb{R}_+^3 \mid t - \varepsilon < \varphi(s, x) < t + \varepsilon\}} n(x)A(s, x) \, dx \end{aligned}$$

for  $(s, t) \in S_0 \times (2\alpha, \infty)$  and  $\varepsilon > 0$  such that  $t - \varepsilon > 2\alpha$  holds. Further, we rewrite this integral by using the transformation theorem. For this reason, we define the map  $\Psi: (t - \varepsilon, t + \varepsilon) \times (0, \pi) \times (0, \pi) \rightarrow \{x \in \mathbb{R}_+^3 \mid t - \varepsilon < \varphi(s, x) < t + \varepsilon\}$  by

$$(T, \phi, \theta) \mapsto \begin{pmatrix} s_1 + \sqrt{\frac{1}{4}T^2 - \alpha^2} \sin(\phi) \cos(\theta) \\ s_2 + \frac{1}{2}T \cos(\phi) \\ \sqrt{\frac{1}{4}T^2 - \alpha^2} \sin(\phi) \sin(\theta) \end{pmatrix}.$$

Then, we obtain

$$\begin{aligned} &\det(\Psi'(T, \phi, \theta)) \\ &= \det \begin{pmatrix} \frac{1}{2} \frac{1}{\sqrt{\frac{1}{4}T^2 - \alpha^2}} \frac{2}{4}T \sin(\phi) \cos(\theta) & \sqrt{\frac{1}{4}T^2 - \alpha^2} \cos(\phi) \cos(\theta) & -\sqrt{\frac{1}{4}T^2 - \alpha^2} \sin(\phi) \sin(\theta) \\ \frac{1}{2} \cos(\phi) & -\frac{1}{2}T \sin(\phi) & 0 \\ \frac{1}{2} \frac{1}{\sqrt{\frac{1}{4}T^2 - \alpha^2}} \frac{2}{4}T \sin(\phi) \sin(\theta) & \sqrt{\frac{1}{4}T^2 - \alpha^2} \cos(\phi) \sin(\theta) & \sqrt{\frac{1}{4}T^2 - \alpha^2} \sin(\phi) \cos(\theta) \end{pmatrix} \\ &= \sin(\phi) \left(-\frac{1}{8}T^2 + \frac{1}{2}\alpha^2 \cos^2(\phi)\right) \end{aligned}$$

for  $(T, \phi, \theta) \in (2\alpha, \infty) \times (0, \pi) \times (0, \pi)$ . As  $T > 2\alpha$  holds, it follows  $\frac{1}{8}T^2 > \frac{1}{2}\alpha^2$  and therefore by using  $\cos^2(\phi) \in (0, 1)$ , we have

$$|\det(\Psi'(T, \phi, \theta))| = \sin(\phi) \left(\frac{1}{8}T^2 - \frac{1}{2}\alpha^2 \cos^2(\phi)\right)$$

for  $(T, \phi, \theta) \in (2\alpha, \infty) \times (0, \pi) \times (0, \pi)$ . Furthermore,  $\sin(\phi) \left(\frac{1}{8}T^2 - \frac{1}{2}\alpha^2 \cos^2(\phi)\right) = 0$  is equivalent to  $\sin(\phi) = 0$  or  $\frac{1}{4\alpha^2}T^2 = \cos^2(\phi)$ . By assumption  $\phi$  lies in  $(0, \pi)$ , so we only have to consider the second condition. Due to  $T > 2\alpha$  and  $\cos^2(\phi) \in (0, 1)$  for  $\phi \in (0, \pi)$  there is no solution of the second equation. Hence,  $|\det(\Psi'(T, \phi, \theta))| \neq 0$  and  $\Psi'(T, \phi, \theta)$  is invertible for all  $(T, \phi, \theta) \in (2\alpha, \infty) \times (0, \pi) \times (0, \pi)$ . Further,  $\Psi$  is injective and continuously differentiable. Thus,  $\Psi: (t - \varepsilon, t + \varepsilon) \times (0, \pi) \times (0, \pi) \rightarrow \Psi((t - \varepsilon, t + \varepsilon) \times (0, \pi) \times (0, \pi)) = \{x \in \mathbb{R}_+^3 \mid t - \varepsilon < \varphi(s, x) < t + \varepsilon\}$  is a diffeomorphism. By the transformation theorem we obtain

$$\begin{aligned} &Fn(s, t) \\ &= \lim_{\varepsilon \rightarrow 0} \frac{1}{2\varepsilon} \int_{t-\varepsilon}^{t+\varepsilon} \int_0^\pi \int_0^\pi n(x(s, T, \phi, \theta))A(s, x(s, T, \phi, \theta)) \sin(\phi) \left(\frac{1}{8}T^2 - \frac{1}{2}\alpha^2 \cos^2(\phi)\right) \, d\phi \, d\theta \, dT \end{aligned}$$

for  $(s, t) \in S_0 \times (2\alpha, \infty)$ .

In order to simplify the integral we compute the function  $A$  in dependence on the prolate spheroidal coordinates with respect to  $(s_1, s_2, 0)^\top$ . We have

$$\begin{aligned}
& |\mathbf{x}_s(s) - x(s, T, \phi, \theta)| |x(s, T, \phi, \theta) - \mathbf{x}_r(s)| \\
&= \sqrt{\left(\frac{1}{4}T^2 - \alpha^2\right) \sin^2(\phi) \cos^2(\theta) + \left(\alpha - \frac{1}{2}T \cos(\phi)\right)^2 + \left(\frac{1}{4}T^2 - \alpha^2\right) \sin^2(\phi) \sin^2(\theta)} \\
&\quad \cdot \sqrt{\left(\frac{1}{4}T^2 - \alpha^2\right) \sin^2(\phi) \cos^2(\theta) + \left(\alpha + \frac{1}{2}T \cos(\phi)\right)^2 + \left(\frac{1}{4}T^2 - \alpha^2\right) \sin^2(\phi) \sin^2(\theta)} \\
&= \sqrt{\left(\frac{1}{4}T^2 - \alpha^2\right) \sin^2(\phi) + \alpha^2 - \alpha T \cos(\phi) + \frac{1}{4}T^2 \cos^2(\phi)} \\
&\quad \cdot \sqrt{\left(\frac{1}{4}T^2 - \alpha^2\right) \sin^2(\phi) + \alpha^2 + \alpha T \cos(\phi) + \frac{1}{4}T^2 \cos^2(\phi)} \\
&= \sqrt{\frac{1}{4}T^2 + \alpha^2 \cos^2(\phi) - \alpha T \cos(\phi)} \sqrt{\frac{1}{4}T^2 + \alpha^2 \cos^2(\phi) + \alpha T \cos(\phi)} \\
&= \left(\frac{1}{2}T - \alpha \cos(\phi)\right) \left(\frac{1}{2}T + \alpha \cos(\phi)\right) = \frac{1}{4}T^2 - \alpha^2 \cos^2(\phi)
\end{aligned}$$

for  $(T, \phi, \theta) \in (2\alpha, \infty) \times (0, \pi) \times (0, \pi)$ , where we used  $T > 2\alpha$  and so  $\frac{1}{2}T > \alpha \cos(\phi)$ . Therewith, we obtain

$$A(s, x(s, T, \phi, \theta)) = \frac{1}{|\mathbf{x}_s(s) - x(s, T, \phi, \theta)| |x(s, T, \phi, \theta) - \mathbf{x}_r(s)|} = \frac{1}{\frac{1}{4}T^2 - \alpha^2 \cos^2(\phi)}$$

for  $(T, \phi, \theta) \in (t - \varepsilon, t + \varepsilon) \times (0, \pi) \times (0, \pi)$ . This yields

$$\begin{aligned}
Fn(s, t) &= \lim_{\varepsilon \rightarrow 0} \frac{1}{2\varepsilon} \int_{t-\varepsilon}^{t+\varepsilon} \int_0^\pi \int_0^\pi \frac{n(x(s, T, \phi, \theta))}{\frac{1}{4}T^2 - \alpha^2 \cos^2(\phi)} \sin(\phi) \left(\frac{1}{8}T^2 - \frac{1}{2}\alpha^2 \cos^2(\phi)\right) d\phi d\theta dT \\
&= \lim_{\varepsilon \rightarrow 0} \frac{1}{2} \frac{1}{2\varepsilon} \int_{t-\varepsilon}^{t+\varepsilon} \int_0^\pi \int_0^\pi n(x(s, T, \phi, \theta)) \sin(\phi) d\phi d\theta dT
\end{aligned}$$

for  $(s, t) \in S_0 \times (2\alpha, \infty)$ . Last, by applying the Lebesgue differentiation theorem, we end up with

$$Fn(s, t) = \frac{1}{2} \int_0^\pi \int_0^\pi n(x(s, t, \phi, \theta)) \sin(\phi) d\phi d\theta \quad (1.17)$$

for  $(s, t) \in S_0 \times (2\alpha, \infty)$ .

In order to extend the representation of  $F$ , we consider the map  $\Psi$  for fixed  $t \in (2\alpha, \infty)$ , which we denote by  $\Psi_t$ . Then, we have  $\Psi_t: (0, \pi) \times (0, \pi) \rightarrow \{x \in \mathbb{R}_+^3 \mid \varphi(s, x) = t\}$ . For fixed  $(s, t) \in S_0 \times (2\alpha, \infty)$  the measure  $\mu(s, t) := A(s, x)\delta(t - \varphi(s, x))$  acts on  $C_c^\infty(\mathbb{R}_+^3)$  via identity (1.17). Since this representation is also well-defined for  $n \in L^1(\Psi_t((0, \pi) \times (0, \pi)))$ , we are able to extend the operator  $F$  on  $L^1(\Psi_t((0, \pi) \times (0, \pi)))$  by

$$Fn(s, t) := \frac{1}{2} \int_0^\pi \int_0^\pi n(x(s, t, \phi, \theta)) \sin(\phi) d\phi d\theta$$

for  $(s, t) \in S_0 \times (2\alpha, \infty)$ , where  $Fn(s, t)$  is measurable for  $(s, t) \in S_0 \times (2\alpha, \infty)$ .

Later on, we consider functions with compact support. Thus, we are able to limit the interval for the angles  $\phi$  and  $\theta$ , where the limits for  $\phi$  depend on  $\theta$ . We conclude

$$Fn(s, t) = \frac{1}{2} \int_{\theta_{\min}}^{\theta_{\max}} \int_{\phi(\theta)_{\min}}^{\phi(\theta)_{\max}} n(x(s, t, \phi, \theta)) \sin(\phi) d\phi d\theta \quad (1.18)$$

for  $(s, t) \in S_0 \times (2\alpha, \infty)$  with

$$\begin{aligned}\theta_{\min} &= \theta_{\min}(s, t) := \min\{\theta \in (0, \pi) \mid x(s, t, \phi, \theta) \in \text{supp}(n)\}, \\ \theta_{\max} &= \theta_{\max}(s, t) := \max\{\theta \in (0, \pi) \mid x(s, t, \phi, \theta) \in \text{supp}(n)\}\end{aligned}$$

and

$$\begin{aligned}\phi(\theta)_{\min} &= \phi(\theta)_{\min}(s, t) := \min\{\phi \in (0, \pi) \mid x(s, t, \phi, \theta) \in \text{supp}(n)\}, \\ \phi(\theta)_{\max} &= \phi(\theta)_{\max}(s, t) := \max\{\phi \in (0, \pi) \mid x(s, t, \phi, \theta) \in \text{supp}(n)\}.\end{aligned}$$

Summarised, for fixed  $(s, t) \in S_0 \times (2\alpha, \infty)$  we integrate over an open half-ellipsoid which intersects the support of the function  $n$ . After the reformulation we determine the minimal and maximal angles defined above such that the point  $x(s, t, \phi, \theta)$  of the open half-ellipsoid lies in  $\text{supp}(n)$  to evaluate  $F_n$  at a point  $(s, t)$ .

We note that this works in the same way if we consider  $\mathbb{R}^3$  instead of  $\mathbb{R}_+^3$ . In this case, we define  $\Psi$  on  $(t - \varepsilon, t + \varepsilon) \times (0, \pi) \times (0, 2\pi)$ . Also the argumentation, why the determinant  $\det(\Psi')$  does not vanish, remains the same. For  $n \in C_c^\infty(\mathbb{R}^3)$  we obtain

$$F_n(s, t) = \int_{\mathbb{R}^3} n(x) A(s, x) \delta(t - \varphi(s, x)) dx = \frac{1}{2} \int_{\theta_{\min}}^{\theta_{\max}} \int_{\phi(\theta)_{\min}}^{\phi(\theta)_{\max}} n(x(s, t, \phi, \theta)) \sin(\phi) d\phi d\theta \quad (1.19)$$

for  $(s, t) \in S_0 \times (2\alpha, \infty)$  with

$$\begin{aligned}\theta_{\min} &= \theta_{\min}(s, t) := \min\{\theta \in [0, 2\pi) \mid x(s, t, \phi, \theta) \in \text{supp}(n)\}, \\ \theta_{\max} &= \theta_{\max}(s, t) := \max\{\theta \in [0, 2\pi) \mid x(s, t, \phi, \theta) \in \text{supp}(n)\}\end{aligned}$$

and

$$\begin{aligned}\phi(\theta)_{\min} &= \phi(\theta)_{\min}(s, t) := \min\{\phi \in [0, \pi) \mid x(s, t, \phi, \theta) \in \text{supp}(n)\}, \\ \phi(\theta)_{\max} &= \phi(\theta)_{\max}(s, t) := \max\{\phi \in [0, \pi) \mid x(s, t, \phi, \theta) \in \text{supp}(n)\}.\end{aligned}$$

In case of  $\mathbb{R}^3$ , we are also able to extend the operator. For  $n \in L^1(\Psi_t((0, \pi) \times (0, 2\pi)))$  we define

$$F_n(s, t) := \frac{1}{2} \int_0^\pi \int_0^\pi n(x(s, t, \phi, \theta)) \sin(\phi) d\phi d\theta$$

for  $(s, t) \in S_0 \times (2\alpha, \infty)$ .

### 1.2.3. A note concerning a non-constant background velocity $c$

At the beginning of Section 1.2 and in the whole thesis we consider the background velocity  $c$  to be constant and even equal to 1. Nevertheless, we take a short look what changes if we allow  $c$  to be not necessarily constant but still smooth.

In this case, we make the same ansatz as stated in the case of constant  $c$  to solve the problem. However,  $\tilde{u}$  is then a solution of

$$\frac{1}{c^2(x)} \partial_t^2 \tilde{u}(t, x; \mathbf{x}_s(s)) - \Delta \tilde{u}(t, x; \mathbf{x}_s(s)) = \delta(x - \mathbf{x}_s(s)) \delta(t) \quad (1.20)$$

for  $t \geq 0$  and  $x \in \mathbb{R}^3$ . Further, the difference  $u_{\text{data}}$  of  $u$  and  $\tilde{u}$  solves

$$\frac{1}{c^2(x)} \partial_t^2 u_{\text{data}}(t, x; \mathbf{x}_s(s)) - \Delta u_{\text{data}}(t, x; \mathbf{x}_s(s)) = -\frac{n(x)}{c^2(x)} \partial_t^2 u(t, x; \mathbf{x}_s(s))$$

for  $t \geq 0$  and  $x \in \mathbb{R}^3$ . Again, by Duhamel's principle we obtain

$$u_{\text{data}}(t, \mathbf{x}_r(s), \mathbf{x}_s(s)) = - \int_0^t \int_{\mathbb{R}_+^3} n(x) \partial_1^2 u(r, x; \mathbf{x}_s(s)) \tilde{u}(t-r, \mathbf{x}_r(s); x) dx dr$$

for  $t \geq 0$  since the fundamental solution is given by  $\tilde{u}$ . As before,  $\partial_1$  denotes the derivative with respect to the first variable. Linearisation leads then to the linearised problem

$$u_{\text{data}}(t, \mathbf{x}_r(s), \mathbf{x}_s(s)) = - \int_0^t \int_{\mathbb{R}_+^3} n(x) \partial_1^2 \tilde{u}(r, x; \mathbf{x}_s(s)) \tilde{u}(t-r, \mathbf{x}_r(s); x) dx dr$$

for  $t \geq 0$ . Since the speed of sound  $c$  is not constant anymore, we do not know the representation of  $\tilde{u}$ . However, if we additionally assume that there exists one and only one ray which connects  $x \in \text{supp}(n)$  with each  $\mathbf{x}_s(s)$  and each  $\mathbf{x}_r(s)$  for  $s \in S_0$ , the solution  $\tilde{u}$  can be approximated by a progressing wave (see [Sym98]). Under this assumption, which is called the geometric optics approximation, we approximate  $\tilde{u}$  by

$$\tilde{u}(t, x; \mathbf{x}_s(s)) \approx a_{\mathbf{x}_s(s)}(x) \delta(t - \tau_{\mathbf{x}_s(s)}(x)) \quad (1.21)$$

for  $t \geq 0$  and  $x \in \mathbb{R}^3$ . Here, the functions  $a_y$  and  $\tau_y$  are smooth for fixed  $y \in \mathbb{R}_+^3$ . Moreover, for fixed  $y \in \mathbb{R}^3$  the travel time  $\tau_y$  solves the eikonal equation

$$|\nabla \tau_y(x)| = \frac{1}{c^2(x)} \quad \text{and} \quad \tau_y(y) = 0$$

for  $x \in \mathbb{R}^3$  and the amplitude  $a_y$  satisfies the transport equation

$$2\nabla_x \tau_y(x) \nabla_x a_y(x) + a_y(x) \Delta_x \tau_y(x) = 0$$

for  $x \in \mathbb{R}^3$  (see Section 3.2.1 in [BCS01]). These conditions are obtained by inserting the progressing wave ansatz (1.21) in equation (1.20) and have to be satisfied. At this point we remark that due to the different solution of  $\tau_y$  for fixed  $y \in \mathbb{R}^3$  the equation  $\tau_{\mathbf{x}_s(s)}(x) + \tau_{\mathbf{x}_r(s)}(x) = t$  for  $x \in \mathbb{R}^3$  and fixed  $(s, t) \in S_0 \times (2\alpha, \infty)$ , which appears later on, does not yield an open half-ellipsoid anymore. With this ansatz we obtain

$$\begin{aligned} u_{\text{data}}(t, \mathbf{x}_r(s); \mathbf{x}_s(s)) &= -\partial_t^2 \int_{\mathbb{R}_+^3} n(x) a_{\mathbf{x}_s(s)}(x) a_{\mathbf{x}_r(s)}(x) \int_0^t \delta(r - \tau_{\mathbf{x}_s(s)}(x)) \delta(t-r - \tau_{\mathbf{x}_r(s)}(x)) dr \\ &= -\partial_t^2 \int_{\mathbb{R}_+^3} n(x) a_{\mathbf{x}_s(s)}(x) a_{\mathbf{x}_r(s)}(x) \delta(t - \tau_{\mathbf{x}_s(s)}(x) - \tau_{\mathbf{x}_r(s)}(x)) dx \end{aligned}$$

for  $t \geq 0$ . As before condition (1.9) has to be fulfilled such that the multiplication in the integral is well-defined. Since  $\tau_y$  satisfies the eikonal equation for fixed  $y \in \mathbb{R}_+^3$ , we have  $|\nabla_x \tau_{\mathbf{x}_s(s)}(x)| = |\nabla_x \tau_{\mathbf{x}_r(s)}(x)| = \frac{1}{c^2(x)}$  for  $x \in \mathbb{R}^3$ . Hence, condition (1.9) is satisfied if  $\nabla_x \tau_{\mathbf{x}_s(s)}(x) + \nabla_x \tau_{\mathbf{x}_r(s)}(x) \neq 0$  for  $x \in \mathbb{R}^3$  holds. Then, we have

$$u_{\text{data}}(t, \mathbf{x}_r(s); \mathbf{x}_s(s)) = -\partial_t^2 \int_{\mathbb{R}_+^3} n(x) a_{\mathbf{x}_s(s)}(x) a_{\mathbf{x}_r(s)}(x) \delta(t - \tau_{\mathbf{x}_s(s)}(x) - \tau_{\mathbf{x}_r(s)}(x)) dx$$

for  $t \geq 0$ .



---

## Preliminaries

---

In this chapter, we collect some known results from the literature we need throughout this thesis. We also provide definitions and notions to make clear under which assumptions we work. Whenever it is helpful for understanding, we give an illustrative example.

This chapter is split into two parts. The first one deals with microlocal analysis. Therein, we give an introduction to this topic. We define the most important notions, give examples and state the results we need later on in this thesis. For convenience of the reader, we present the proofs of some results.

The topic of the second part are generalised Radon transforms. We prepare the definition of such a transform by providing the notions needed from measure theory. Finally, we close with the definition of a generalised Radon transform and its dual.

### 2.1. Basics of microlocal analysis

The theory of microlocal analysis was developed in the 1960s and 1970s. It derives from the theory of partial differential equations and Fourier analysis. At that time, the dominating research topics in mathematical analysis were functional analysis and distribution theory. The mathematicians were interested the existence of solutions for linear partial differential equations.

However, some of them developed these topics further. For example by the generalisation of terms like the singular support of a distribution or pseudodifferential operators which existed already. In this context, we have to mention two persons, Lars Hörmander and Mikio Sato. Both encouraged the theory of microlocal analysis in their different mathematical perspectives.

The essential thing in microlocal analysis is to analyse a distribution in a local sense. A good example is the comparison of the just mentioned singular support and its expansion in microlocal analysis, the wave front set. An element is not in the singular support of a distribution if it coincides with a  $C^\infty$ -function in a neighbourhood of this element. The wave front set additionally contains the related directions of the singularity. Hence, not only the location of a singularity is a part of the wave front set but also its directions. A direction is related to a singularity if a certain property is satisfied in a conic neighbourhood of the direction. In this way, it yields more information about the local behaviour of a distribution concerning its singularities.

Another significant part in the theory of microlocal analysis are Fourier integral operators. These are a generalisation of the Fourier transform introduced by Hörmander.

There are three publications [Hör65], [Hör70] and [Hör71] by Hörmander which con-

tain all his important results concerning this topic. Further, we refer to the books [Pet83] and [Shu87] by Bent E. Petersen and Mikhail A. Shubin, respectively, and the two volumes [Tre801] and [Tre802] by François Trèves. In there, the content is presented more elaborate than in the original publications by Hörmander. There is also the worth reading introduction [BDH14] to wave front sets by Christian Brouder, Nguyen V. Dang and Frédéric Hélein.

For a first general impression of microlocal analysis we recommend the publication [KQ15] by Venkateswaran P. Krishnan and E. Todd Quinto. This paper also has a link to the second large topic of this introductory chapter which are Radon transforms.

### 2.1.1. Basic definitions and results

In this section, we present some elementary tools from microlocal analysis. For  $n_Y, n_X \in \mathbb{N}$  we assume  $Y \subseteq \mathbb{R}^{n_Y}$  and  $X \subseteq \mathbb{R}^{n_X}$  to be open subsets of  $\mathbb{R}^{n_Y}$  and  $\mathbb{R}^{n_X}$ , respectively, and let  $N \in \mathbb{N}$  be given.

Before we are able to give the definitions of pseudodifferential and Fourier integral operators we define the term of a symbol which is one essential part of them.

For  $m \in \mathbb{Z}$  a function  $p \in C^\infty(Y \times X \times \mathbb{R}^N \setminus \{0\})$  is a *symbol of order  $m$  on  $Y \times X \times \mathbb{R}^N$*  if for every compact set  $K \subseteq Y \times X$  and all multi-indices  $\alpha \in \mathbb{N}_0^N, \beta \in \mathbb{N}_0^{n_X}$  and  $\gamma \in \mathbb{N}_0^{n_Y}$  there exists a constant  $C_{K,\alpha,\beta,\gamma} > 0$  such that

$$|D_\xi^\alpha D_x^\beta D_y^\gamma p(y, x, \xi)| \leq C_{K,\alpha,\beta,\gamma} (1 + |\xi|)^{m-|\alpha|} \quad (2.1)$$

for all  $(y, x) \in K$  and  $|\xi| \geq 1$  holds and if  $p$  is locally integrable on  $K \times \{\xi \in \mathbb{R}^N \mid |\xi| \leq 1\}$ .

We observe that a function  $p \in C^\infty(Y \times X \times \mathbb{R}^N)$  which satisfies estimate (2.1) for  $\xi \in \mathbb{R}^N$  is locally integrable. For this reason, we often only show estimate (2.1) for all  $\xi \in \mathbb{R}^N$  when we verify that a function  $p \in C^\infty(Y \times X \times \mathbb{R}^N)$  is a symbol.

We denote the set of all symbols of order  $m$  on  $Y \times X \times \mathbb{R}^N$  by  $S^m(Y \times X \times \mathbb{R}^N)$ . Further, we define the set  $S^{-\infty}(Y \times X \times \mathbb{R}^N) := \bigcap_{m \in \mathbb{Z}} S^m(Y \times X \times \mathbb{R}^N)$ .

Likewise, we define a *symbol of order  $m$  on  $X \times \mathbb{R}^N$*  depending only on two variables. Such a symbol  $p \in S^m(X \times \mathbb{R}^N)$  of order  $m$  is *elliptic* if for every compact set  $K \subseteq X$  there exist constants  $C_K > 0$  and  $M > 0$  such that

$$|p(x, \xi)| \geq C_K (1 + |\xi|)^m$$

for all  $x \in K$  and all  $\xi \in \mathbb{R}^N$  with  $|\xi| \geq M$ .

There is also a localised version of ellipticity. In order to characterise what localised means in this situation we introduce the notion of a conic neighbourhood.

A set  $V \subseteq \mathbb{R}^N \setminus \{0\}$  is a *conic neighbourhood* of an element  $\xi_0 \in \mathbb{R}^N \setminus \{0\}$  if  $\xi_0 \in V$  holds,  $B_\varepsilon(\xi_0) \subseteq V$  is satisfied for some  $\varepsilon > 0$  and  $\xi \in V$  implies  $\lambda\xi \in V$  for all  $\lambda > 0$ . Furthermore, a conic neighbourhood  $V$  of  $(x_0, \xi_0) \in X \times \mathbb{R}^N \setminus \{0\}$  is a notion for an open neighbourhood  $U \subseteq X$  of  $x_0$  and a conic neighbourhood  $\tilde{V} \subseteq \mathbb{R}^N \setminus \{0\}$  of  $\xi_0$ , i.e.  $V = U \times \tilde{V}$ .

Now, let  $(x_0, \xi_0) \in X \times \mathbb{R}^N \setminus \{0\}$ . Then, a symbol  $p \in S^m(X \times \mathbb{R}^N)$  is *microlocally elliptic of order  $m$*  at  $(x_0, \xi_0)$  if there are an open neighbourhood  $U \subseteq X$  of  $x_0$ , a conic neighbourhood  $V \subseteq \mathbb{R}^N \setminus \{0\}$  of  $\xi_0$  and constants  $M > 0$  and  $C_{U,V,M} > 0$  such that

$$|p(x, \xi)| \geq C_{U,V,M} (1 + |\xi|)^m$$

for all  $x \in U$  and all  $\xi \in V$  with  $|\xi| \geq M$ .

We remark that we consider functions  $p \in C^\infty(Y \times X \times \mathbb{R}^N)$  in the following two lemmas. Thus, we obtain in the second lemma estimate (2.1) for all  $\xi \in \mathbb{R}^N$ . Both lemmas are also

valid if the function  $p$  is in  $C^\infty(Y \times X \times \mathbb{R}^N \setminus \{0\})$  and locally integrable for  $(y, x) \in K$  and  $|\xi| \leq 1$  for every compact set  $K \subseteq Y \times X$ . Then, estimate (2.1) is only satisfied for  $(y, x) \in K$  and  $|\xi| \leq 1$  as stated above.

We now consider a special kind of homogeneous functions. In order to prove that these functions are symbols, we need the following lemma.

**2.1 Lemma.** *Let  $p \in C^\infty(Y \times X \times \mathbb{R}^N)$  be positive homogeneous of degree  $l \in \mathbb{Z}$  with respect to the last component, i. e.*

$$p(y, x, \lambda\xi) = \lambda^l p(y, x, \xi)$$

for all  $(y, x, \xi) \in Y \times X \times \mathbb{R}^N$  and  $\lambda > 0$ . Further, let  $\alpha \in \mathbb{N}_0^N$  be a multi-index. Then, the derivative  $D_\xi^\alpha$  is homogeneous of degree  $l - |\alpha|$ .

*Proof.* On the one hand, we have

$$D_\xi^\alpha(p(y, x, \lambda\xi)) = \lambda^{|\alpha|} [D_\xi^\alpha p](y, x, \lambda\xi)$$

for  $(y, x, \xi) \in Y \times X \times \mathbb{R}^N$  and  $\lambda \in \mathbb{R}$ . On the other hand, by the homogeneity of  $p$ , it holds

$$D_\xi^\alpha(p(y, x, \lambda\xi)) = D_\xi^\alpha(\lambda^l p(y, x, \xi)) = \lambda^l D_\xi^\alpha p(y, x, \xi)$$

for  $(y, x, \xi) \in Y \times X \times \mathbb{R}^N$  and  $\lambda > 0$ . Equating both equations yields

$$\lambda^{|\alpha|} [D_\xi^\alpha p](y, x, \lambda\xi) = \lambda^l D_\xi^\alpha p(y, x, \xi)$$

and we conclude

$$[D_\xi^\alpha p](y, x, \lambda\xi) = \lambda^{l-|\alpha|} D_\xi^\alpha p(y, x, \xi)$$

for  $(y, x, \xi) \in Y \times X \times \mathbb{R}^N$  and  $\lambda > 0$ . Hence,  $D_\xi^\alpha p$  is homogeneous of degree  $l - |\alpha|$ .  $\square$

Using this assertion, we are now able to verify that the functions defined in the following lemma are indeed examples of symbols.

**2.2 Lemma.** *Let  $p \in C^\infty(Y \times X \times \mathbb{R}^N)$  be asymptotically positive homogeneous of degree  $l \in \mathbb{Z}$  in the sense that*

$$p(y, x, \lambda\xi) = \lambda^l p(y, x, \xi) \tag{2.2}$$

for all  $(y, x, \xi) \in Y \times X \times \mathbb{R}^N$  with  $|\xi| \geq 1$  and  $\lambda \geq 1$ . Then,  $p$  is a symbol of order  $l$ .

We notice that we obtain estimate (2.1) for all  $\xi \in \mathbb{R}^N$  as the function  $p$  is smooth at zero.

*Proof.* Let  $\alpha \in \mathbb{N}_0^N, \beta \in \mathbb{N}_0^{n_x}$  and  $\gamma \in \mathbb{N}_0^{n_y}$  be multi-indices. First, we consider  $\xi \in \mathbb{R}^N$  with  $|\xi| \geq 1$ . We observe that since  $p$  satisfies (2.2) and the derivatives  $D_x^\beta$  and  $D_y^\gamma$  do not operate on  $\xi$ , identity (2.2) also holds for the function  $D_x^\beta D_y^\gamma p$ . We therefore have

$$D_\xi^\alpha D_x^\beta D_y^\gamma p(y, x, \xi) = [D_\xi^\alpha D_x^\beta D_y^\gamma p](y, x, |\xi| \frac{\xi}{|\xi|}) = |\xi|^{l-|\alpha|} [D_\xi^\alpha D_x^\beta D_y^\gamma p](y, x, \frac{\xi}{|\xi|})$$

for  $(y, x, \xi) \in Y \times X \times \mathbb{R}^N$  with  $|\xi| \geq 1$  by the homogeneity assumption and Lemma 2.1. For  $l - |\alpha| \geq 0$  we have

$$\begin{aligned} |D_\xi^\alpha D_x^\beta D_y^\gamma p(y, x, \xi)| &\leq |\xi|^{l-|\alpha|} \max_{\xi \in \mathbb{R}^N, |\xi| \geq 1} |[D_\xi^\alpha D_x^\beta D_y^\gamma p](y, x, \frac{\xi}{|\xi|})| \\ &= |\xi|^{l-|\alpha|} \max_{\xi \in \mathbb{R}^N, |\xi|=1} |[D_\xi^\alpha D_x^\beta D_y^\gamma p](y, x, \xi)| \\ &\leq (1 + |\xi|)^{l-|\alpha|} \max_{\xi \in \mathbb{R}^N, |\xi|=1} |[D_\xi^\alpha D_x^\beta D_y^\gamma p](y, x, \xi)| \end{aligned}$$

for  $(y, x, \xi) \in Y \times X \times \mathbb{R}^N$  with  $|\xi| \geq 1$ , where the maximum

$$|[D_x^\beta D_y^\gamma p](y, x, \xi^*)| = \max_{\xi \in \mathbb{R}^N, |\xi|=1} |[D_\xi^\alpha D_x^\beta D_y^\gamma p](y, x, \xi)|$$

exists since  $D_\xi^\alpha D_x^\beta D_y^\gamma p$  is continuous and the set  $\{\xi \in \mathbb{R}^N \mid |\xi| = 1\}$  is compact. Further, we take the maximum of  $|[D_x^\beta D_y^\gamma p](\cdot, \cdot, \xi^*)|$  over an arbitrary compact subset  $K \subseteq Y \times X$ . By continuity this exists and so we obtain for every compact set  $K \subseteq Y \times X$  and all multi-indices  $\alpha, \beta, \gamma$  estimate (2.1) for  $(x, y) \in K$  and  $\xi \in \mathbb{R}^N$  with  $|\xi| \geq 1$ .

In case of  $l - |\alpha| < 0$  we observe

$$\begin{aligned} |D_\xi^\alpha D_x^\beta D_y^\gamma p(y, x, \xi)| &\leq |\xi|^{l-|\alpha|} \max_{\xi \in \mathbb{R}^N, |\xi| \geq 1} |[D_\xi^\alpha D_x^\beta D_y^\gamma p](y, x, \frac{\xi}{|\xi|})| \\ &= |\xi|^{l-|\alpha|} \max_{\xi \in \mathbb{R}^N, |\xi|=1} |[D_\xi^\alpha D_x^\beta D_y^\gamma p](y, x, \xi)| \\ &= (1 + |\xi|)^{l-|\alpha|} \left(\frac{|\xi|}{1 + |\xi|}\right)^{l-|\alpha|} \max_{\xi \in \mathbb{R}^N, |\xi|=1} |[D_\xi^\alpha D_x^\beta D_y^\gamma p](y, x, \xi)| \\ &\leq 2^{|\alpha|-l} (1 + |\xi|)^{l-|\alpha|} \max_{\xi \in \mathbb{R}^N, |\xi|=1} |[D_\xi^\alpha D_x^\beta D_y^\gamma p](y, x, \xi)| \end{aligned}$$

for  $(y, x, \xi) \in Y \times X \times \mathbb{R}^N$  with  $|\xi| \geq 1$ , where we used the monotonicity of  $z \mapsto \frac{1+z}{z}$  for  $z \geq 0$ . The appearing maximum exists by the arguments given above. Further, we continue as in case of  $l - |\alpha| \geq 0$  to obtain estimate (2.1).

Second, we consider  $\xi \in \mathbb{R}^N$  with  $|\xi| < 1$ . For  $l - |\alpha| \geq 0$  we have

$$|D_\xi^\alpha D_x^\beta D_y^\gamma p(y, x, \xi)| \leq \max_{|\xi| \leq 1} |D_\xi^\alpha D_x^\beta D_y^\gamma p(y, x, \xi)| \leq (1 + |\xi|)^{l-|\alpha|} \max_{|\xi| \leq 1} |D_\xi^\alpha D_x^\beta D_y^\gamma p(y, x, \xi)|$$

whereas for  $l - |\alpha| < 0$  we observe

$$\begin{aligned} |D_\xi^\alpha D_x^\beta D_y^\gamma p(y, x, \xi)| &\leq \max_{|\xi| \leq 1} |D_\xi^\alpha D_x^\beta D_y^\gamma p(y, x, \xi)| \\ &= (1 + |\xi|)^{-(l-|\alpha|)} (1 + |\xi|)^{l-|\alpha|} \max_{|\xi| \leq 1} |D_\xi^\alpha D_x^\beta D_y^\gamma p(y, x, \xi)| \\ &\leq 2^{|\alpha|-l} (1 + |\xi|)^{l-|\alpha|} \max_{|\xi| \leq 1} |D_\xi^\alpha D_x^\beta D_y^\gamma p(y, x, \xi)| \end{aligned}$$

for  $(x, y, \xi) \in Y \times X \times \mathbb{R}^N$  with  $|\xi| < 1$ . As before, the maximum

$$|D_x^\beta D_y^\gamma p(y, x, \xi_*)| = \max_{|\xi| \leq 1} |D_\xi^\alpha D_x^\beta D_y^\gamma p(y, x, \xi)|$$

exists because  $D_\xi^\alpha D_x^\beta D_y^\gamma p$  is continuous and the set  $\{\xi \in \mathbb{R}^N \mid |\xi| \leq 1\}$  is compact. Again, we consider the maximum of  $|[D_x^\beta D_y^\gamma p](\cdot, \cdot, \xi_*)|$  over an arbitrary compact subset  $K \subseteq Y \times X$ , which exists as  $[D_x^\beta D_y^\gamma p](\cdot, \cdot, \xi_*)$  is continuous. Hence, we find in both cases for every compact set  $K \subseteq Y \times X$  and all multi-indices  $\alpha, \beta, \gamma$  estimate (2.1) for  $(x, y) \in K$  and  $\xi \in \mathbb{R}^N$  satisfying  $|\xi| < 1$  with two different constants.

Finally, we take the maximum of the four constants related to the four considered cases to deduce estimate (2.1) on  $K \times \mathbb{R}^N$  for every compact set  $K \subseteq Y \times X$  and all multi-indices  $\alpha, \beta, \gamma$ .  $\square$

In order to define a Fourier integral operator the following function is essential.

A real valued function  $\phi: Y \times X \times \mathbb{R}^N \setminus \{0\} \rightarrow \mathbb{R}$  is called a *phase function* if

- (i)  $\phi \in C^\infty(Y \times X \times \mathbb{R}^N \setminus \{0\})$  is satisfied,

- (ii)  $\phi$  is positive homogeneous of degree 1 in the last variable, i.e. for  $\lambda > 0$  we have  $\phi(y, x, \lambda\xi) = \lambda\phi(y, x, \xi)$  for all  $(y, x, \xi) \in Y \times X \times \mathbb{R}^N \setminus \{0\}$ , and
- (iii)  $(\nabla_y \phi, \nabla_\xi \phi)$  and  $(\nabla_x \phi, \nabla_\xi \phi)$  do not vanish on  $Y \times X \times \mathbb{R}^N \setminus \{0\}$ .

Moreover, a phase function  $\phi: Y \times X \times \mathbb{R}^N \setminus \{0\} \rightarrow \mathbb{R}$  is called a *non-degenerate phase function* if the rank of the matrix

$$\begin{pmatrix} \partial_\xi \partial_{\xi_1} \phi(y, x, \xi) & \partial_y \partial_{\xi_1} \phi(y, x, \xi) & \partial_x \partial_{\xi_1} \phi(y, x, \xi) \\ \vdots & \vdots & \vdots \\ \partial_\xi \partial_{\xi_N} \phi(y, x, \xi) & \partial_y \partial_{\xi_N} \phi(y, x, \xi) & \partial_x \partial_{\xi_N} \phi(y, x, \xi) \end{pmatrix} \quad (2.3)$$

for  $(y, x, \xi) \in \Sigma_\phi$  is equal to  $N$ , where

$$\Sigma_\phi := \{(y, x, \xi) \in Y \times X \times \mathbb{R}^N \setminus \{0\} \mid \nabla_\xi \phi(y, x, \xi) = 0\}. \quad (2.4)$$

In detail we consider the matrix

$$\begin{pmatrix} \partial_{\xi_1} \partial_{\xi_1} \phi & \dots & \partial_{\xi_N} \partial_{\xi_1} \phi & \partial_{y_1} \partial_{\xi_1} \phi & \dots & \partial_{y_{N_Y}} \partial_{\xi_1} \phi & \partial_{x_1} \partial_{\xi_1} \phi & \dots & \partial_{x_{N_X}} \partial_{\xi_1} \phi \\ \vdots & \vdots \\ \partial_{\xi_1} \partial_{\xi_N} \phi & \dots & \partial_{\xi_N} \partial_{\xi_N} \phi & \partial_{y_1} \partial_{\xi_N} \phi & \dots & \partial_{y_{N_Y}} \partial_{\xi_N} \phi & \partial_{x_1} \partial_{\xi_N} \phi & \dots & \partial_{x_{N_X}} \partial_{\xi_N} \phi \end{pmatrix}$$

on the set  $\Sigma_\phi$ .

Using these two notions of a symbol and a phase function, we now define a Fourier integral operator.

Let  $p \in S^m(Y \times X \times \mathbb{R}^N)$  be a symbol of order  $m$  and  $\phi \in C^\infty(Y \times X \times \mathbb{R}^N \setminus \{0\})$  be a phase function. A *Fourier integral operator of order  $k$*  is an operator  $F$  given by

$$Fu(y) = \int_{\mathbb{R}^N} \int_X p(y, x, \xi) u(x) e^{i\phi(y, x, \xi)} dx d\xi$$

for  $y \in Y$  and  $u \in C_c^\infty(X)$ . This operator  $F$  maps  $C_c^\infty(X)$  continuously into  $C^\infty(Y)$  and extends to a continuous linear map from  $\mathcal{E}'(X)$  into  $\mathcal{D}'(Y)$  (see Theorem VIII.5.1 in [Tre802]).

In case the phase function of a Fourier integral operator is non-degenerate, the order of the operator is given by  $k := m - (\frac{n_X + n_Y}{4} - \frac{N}{2})$ . For this result, we refer to the text following equation (5.3) on page 456 in [Tre802].

The dual operator  $F^*$  of  $F$  is given by

$$F^*v(x) = \int_{\mathbb{R}^N} \int_Y p^*(x, y, \xi) v(y) e^{i\phi^*(x, y, \xi)} dy d\xi$$

for  $v \in C_c^\infty(Y)$  with  $p^*(x, y, \xi) = p(y, x, \xi)$  and  $\phi^*(x, y, \xi) = \phi(y, x, \xi)$  for  $x \in X$ ,  $y \in Y$  and  $\xi \in \mathbb{R}^N \setminus \{0\}$ .

In the following, we consider pseudodifferential operators which are a special kind of Fourier integral operators (see Example 2.3). Since we only regard symbols depending on the two variables  $y$  and  $\xi$  later on, we only consider symbols defined on  $Y \times \mathbb{R}^N$ . In principle, the dependency on three variables is also possible and works analogously.

From now on, we set  $Y = X$  and  $n_X = N$ . Let  $a \in S^m(X \times \mathbb{R}^N)$  be a symbol of order  $m$ . For  $u \in C_c^\infty(X)$  an operator  $P$  of the form

$$Pu(y) = \frac{1}{(2\pi)^N} \int_{\mathbb{R}^N} \int_X a(y, \xi) u(x) e^{i(y-x)\cdot\xi} dx d\xi$$

for  $y \in Y$  is a *pseudodifferential operator of order  $m$* . Such an operator  $P$  maps  $C_c^\infty(X)$  continuously into  $C^\infty(X)$  and extends uniquely to a continuous linear map from  $\mathcal{E}'(X)$  into  $\mathcal{D}'(X)$  (see Theorem 3.2.4 and Corollary 3.3.13 in [Pet83]).

Some properties of pseudodifferential operators are determined by a part of their symbol, the top order symbol. A function  $\sigma(P) \in S^m(X \times \mathbb{R}^N)$  is the *top order symbol of  $P$*  if  $a - \sigma(P) \in S^{m'}(X \times \mathbb{R}^N)$  holds for some  $m' \in \mathbb{Z}$  with  $m' < m$  and  $\sigma(P)$  is positively homogeneous of order  $m$  in the last variable.

A pseudodifferential operator with symbol  $a \in S^{-\infty}(X \times \mathbb{R}^N)$  is termed a *smoothing operator* since it maps from  $\mathcal{E}'(X)$  into  $C^\infty(X)$  (see Lemma 3.3.14 in [Pet83]).

We now take a look at the connection between ellipticity and the symbol of a pseudodifferential operator. A pseudodifferential operator  $P$  is *elliptic* if its symbol is elliptic on  $X \times \mathbb{R}^N$ . Similarly, a pseudodifferential operator is *microlocally elliptic* at a point  $y$  if its symbol is microlocally elliptic at  $(y, \xi)$  with an appropriate  $\xi \in \mathbb{R}^N \setminus \{0\}$ . Moreover, if  $P$  is of order  $m$  adding an element of  $S^{m'}(X \times \mathbb{R}^N)$  with  $m' < m$  to the symbol does not change whether the pseudodifferential operator is microlocally elliptic at a point or not as we will see in the following. Let the symbol  $a \in S^m(X \times \mathbb{R}^N)$  of  $P$  be microlocally elliptic at a point  $(y_0, \xi_0) \in X \times \mathbb{R}^N \setminus \{0\}$ . Then, there exists a neighbourhood  $U \subseteq X$  of  $y_0$ , a conic neighbourhood  $V \subseteq \mathbb{R}^N \setminus \{0\}$  of  $\xi_0$  and constants  $M, C > 0$  such that

$$|a(y, \xi)| \geq C(1 + |\xi|)^m$$

for  $y \in U$  and  $\xi \in V$  with  $|\xi| \geq M$ . Now, we take a symbol  $b \in S^{m'}(X \times \mathbb{R}^N)$  with  $m' < m$ , i.e.

$$|b(y, \xi)| \leq C^*(1 + |\xi|)^{m'}$$

for all  $y \in U$  and  $\xi \in \mathbb{R}^N$ . We have

$$\begin{aligned} |a(y, \xi) + b(y, \xi)| &\geq C(1 + |\xi|)^m - C^*(1 + |\xi|)^{m'} \\ &= C(1 + |\xi|)^m \left(1 - \frac{C^*}{C(1 + |\xi|)^{m-m'}}\right) \\ &\geq C(1 + |\xi|)^m \left(1 - \frac{C^*}{C(1+M)^{m-m'}}\right) \\ &= C \left(1 - \frac{C^*}{C(1+M)^{m-m'}}\right) (1 + |\xi|)^m \end{aligned}$$

for  $y \in U$  and  $\xi \in V$  with  $|\xi| \geq M$ . By choosing  $M^* > M > 0$  large enough the term  $C \left(1 - \frac{C^*}{C(1+M^*)^{m-m'}}\right)$  is strictly positive and so, we have shown that  $a + b$  is microlocally elliptic in  $(y_0, \xi_0)$ . We observe that ellipticity is a property of the top order symbol.

As mentioned before, we verify that pseudodifferential operators are a special kind of Fourier integral operators.

**2.3 Example.** Let  $P$  be a pseudodifferential operator of order  $m$  and the function  $\phi: X \times X \times \mathbb{R}^N \rightarrow \mathbb{R}$  be defined by  $\phi(y, x, \xi) := (y - x) \cdot \xi$ . Then, we have  $\phi \in C^\infty(X \times X \times \mathbb{R}^N)$  and  $\phi(y, x, \lambda\xi) = \lambda\phi(y, x, \xi)$  for  $(y, x, \xi) \in X \times X \times \mathbb{R}^N$  and  $\lambda > 0$ . Moreover, it holds

$$\nabla_y \phi(y, x, \xi) = \xi, \quad \nabla_x \phi(y, x, \xi) = -\xi \quad \text{and} \quad \nabla_\xi \phi(y, x, \xi) = y - x$$

for  $(y, x, \xi) \in X \times X \times \mathbb{R}^N$ . Since the first two derivatives do not vanish for  $(y, x, \xi) \in X \times X \times \mathbb{R}^N \setminus \{0\}$  the terms  $(\nabla_y \phi(y, x, \xi), \nabla_\xi \phi(y, x, \xi)) = (-\xi, y - x)$  and  $(\nabla_x \phi(y, x, \xi), \nabla_\xi \phi(y, x, \xi)) = (\xi, y - x)$  do not vanish on  $X \times X \times \mathbb{R}^N \setminus \{0\}$ . Hence,  $P$  is a Fourier integral operator.

To investigate whether the phase function  $\phi$  is non-degenerate we consider the matrix given in (2.3). In this special case, we calculate

$$\begin{pmatrix} 0 & I & -I \end{pmatrix},$$

where 0 is the zero matrix in  $\mathbb{R}^{N \times N}$  and I the unit matrix in  $\mathbb{R}^{N \times N}$ . This matrix has rank  $N$  and thus  $\phi$  is non-degenerate. As a consequence, the order of  $P$  is  $k = m - (\frac{N+N}{4} - \frac{N}{2}) = m$  by definition. This coincides with the order of  $P$  as pseudodifferential operator.

Linear differential operators are possibly the most popular kind of pseudodifferential operators. We take a closer look at them in the next example.

**2.4 Example.** Let  $d \in \mathbb{N}$  and  $P: C_c^\infty(\mathbb{R}^d) \rightarrow C_c^\infty(\mathbb{R}^d)$  be a linear differential operator of order  $m$ , which means that  $P$  is given by

$$Pu(x) = \sum_{|\alpha| \leq m} a_\alpha(x) D^\alpha u(x)$$

for  $x \in \mathbb{R}^d$  with a multi-index  $\alpha \in \mathbb{N}_0^d$  and functions  $a_\alpha \in C^\infty(\mathbb{R}^d)$ . From the identity

$$(\mathcal{F}(D^\alpha u))(x) = i^{|\alpha|} x^\alpha (\mathcal{F}f)(x)$$

it follows that

$$\begin{aligned} Pu(x) &= \sum_{|\alpha| \leq m} a_\alpha(x) (\mathcal{F}^{-1} \mathcal{F} D^\alpha u)(x) = \sum_{|\alpha| \leq m} a_\alpha(x) \mathcal{F}^{-1} (i^{|\alpha|} \cdot x^\alpha \widehat{u})(x) \\ &= \sum_{|\alpha| \leq m} a_\alpha(x) \frac{1}{(2\pi)^{\frac{d}{2}}} \int_{\mathbb{R}^d} i^{|\alpha|} \xi^\alpha \widehat{u}(\xi) e^{ix \cdot \xi} d\xi \\ &= \frac{1}{(2\pi)^d} \int_{\mathbb{R}^d} \int_{\mathbb{R}^d} \sum_{|\alpha| \leq m} a_\alpha(x) i^{|\alpha|} \xi^\alpha u(y) e^{i(x-y) \cdot \xi} dy d\xi \end{aligned}$$

for  $x \in \mathbb{R}^d$  as the Fourier transform  $\mathcal{F}$  is an isomorphism on  $\mathcal{S}(\mathbb{R}^d)$  and  $C_c^\infty(\mathbb{R}^d) \subsetneq \mathcal{S}(\mathbb{R}^d)$ . Thus,  $P$  is a pseudodifferential operator with symbol  $a(x, \xi) = \sum_{|\alpha| \leq m} a_\alpha(x) i^{|\alpha|} \xi^\alpha$  for  $x, \xi \in \mathbb{R}^d$  from which it can be easily deduced that  $P$  is of order  $m$ .

Further, we calculate the explicit symbols of two differential operators in  $\mathbb{R}^3$  we need later on.

First, we consider the Laplace operator  $\Delta$ . In order to write this operator using multi-indices, we define the set  $A := \{(2, 0, 0), (0, 2, 0), (0, 0, 2)\}$  of multi-indices with length equal to 2. With this set we have  $\Delta u(x) = \sum_{\alpha \in A} D^\alpha u(x) = \partial_{x_1}^2 u(x) + \partial_{x_2}^2 u(x) + \partial_{x_3}^2 u(x)$  for  $u \in \mathcal{S}(\mathbb{R}^3)$ , so the symbol of  $\Delta$  is given by  $a(x, \xi) = i^2(\xi_1^2 + \xi_2^2 + \xi_3^2) = -|\xi|^2$  for  $x, \xi \in \mathbb{R}^3$ . Hence,  $\Delta$  is a pseudodifferential operator of order 2 which is even elliptic as is easy to check.

Besides this, we denote by  $\partial_3$  the derivative in the third space direction, which can be described as  $\partial_3 u(x) = \sum_{\alpha \in B} D^\alpha u(x) = \partial_{x_3} u(x)$  with  $B := \{(0, 0, 1)\}$  for  $u \in \mathcal{S}(\mathbb{R}^3)$ . Thus, the symbol is  $a(x, \xi) = i \xi_3$  for  $x, \xi \in \mathbb{R}^3$  and  $\partial_3$  is a pseudodifferential operator of order 1.

Another example of a pseudodifferential operator is the following one.

**2.5 Example.** We consider the multiplication operator  $M: C_c^\infty(\mathbb{R}^3) \rightarrow C_c^\infty(\mathbb{R}^3)$  defined by  $Mu(x) := x_3^2 u(x)$  for  $x \in \mathbb{R}^3$ . Then, we have

$$\begin{aligned} Mu(x) &= x_3^2 u(x) = x_3^2 \mathcal{F}^{-1} \mathcal{F} u(x) = x_3^2 \mathcal{F}^{-1} \left( x \mapsto \frac{1}{(2\pi)^{\frac{3}{2}}} \int_{\mathbb{R}^3} u(y) e^{-ix \cdot y} dy \right) \\ &= x_3^2 \frac{1}{(2\pi)^3} \int_{\mathbb{R}^3} \int_{\mathbb{R}^3} u(y) e^{i(x-y) \cdot \xi} dy d\xi = \frac{1}{(2\pi)^3} \int_{\mathbb{R}^3} \int_{\mathbb{R}^3} x_3^2 u(y) e^{i(x-y) \cdot \xi} dy d\xi \end{aligned}$$

for  $x \in \mathbb{R}^3$  since the Fourier transform is bijective on  $\mathcal{S}(\mathbb{R}^3)$  and  $C_c^\infty(\mathbb{R}^3) \subsetneq \mathcal{S}(\mathbb{R}^3)$ . Hence, the operator  $M$  is a pseudodifferential operator of order 0 with symbol  $a(x, \xi) = x_3^2$  for  $(x, \xi) \in \mathbb{R}^3 \times \mathbb{R}^3$ .

As we noted before, pseudodifferential operators map  $C_c^\infty(X)$  into  $C^\infty(X)$  and  $\mathcal{E}'(X)$  into  $\mathcal{D}'(X)$ . In general, it is therefore not possible to compose two of them. Nevertheless, with an additional assumption on the first operator the composition is well defined. Before we state this assumption, we need to define another term.

The *support of a pseudodifferential operator*  $P$ , which we denote by  $\text{supp}(P)$ , is the complement of the largest open subset  $U$  of  $X \times X$  such that for all open subsets  $W_1$  and  $W_2$  of  $X$  with  $W_1 \times W_2 \subseteq U$  we have  $Pu = 0$  on  $W_1$  for each  $u \in C_c^\infty(W_2)$ . A pseudodifferential operator  $P$  is *properly supported* if the two projection maps from  $\text{supp}(P)$  onto its first and second component are proper, i.e. the preimage of every compact set in  $X$  under the projection map is compact in  $\text{supp}(P)$ . This is an important property since a properly supported pseudodifferential operator  $P: C_c^\infty(X) \rightarrow C^\infty(X)$  extends uniquely to a continuous linear map from  $C^\infty(X)$  into  $C^\infty(X)$  (see Lemma 3.3.8 in [Pet83]).

For a pseudodifferential operator  $P$  with symbol  $a \in S^m(X \times \mathbb{R}^N)$  there exists a properly supported pseudodifferential operator  $Q$  with symbol  $q \in S^m(X \times \mathbb{R}^N)$  such that the symbol of the operator  $P - Q$  is an element of  $S^{-\infty}(X \times \mathbb{R}^N)$ . In this sense the symbol of a pseudodifferential operator is unique.

With the above introduced property we are able to extend the domain of a pseudodifferential operator once again. If  $P$  is a properly supported pseudodifferential operator,  $P$  maps  $C_c^\infty(X)$  into  $C_c^\infty(X)$  and  $\mathcal{D}'(X)$  into  $\mathcal{D}'(X)$  (see Theorem 3.3.13 in [Pet83]). Moreover, properly supported operators with symbol  $a \in S^{-\infty}(X \times \mathbb{R}^N)$  map  $\mathcal{D}'(X)$  into  $C^\infty(X)$  (see Lemma 3.3.14 in [Pet83]). Hence, these are smoothing operators.

Before we finish this section, we introduce two important sets associated with Fourier integral operators. We have already mentioned the first one in the context of a non-degenerate phase function. Later on, we will see that these sets are important in how a Fourier integral operator maps singularities.

Let  $F$  be a Fourier integral operator. As defined in (2.4), the set  $\Sigma_\phi$  is given by

$$\Sigma_\phi = \{(y, x, \xi) \in Y \times X \times \mathbb{R}^N \setminus \{0\} \mid \nabla_\xi \phi(y, x, \xi) = 0\}.$$

The *canonical relation*  $C \subseteq (Y \times \mathbb{R}^{n_Y} \setminus \{0\}) \times (X \times \mathbb{R}^{n_X} \setminus \{0\})$  is defined by

$$C := \{(y, \nabla_y \phi(y, x, \xi); x, -\nabla_x \phi(y, x, \xi)) \mid (y, x, \xi) \in \Sigma_\phi\}. \quad (2.5)$$

Here,  $C \subseteq (Y \times \mathbb{R}^{n_Y} \setminus \{0\}) \times (X \times \mathbb{R}^{n_X} \setminus \{0\})$  holds as  $\nabla_y \phi(y, x, \xi)$  and  $\nabla_x \phi(y, x, \xi)$  cannot be zero for  $(y, x, \xi) \in \Sigma_\phi$  by the third assumption on a phase function  $\phi$ .

Besides this, we observe that for the canonical relation  $C^\top$  of the dual  $F^*$  it holds

$$C^\top = \{(x, \xi; y, \eta) \mid (y, \eta; x, \xi) \in C\} \quad (2.6)$$

and thus  $C^\top \subseteq (X \times \mathbb{R}^{n_X} \setminus \{0\}) \times (Y \times \mathbb{R}^{n_Y} \setminus \{0\})$ .

In the next example, we explicitly determine these sets for a pseudodifferential operator.

**2.6 Example.** According to Example 2.3, every pseudodifferential operator is a Fourier integral operator with phase function  $\phi(y, x, \xi) = \xi \cdot (y - x)$  for  $(y, x, \xi) \in X \times X \times \mathbb{R}^N$ . Using this observation, we get

$$\Sigma_\phi = \{(y, x, \xi) \in X \times X \times \mathbb{R}^N \setminus \{0\} \mid x - y = 0\}.$$

Consequently, the canonical relation  $C \subseteq (X \times \mathbb{R}^N \setminus \{0\}) \times (X \times \mathbb{R}^N \setminus \{0\})$  is given by

$$C = \{(y, \xi; x, \xi) \mid (y, x, \xi) \in \Sigma_\phi\} = \{(x, \xi; x, \xi) \mid \xi \neq 0\}.$$

For the composition of the canonical relation  $C$  and its transpose or the composition with other sets, the following definitions apply.

**2.7 Definition.** Let the sets  $C \subseteq (Y \times \mathbb{R}^{n_Y} \setminus \{0\}) \times (X \times \mathbb{R}^{n_X} \setminus \{0\})$ ,  $\tilde{C} \subseteq (X \times \mathbb{R}^{n_X} \setminus \{0\}) \times (Y \times \mathbb{R}^{n_Y} \setminus \{0\})$ ,  $A \subseteq X \times \mathbb{R}^{n_X} \setminus \{0\}$  and  $B \subseteq Y \times \mathbb{R}^{n_Y} \setminus \{0\}$  be given. We define the compositions

$$\tilde{C} \circ C := \{(\tilde{x}, \tilde{\xi}; x, \xi) \mid \text{there exists } (y, \eta) \text{ with } (\tilde{x}, \tilde{\xi}; y, \eta) \in \tilde{C} \text{ and } (y, \eta; x, \xi) \in C\},$$

$$C \circ A := \{(y, \eta) \mid \text{there exists } (x, \xi) \in A \text{ with } (y, \eta; x, \xi) \in C\},$$

$$C^\top \circ B := \{(x, \xi) \mid \text{there exists } (y, \eta) \in B \text{ with } (x, \xi; y, \eta) \in C^\top\},$$

which are special cases of compositions of general relations.

As a consequence of the first definition given above, we find

$$C^\top \circ C := \{(x, \xi; x, \xi) \mid \text{there exists } (y, \eta) \text{ with } (y, \eta; x, \xi) \in C\}.$$

In the next lemma, we present different expressions for the last two compositions. For this reason, we introduce the two canonical projections each from the canonical relation onto one of its two two-part components. Let  $\Pi_L: C \rightarrow Y \times \mathbb{R}^{n_Y} \setminus \{0\}$  be the projection onto the first two single components and  $\Pi_R: C \rightarrow X \times \mathbb{R}^{n_X} \setminus \{0\}$  the projection onto the last two single components. The subsequent figure illustrates these relations.

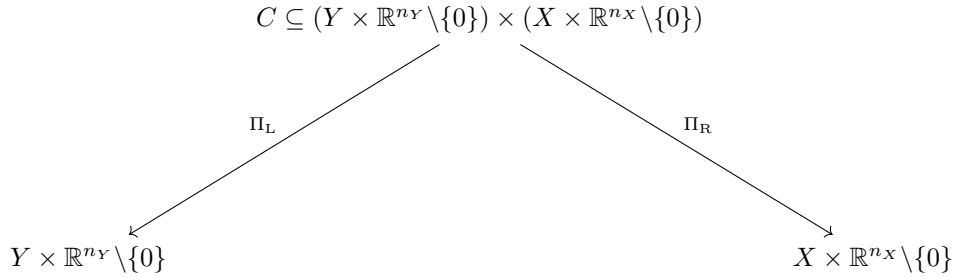


**Figure 2.1:** The two canonical projections of the canonical relation  $C$ .

**2.8 Lemma.** Let  $A \subseteq X \times \mathbb{R}^{n_X} \setminus \{0\}$  and  $B \subseteq Y \times \mathbb{R}^{n_Y} \setminus \{0\}$ . Then,

$$C \circ A = \Pi_L(\Pi_R^{-1}(A)) \quad \text{and} \quad C^\top \circ B = \Pi_R(\Pi_L^{-1}(B)).$$

*Proof.* By the definitions of the two projections  $\Pi_L$  and  $\Pi_R$  (see also Figure 2.1) we obtain

$$\begin{aligned} \Pi_L(\Pi_R^{-1}(A)) &= \Pi_L(\{(y, \eta; x, \xi) \in C \mid (x, \xi) \in A\}) \\ &= \{(y, \eta) \mid \text{there exists } (x, \xi) \in A \text{ with } (y, \eta; x, \xi) \in C\} = C \circ A. \end{aligned}$$

Analogously, we observe

$$\begin{aligned} \Pi_R(\Pi_L^{-1}(B)) &= \Pi_R(\{(y, \eta; x, \xi) \in C \mid (y, \eta) \in B\}) \\ &= \{(x, \xi) \mid \text{there exists } (y, \eta) \in B \text{ with } (y, \eta; x, \xi) \in C\} \\ &= \{(x, \xi) \mid \text{there exists } (y, \eta) \in B \text{ with } (x, \xi; y, \eta) \in C^\top\} = C^\top \circ B, \end{aligned}$$

where we additionally used that  $(y, \eta; x, \xi) \in C$  if and only if  $(x, \xi; y, \eta) \in C^\top$  holds.  $\square$

### 2.1.2. Singularities and their propagation

We start this section with some elementary notions concerning singularities of distributions. First, we consider the singularities given by the points at which a function is not  $C^\infty$ -smooth. We describe the location of these singularities and state a related direction in which the singularities are relevant. For this reason, we consider localised Fourier transforms. Afterwards, we discuss the impact of Fourier integral and pseudodifferential operators on wave front sets which collect all necessary information on the singularities of a distribution.

In a second step we extend this concept to Sobolev spaces. Hence, we consider no longer only points where a distribution is not  $C^\infty$ -smooth but also where it is not locally in a Sobolev space  $H^r$  for  $r \in \mathbb{R}$ . As in the smooth case, we examine the impact on the singularities of a distribution when applying the just introduced operators to it.

In Chapter 3 we show that the operator  $F$  is a Fourier integral operator. Moreover, the composition  $F^*\psi F$  is a pseudodifferential operator, where  $\psi$  is a cut-off function which makes sure that the composition is well defined. At this point, we use the terms we define in this section to investigate the behaviour of the composition concerning singularities.

Now, let  $\Omega \subseteq \mathbb{R}^d$  with  $d \in \mathbb{N}$  be open. For  $u \in \mathcal{D}(\Omega)$  we define the *singular support* of  $u$  by

$$\text{sing supp}(u) := \Omega \setminus \{x \in \Omega \mid u \text{ coincides with a } C^\infty\text{-function in a neighbourhood of } x_0\}.$$

Thus,  $\text{sing supp}(u)$  is the complement in  $\Omega$  of the largest open set in  $\Omega$  on which  $u$  coincides with a  $C^\infty$ -function. In other words, an element  $x_0 \in \Omega$  is not in the singular support  $\text{sing supp}(u)$  of  $u$  if  $u$  is  $C^\infty$ -smooth in a neighbourhood of  $x_0$ .

Further, we are also interested in the directions in which an element of the singular support is not smooth. To describe these directions we introduce a decrease condition for a function. A function  $f: \mathbb{R}^d \rightarrow \mathbb{C}$  is *rapidly decaying at infinity on the cone*  $V \subseteq \mathbb{R}^d$  if for every  $N \in \mathbb{N}_0$  there is a constant  $C_N > 0$  such that

$$|f(x)| \leq C_N(1 + |x|)^{-N} \quad (2.7)$$

for all  $x \in V$ .

The next theorem yields that the Fourier transform of an element in  $\mathcal{E}'(\mathbb{R}^d)$  is smooth. Hence, we are able to evaluate its Fourier transform at a point.

**2.9 Theorem.** *Let  $f$  be in  $\mathcal{E}'(\mathbb{R}^d)$ . Then, we have  $\hat{f} \in C^\infty(\mathbb{R}^d)$  and*

$$\hat{f}(x) = \frac{1}{(2\pi)^{\frac{d}{2}}} \int_{\mathbb{R}^d} e^{-ix \cdot y} f(y) dy$$

for  $x \in \mathbb{R}^d$ .

For a proof of this theorem we refer to Theorem 2.8.1 in [Pet83]. The above condition (2.7) is related to the smoothness of a distribution  $u$  by the following lemma (see Lemma 2.13.1 in [Pet83]).

**2.10 Lemma.** *A distribution  $u \in \mathcal{E}'(\Omega)$  is in  $C_c^\infty(\Omega)$  if and only if its Fourier transform  $\hat{u}$  is rapidly decaying at infinity on  $\mathbb{R}^d$ , i.e. for each  $N \in \mathbb{N}_0$  there exists a constant  $C_N > 0$  such that*

$$|\hat{u}(\xi)| \leq C_N(1 + |\xi|)^{-N} \quad (2.8)$$

for  $\xi \in \mathbb{R}^d$ .

Thus, if  $u$  is not  $C^\infty$ -smooth, there are non-zero frequency directions  $\xi$  such that the Fourier transform  $\widehat{u}$  of  $u$  does not satisfy estimate (2.8) in any conic neighbourhood  $V$  of  $\xi$ .

Next, we are looking for a similar criterion for distributions  $u \in \mathcal{D}'(\Omega)$ . Therefore, we first note that  $\phi u \in \mathcal{E}'(\Omega)$  holds for  $\phi \in C_c^\infty(\Omega)$ . Moreover, we obtain that the Fourier transform of an element in  $\mathcal{E}'(\Omega)$  is smooth in consequence of Theorem 2.9. These considerations yield the subsequent corollary (see Corollary 2.13.2 in [Pet83]).

**2.11 Corollary.** *Let  $u \in \mathcal{D}'(\Omega)$  and  $U \subseteq \Omega$  be an open subset. Then,  $u|_U \in C^\infty(U)$  is satisfied if and only if  $\widehat{\phi u}$  is rapidly decaying at infinity on  $\mathbb{R}^d$  for each  $\phi \in C_c^\infty(U)$ , i.e. for each  $\phi \in C_c^\infty(U)$  and each integer  $N \in \mathbb{N}_0$  there exists a constant  $C_{N,\phi} > 0$  such that*

$$|\widehat{\phi u}(\xi)| \leq C_{N,\phi}(1 + |\xi|)^{-N}$$

for all  $\xi \in \mathbb{R}^d$ .

Hence, the above corollary yields the searched for criterion when a distribution is smooth.

For a relation to the elements of the singular support, the points where a distribution  $u$  is not  $C^\infty$ -smooth, we consider the non-zero directions  $\xi$  where a localised Fourier transform of  $u$  does not satisfy this decrease condition.

**2.12 Definition.** *A distribution  $u \in \mathcal{D}'(\Omega)$  is microlocally  $C^\infty$  at  $(x_0, \xi_0) \in \Omega \times \mathbb{R}^d \setminus \{0\}$  if for some neighbourhood  $U$  of  $x_0$  in  $\Omega$  and some conic neighbourhood  $V$  of  $\xi_0$  in  $\mathbb{R}^d \setminus \{0\}$ , the Fourier transform  $\widehat{\phi u}$  is rapidly decaying on  $V$  for all  $\phi \in C_c^\infty(U)$ .*

According to Theorem 2.13.5 in [Pet83], we are able to restrict the set of functions  $\phi$  in the above definition. By this result it is sufficient that there exists a function  $\phi \in C_c^\infty(\Omega)$  with  $\phi(x_0) \neq 0$  and a neighbourhood  $V$  of  $\xi_0$  in  $\mathbb{R}^d \setminus \{0\}$  such that  $\widehat{\phi u}$  is rapidly decaying on  $V$ .

We are interested in the points where a distribution is not microlocally  $C^\infty$ . Thus, we introduce the set

$$\text{WF}(u) = \{(x, \xi) \in \Omega \times \mathbb{R}^d \setminus \{0\} \mid u \text{ is not microlocally } C^\infty \text{ at } (x, \xi)\}, \quad (2.9)$$

which is called the *wave front set* of  $u$ .

The original definition suggested by Hörmander differs from the one above. Therein, the wave front set is described as an intersection of characteristic sets over a fixed kind of pseudodifferential operators (see page 120 in [Hör71]). There are also some other equivalent definitions which are discussed in [BDH14]. Anyway, [BDH14] is a very detailed written publication worth reading with many examples of wave front sets of special distributions.

In the next lemma, we observe that the first component of  $\text{WF}(u)$  for a distribution  $u$  is just given by its singular support. So, if  $u$  is not microlocally  $C^\infty$  at  $(x_0, \xi_0)$ , the point  $x_0$  is an element of the singular support of  $u$ . With  $\xi_0$  we obtain an associated direction in which it is not smooth. Since the proof of the following lemma in [Pet83] (see Lemma 2.13.3 in [Pet83]) is kept very short in parts, we give a detailed proof at this point.

**2.13 Lemma.** *Let  $u \in \mathcal{D}'(\Omega)$  be a distribution. Then, the following assertions are valid.*

- (a)  $\text{WF}(u)$  is a closed conic set in  $\Omega \times \mathbb{R}^d \setminus \{0\}$ .
- (b)  $\text{WF}(\phi u) \subseteq \text{WF}(u)$  is satisfied for all  $\phi \in C^\infty(\Omega)$ .
- (c)  $\text{sing supp}(u) = \pi(\text{WF}(u))$  holds, where  $\pi$  denotes the projection of  $\Omega \times \mathbb{R}^d \setminus \{0\}$  onto  $\Omega$ .

By part (a) the wave front set is conic in the sense that it is invariant under multiplication of the second variable by non-negative scalars. Thus, we are able to consider the wave front set as a subset of  $\Omega \times S^{d-1}$ .

Before we prove this lemma, we mention another case where the singular support and the wave front set are important. A product of a distribution  $u \in \mathcal{D}'(\Omega)$  with a function  $w \in C^\infty(\Omega)$  is always well defined. However, in general it is not possible to consider the product of two distributions. Here, the wave front set plays an important role. If we have two distributions  $u$  and  $v$  in  $\mathcal{D}'(\Omega)$  such that  $\text{sing supp}(u) \cap \text{sing supp}(v) = \emptyset$ , the product  $uv$  is well defined. This means that at every point, where one of the distributions is not smooth, the other one certainly is as there is no point where none of both is smooth. For a precise explanation we refer to page 55 in [Hör90]. The set of distributions for which such a product is well defined gets larger by additionally considering the directions related to the singular support or, in short, the wave front set. Let  $u$  and  $v$  be again two distributions in  $\mathcal{D}'(\Omega)$ . If there is no point  $(x, \xi) \in \text{WF}(u)$  such that  $(x, -\xi) \in \text{WF}(v)$  holds, the product  $uv$  is well defined. These condition is called Hörmander's condition. It is stated in Theorem 13 in [BDH14] and based on page 267 in [Hör90].

*Proof of Lemma 2.13* (a) By definition, the complement of  $\text{WF}(u)$  is the union of the neighbourhoods  $U \times V$  of  $(x_0, \xi_0)$  from Definition 2.12. Thus,  $\text{WF}(u)$  is closed. Moreover, if  $u$  is microlocally  $C^\infty$  at  $(x_0, \xi_0)$  it follows by definition that  $u$  is microlocally  $C^\infty$  at  $(x_0, \lambda\xi)$  for  $\lambda \geq 0$ . Hence,  $\text{WF}(u)$  is conic.

- (b) Let  $(x_0, \xi_0) \notin \text{WF}(u)$ . Since we have  $|\widehat{\psi\phi u}(\xi)| \leq \|\psi\|_\infty |\widehat{\phi u}(\xi)|$  for  $\xi$  in a neighbourhood  $V$  of  $\xi_0$ , it follows  $(x_0, \xi_0) \notin \text{WF}(\phi u)$ .
- (c) To show the first inclusion, we assume  $x_0 \notin \text{sing supp}(u)$ . By definition there exists a neighbourhood  $U$  of  $x_0$  with  $u|_U \in C^\infty(U)$ . According to Corollary 2.11, it follows that  $\widehat{\phi u}$  is rapidly decreasing on  $\mathbb{R}^d$  for each  $\phi \in C_c^\infty(\Omega)$ , which in turn means that  $u$  is microlocally  $C^\infty$  at  $(x_0, \xi)$  for  $\xi \in \mathbb{R}^d \setminus \{0\}$ . Therefore, we get  $(x_0, \xi) \notin \text{WF}(u)$  for each  $\xi \in \mathbb{R}^d \setminus \{0\}$  and conclude  $x_0 \notin \pi(\text{WF}(u))$ .

For the second inclusion, we assume  $x_0 \notin \pi(\text{WF}(u))$ . By definition this means that for all  $\xi_0 \in \mathbb{R}^d \setminus \{0\}$  there exists a neighbourhood  $U$  of  $x_0$  and a conic neighbourhood  $V$  of  $\xi_0$  such that for each  $\phi \in C_c^\infty(U)$  and each  $N \in \mathbb{N}_0$  there exists a constant  $C_{N,\phi} > 0$  such that

$$|\widehat{\phi u}(\xi)| \leq C_{N,\phi} (1 + |\xi|)^{-N} \quad (2.10)$$

for all  $\xi \in V$ . As we have already observed, the wave front set  $\text{WF}(u)$  is a conic set, i.e. it is sufficient to consider  $\xi \in S^{d-1}$ . Thus, we take all  $\xi_0 \in S^{d-1}$  and obtain a covering of  $S^{d-1}$  which contains the related conic neighbourhoods  $V$ . The compactness of the sphere  $S^{d-1}$  implies the existence of a finite subcovering of neighbourhoods  $V$  of finitely many  $\xi_0 \in S^{d-1}$ . For each of these  $\xi_0$  we have estimate (2.10) with a different constant  $C_{N,\phi} > 0$  on a neighbourhood  $V$  of  $\xi_0$ . By taking the maximum  $C_{N,\phi}^* > 0$  of this finite number of constants we obtain that for all  $\xi \in S^{d-1}$  there exists a neighbourhood  $U$  of  $x_0$  such that for each  $\phi \in C_c^\infty(U)$  and each  $N \in \mathbb{N}_0$  we have

$$|\widehat{\phi u}(\xi)| \leq C_{N,\phi}^* (1 + |\xi|)^{-N}$$

for all  $\xi \in S^{d-1} \setminus \{0\}$ . Since the wave front set is conic, this estimate is valid for all  $\xi \in \mathbb{R}^d \setminus \{0\}$ . Corollary 2.11 thus yields that  $u|_U$  is in  $C^\infty$  for each neighbourhood  $U$  of  $x_0$ . Hence, we obtain  $x_0 \notin \text{sing supp}(u)$ .  $\square$

For an impression of how a wave front set might look like, we determine it in case of some characteristic functions.

**2.14 Example.** (a) We consider the square  $S := [0, 1]^2$  in  $\mathbb{R}^2$ . Further, let  $\chi_S$  be the characteristic function on  $S$ , i. e.

$$\chi_S(x, y) = \begin{cases} 1, & \text{if } (x, y) \in S, \\ 0, & \text{otherwise,} \end{cases}$$

for  $(x, y) \in \mathbb{R}^2$ . Here,  $\chi_S$  coincides with a  $C^\infty$ -function on the interior of the square  $S$  and on the complement of  $S$  in  $\mathbb{R}^2$ . Only where it jumps between the values 0 and 1, the function  $\chi_S$  is not  $C^\infty$  smooth. Thus, the singular support of  $u$  is given by the boundary of  $S$ . The associated directions to a point of the boundary except the four corner points are all non-zero directions perpendicular to the boundary at this point. The four corner points with all non-zero directions are also an element of the wave front set of  $u$ . For a proof we refer to Example 5 in [KQ15]. These results are illustrated in Figure 2.2.

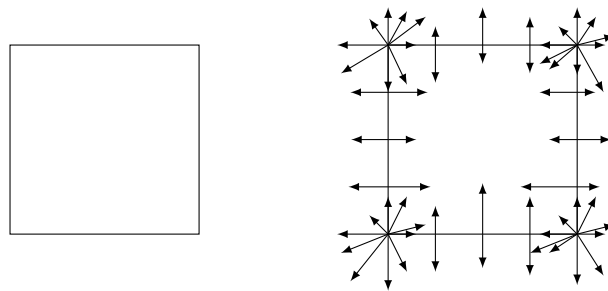


**Figure 2.2:** The singular support and some elements of the wave front set of  $\chi_S$ . We note that the directions are not normalised.

(b) Furthermore, we consider a generalisation of part (a). Let  $\Omega \subseteq \mathbb{R}^d$  with a  $C^\infty$ -boundary. Then

$$\text{WF}(\chi_\Omega) = \{(x, \xi) \in \mathbb{R}^d \times \mathbb{R}^d \setminus \{0\} \mid x \in \partial\Omega, \xi \perp \partial\Omega \text{ at } x\}.$$

This result follows by Example 8.2.5 in [Hör90] and is given in this form as Example 6 in [KQ15] or Proposition 20 in [BDH14].

(c) For  $r > 0$  and  $p \in \mathbb{R}^d$  we consider the characteristic function of  $B_r(p)$  in  $\mathbb{R}^d$ , i.e.

$$\chi_{B_r(p)}(x) = \begin{cases} 1, & \text{if } x \in B_r(p), \\ 0, & \text{otherwise,} \end{cases}$$

for  $x \in \mathbb{R}^d$ . By part (b) the singular support of  $\chi_{B_r(p)}$  is given by  $\partial B_r(p)$  and the associated directions are perpendicular to  $\partial B_r(p)$  at each point of the singular support.

Hence,

$$\text{WF}(\chi_{B_r(p)}) = \{(x, \xi) \in \mathbb{R}^d \times \mathbb{R}^d \setminus \{0\} \mid x \in \partial B_r(p), \xi \perp \partial B_r(p) \text{ at } x\}.$$

An illustration of the singular support and the wave front set is given in Figure 2.3.

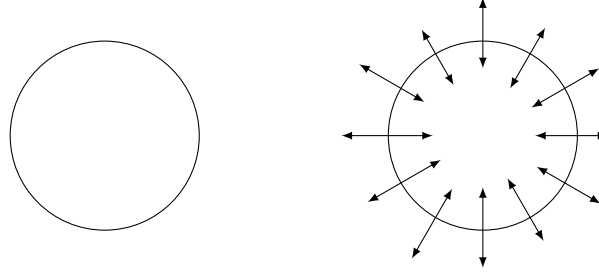


**Figure 2.3:** A cross section of the singular support and parts of the wave front set of  $\chi_{B_r(p)}$ . Again, the directions are not normalised.

The previous example illustrates why characteristic functions are widely used in applications. By choosing an appropriate characteristic function representing an object, the wave front set is its boundary, which to know is sufficient to locate it. In seismic imaging and many other applications in tomography this is exactly what we are interested in.

The next theorem yields a set wherein the wave front set of a pseudodifferential operator is included. In this theorem, the notion of the essential support of a pseudodifferential operator appears. We first establish what the essential support of a symbol is. For a symbol  $a \in S^m(\Omega \times \mathbb{R}^d)$  the *essential support* is defined as the complement of the largest open conic set  $V$  in  $\Omega \times \mathbb{R}^d \setminus \{0\}$  such that  $a|_V \in S^{-\infty}(V)$ . Since the symbol of a pseudodifferential operator is uniquely determined modulo  $S^{-\infty}(\Omega \times \mathbb{R}^d)$ , we define the *essential support of a pseudodifferential operator*  $P$ , abbreviated by  $\text{ess supp}(P)$ , to be the essential support of its symbol. We note that  $P$  is a smoothing operator if and only if the essential support of  $P$  is empty. Moreover, we observe that the essential support of an elliptic pseudodifferential operator is given by the whole domain  $\Omega \times \mathbb{R}^d$  as the symbol of such an operator does not vanish at any point.

**2.15 Theorem.** *Let  $P$  be a pseudodifferential operator of order  $m$  and  $u \in \mathcal{E}'(\Omega)$ . Then,*

$$\text{WF}(Pu) \subseteq \text{WF}(u) \cap \text{ess supp } P.$$

*Furthermore, if  $P$  is properly supported, the inclusion even holds for  $u \in \mathcal{D}'(\Omega)$ .*

For a proof we refer to Theorem 3.8.3 in [Pet83]. Also the next lemma can be found in [Pet83] as Lemma 3.9.4.

**2.16 Lemma.** *Let  $P$  be a pseudodifferential operator of order  $m$  and furthermore microlocally elliptic at a point  $(x_0, \xi_0) \in \Omega \times \mathbb{R}^d \setminus \{0\}$ . Then, there exists a properly supported pseudodifferential operator  $Q$  of order  $-m$  and an open conic neighbourhood  $V$  of  $(x_0, \xi_0)$  such that the operator  $QP - \text{Id}$  is smoothing in  $V$ .*

The operator  $Q$  is a kind of inverse to  $P$  on the conic set  $V$ . Here,  $P$  has to be elliptic as we need the symbol  $a$  of  $P$  to be bounded from below to define the symbol of  $Q$ , in which the reciprocal of  $a$  appears.

**2.17 Theorem** (Pseudolocal property). *If  $P$  is a pseudodifferential operator, it holds*

$$\text{sing supp}(Pu) \subseteq \text{sing supp}(u) \quad \text{and} \quad \text{WF}(Pu) \subseteq \text{WF}(u)$$

for  $u \in \mathcal{E}'(\Omega)$ . If  $P$  is additionally microlocally elliptic at all points  $(x, \xi) \in \Omega \times \mathbb{R}^d$ , we even obtain equality in both cases

$$\text{sing supp}(Pu) = \text{sing supp}(u) \quad \text{and} \quad \text{WF}(Pu) = \text{WF}(u)$$

for  $u \in \mathcal{E}'(\Omega)$ . If  $P$  is properly supported, all assertions hold for  $u \in \mathcal{D}'(\Omega)$ .

*Proof.* The first two assertions follow from Theorem 2.15 as  $\text{WF}(Pu) \cap \text{ess supp } P \subseteq \text{WF}(u)$  is satisfied.

For the proof of the elliptic case let  $(x_0, \xi_0) \notin \text{WF}(Pu)$ . Since  $P$  is microlocally elliptic in  $(x_0, \xi_0)$ , there exists a properly supported pseudodifferential operator  $Q$  of order  $-m$  and an open conic neighbourhood  $V$  of  $(x_0, \xi_0)$  such that  $S := QP - \text{Id}$  is smoothing on  $V$  by Lemma 2.16. Therefore, we find  $u = QPu - Su$  on  $V$ . In the following, we consider the wave front set restricted to the conic neighbourhood  $V$  denoted by  $\text{WF}|_V$ . Since  $S$  is smoothing on  $V$ , we observe  $\text{WF}|_V(Su) = \emptyset$  and according to Theorem 2.15, we obtain

$$\text{WF}|_V(u) \subseteq \text{WF}|_V(QPu) \cup \text{WF}|_V(Su) \subseteq \text{WF}|_V(Pu) \cap \text{ess supp}(Q) \subseteq \text{WF}|_V(Pu)$$

as  $Q$  is of order  $-m$ . Thus, we obtain  $(x_0, \xi_0) \notin \text{WF}(u)$ . Finally, the elliptic case follows with the first two assertions.  $\square$

By the above theorem it follows that

$$\text{WF}(u) \subseteq \text{WF}(Pu) \cup \{(x, \xi) \in \Omega \times \mathbb{R}^d \setminus \{0\} \mid P \text{ is not microlocally elliptic in } (x, \xi)\}$$

for a pseudodifferential operator  $P$  and a distribution  $u \in \mathcal{D}'(\Omega)$ . According to the remarks related to ellipticity, we obtain the equivalent assertion

$$\text{WF}(u) \subseteq \text{WF}(Pu) \cup \{(x, \xi) \in \Omega \times \mathbb{R}^d \setminus \{0\} \mid \sigma(P)(x, \xi) = 0\}.$$

**2.18 Theorem** (Hörmander-Sato Lemma). *Let  $u \in \mathcal{E}'(\Omega)$  and  $P, P_1$  and  $P_2$  be Fourier integral operators with canonical relations  $C, C_1$  and  $C_2$ , respectively. Furthermore, let the composition  $P_1P_2$  be defined on  $\mathcal{E}'(\Omega)$ . Then, we have*

$$\begin{aligned} \text{WF}(Pu) &\subseteq C \circ \text{WF}(u), \\ \text{WF}((P_1P_2)u) &\subseteq (C_1 \circ C_2) \circ \text{WF}(u). \end{aligned}$$

In short, we write

$$\text{WF}(P_1P_2) \subseteq C_1 \circ C_2,$$

which means precisely what is written above for  $u$  in a suitable function space.

The assertions in the theorem above follow by results in [Hör90] and are written in this form in Theorem 15 and Theorem 16 in [KQ15].

Up to now, we considered points where a distribution is not  $C^\infty$ -smooth and their associated directions, which are combined in the wave front set. Now, we expand this concept and look for points where a distribution is locally not in  $H^r$  for some  $r \in \mathbb{R}$ .

For this, we define the  $H^r$ -singular support of  $u$  to be the complement in  $\Omega$  of the largest open subset  $U$  of  $\Omega$  such that  $u|_U \in H_{\text{loc}}^r(U)$  is satisfied. Analogously to the definition of the property to be microlocally  $C^\infty$ , we define the condition for a distribution to be microlocally  $H^r$  at a point. A distribution  $u \in \mathcal{D}'(\Omega)$  is *microlocally  $H^r$*  at  $(x_0, \xi_0) \in \Omega \times \mathbb{R}^d \setminus \{0\}$  if for some neighbourhood  $U$  of  $x_0$  in  $\Omega$  and some conic neighbourhood  $V$  of  $\xi_0$  in  $\mathbb{R}^d \setminus \{0\}$  we have

$$\int_V |\widehat{\phi u}(\xi)|^2 (1 + |\xi|^2)^r \, d\xi < \infty$$

for all  $\phi \in C_c^\infty(U)$ .

Further, we define the  $H^r$ -wave front set of  $u$  for some  $r \in \mathbb{R}$  by

$$\text{WF}^r(u) = \{(x, \xi) \in \Omega \times \mathbb{R}^d \setminus \{0\} \mid u \text{ is not microlocally } H^r \text{ at } (x, \xi)\}.$$

We note that if  $u$  is in  $H_{\text{loc}}^r(\Omega)$ , the  $H^r$ -singular support of  $u$  and hence the  $H^r$ -wave front set are empty.

Analogously, to the  $C^\infty$ -case the first component of the  $H^r$ -wave front set is the  $H^r$ -singular support. For a proof of this assertion, which is formulated in the next theorem, we refer to Theorem 4.6.4 in [Pet83].

**2.19 Theorem.** *Let  $\pi: \Omega \times \mathbb{R}^d \setminus \{0\} \rightarrow \Omega$  be the projection map. If  $u \in \mathcal{D}'(\Omega)$  we have*

$$H^r - \text{sing supp}(u) = \pi(\text{WF}^r(u))$$

for  $r \in \mathbb{R}$ .

For a distribution  $u \in \mathcal{D}'(\Omega)$  the elements that might be in the  $H^r$ -wave front set for some  $r \in \mathbb{R}$  are the elements of the wave front set. Only at the therein contained points  $u$  is not microlocally  $C^\infty$ . Thus, these are just the elements at which it is possible that  $u$  is not microlocally  $H^r$ . Further, we have

$$H_{\text{loc}}^s(\Omega) \subseteq H_{\text{loc}}^r(\Omega)$$

for  $r, s \in \mathbb{R}$  with  $r < s$ . These considerations yield the subsequent corollary.

**2.20 Corollary.** *Let  $u \in \mathcal{D}'(\Omega)$  and  $r, s \in \mathbb{R}$ . If  $r < s$ , we have  $\text{WF}^r(u) \subseteq \text{WF}^s(u) \subseteq \text{WF}(u)$ .*

Next, we are interested in the range of a pseudodifferential operator defined on distributions  $u \in \mathcal{E}'(\Omega)$  lying in  $H^r(\Omega)$  for some  $r \in \mathbb{R}$ . Hence, we define

$$H_c^r(\Omega) := H^r(\Omega) \cap \mathcal{E}'(\Omega)$$

for  $r \in \mathbb{R}$ . The next theorem is Theorem 4.5.12 in [Pet83].

**2.21 Theorem.** *Let  $P$  be a pseudodifferential operator of order  $m$ . Then,  $P$  maps  $H_c^r(\Omega)$  continuously into  $H_{\text{loc}}^{r-m}(\Omega)$ .*

For  $u \in H_c^r(\Omega)$  this theorem yields  $H^{r-m} - \text{sing supp}(Pu) = \emptyset$  and thus  $\text{WF}^{r-m}(Pu) = \emptyset$  for a pseudodifferential operator of order  $m$ . The decomposition of  $u \in \mathcal{D}'(\Omega)$  in the following theorem is shown in the proof of Theorem 4.6.1 in [Pet83]. We need it to show the assertion of Theorem 2.23.

**2.22 Theorem.** *Let  $u \in \mathcal{D}'(\Omega)$  and  $(x, \xi) \in \Omega \times \mathbb{R}^d \setminus \{0\}$ . Then,  $(x, \xi) \notin \text{WF}^r(u)$  if and only if there exist  $u_1 \in H_c^r(\Omega)$  and  $u_2 \in \mathcal{D}'(\Omega)$  in such a way that  $u = u_1 + u_2$  and  $(x, \xi) \notin \text{WF}(u_2)$ .*

The next theorem is very important to determine which  $H^r$ -singularities for  $r \in \mathbb{R}$  are preserved by a pseudodifferential operator  $P$ . Moreover, it tells us how their smoothness changes. Depending on the sign of the order of  $P$ , they get emphasised or deemphasised. Analogously to the smooth case, microlocal ellipticity plays the crucial role.

**2.23 Theorem.** *Let  $P$  be a pseudodifferential operator of order  $m$ . If  $P$  is microlocally elliptic at  $(x_0, \xi_0)$ , we have*

$$(x_0, \xi_0) \in \text{WF}^r(u) \text{ if and only if } (x_0, \xi_0) \in \text{WF}^{r-m}(Pu)$$

for  $u \in \mathcal{E}'(\Omega)$  and  $r \in \mathbb{R}$ .

*Proof.* Before we prove the claimed equivalence, we show

$$\text{WF}^{r-m}(Pu) \subseteq \text{WF}^r(u) \cap \text{ess supp}(P)$$

which is the analogue statement in the  $H^r$ -case to Theorem 2.15 in the smooth case.

For this reason, let  $(x_0, \xi_0) \in \Omega \times \mathbb{R}^d \setminus \{0\}$ . If we have  $(x_0, \xi_0) \notin \text{ess supp}(P)$ , we obtain  $(x_0, \xi_0) \notin \text{WF}(Pu)$  by Theorem 2.15. In particular, we deduce  $(x_0, \xi_0) \notin \text{WF}^{r-m}(Pu)$ .

In order to prove the first implication given in the theorem, let  $(x_0, \xi_0) \notin \text{WF}^r(u)$ . Then, according to Theorem 2.22 there exist  $u_1 \in H_c^r(\Omega)$  and  $u_2 \in \mathcal{D}'(\Omega)$  such that  $u = u_1 + u_2$  and  $(x_0, \xi_0) \notin \text{WF}(u_2)$ . By Theorem 2.15, we obtain  $(x_0, \xi_0) \notin \text{WF}(Pu_2)$  and hence  $(x, \xi) \notin \text{WF}^r(Pu_2)$  by Corollary 2.20. Moreover, we have  $Pu_1 \in H_{\text{loc}}^{r-m}(\Omega)$  according to Theorem 2.21. Hence, we achieve  $(x_0, \xi_0) \notin \text{WF}^{r-m}(Pu_1)$  and thus  $(x_0, \xi_0) \notin \text{WF}^{r-m}(Pu)$ .

Additionally, with the just proven assertion we easily obtain

$$\text{WF}^{r-m}(Pu) \subseteq \text{WF}^r(u)$$

and by this means, the first direction of Theorem 2.23.

We note, that this statement is satisfied for every pseudodifferential operator of order  $m$  independent of ellipticity.

For the proof of the second implication, let  $(x, \xi) \in \text{WF}^r(u)$ . Since  $P$  is microlocally elliptic in  $(x, \xi)$ , there exists by Lemma 2.16 a properly supported pseudodifferential operator  $Q$  of order  $-m$  and an open conic neighbourhood  $V$  of  $(x, \xi)$  such that  $S := QP - \text{Id}$  is smoothing on  $V$ . As a consequence, it holds  $u = QPu - Su$  on  $V$ . In the following, we consider the wave front set restricted to the conic neighbourhood  $V$ , which we denote by  $\text{WF}_{|V}^r$ . As  $S$  is smoothing on  $V$ , we have  $\text{WF}_{|V}^r(Su) = \emptyset$  and according to Theorem 2.15, we obtain

$$\text{WF}_{|V}^r(u) \subseteq \text{WF}_{|V}^r(QPu) \cup \text{WF}_{|V}^r(Su) \subseteq \text{WF}_{|V}^{r-m}(Pu) \cap \text{ess supp}(Q) \subseteq \text{WF}_{|V}^{r-m}(Pu),$$

where we used that  $Q$  is of order  $-m$ . This finishes the proof of the claimed equivalence.  $\square$

As in the smooth case, for a pseudodifferential operator  $P$  and a distribution  $u \in \mathcal{D}'(\Omega)$  we have

$$\begin{aligned} \text{WF}^r(u) &\subseteq \text{WF}^r(Pu) \cup \{(x, \xi) \in \Omega \times \mathbb{R}^d \setminus \{0\} \mid P \text{ is not microlocally elliptic in } (x, \xi)\} \\ &= \text{WF}^r(Pu) \cup \{(x, \xi) \in \Omega \times \mathbb{R}^d \setminus \{0\} \mid \sigma(P)(x, \xi) = 0\}. \end{aligned}$$

for  $r \in \mathbb{R}$ .

We finish this issue by determining the  $H^r$ -wave front set of two characteristic functions.

**2.24 Example.** (a) Let  $\chi_{B_R(p)}$  be the characteristic function of the open ball  $B_R(p)$  for  $R > 0$  and  $p \in \mathbb{R}^3$ . For  $\delta > 0$  we define by  $(\partial B_R(p))_\delta$  the  $\delta$ -tube around  $B_R(p)$  consisting of all points in  $\mathbb{R}^3$  with distance  $\delta$  to the boundary  $\partial B_R(p)$ , i.e.

$$(\partial B_R(p))_\delta := \{x \in \mathbb{R}^3 \mid R - \delta \leq |x - p| \leq R + \delta\}.$$

By Lemma 1.1 in [FR12], the characteristic function  $\chi_{B_R(p)}$  is in  $H^r(\mathbb{R}^3)$  for  $r > 0$  if

$$\int_0^1 |(\partial B_R(p))_\delta| \frac{1}{\delta^{1+2r}} d\delta < \infty$$

is satisfied. We observe

$$|(\partial B_R(p))_\delta| = \frac{4}{3}\pi((R + \delta)^3 - (R - \delta)^3) = 8\pi R^2\delta + \frac{8}{3}\pi\delta^3$$

and deduce

$$\int_0^1 |(\partial B_R(p))_\delta| \frac{1}{\delta^{1+2r}} d\delta = 8\pi R^2 \int_0^1 \frac{1}{\delta^{2r}} d\delta + \frac{8}{3}\pi \int_0^1 \frac{1}{\delta^{2r-2}} d\delta.$$

The integrals on the right-hand side exist if  $2r < 1$  and  $2r - 2 < 1$  holds, so the integral on the left hand side exists if  $r < \frac{1}{2}$  is satisfied. By the lemma mentioned above, we obtain  $\chi_{B_R(p)} \in H^{1/2-\varepsilon}(\mathbb{R}^3)$  for any  $\varepsilon > 0$ .

Further, for the wave front set of  $\chi_{B_R(p)}$  we have

$$\text{WF}(\chi_{B_R(p)}) = \{(x, \xi) \in \mathbb{R}^3 \times \mathbb{R}^3 \setminus \{0\} \mid x \in \partial B_R(p), \xi \perp \partial B_R(p) \text{ at } x\}$$

by Example 2.14 (c). Using the calculations above, we obtain

$$\text{WF}^{1/2+\gamma}(\chi_{B_R(p)}) = \text{WF}(\chi_{B_R(p)})$$

for  $\gamma \geq 0$  since  $\chi_{B_R(p)}$  is not in  $H^{1/2+\gamma}(\mathbb{R}^3)$  for  $\gamma \geq 0$  and

$$\text{WF}^{1/2-\varepsilon}(\chi_{B_R(p)}) = \emptyset$$

for any  $\varepsilon > 0$ , so in the remaining cases of  $r \in \mathbb{R}$  the  $H^r$ -wave front set is empty.

(b) Let  $\chi_{\{x_3 \geq b\}}$  be the characteristic function of the half-space  $\{x \in \mathbb{R}^3 \mid x_3 \geq b\}$  for some  $b > 0$ . We show that  $\chi_{\{x_3 \geq b\}}$  is in  $H_{\text{loc}}^{1/2-\varepsilon}(\mathbb{R}^3)$  for any  $\varepsilon > 0$ . Therefore, let  $\phi \in C_c^\infty(\mathbb{R}^3)$ . Since  $\text{supp}(\phi)$  is compact, there exists a cube  $Q_a$  with length  $a > 0$  such that

$$\text{supp}(\phi\chi_{\{x_3 \geq b\}}) \subseteq Q_a \subsetneq \{x_3 \geq b\}$$

and a function  $f \in C_c^\infty(\mathbb{R}^3)$  with  $\text{supp}(f) = \text{supp}(\phi) \cap \{x \in \mathbb{R}^3 \mid x_3 \geq b\}$  and

$$\phi(x)\chi_{\{x_3 \geq b\}}(x) = f(x)\chi_{Q_a}(x) \tag{2.11}$$

for  $x \in \mathbb{R}^3$ . Now, we show analogously to part (a) that  $\chi_{Q_a}$  is in  $H^{1/2-\varepsilon}(\mathbb{R}^3)$  for any  $\varepsilon > 0$ . Hence, we define the  $\delta$ -tube of  $Q_a$  by  $(\partial Q_a)_\delta = \{x \in \mathbb{R}^3 \mid \text{dist}(x, \partial Q_a) \leq \delta\}$  for  $\delta > 0$ . Further, we have

$$|(\partial Q_a)_\delta| = (a + 2\delta)^3 - (a - 2\delta)^3 = 12a^2\delta + 16\delta^3$$

and thus, we obtain

$$\int_0^1 |(\partial Q_a)_\delta| \frac{1}{\delta^{1+2r}} d\delta = 12a^2 \int_0^1 \frac{1}{\delta^{2r}} d\delta + 16 \int_0^1 \frac{1}{\delta^{2r-2}} d\delta.$$

As in part (a) the integral on the left hand side exists if  $r < \frac{1}{2}$  holds. Again by Lemma 1.1 in [FR12], we conclude that  $\chi_{\{x_3 \geq b\}} \in H^{1/2-\varepsilon}(\mathbb{R}^3)$  for any  $\varepsilon > 0$ . Since  $f$  is contained in  $C_c^\infty(\mathbb{R}^3)$ , the product  $f\chi_{Q_a}$  is also in  $H^{1/2-\varepsilon}(\mathbb{R}^3)$  for any  $\varepsilon > 0$ . By equality (2.11) this finally yields  $\phi\chi_{\{x_3 \geq b\}} \in H^{1/2-\varepsilon}(\mathbb{R}^3)$  and thus,  $\chi_{\{x_3 \geq b\}} \in H_{\text{loc}}^{1/2-\varepsilon}(\mathbb{R}^3)$  for any  $\varepsilon > 0$ .

By Example 2.14 (b) we deduce

$$\text{WF}(\chi_{\{x_3 \geq b\}}) = \{(x, \xi) \in \mathbb{R}^3 \times \mathbb{R}^3 \setminus \{0\} \mid x_3 = b, \xi \perp \{y \in \mathbb{R}^3 \mid y_3 = b\} \text{ at } x\}$$

for the wave front set of  $\chi_{\{x_3 \geq b\}}$ , which is explicitly calculated in the case of the upper half-plane in Section 4.1 in [BDH14]. In addition, we conclude

$$\text{WF}^{1/2+\gamma}(\chi_{\{x_3 \geq b\}}) = \text{WF}(\chi_{\{x_3 \geq b\}})$$

for  $\gamma \geq 0$  using the same arguments as in part (a). Again, the  $H^r$ -wave front set is empty in the remaining cases of  $r \in \mathbb{R}$ , so

$$\text{WF}^{1/2-\varepsilon}(\chi_{\{x_3 \geq b\}}) = \emptyset$$

for any  $\varepsilon > 0$ .

## 2.2. The generalised Radon transform in terms of defining measures

At first glance, the second topic of this chapter has no direct relation to the first one. However, we see later on that the operator  $F$  from (1.12) is both a Fourier integral operator and a generalised Radon transform. Consequently, there is indeed a connection.

In this section, we collect some notions from differential geometry as well as definitions and results of measure theory, which we need to define a generalised Radon transform. For the definition of such a transform we follow the lines of [Quin80].

**2.25 Definition.** *Let  $B, E$  and  $F$  be manifolds. The map  $\pi: E \rightarrow B$  is a fibre map with the fibre  $F$  if  $\pi$  is surjective and locally trivialised with the fibre  $F$ , i.e. for each  $p \in B$  there is an open neighbourhood  $U \subseteq B$  of  $p$  and a homeomorphism  $\varphi: \pi^{-1}(U) \rightarrow U \times F$  in such a way that the following diagram commutes*

$$\begin{array}{ccc} \pi^{-1}(U) & \xrightarrow{\varphi} & U \times F \\ \downarrow \pi & \swarrow \Pi & \\ U & & \end{array}$$

where  $\Pi: U \times F \rightarrow U$  is the natural projection onto the first factor, so we have  $\Pi \circ \varphi = \pi$ . We call  $(E, B, \pi, F)$  a fibre bundle.

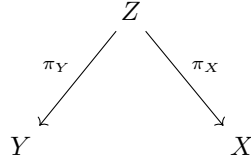
Hence, for each  $p \in B$  the preimage  $\pi^{-1}(\{p\})$  is homeomorphic to  $F$ .

Roughly speaking, this means  $E$  is locally a product space. To illustrate this definition, we take a look at the *trivial bundle*.

**2.26 Example.** Let  $E = B \times F$  and  $\pi: E \rightarrow B$  be the projection onto the first factor. Then,  $(E, B, \pi, F)$  is a fibre bundle, the trivial one.

Next, we formulate the assumption we need to apply one of the central theorems in [Quin80].

**2.27 Assumption.** Let  $X, Y$  be open connected subsets of  $\mathbb{R}^n$ , i.e. connected smooth manifolds of dimension  $n > 0$ , and  $Z$  be a closed submanifold of  $Y \times X$  with codimension  $k > 0$ .



We denote by  $\pi_X$  and  $\pi_Y$  the projections onto  $X$  and  $Y$ , respectively, and assume both to be fibre maps with connected fibres.

In comparison to [Quin80] we do not assume that  $\pi_X$  is proper because this is not true for the projection  $\pi_X$  in our case of application. In [Quin80] this property of  $\pi_X$  is necessary to compose a generalised Radon transform  $R$  with its dual  $R^*$ . To compensate this, we multiply our special Radon transform  $F$  with the cut-off function  $\psi$ , so the composition of  $F^*$  with  $\psi F$  is well defined. This allows us to apply Theorem 2.1 in [Quin80] to  $F^*\psi F$ .

Since  $Z$  is an embedded submanifold of  $Y \times X$ , the inclusion  $f: Z \rightarrow Y \times X$  is smooth. Moreover, the canonical projections  $p_X: Y \times X \rightarrow X$  and  $p_Y: Y \times X \rightarrow Y$  are smooth as  $X$  and  $Y$  are smooth manifolds. Thus, the two projections  $\pi_X = p_X \circ f: Z \rightarrow X$  and  $\pi_Y = p_Y \circ f: Z \rightarrow Y$  are also smooth. We conclude that

$$G(x) := \pi_Y \pi_X^{-1}(x) = \{y \in Y \mid (y, x) \in Z\}$$

for each  $x \in X$  is a closed submanifold of  $Y$  diffeomorphic to the fibre  $\pi_X^{-1}(x)$  with codimension  $k$ . Analogously, for each  $y \in Y$  the set

$$H(y) := \pi_X \pi_Y^{-1}(y) = \{x \in X \mid (y, x) \in Z\}$$

is a closed submanifold of  $X$  diffeomorphic to the fibre  $\pi_Y^{-1}(y)$  with codimension  $k$ . Thus, for each  $x \in X$  we can identify the fibre  $\pi_X^{-1}(x)$  with  $G(x)$  and analogously for each  $y \in Y$  the fibre  $\pi_Y^{-1}(y)$  can be identified with  $H(y)$ .

**2.28 Assumption.** We assume that  $G(x_1) = G(x_2)$  is satisfied if and only if  $x_1 = x_2$  holds and  $H(y_1) = H(y_2)$  if and only if  $y_1 = y_2$  is valid. Hence, each  $x \in X$  corresponds to a unique  $G(x)$  and each  $y \in Y$  to a unique  $H(y)$ .

In contrast to [Quin80], we omit the assumption on  $X$ ,  $Y$  and  $Z$  to be paracompact because, as a consequence of the second axiom of countability and the Hausdorff property, smooth manifolds are always paracompact.

The generalised Radon transform is given by a relation of measures. More precisely, it is defined in terms of push forward measures we define next.

**2.29 Definition.** Let  $(X, \mathcal{A}, \mu)$  be a measure space,  $(Y, \mathcal{B})$  a measurable space and  $f: X \rightarrow Y$  an  $\mathcal{A}$  –  $\mathcal{B}$ -measurable function. Then, there is a measure  $f_*\mu: \mathcal{B} \rightarrow [0, \infty]$  on  $(Y, \mathcal{B})$  defined by

$$B \mapsto \mu \circ f^{-1}(B) = \mu(f^{-1}(B))$$

for  $B \in \mathcal{B}$ . This measure is called the push forward of  $\mu$  with respect to  $f$ .

Further, we observe that a measurable function  $g: Y \rightarrow \overline{\mathbb{R}} := \mathbb{R} \cup \{-\infty, +\infty\}$  is integrable with respect to the push forward measure  $f_*\mu$  if and only if  $g \circ f$  is integrable with respect to  $\mu$ . If this is the case, the two integrals coincide, so we have

$$\int_Y g \, d f_*\mu = \int_X g \circ f \, d\mu.$$

In our case of application, we also want to determine the push forward for measures that not necessarily have non-negative values. Therefore, we introduce the following notions and the corresponding notations.

Let  $(X, \mathcal{A}, \mu)$  be a measure space. For  $h: X \rightarrow [0, \infty]$  measurable we define the measure  $h \odot \mu: \mathcal{A} \rightarrow [0, \infty]$  on  $\mathcal{A}$  by

$$(h \odot \mu)(A) := \int_X h \cdot \chi_A \, d\mu$$

for  $A \in \mathcal{A}$ . Then,  $h \odot \mu$  is a measure on  $X$  with density  $h$  with respect to  $\mu$  (see Satz IV.2.10 in [El11]) and for measurable  $g: X \rightarrow [0, \infty]$  we have

$$\int_X g \, d(h \odot \mu) = \int_X g \cdot h \, d\mu \quad (2.12)$$

(see Satz IV.2.12 in [El11]). Additionally,  $h \odot \mu$  is absolutely continuous with respect to  $\mu$ , i.e. for  $A \in \mathcal{A}$  with  $\mu(A) = 0$  it follows  $(h \odot \mu)(A) = 0$  (see Korollar IV.2.11 in [El11]).

We also consider measures with non-positive densities. These are examples of so called *signed measures*. A signed measure is a measure with values not only in  $[0, \infty]$ , but in  $(-\infty, \infty]$ .

For a function  $h: X \rightarrow \mathbb{R}$  we define the *positive part*  $h^+$  of  $h$  by  $h^+ = \max\{h, 0\}$  and the *negative part*  $h^-$  by  $h^- = \max\{-h, 0\}$ . Using this notation for a density function  $h: X \rightarrow \mathbb{R}$  with respect to the measure  $\mu$ , we get two measures  $h^+ \odot \mu$  and  $h^- \odot \mu$ . If at least one of them is finite, we can write

$$\nu := h \odot \mu = h^+ \odot \mu - h^- \odot \mu \quad (2.13)$$

and hence, we find a representation of  $\nu$  as difference of two measures. If  $h$  is integrable with respect to  $\mu$ , both of these measures are finite.

By means of this composition, we conclude that equality (2.12) holds for such measures  $\nu$  with real valued densities and that these are absolutely continuous with respect to  $\mu$ . Furthermore, we are able to define the push forward for measures with real valued densities. This follows using Definition 2.29 and composition (2.13).

**2.30 Definition.** Let  $(X, \mathcal{A}, \mu)$  be a measure space,  $(Y, \mathcal{B})$  a measurable space and  $f: X \rightarrow Y$  an  $\mathcal{A} - \mathcal{B}$ -measurable function. Additionally, let  $\nu$  be a measure with a real valued density  $h: X \rightarrow \mathbb{R}$  with respect to  $\mu$ , i.e.  $\nu = h \odot \mu$ . Then, there is a measure  $f_*\nu: \mathcal{B} \rightarrow [0, \infty]$  on  $(Y, \mathcal{B})$  defined by

$$B \mapsto \nu \circ f^{-1}(B) = (h^+ \odot \mu)(f^{-1}(B)) - (h^- \odot \mu)(f^{-1}(B))$$

for  $B \in \mathcal{B}$ . This measure is the push forward of  $\nu$  with respect to  $f$ .

Further, a measurable function  $g: Y \rightarrow \mathbb{R}$  is integrable with respect to the push forward measure  $f_*\nu$  if and only if  $g \circ f$  is integrable with respect to  $\nu$ . If this is the case, these two

integrals coincide and it holds

$$\begin{aligned} \int_Y g \, d f_* \nu &= \int_Y g \, d f_*(h^+ \odot \mu) - \int_Y g \, d f_*(h^- \odot \mu) \\ &= \int_X g \circ f \, d(h^+ \odot \mu) - \int_X g \circ f \, d(h^- \odot \mu) = \int_X g \circ f \, d\nu. \end{aligned}$$

In the following example, we show some assertions using the push forward measure and the existence of some integrals with respect to it.

**2.31 Example.** Let  $(X, \mathcal{A}, \mu)$  be a measure space,  $(Y, \mathcal{B})$  a measurable space with  $X \subseteq \mathbb{R}^n$  and  $Y \subseteq \mathbb{R}^m$  for  $m, n > 0$  and a Radon measure  $\mu$ . Further, let  $f: X \rightarrow Y$  be an  $\mathcal{A}$ - $\mathcal{B}$ -measurable function.

- (a) If  $\mu$  additionally has compact support and  $f$  is continuous, the push forward  $f_*\mu$  is also a measure with compact support.

*Proof.* If we show that the inclusion

$$\text{supp}(\mu_*f) \subseteq f(\text{supp}(\mu)) \tag{2.14}$$

is true, we are able to conclude the claimed assertion from the following arguments. Since  $f$  is a continuous function and the measure  $\mu$  has compact support, the set  $f(\text{supp}(\mu))$  is a compact subset of  $Y$ . Furthermore, the support of a measure is a closed set by definition. According to the above inclusion (2.14) the set  $\text{supp}(\mu_*f)$  is a closed subset of a compact set and thus itself compact. It remains to show inclusion (2.14). Therefore, we consider the equivalent assertion  $\text{supp}(f_*\mu)^c \supseteq f(\text{supp}(\mu))^c$ . This in turn is equivalent to the validity of the inclusion

$$\bigcup_{i \in I} \mu(f^{-1}(U_i)) \supseteq f(\text{supp}(\mu))^c,$$

where  $U_i$  for  $i \in I$  are all open subsets of  $Y$  with  $\mu(f^{-1}(U_i)) = 0$  with an index set  $I$ . To show the last claim, let  $U \subseteq f(\text{supp}(\mu))^c$  be open. Then, we have  $U \cap f(\text{supp}(\mu)) = \emptyset$  and further  $f^{-1}(U) \cap \text{supp}(\mu) = \emptyset$  which leads to  $\mu(f^{-1}(U)) = 0$  by the definition of the support of a measure since  $f^{-1}(U)$  is open as  $f$  is continuous. Hence, every open set  $U$  in  $f(\text{supp}(\mu))^c$  is contained in  $\bigcup_{i \in I} U_i$  and the assertion is proved.  $\square$

- (b) Additionally, let  $f$  be proper and  $g \in C_c^\infty(Y)$ . Then, the integral with respect to the push forward  $f_*\mu$  given in Definition 2.29 by

$$\int_Y g(y) \, d f_*\mu(y) = \int_X (g \circ f)(x) \, d\mu(x) = \int_X g(f(x)) \, d\mu(x)$$

exists.

*Proof.* By assumption,  $\text{supp}(g)$  is compact and therefore,  $K := f^{-1}(\text{supp}(g))$  is also compact as  $f$  is proper. Further, the integrand  $g \circ f$  vanishes if  $x \notin K$  and we obtain

$$\int_X g(f(x)) \, d\mu(x) = \int_K g(f(x)) \, d\mu(x).$$

Since  $\mu$  is a Radon measure, the measure of  $K$  is finite (see Folgerungen VIII.1.2 b) in [El11]) and therefore the integral exists, i.e. functions in  $C_c^\infty(Y)$  are integrable with respect to  $f_*\mu$ .  $\square$

- (c) In addition, let  $f$  be proper,  $g \in C_c^\infty(Y)$  and  $\nu$  the measure with continuous density  $l: X \rightarrow \mathbb{R}$  with respect to  $\mu$ , i.e.  $\nu = (f \circ h) \odot \mu$ . Then, we achieve

$$\int_Y g(y) \, df_*(l \odot \mu)(y) = \int_X (g \circ f)(x) \, d(l \odot \mu)(x) = \int_X g(f(x))l(x) \, d\mu(x)$$

according to Definition 2.30. Since the density  $l$  is continuous, the existence of the last integral follows analogously to part (b).

- (d) Further, let the measurable space  $(Z, \mathcal{C})$  be given and  $f$  be proper. Moreover, let  $k: X \rightarrow Z$  be continuous,  $l \in C_c^\infty(Y)$  and  $g \in C^\infty(Z)$ . Then, the integral

$$\int_Z g(z) \, dk_*((l \circ f) \odot \mu)(z)$$

exists.

*Proof.* By Definition 2.30, we obtain

$$\int_Z g(z) \, dk_*((l \circ f) \odot \mu)(z) = \int_X (g \circ k)(x) \, d((l \circ f) \odot \mu)(x) = \int_X g(k(x))l(f(x)) \, d\mu(x).$$

Moreover, the set  $K := f^{-1}(\text{supp}(l))$  is compact since  $\text{supp}(l)$  is compact and  $f$  is proper. Using this and the fact that  $g \circ k$  is continuous, we argue as in part (b) to show the existence of the integral.  $\square$

The subsequent definition follows [Quin80] with the difference that in our case we do not assume  $\pi_X$  to be proper but  $\pi_Y$ . As the definitions for the generalised Radon transform and its dual are analogue to each other, we interchange the mapping properties of both in the following.

But before we formulate the definition of the generalised Radon transform, we recall that a measure  $\mu$  on a manifold is smooth if  $\mu$  is absolutely continuous with respect to the Lebesgue measure and the associated density is a smooth function on each chart of the manifold.

**2.32 Definition.** *Let Assumption 2.27 and Assumption 2.28 be satisfied and  $\mu, \nu_X$  and  $\nu_Y$  be smooth Radon measures with associated positive nowhere zero densities given on  $Z, X$  and  $Y$ , respectively. Additionally, let  $\pi_Y$  be proper.*

*The generalised Radon transform  $R: C^\infty(X) \rightarrow C^\infty(Y)$  is defined by the relation*

$$Rf \odot \nu_Y = \pi_{Y*}((f \circ \pi_X) \odot \mu)$$

for  $f \in C^\infty(X)$ .

We observe that due to the non-vanishing assumption in Definition 2.32 the measures  $\mu, \nu_X$  and  $\nu_Y$  have compact support if and only if the associated spaces are compact.

By assumption,  $f \circ \pi_X$  is continuous and  $\pi_Y$  proper. According to Example 2.31 (c), the push forward of  $(f \circ \pi_X) \odot \mu$  with respect to  $\pi_Y$  is defined and we have

$$\begin{aligned} \int_Y g(y) \, d(Rf \odot \nu_Y)(y) &= \int_Y g(y) \, d\pi_{Y*}((f \circ \pi_X) \odot \mu)(y) \\ &= \int_Z (g \circ \pi_Y)(z) \, d((f \circ \pi_X) \odot \mu)(z), \end{aligned}$$

where all integrals exist.

In addition,  $f \circ \pi_X$  is smooth and so  $(f \circ \pi_X) \odot \mu$  is a smooth measure. As  $\pi_Y$  is a proper fibre map the measure  $\pi_{Y*}((f \circ \pi_X) \odot \mu)$  is again smooth (see page 333 in [Quin80]). Thus, also  $Rf \odot \nu_Y$  is smooth and with the smoothness of  $\nu_Y$  we conclude the density  $Rf$  to be smooth.

For the dual Radon transform we formally calculate

$$\begin{aligned} \int_Y g(y) d(Rf \odot \nu_Y)(y) &= \int_Y g(y) d\pi_{Y*}((f \circ \pi_X) \odot \mu)(y) \\ &= \int_Z (g \circ \pi_Y)(z) d((f \circ \pi_X) \odot \mu)(z) = \int_Z (f \circ \pi_X)(z) d((g \circ \pi_Y) \odot \mu)(z) \\ &= \int_X f(x) d\pi_{X*}((g \circ \pi_Y) \odot \mu)(x) \end{aligned}$$

for  $f \in C^\infty(X)$  and  $g \in C_c^\infty(Y)$ .

The last calculation motivates the following definition of the dual generalised Radon transform.

**2.33 Definition.** *Let the assumptions of Definition 2.32 be satisfied. We define the dual generalised Radon transform  $R^* : C_c^\infty(Y) \rightarrow C_c^\infty(X)$  to the Radon transform  $R$  by*

$$R^*g \odot \nu_X = \pi_{X*}((g \circ \pi_Y) \odot \mu)$$

for  $g \in C_c^\infty(Y)$ .

The composition  $f \circ \pi_X$  is continuous and  $\pi_Y$  proper. By Example 2.31 (d), we obtain

$$\begin{aligned} \int_X f(x) d(R^*g \odot \nu_X)(x) &= \int_X f(x) d\pi_{X*}((g \circ \pi_Y) \odot \mu)(x) \\ &= \int_X (f \circ \pi_X)(z) d((g \circ \pi_Y) \odot \mu)(z) \end{aligned}$$

and the existence of these integrals. In addition,  $(g \circ \pi_Y) \odot \mu$  is a measure of compact support because  $\pi_Y$  is proper. By part (a) of Example 2.31 and the continuity of  $\pi_X$ , the push forward  $\pi_{X*}((g \circ \pi_Y) \odot \mu)$  is a measure of compact support. Thus, the equation defining  $R^*$  yields that  $R^*g \odot \nu_X$  is also a measure of compact support. Since  $\nu_X$  has compact support if and only if  $X$  is compact (see also the text after Definition 2.32), the support of  $\nu_X$  is not compact in general. Hence, the density  $R^*g$  has compact support.

Moreover,  $(g \circ \pi_Y) \odot \mu$  is not only of compact support but also smooth because  $g \circ \pi_Y$  is smooth. Since  $\pi_X$  is a fibre map, the measure  $\pi_{X*}((g \circ \pi_Y) \odot \mu)$  is smooth according to the assertion on page 333 in [Quin80]. Thus,  $R^*g \odot \nu_X$  is a smooth measure and  $R^*g$  therefore a smooth density as  $\nu_X$  is smooth.

---

## Theoretical results concerning the operator $F$

---

Chapter 3 contains all theoretical considerations related to the operator  $F$ . First, we show that  $F$  and its dual operator are generalised Radon transforms. For further investigations we deduce their representations as Fourier integral operators.

Afterwards we compose these two operators which is possible since we introduce a cut-off function  $\psi$ . Then, we analyse the normal operator  $F^*\psi F$ , show that  $F^*\psi F$  is a pseudodifferential operator and define the reconstruction operator  $\Lambda$  based on  $F^*\psi F$ .

In a further step, we calculate the top order symbol of  $\Lambda$  and analyse its behaviour depending on the offset  $\alpha$ . Finally, we introduce modified reconstruction operators in order to obtain reconstructions independent of  $\alpha$  and the distance to the surface.

### 3.1. The operator $F$ – A generalised Radon transform

In this section, we verify that the operator  $F$  is a generalised Radon transform in terms of defining measures as described in Section 2.2. In order to prove this, we have to confirm a few assumptions.

Before we introduce the setting relevant for our case of application, we show two lemmas we apply on the following pages a few times. The first one states two equivalent representations of an open half-ellipsoid.

We recall the set  $S_0$  which is an open, bounded and connected subset in  $\mathbb{R}^2$ .

**3.1 Lemma.** *Let  $(s, t, x) \in S_0 \times (2\alpha, \infty) \times \mathbb{R}_+^3$ . Then, the equation*

$$\frac{(x_1 - s_1)^2}{\frac{1}{4}t^2 - \alpha^2} + \frac{(x_2 - s_2)^2}{\frac{1}{4}t^2} + \frac{x_3^2}{\frac{1}{4}t^2 - \alpha^2} = 1$$

is equivalent to

$$\varphi(s, x) = |\mathbf{x}_s(s) - x| + |x - \mathbf{x}_r(s)| = t.$$

Further, for fixed  $(s, t) \in S_0 \times (2\alpha, \infty)$  we have

$$\{x \in \mathbb{R}_+^3 \mid \varphi(s, x) = t\} = \left\{x \in \mathbb{R}_+^3 \mid \frac{4(x_1 - s_1)^2}{t^2 - 4\alpha^2} + \frac{4(x_2 - s_2)^2}{t^2} + \frac{4x_3^2}{t^2 - 4\alpha^2} = 1\right\}.$$

So, this set yields an open half-ellipsoid with major half-axis  $\frac{1}{2}t$  in  $x_2$ -direction and minor half-axes  $\sqrt{\frac{1}{4}t^2 - \alpha^2}$  in  $x_1$ - and  $x_3$ -direction.

*Proof.* First, we rearrange  $\varphi(s, x) = |\mathbf{x}_s(s) - x| + |x - \mathbf{x}_r(s)| = t$  to

$$\sqrt{(s_1 - x_1)^2 + (s_2 - \alpha - x_2)^2 + x_3^2} = t - \sqrt{(x_1 - s_1)^2 + (x_2 - s_2 - \alpha)^2 + x_3^2}.$$

As both sides are positive, we obtain after squaring the equivalent representation

$$(s_2 - \alpha - x_2)^2 = t^2 - 2t\sqrt{(x_1 - s_1)^2 + (x_2 - s_2 - \alpha)^2 + x_3^2} + (x_2 - s_2 - \alpha)^2.$$

Then, we reorganise these terms such that just the square root remains on the left hand-side

$$2t\sqrt{(x_1 - s_1)^2 + (x_2 - s_2 - \alpha)^2 + x_3^2} = t^2 + 4\alpha(s_2 - x_2).$$

Further, we have  $s_2 - \frac{t}{2} < x_2 < s_2 + \frac{t}{2}$  for all  $x_2 \in \mathbb{R}$  using that  $t$  is the travel time. Thus, we obtain

$$t^2 + 4\alpha(s_2 - x_2) > t^2 - 2\alpha t = t(t - 2\alpha) > 0$$

since we consider  $t > 2\alpha$ . This yields that again both sides are positive. By squaring both we obtain the equivalent formulation

$$4(x_1 - s_1)^2 + (4 - \frac{16}{t^2}\alpha^2)(x_2 - s_2)^2 + 4x_3^2 = t^2 - 4\alpha^2.$$

After reformulation we deduce

$$\frac{4(x_1 - s_1)^2}{t^2 - 4\alpha^2} + \frac{4(x_2 - s_2)^2}{t^2} + \frac{4x_3^2}{t^2 - 4\alpha^2} = 1$$

or equivalently

$$\frac{(x_1 - s_1)^2}{\frac{1}{4}t^2 - \alpha^2} + \frac{(x_2 - s_2)^2}{\frac{1}{4}t^2} + \frac{x_3^2}{\frac{1}{4}t^2 - \alpha^2} = 1$$

where we simply read off the three half-axes.  $\square$

We consider  $\varphi(s, z)$ ,  $\partial_{z_1}\varphi(s, z)$  and  $\partial_{z_2}\varphi(s, z)$  for fixed  $s \in S_0$  and two different values for  $z \in \mathbb{R}_+^3$ . These three identities determine the value of  $z \in \mathbb{R}_+^3$  uniquely as we show in the following lemma. Later on, we take this valuable statement a few times into account. An analogue result for the two-dimensional case in the full space is shown in [KLQ12].

**3.2 Lemma.** *Let  $s \in S_0$  be fixed. For all  $x, y \in \mathbb{R}_+^3$  which satisfy the following equations*

$$|\mathbf{x}_s(s) - x| + |x - \mathbf{x}_r(s)| = |\mathbf{x}_s(s) - y| + |y - \mathbf{x}_r(s)|, \quad (3.1)$$

$$\frac{x_1 - s_1}{|\mathbf{x}_s(s) - x|} + \frac{x_1 - s_1}{|x - \mathbf{x}_r(s)|} = \frac{y_1 - s_1}{|\mathbf{x}_s(s) - y|} + \frac{y_1 - s_1}{|y - \mathbf{x}_r(s)|}, \quad (3.2)$$

$$\frac{x_2 - (s_2 - \alpha)}{|\mathbf{x}_s(s) - x|} + \frac{x_2 - (s_2 + \alpha)}{|x - \mathbf{x}_r(s)|} = \frac{y_2 - (s_2 - \alpha)}{|\mathbf{x}_s(s) - y|} + \frac{y_2 - (s_2 + \alpha)}{|y - \mathbf{x}_r(s)|} \quad (3.3)$$

we have necessarily  $x = y$ .

If we consider  $x, y$  in the full space  $\mathbb{R}^3$  the result of the lemma above changes to  $x_1 = y_1$ ,  $x_2 = y_2$  and  $x_3 = \pm y_3$ . For more details regarding this circumstance, we refer to Remark 3.3.

*Proof.* For the proof we shift the coordinates of  $x$  and  $y$  to prolate spheroidal coordinates which we introduced in Subsection 1.2.1 and which are explicitly given in (1.15). As a consequence, we have

$$\begin{aligned} x_1 &= s_1 + \sqrt{\frac{1}{4}t^2 - \alpha^2} \sin(\phi) \cos(\theta), \\ x_2 &= s_2 + \frac{1}{2}t \cos(\phi), \\ x_3 &= \sqrt{\frac{1}{4}t^2 - \alpha^2} \sin(\phi) \sin(\theta) \end{aligned}$$

for  $\phi \in (0, \pi)$ ,  $\theta \in (0, \pi)$  and  $t \in (2\alpha, \infty)$  since  $x_3 > 0$  holds. Analogously, let  $y$  be given by

$$\begin{aligned} y_1 &= s_1 + \sqrt{\frac{1}{4}(t')^2 - \alpha^2 \sin(\phi') \cos(\theta')}, \\ y_2 &= s_2 + \frac{1}{2}t' \cos(\phi'), \\ y_3 &= \sqrt{\frac{1}{4}(t')^2 - \alpha^2 \sin(\phi') \sin(\theta')} \end{aligned}$$

for  $\phi' \in (0, \pi)$ ,  $\theta' \in (0, \pi)$  and  $t' \in (2\alpha, \infty)$ .

First, we consider condition (3.1). We calculate

$$\begin{aligned} |\mathbf{x}_s(s) - x| &= \sqrt{(s_1 - x_1)^2 + (s_2 - \alpha - x_2)^2 + x_3^2} \\ &= \sqrt{(\frac{1}{4}t^2 - \alpha^2) \sin^2(\phi) \cos^2(\theta) + (-\alpha - \frac{1}{2}t \cos(\phi))^2 + (\frac{1}{4}t^2 - \alpha^2) \sin^2(\phi) \sin^2(\theta)} \\ &= \sqrt{(\frac{1}{4}t^2 - \alpha^2) \sin^2(\phi) + \alpha^2 + \alpha t \cos(\phi) + \frac{1}{4}t^2 \cos^2(\phi)} \\ &= \sqrt{\frac{1}{4}t^2 + \alpha^2 \cos^2(\phi) + \alpha t \cos(\phi)} = \sqrt{(\frac{1}{2}t + \alpha \cos(\phi))^2} = \frac{1}{2}t + \alpha \cos(\phi) \end{aligned}$$

and analogously

$$|x - \mathbf{x}_r(s)| = \sqrt{(\frac{1}{2}t - \alpha \cos(\phi))^2} = \frac{1}{2}t - \alpha \cos(\phi)$$

using that  $t > 2\alpha$  is satisfied. Hence, equation (3.1) is equivalent to

$$\frac{1}{2}t + \alpha \cos(\phi) + \frac{1}{2}t - \alpha \cos(\phi) = \frac{1}{2}t' + \alpha \cos(\phi') + \frac{1}{2}t' - \alpha \cos(\phi')$$

which yields  $t = t'$ . Inserting this in the last equation (3.3), we deduce

$$\frac{\frac{1}{2}t \cos(\phi) + \alpha}{\frac{1}{2}t + \alpha \cos(\phi)} + \frac{\frac{1}{2}t \cos(\phi) - \alpha}{\frac{1}{2}t - \alpha \cos(\phi)} = \frac{\frac{1}{2}t \cos(\phi') + \alpha}{\frac{1}{2}t + \alpha \cos(\phi')} + \frac{\frac{1}{2}t \cos(\phi') - \alpha}{\frac{1}{2}t - \alpha \cos(\phi')}$$

and obtain the equivalent equation

$$\frac{\cos(\phi)}{\frac{1}{4}t^2 - \alpha^2 \cos^2(\phi)} = \frac{\cos(\phi')}{\frac{1}{4}t^2 - \alpha^2 \cos^2(\phi')}. \quad (3.4)$$

Now, if the function given by  $\cos(\phi) \mapsto \frac{\cos(\phi)}{\frac{1}{4}t^2 - \alpha^2 \cos^2(\phi)}$  is injective, equation (3.4) yields  $\cos(\phi) = \cos(\phi')$ . Hence, in order to show injectivity we define

$$z := \frac{\cos(\phi)}{\frac{1}{4}t^2 - \alpha^2 \cos^2(\phi)}$$

which yields  $\alpha^2 z \cos^2(\phi) + \cos(\phi) - z \frac{1}{4}t^2 = 0$  and further  $\cos(\phi) = \frac{-1 \pm \sqrt{1 + \alpha^2 z^2 t^2}}{2\alpha^2 z}$ .

First, we assume that  $z = \frac{\cos(\phi)}{\frac{1}{4}t^2 - \alpha^2 \cos^2(\phi)} > 0$  holds. Since  $t > 2\alpha$  is satisfied by assumption, for the denominator  $\frac{1}{4}t^2 - \alpha^2 \cos^2(\phi) > 0$  holds. It follows  $\cos(\phi) > 0$  and so  $\cos(\phi) = \frac{-1 + \sqrt{1 + \alpha^2 z^2 t^2}}{2\alpha^2 z}$  is valid. In case  $z = \frac{\cos(\phi)}{\frac{1}{4}t^2 - \alpha^2 \cos^2(\phi)} < 0$  is satisfied, we have  $\cos(\phi) < 0$

and hence  $\cos(\phi) = \frac{-1 - \sqrt{1 + \alpha^2 z^2 t^2}}{2\alpha^2 z}$ . Thus,  $\cos(\phi)$  is uniquely determined by the value of  $\frac{\cos(\phi)}{\frac{1}{4}t^2 - \alpha^2 \cos^2(\phi)}$ . According to equation (3.4), we conclude  $\cos(\phi) = \cos(\phi')$ . Since we have  $\phi, \phi' \in (0, \pi)$  by assumption and  $\cos$  is bijective on  $(0, \pi)$ , it follows  $\phi = \phi'$  and thus  $x_2 = y_2$ .

Last, we consider the second equation (3.2) and insert both obtained conditions  $t = t'$  and  $\phi = \phi'$ . This yields

$$\frac{\cos(\theta)}{\frac{1}{2}t + \alpha \cos(\phi)} + \frac{\cos(\theta)}{\frac{1}{2}t - \alpha \cos(\phi)} = \frac{\cos(\theta')}{\frac{1}{2}t + \alpha \cos(\phi)} + \frac{\cos(\theta')}{\frac{1}{2}t - \alpha \cos(\phi)} \quad (3.5)$$

since  $\sqrt{\frac{1}{4}t^2 - \alpha^2 \sin(\phi)} > 0$  holds as  $t > 2\alpha$  and  $\phi > 0$  are satisfied by assumption. Further, (3.5) is equivalent to  $\cos(\theta) = \cos(\theta')$ . Again using that  $\cos$  is bijective on  $(0, \pi)$ , we end up with  $\theta = \theta'$ . Altogether, we showed  $x_1 = y_1$ ,  $x_2 = y_2$  and  $x_3 = y_3$ .  $\square$

**3.3 Remark.** If we consider the full space  $\mathbb{R}^3$ , we get the conditions  $t, t' > 2\alpha$ ,  $\phi, \phi' \in [0, \pi)$  and  $\theta, \theta' \in [0, 2\pi)$  after the shift of coordinates. As before, we obtain  $t = t'$  and  $\phi = \phi'$ . However, from the last equation we get  $\cos(\theta) = \cos(\theta')$  and consider then the two cases  $\theta = \theta'$  and  $\theta = -\theta'$ . In the first case, we get  $\sin(\theta) = \sin(\theta')$  and so  $x_1 = y_1$ ,  $x_2 = y_2$  and  $x_3 = y_3$ . Considering the second case we have  $\sin(\theta) = -\sin(\theta')$  which yields  $x_1 = y_1$ ,  $x_2 = y_2$  and  $x_3 = -y_3$ . Hence, we also obtain the mirror point  $(x_1, x_2, -x_3)^\top$  of  $(x_1, x_2, x_3)^\top$ .

Next, we present the setting we assume to show that  $F$  is a generalised Radon transform. The considered setting has to satisfy the assumptions stated in Assumption 2.27.

**3.4 Setting.** We set  $X = \mathbb{R}_+^3$  and  $Y = S_0 \times (2\alpha, \infty)$ . Both are open and connected subsets of  $\mathbb{R}^3$  and consequently connected and smooth manifolds of dimension 3. Further, let

$$Z = \{(s, t, x) \in S_0 \times (2\alpha, \infty) \times \mathbb{R}_+^3 \mid \varphi(s, x) = t\}.$$

Since

$$\nabla_x \varphi(s, x) = \left( \frac{x_1 - s_1}{|\mathbf{x}_s(s) - x|} + \frac{x_1 - s_1}{|x - \mathbf{x}_r(s)|}, \frac{x_2 - s_2 + \alpha}{|\mathbf{x}_s(s) - x|} + \frac{x_2 - s_2 - \alpha}{|x - \mathbf{x}_r(s)|}, \frac{x_3}{|\mathbf{x}_s(s) - x|} + \frac{x_3}{|x - \mathbf{x}_r(s)|} \right)^\top$$

does not vanish as  $x_3 > 0$  holds, the gradient  $\nabla_{(s,t,x)}(\varphi(s, x) - t)$  is nowhere zero. This yields that  $Z$  is a submanifold of  $X \times Y$  with codimension 1 as a level set of the function  $\Phi(s, t, x) = t - \varphi(s, x)$  for  $(s, t, x) \in S_0 \times (2\alpha, \infty) \times \mathbb{R}_+^3$ . Moreover,  $Z$  is closed as  $\varphi$  is continuous.

In the following, we consider  $\pi_{S_0 \times (2\alpha, \infty)}: Z \rightarrow S_0 \times (2\alpha, \infty)$  and  $\pi_{\mathbb{R}_+^3}: Z \rightarrow \mathbb{R}_+^3$  which are the projections onto the first respectively the second factor of  $Z$ .

$$\begin{array}{ccc} & Z = \{(s, t, x) \in S_0 \times (2\alpha, \infty) \times \mathbb{R}_+^3 \mid \varphi(s, x) = t\} & \\ \swarrow \pi_{S_0 \times (2\alpha, \infty)} & & \searrow \pi_{\mathbb{R}_+^3} \\ S_0 \times (2\alpha, \infty) & & \mathbb{R}_+^3 \end{array}$$

Before we define the generalised Radon transform associated with Setting 3.4, we have to verify that the projections  $\pi_{S_0 \times (2\alpha, \infty)}$  and  $\pi_{\mathbb{R}_+^3}$  are fibre maps. Therefore, we need an auxiliary function  $\zeta$ , which we consider in the subsequent lemma.

**3.5 Lemma.** We define  $\zeta: S_0 \times (2\alpha, \infty) \times \mathbb{R}^2 \rightarrow \mathbb{R}_+ \cup \{0\}$  by

$$\zeta(s, t, x_1, x_2) := \begin{cases} x_3, & \text{if } \frac{4(x_1 - s_1)^2}{t^2 - 4\alpha^2} + \frac{4(x_2 - s_2)^2}{t^2} < 1, \\ 0, & \text{if } \frac{4(x_1 - s_1)^2}{t^2 - 4\alpha^2} + \frac{4(x_2 - s_2)^2}{t^2} \geq 1, \end{cases}$$

where  $x_3$  is given by

$$x_3 = \sqrt{\frac{1}{4}t^2 - \alpha^2 - (x_1 - s_1)^2 - (x_2 - s_2)^2 + \frac{4\alpha^2(x_2 - s_2)^2}{t^2}}.$$

Then,  $\zeta$  is well defined and continuous.

Especially, in the first case, i.e. if  $\frac{4(x_1 - s_1)^2}{t^2 - 4\alpha^2} + \frac{4(x_2 - s_2)^2}{t^2} < 1$  is satisfied,  $\zeta$  yields for given  $(s, t, x_1, x_2)$  the unique  $x_3$  in  $\mathbb{R}_+$  such that  $\varphi(s, x) = t$  is satisfied.

Before we prove the assertions of this lemma, we describe the function  $\zeta$  illustrated in Figure 3.1. For given  $s \in S_0$ ,  $t \in (2\alpha, \infty)$  and  $(x_1, x_2)^\top \in \mathbb{R}^2$  the function  $\zeta$  assigns a value for  $x_3 \in \mathbb{R}_+ \cup \{0\}$ . If there is a value for  $x_3$  such that  $(x_1, x_2, x_3)^\top \in \mathbb{R}_+^3$  is an element of the open half-ellipsoid given by  $\varphi(s, x) = t$ , the function  $\zeta$  maps  $(s, t, x_1, x_2)$  to it. Otherwise  $\zeta$  maps  $(s, t, x_1, x_2)$  to zero.

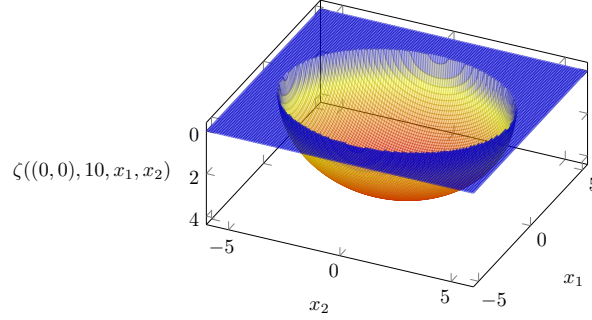


**Figure 3.1:** An illustration of the function  $\zeta$  defined in Lemma 3.5 for  $\alpha = 3$ ,  $s = (0, 0)$  and  $t = 10$ .

In other words, to an open half-ellipsoid given by  $s \in S_0$  and  $t \in (2\alpha, \infty)$  we take a point  $(x_1, x_2)^\top \in \mathbb{R}^2$ . If this point extended to  $(x_1, x_2, 0)^\top$ , is an element of the interior of the ellipse determined by the open half-ellipsoid in the  $x_1$ - $x_2$ -plane, we project this point onto the open half-ellipsoid. This means, that we assign to  $x_1$  and  $x_2$  the  $x_3$ -value such that  $x$  satisfies  $\varphi(s, x) = t$ . This value is unique since we consider the half-space, i.e.  $x_3 > 0$  holds. If the point  $(x_1, x_2, 0)^\top$  is outside or on the boundary of the ellipse in the  $x_1$ - $x_2$ -plane, the function  $\zeta$  assigns the value zero to  $x_1$  and  $x_2$  as third component in  $\mathbb{R}_+^3 \cup \{y \in \mathbb{R}^3 \mid y_3 = 0\}$ .

So, for fixed  $(s, t) \in S_0 \times (2\alpha, \infty)$  applying  $\zeta$  on  $(x_1, x_2)^\top \in \mathbb{R}^2$  yields an open half-ellipsoid with foci on the  $x_1$ - $x_2$ -plane given by  $(s_1, s_2 - \alpha, 0)^\top$  and  $(s_1, s_2 + \alpha, 0)^\top$  and travel time  $t$  continued by zero on the  $x_1$ - $x_2$ -plane.

We note that the assigned  $x_3$  in  $\mathbb{R}_+$  is unique as we do not allow negative values for  $x_3$ . Hence, in the full space setting there is no possibility to get a unique value in this way.

*Proof of Lemma 3.5.* First, we show that  $\zeta$  is well defined. We consider the set

$$A := \left\{ (s, t, x_1, x_2) \in S_0 \times (2\alpha, \infty) \times \mathbb{R}^2 \mid \frac{4(x_1 - s_1)^2}{t^2 - 4\alpha^2} + \frac{4(x_2 - s_2)^2}{t^2} < 1 \right\}.$$

Let  $(s, t, x_1, x_2)$  be in  $A$ . The inequality

$$\frac{4(x_1 - s_1)^2}{t^2 - 4\alpha^2} + \frac{4(x_2 - s_2)^2}{t^2} < 1$$

is equivalent to

$$\frac{1}{4}t^2 - \alpha^2 - (x_1 - s_1)^2 - (x_2 - s_2)^2 + \frac{4\alpha^2(x_2 - s_2)^2}{t^2} > 0$$

and so the square root which determines  $x_3$  is well defined and thus  $\zeta$ .

Next, we prove the continuity of  $\zeta$ . On the set  $A$  the function  $\zeta$  is continuous as composition of continuous functions and on

$$\left\{ (s, t, x_1, x_2) \in S_0 \times (2\alpha, \infty) \times \mathbb{R}^2 \mid \frac{4(x_1 - s_1)^2}{t^2 - 4\alpha^2} + \frac{4(x_2 - s_2)^2}{t^2} > 1 \right\}$$

as a constant function. Moreover, the equation

$$\frac{4(x_1 - s_1)^2}{t^2 - 4\alpha^2} + \frac{4(x_2 - s_2)^2}{t^2} = 1$$

has the equivalent reformulation

$$\frac{1}{4}t^2 - \alpha^2 - (x_1 - s_1)^2 - (x_2 - s_2)^2 + \frac{4\alpha^2(x_2 - s_2)^2}{t^2} = 0.$$

Using the representation of  $x_3$  given in the lemma, we deduce  $x_3 = 0 = \zeta(s, t, x_1, x_2)$  for  $(s, t, x_1, x_2)$  on the boundary  $\partial A$  of  $A$ . Thus,  $\zeta$  is continuous.

For the proof of the last assertion we use the other representation of an open half-ellipsoid. According to Lemma 3.1, the condition  $\varphi(s, x) = t$  is equivalent to

$$\frac{4(x_1 - s_1)^2}{t^2 - 4\alpha^2} + \frac{4(x_2 - s_2)^2}{t^2} + \frac{4x_3^2}{t^2 - 4\alpha^2} = 1.$$

If we solve this equation for  $x_3^2$ , we end up with

$$x_3^2 = \frac{1}{4}t^2 - \alpha^2 - (x_1 - s_1)^2 - (x_2 - s_2)^2 + \frac{4\alpha^2(x_2 - s_2)^2}{t^2}.$$

Further, we choose the positive solution of the quadratic equation given by

$$x_3 = \sqrt{\frac{1}{4}t^2 - \alpha^2 - (x_1 - s_1)^2 - (x_2 - s_2)^2 + \frac{4\alpha^2(x_2 - s_2)^2}{t^2}}$$

as we assume  $x_3 > 0$ . This is exactly the representation of  $x_3$  stated in the lemma. Thus, for given  $(s, t, x_1, x_2) \in A$  we get a unique  $x_3 > 0$  such that  $(x_1, x_2, x_3)^\top$  is part of the open half-ellipsoid with the two foci  $(s_1, s_2 - \alpha, 0)^\top$  and  $(s_1, s_2 + \alpha, 0)^\top$ , i.e.  $\varphi(s, x) = t$  is satisfied.  $\square$

Using the function  $\zeta$  defined in the last lemma, we are able to prove the first essential assumption to define a generalised Radon transform.

### 3.6 Lemma. *The two projections*

$$\pi_{S_0 \times (2\alpha, \infty)} : \{(s, t, x) \in S_0 \times (2\alpha, \infty) \times \mathbb{R}_+^3 \mid \varphi(s, x) = t\} \rightarrow S_0 \times (2\alpha, \infty)$$

and

$$\pi_{\mathbb{R}_+^3} : \{(s, t, x) \in S_0 \times (2\alpha, \infty) \times \mathbb{R}_+^3 \mid \varphi(s, x) = t\} \rightarrow \mathbb{R}_+^3$$

are fibre maps with connected fibres  $\mathbb{R}^2$  and  $S_0$ , respectively.

*Proof.* First, we consider the projection  $\pi_{S_0 \times (2\alpha, \infty)}$ . In order to show that  $\pi_{S_0 \times (2\alpha, \infty)}$  is surjective, let  $(s, t) = (s_1, s_2, t) \in S_0 \times (2\alpha, \infty)$  be arbitrary. By choosing  $x_1 = s_1$ ,  $x_2 = s_2$  and  $x_3 = \sqrt{\frac{t^2}{4} - \alpha^2}$ , we have  $x \in \mathbb{R}_+^3$  as  $t > 2\alpha$  holds. Moreover, we obtain

$$\varphi(s, x) = |\mathbf{x}_s(s) - x| + |x - \mathbf{x}_r(s)| = \sqrt{\alpha^2 + \frac{1}{4}t^2 - \alpha^2} + \sqrt{\alpha^2 + \frac{1}{4}t^2 - \alpha^2} = t.$$

Thus,  $\pi_{S_0 \times (2\alpha, \infty)}$  is surjective.

Further, let  $(p, q) \in S_0 \times (2\alpha, \infty)$  and we choose  $U$  to be  $U = S_0 \times (2\alpha, \infty)$ . Then,  $U$  is an open neighbourhood of  $(p, q)$ . We define  $\Psi : \pi_{S_0 \times (2\alpha, \infty)}^{-1}(U) \rightarrow U \times \mathbb{R}^2$  by  $(s, t, x) \mapsto (s, t, x_1, x_2)$  and  $\Psi^{-1} : U \times \mathbb{R}^2 \rightarrow \pi_{S_0 \times (2\alpha, \infty)}^{-1}(U)$  by  $(s, t, x_1, x_2) \mapsto (s, t, x_1, x_2, \zeta(s, t, x_1, x_2))$ , where  $\zeta : S_0 \times (2\alpha, \infty) \times \mathbb{R}^2 \rightarrow \mathbb{R}_+ \cup \{0\}$  is defined in Lemma 3.5. We show, that  $\Psi$  and  $\Psi^{-1}$  define a homeomorphism in such a way that the following diagram commutes

$$\begin{array}{ccc}
\pi_{S_0 \times (2\alpha, \infty)}^{-1}(U) & \xrightarrow{\Psi} & U \times \mathbb{R}^2 \\
\pi_{S_0 \times (2\alpha, \infty)} \downarrow & & \swarrow \Pi \\
U & & 
\end{array}$$

where  $\Pi$  is the natural projection onto the first factor (see Definition 2.25).

But before we prove this, we determine the preimage of  $U$  under  $\pi_{S_0 \times (2\alpha, \infty)}^{-1}$  by

$$\begin{aligned}
\pi_{S_0 \times (2\alpha, \infty)}^{-1}(U) &= \{(s, t, x) \in U \times \mathbb{R}_+^3 \mid \pi_{S_0 \times (2\alpha, \infty)}(s, t, x) = (s, t)\} \\
&= \{(s, t, x) \in U \times \mathbb{R}_+^3 \mid \varphi(s, x) = t\}.
\end{aligned}$$

First, we show that  $\Psi$  is bijective and  $\Psi^{-1}$  is the corresponding inverse. Hence, let  $(s, t, x) \in \pi_{S_0 \times (2\alpha, \infty)}^{-1}(U)$ . Then, we have  $(s, t, x) \in U \times \mathbb{R}_+^3$  such that  $\varphi(s, x) = t$  is fulfilled. Further, we get

$$(\Psi^{-1} \circ \Psi)(s, t, x) = \Psi^{-1}(s, t, x_1, x_2) = (s, t, x_1, x_2, \zeta(s, t, x_1, x_2)) = (s, t, x),$$

where we explain the last step in the following. The given condition  $\varphi(s, x) = t$  is equivalent to

$$\frac{4(x_1 - s_1)^2}{t^2 - 4\alpha^2} + \frac{4(x_2 - s_2)^2}{t^2} + \frac{4x_3^2}{t^2 - 4\alpha^2} = 1$$

by Lemma 3.1. As a consequence,  $(s, t, x_1, x_2)$  satisfies  $\frac{4(x_1 - s_1)^2}{t^2} + \frac{4(x_2 - s_2)^2}{t^2 - 4\alpha^2} < 1$  since  $x_3$  is strictly positive by assumption. Thus, according to Lemma 3.5 the function  $\zeta$  yields the unique  $x_3$  corresponding to  $(s, t, x_1, x_2)$  such that  $\varphi(s, x) = t$  is satisfied and we obtain the claimed equality.

For the reversed composition let  $(s, t, x_1, x_2) \in U \times \mathbb{R}^2$  be given. We have

$$(\Psi \circ \Psi^{-1})(s, t, x_1, x_2) = \Psi(s, t, x_1, x_2, \zeta(s, t, x_1, x_2)) = (s, t, x_1, x_2).$$

Hence,  $\Psi^{-1}$  is the inverse to  $\Psi$  and so  $\Psi$  is bijective.

Moreover, as a projection  $\Psi$  is continuous. By Lemma 3.5 the function  $\zeta$  is continuous and thus the inverse  $\Psi^{-1}$ . All in all,  $\Psi$  is a homeomorphism and  $\pi_{S_0 \times (2\alpha, \infty)}$  a fibre map with the connected set  $\mathbb{R}^2$  as fibre.

Now, we consider the second projection  $\pi_{\mathbb{R}_+^3}$ . Therefore, let  $x = (x_1, x_2, x_2)^\top$  be given. For arbitrary  $s \in S_0$  we achieve

$$\begin{aligned}
t = \varphi(s, x) &> \sqrt{(s_1 - x_1)^2 + (s_2 - \alpha - x_2)^2} + \sqrt{(x_1 - s_1)^2 + (x_2 - (s_2 + \alpha))^2} \\
&\geq \sqrt{(s_2 - \alpha - x_2)^2} + \sqrt{(x_2 - s_2 - \alpha)^2} = |s_2 - \alpha - x_2| + |x_2 - s_2 - \alpha| \\
&\geq |s_2 - \alpha - x_2 + x_2 - s_2 - \alpha| = 2\alpha
\end{aligned}$$

using once again that we assume  $x_3 > 0$ . Hence, given  $x = (x_1, x_2, x_2)^\top$  we find  $t \in (2\alpha, \infty)$  for arbitrary  $s_1$  and  $s_2$ . Thus,  $\pi_{\mathbb{R}_+^3}$  is surjective.

For the proof concerning the commutative diagram let  $p \in \mathbb{R}_+^3$  be given and we choose  $U$  to be  $U = \mathbb{R}_+^3$ , which is an open neighbourhood of  $p$ . We define  $\Phi: \pi_{\mathbb{R}_+^3}^{-1}(U) \rightarrow U \times S_0$  by  $(s, t, x) \mapsto (x, s)$  and  $\Phi^{-1}: U \times S_0 \rightarrow \pi_{\mathbb{R}_+^3}^{-1}(U)$  by  $(x, s) \mapsto (s, \varphi(s, x), x)$ . Using these maps we claim that the following diagram commutes

$$\begin{array}{ccc}
\pi_{\mathbb{R}_+^3}^{-1}(U) & \xrightarrow{\Phi} & U \times S_0 \\
\pi_{\mathbb{R}_+^3} \downarrow & \swarrow \Pi & \\
U & & 
\end{array}$$

where  $\Pi$  projects again onto the first factor.

Again, we reformulate the preimage  $\pi_{\mathbb{R}_+^3}^{-1}(U)$  of  $U$  before we prove the assertion. We observe

$$\begin{aligned}
\pi_{\mathbb{R}_+^3}^{-1}(U) &= \{(s, t, x) \in S_0 \times (2\alpha, \infty) \times U \mid \pi_{\mathbb{R}_+^3}(s, t, x) = x\} \\
&= \{(s, t, x) \in S_0 \times (2\alpha, \infty) \times U \mid \varphi(s, x) = t\}.
\end{aligned}$$

Now, let  $(s, t, x)$  be in  $\pi_{\mathbb{R}_+^3}^{-1}(U)$ . Then, it follows

$$(\Phi^{-1} \circ \Phi)(s, t, x) = \Phi^{-1}(x, s) = (s, \varphi(s, x), x) = (s, t, x)$$

since  $(s, t, x)$  is an element of  $\pi_{\mathbb{R}_+^3}^{-1}(U)$  by assumption. Further for  $(x, s) \in U \times S_0$  we have

$$(\Phi \circ \Phi^{-1})(x, s) = \Phi(s, \varphi(s, x), x) = (x, s).$$

Hence,  $\Phi$  is bijective with inverse  $\Phi^{-1}$ .

The maps  $\Phi$  and  $\Phi^{-1}$  are continuous since projections are continuous and  $\varphi$  is continuous. Thus,  $\Phi$  is a homeomorphism and so the projection  $\pi_{\mathbb{R}_+^3}$  a fibre map with fibre  $S_0$ , a connected set by assumption.  $\square$

In the next lemma, we consider the two sets we obtain from  $Z = \{(s, t, x) \in S_0 \times (2\alpha, \infty) \times \mathbb{R}_+^3 \mid \varphi(s, x) = t\}$  by firstly fixing  $(s, t) \in S_0 \times (2\alpha, \infty)$  and secondly fixing  $x \in \mathbb{R}_+^3$ .

**3.7 Lemma.** *We consider the two sets*

$$E(s, t) = \{x \in \mathbb{R}_+^3 \mid \varphi(s, x) = t\}$$

for given  $(s, t) \in S_0 \times (2\alpha, \infty)$  and

$$\tilde{E}(x) = \{(s, t) \in S_0 \times (2\alpha, \infty) \mid \varphi(s, x) = t\}$$

for given  $x \in \mathbb{R}_+^3$ .

*Then, the set  $E(s, t)$  determines  $(s, t) \in S_0 \times (2\alpha, \infty)$  uniquely and the set  $\tilde{E}(x)$  determines  $x \in \mathbb{R}_+^3$  uniquely. So,  $E(s, t) = E(u, v)$  is satisfied if and only if  $(s, t) = (u, v)$  is satisfied. Further,  $\tilde{E}(x) = \tilde{E}(\bar{x})$  holds if and only if  $x = \bar{x}$  is valid.*

For fixed  $(s, t) \in S_0 \times (2\alpha, \infty)$  the set  $E(s, t)$  describes the open half-ellipsoid with the two foci  $\mathbf{x}_s(s) = (x_1, x_2 - \alpha, 0)^\top$  and  $\mathbf{x}_r(s) = (x_1, x_2 + \alpha, 0)^\top$  and travel time  $t$ . So, by the lemma above knowing the open half-ellipsoid, we get the two foci and the associated travel time of it.

Conversely, the set  $\tilde{E}(x)$  for fixed  $x \in \mathbb{R}_+^3$  contains pairs of foci determined by an element of  $S_0$  and travel times  $t$  in  $(2\alpha, \infty)$  going through  $x$ . Thus, a point  $x \in \mathbb{R}_+^3$  is uniquely determined by the open half-ellipsoids containing this point.

*Proof.* We start with the set  $E(s, t)$  for fixed  $(s, t) \in S_0 \times (2\alpha, \infty)$  and show that we are able to determine  $(s, t)$  uniquely. The closure of  $E(s, t)$  is given by

$$\overline{E(s, t)} = \{x = (x_1, x_2, x_3) \in \mathbb{R} \times \mathbb{R} \times (\mathbb{R}_+ \cup \{0\}) \mid \varphi(s, x) = t\}.$$

This set is compact and thus the following extrema exist

$$\begin{aligned} \overline{x}_1 &:= \max\{x_1 \mid (x_1, x_2, x_3)^\top \in E(s, t)\} & \text{and} & & \underline{x}_1 &:= \min\{x_1 \mid (x_1, x_2, x_3)^\top \in E(s, t)\}, \\ \overline{x}_2 &:= \max\{x_2 \mid (x_1, x_2, x_3)^\top \in E(s, t)\} & \text{and} & & \underline{x}_2 &:= \min\{x_2 \mid (x_1, x_2, x_3)^\top \in E(s, t)\}, \\ \overline{x}_3 &:= \max\{x_3 \mid (x_1, x_2, x_3)^\top \in E(s, t)\}. \end{aligned}$$

Since we maximise respectively minimise over the closed half-ellipsoid, these extrema are unique. Now, we set  $s_1 := \frac{1}{2}(\overline{x}_1 + \underline{x}_1)$ ,  $s_2 := \frac{1}{2}(\overline{x}_2 + \underline{x}_2)$  and determine the travel time  $t$  by calculating  $t = \varphi(s, \hat{x})$  with  $\hat{x} = (s_1, s_2, \overline{x}_3)^\top$ . This point is an element of  $E(s, t)$ , the deepest one. Hence, we get  $(s, t)$  uniquely in the above way. Clearly, we get  $E(s, t) = E(u, v)$  for  $(s, t) = (u, v)$ .

For the proof of the second assertion we assume  $\tilde{E}(x) = \tilde{E}(y)$  for  $x, y \in \mathbb{R}_+^3$ . This means that  $x$  is an element of every open half-ellipsoid which contains  $y$  and the other way round. Thus, we get

$$\varphi(s, x) = \varphi(s, y) \tag{3.6}$$

for all  $s \in S_0$ . Now, let  $s = (s_1, s_2) \in S_0$  be fixed. As the set  $S_0$  is open by assumption, there exists  $\varepsilon > 0$  such that  $(s_1 + h, s_2) \in S_0$  and  $(s_1, s_2 + h) \in S_0$  for all  $h > 0$  with  $|h| < \varepsilon$ . By (3.6) we obtain

$$\begin{aligned} \varphi(s, x) &= \varphi(s, y), & (3.7) \\ \varphi((s_1 + h, s_2), x) &= \varphi((s_1 + h, s_2), y), \\ \varphi((s_1, s_2 + h), x) &= \varphi((s_1, s_2 + h), y) \end{aligned}$$

for all  $h > 0$  with  $|h| < \varepsilon$ . These identities yield

$$\frac{\varphi((s_1 + h, s_2), x) - \varphi((s_1, s_2), x)}{h} = \frac{\varphi((s_1 + h, s_2), y) - \varphi((s_1, s_2), y)}{h}$$

and

$$\frac{\varphi((s_1, s_2 + h), x) - \varphi((s_1, s_2), x)}{h} = \frac{\varphi((s_1, s_2 + h), y) - \varphi((s_1, s_2), y)}{h}$$

for all  $h > 0$  with  $|h| < \varepsilon$ . By taking the limit  $h \rightarrow 0$  we achieve

$$\partial_{s_1} \varphi(s, x) = \partial_{s_1} \varphi(s, y)$$

and

$$\partial_{s_2} \varphi(s, x) = \partial_{s_2} \varphi(s, y).$$

Together with (3.7) we get the following three equations

$$\begin{aligned} |\mathbf{x}_s(s) - x| + |x - \mathbf{x}_r(s)| &= |\mathbf{x}_s(s) - y| + |y - \mathbf{x}_r(s)|, \\ \frac{x_1 - s_1}{|\mathbf{x}_s(s) - x|} + \frac{x_1 - s_1}{|x - \mathbf{x}_r(s)|} &= \frac{y_1 - s_1}{|\mathbf{x}_s(s) - y|} + \frac{y_1 - s_1}{|y - \mathbf{x}_r(s)|}, \\ \frac{x_2 - (s_2 - \alpha)}{|\mathbf{x}_s(s) - x|} + \frac{x_2 - (s_2 + \alpha)}{|x - \mathbf{x}_r(s)|} &= \frac{y_2 - (s_2 - \alpha)}{|\mathbf{x}_s(s) - y|} + \frac{y_2 - (s_2 + \alpha)}{|y - \mathbf{x}_r(s)|}. \end{aligned}$$

By Lemma 3.2, we obtain  $x = y$ , so one direction is proved. For the other, we assume  $x = y$ . This yields obviously  $\tilde{E}(x) = \tilde{E}(y)$ . Hence, the proof is finished.  $\square$

According to Setting 3.4, Lemma 3.6 and Lemma 3.7 the choices we made in Setting 3.4 in order to define a generalised Radon transform by defining measures satisfy Assumption 2.27 and Assumption 2.28. But before we are able to define the related generalised Radon transforms, we have to verify one last assumption. This is,  $\pi_{S_0 \times (2\alpha, \infty)}$  has to be proper. We show this in the following Lemma.

**3.8 Lemma.** *The projection  $\pi_{S_0 \times (2\alpha, \infty)}: Z = \{(s, t, x) \in S_0 \times (2\alpha, \infty) \times \mathbb{R}_+^3 \mid \varphi(s, x) = t\} \rightarrow S_0 \times (2\alpha, \infty)$  is proper.*

*Proof.* Let  $a, b \in (2\alpha, \infty)$  be arbitrary with  $a < b$  and  $K$  be an arbitrary compact subset of  $S_0$ . Then,  $K \times [a, b]$  is compact subset of  $S_0 \times (2\alpha, \infty)$ .

First, we show that

$$\pi_{S_0 \times (2\alpha, \infty)}^{-1}(K \times [a, b]) = \{(s, t, x) \in K \times [a, b] \times \mathbb{R}_+^3 \mid \varphi(s, x) = t\}$$

is bounded. As  $t \in [a, b]$ , we get

$$b \geq t = \varphi(s, x) = |\mathbf{x}_s(s) - x| + |x - \mathbf{x}_r(s)| \geq |x - \mathbf{x}_s(s)|$$

and further

$$b \geq |x| - |\mathbf{x}_s(s)|.$$

Consequently, we have

$$|x| \leq b + |(s_1, s_2 - \alpha, 0)^\top|.$$

Thus, all  $x \in \mathbb{R}_+^3$  such that  $(s, t, x) \in \pi_{S_0 \times (2\alpha, \infty)}^{-1}(K \times [a, b])$  holds are bounded as  $s = (s_1, s_2) \in K$  is satisfied. As a consequence,  $\pi_{S_0 \times (2\alpha, \infty)}^{-1}(K \times [a, b])$  is bounded.

Further, the set  $\pi_{S_0 \times (2\alpha, \infty)}^{-1}(K \times [a, b])$  is closed as preimage of the closed set  $K \times [a, b]$  under the continuous map  $\pi_{S_0 \times (2\alpha, \infty)}$ .

Altogether,  $\pi_{S_0 \times (2\alpha, \infty)}^{-1}(K \times [a, b])$  is compact as bounded and closed subset of  $\mathbb{R}^6$  and thus  $\pi_{S_0 \times (2\alpha, \infty)}^{-1}$  is proper.  $\square$

Except for the defining measures we have everything needed to define the generalised Radon transform in the considered setting. Before we state these, we look closely at one of the measures we choose.

**3.9 Remark.** By  $\lambda_x, \lambda_s$  and  $\lambda_t$  we denote the Lebesgue measures on  $\mathbb{R}_+^3, S_0$  and  $(2\alpha, \infty)$ , respectively. Therewith, we define the measure  $\mu$  on  $Z$  by  $\mu = \delta(t - \varphi(s, x))A(s, x) \lambda_s \otimes \lambda_t \otimes \lambda_x$ , where  $A$  is given by  $A(s, x) = \frac{1}{|\mathbf{x}_s(s) - x| |x - \mathbf{x}_r(s)|}$  for  $s \in S_0$  and  $x \in \mathbb{R}_+^3$  according to definition (1.11).

For fixed  $(s, t) \in S_0 \times (2\alpha, \infty)$  we have  $\mu(s, t) = \delta(t - \varphi(s, x))A(s, x)\lambda_x$ , which is a measure on  $\mathbb{R}_+^3$  supported on the set  $E(s, t)$ , i.e. on the open half-ellipsoid determined by  $s$  and  $t$ . In Subsection 1.2.2 we analysed how  $\mu(s, t)$  acts on  $C_c^\infty(\mathbb{R}_+^3)$  for fixed  $(s, t) \in S_0 \times (2\alpha, \infty)$ . We have

$$\mu(s, t)(f) = \int_{\mathbb{R}_+^3} f(x)A(s, x)\delta(t - \varphi(s, x)) dx = \frac{1}{2} \int_0^\pi \int_0^\pi f(x(s, t, \phi, \theta)) \sin(\phi) d\phi d\theta$$

for  $f \in C_c^\infty(\mathbb{R}_+^3)$ . We deduce

$$\begin{aligned}\mu(f) &= \int_{S_0} \int_{2\alpha}^{\infty} \int_{\mathbb{R}_+^3} f(x) A(s, x) \delta(t - \varphi(s, x)) \, dx \, dt \, ds \\ &= \frac{1}{2} \int_{S_0} \int_{2\alpha}^{\infty} \int_0^\pi \int_0^\pi f(x(s, t, \phi, \theta)) \sin(\phi) \, d\phi \, d\theta \, dt \, ds\end{aligned}\quad (3.8)$$

for  $f \in C_c^\infty(\mathbb{R}_+^3)$ . Thus, the measure  $\mu$  acts on  $C_c^\infty(\mathbb{R}_+^3)$  via identity (3.8). Its density given by  $\phi \mapsto \frac{1}{2} \sin(\phi)$  for  $\phi \in (0, \pi)$  is smooth. In this sense  $\mu$  is a smooth measure on  $Z$ .

**3.10 Definition.** By Lemma 3.6 and Lemma 3.7 the Setting 3.4 satisfies Assumption 2.27 and Assumption 2.28. Moreover, the projection  $\pi_{S_0 \times (2\alpha, \infty)}$  is proper according to Lemma 3.8

We choose  $\nu_X = \lambda_x$ ,  $\nu_Y = \lambda_s \otimes \lambda_t$  and  $\mu = \delta(t - \varphi(s, x)) A(s, x) \lambda_s \otimes \lambda_t \otimes \lambda_x$  as smooth Radon measures on  $X, Y$  and  $Z$  (see Remark 3.9).

Then, by Definition 2.32 the corresponding generalised Radon transform  $F: C^\infty(\mathbb{R}_+^3) \rightarrow C^\infty(S_0 \times (2\alpha, \infty))$  is given by the relation

$$Ff \odot \lambda_s \otimes \lambda_t = \pi_{S_0 \times (2\alpha, \infty)*}((f \circ \pi_{\mathbb{R}_+^3}) \odot \mu).$$

After a calculation we obtain the following representation

$$Ff(s, t) = \int_{\mathbb{R}_+^3} f(x) \delta(t - \varphi(s, x)) A(s, x) \, dx$$

for  $F$  (see below this definition). Here, and in the following we write  $dx$ ,  $ds$  and  $dt$  for integrating with respect to  $\lambda_x$ ,  $\lambda_s$  and  $\lambda_t$ , respectively. Since  $\varphi(s, x) = t$  with  $(s, t, x) \in S_0 \times (2\alpha, \infty) \times \mathbb{R}_+^3$  describes an open half-ellipsoid (see Lemma 3.1),  $F$  is often called the elliptic generalised Radon transform.

In order to get the above representation of  $F$  let  $f \in C_c^\infty(\mathbb{R}_+^3)$  and  $g \in C^\infty(S_0 \times (2\alpha, \infty))$  be given. Then, we have

$$\begin{aligned}& \int_{S_0 \times (2\alpha, \infty)} g(s, t) \, d(Ff \odot \lambda_s \lambda_t)(s, t) \\ &= \int_{S_0 \times (2\alpha, \infty)} g(s, t) \, d\pi_{S_0 \times (2\alpha, \infty)*}((f \circ \pi_{\mathbb{R}_+^3}) \odot \mu)(s, t) \\ &= \int_Z (g \circ \pi_{S_0 \times (2\alpha, \infty)})(s, t, x) \, d((f \circ \pi_{\mathbb{R}_+^3}) \odot \mu)(s, t, x) \\ &= \int_Z (g \circ \pi_{S_0 \times (2\alpha, \infty)})(s, t, x) (f \circ \pi_{\mathbb{R}_+^3})(s, t, x) \, d\mu(s, t, x) \\ &= \int_{S_0 \times (2\alpha, \infty) \times \mathbb{R}_+^3} g(s, t) f(x) \delta(t - \varphi(s, x)) A(s, x) \, d(s, t, x) \\ &= \int_{S_0 \times (2\alpha, \infty)} g(s, t) \int_{\mathbb{R}_+^3} f(x) \delta(t - \varphi(s, x)) A(s, x) \, dx \, d(s, t).\end{aligned}$$

**3.11 Definition.** As mentioned in Definition 3.10 the assumptions we need to apply Definition 2.32 and thus Definition 2.33 are satisfied. With the same measures as in Definition 3.10 we define the corresponding dual generalised Radon transform  $F^*: C_c^\infty(S_0 \times (2\alpha, \infty)) \rightarrow C_c^\infty(\mathbb{R}_+^3)$  by the relation

$$F^*g \odot \lambda_x = \pi_{\mathbb{R}_+^3*}((g \circ \pi_{S_0 \times (2\alpha, \infty)}) \odot \mu)$$

according to Definition 2.33. Again, a calculation (see below this definition) yields

$$F^*g(x) = \int_{S_0 \times (2\alpha, \infty)} g(s, t) \delta(t - \varphi(s, x)) A(s, x) d(s, t) = \int_{S_0} g(s, \varphi(s, x)) A(s, x) ds.$$

For the calculation of the representation of  $F^*$  let  $f \in C_c^\infty(\mathbb{R}_+^3)$  and  $g \in C^\infty(S_0 \times (2\alpha, \infty))$  be given. We obtain

$$\begin{aligned} \int_{\mathbb{R}_+^3} f(x) d(F^*g \odot \lambda_x)(x) &= \int_{\mathbb{R}_+^3} f(x) d\pi_{\mathbb{R}_+^3}((g \circ \pi_{S_0 \times (2\alpha, \infty)}) \odot \mu)(x) \\ &= \int_Z (f \circ \pi_{\mathbb{R}_+^3})(s, t, x) d((g \circ \pi_{S_0 \times (2\alpha, \infty)}) \odot \mu)(s, t, x) \\ &= \int_Z (f \circ \pi_{\mathbb{R}_+^3})(s, t, x) (g \circ \pi_{S_0 \times (2\alpha, \infty)})(s, t, x) d\mu(s, t, x) \\ &= \int_{S_0 \times (2\alpha, \infty) \times \mathbb{R}_+^3} f(x) g(s, t) \delta(t - \varphi(s, x)) A(s, x) d(s, t, x) \\ &= \int_{\mathbb{R}_+^3} f(x) \int_{S_0 \times (2\alpha, \infty)} g(s, t) \delta(t - \varphi(s, x)) A(s, x) d(s, t) dx. \end{aligned}$$

In Subsection 3.2.1 we confirm that  $F^*$  is the dual operator to  $F$  from another point of view.

## 3.2. Properties of $F$

In Chapter 1 we obtained the equation

$$Fn = y$$

for the quantity  $n$  we are interested in with the measured data  $y$ . Since there is no inversion formula for  $F$  known, we are not able to solve this equation directly for  $n$ . In our application, we do not need the exact values of  $n$ . It is sufficient if we know where the jumps of  $n$  appear since these describe the material changes below the surface. In this way, we are able to locate different materials (see also Introduction and Chapter 1).

In order to obtain information about the singularities, we aim to apply a reconstruction algorithm. For this purpose, we choose a suitable reconstruction operator  $\Lambda$  which is defined by  $\Lambda := \tilde{F}F$  where  $\tilde{F}$  has to be chosen later on.

At this point, the microlocal analysis comes into play. With the help of the results available in this theory we are able to predict which singularities are reconstructed or not and which are added by the reconstruction operator  $\Lambda$ . Knowing this, we draw conclusions on  $n$  by knowing  $\Lambda n$ .

In short, this means we have to find an operator  $\Lambda$  which preserves the singularities of  $n$  and does not add any. Also, the strength of the singularities should ideally increase and not decrease.

In Chapter 2 we have seen that elliptic pseudodifferential operators preserve the wave front set and in particular, the singularities. Further, there is a result on page 371 in [GS77] that the normal operator  $R^*R$  for a generalised Radon transform  $R$  is an elliptic pseudodifferential operator if an additional condition, the Bolker condition, holds. Moreover, the composition  $R^*R$  has to be well defined. Since we verified in Section 3.1 that  $F$  is a generalised Radon transform, we start analysing the the normal operator of  $F$ .

However, before we go on with the normal operator of  $F$ , we verify that  $F$  and its dual  $F^*$  are Fourier integral operators. We will benefit from this knowledge later on when we consider the normal operator of  $F$ .

### 3.2.1. $F$ as Fourier integral operator

In Section 3.1 we defined the elliptic Radon transform  $F: C^\infty(\mathbb{R}_+^3) \rightarrow C^\infty(S_0 \times (2\alpha, \infty))$  and its dual  $F^*: C_c^\infty(S_0 \times (2\alpha, \infty)) \rightarrow C_c^\infty(\mathbb{R}_+^3)$ . As we are interested in quantities  $n$  which are non-smooth, we continue the operator  $F|_{C_c^\infty(\mathbb{R}_+^3)}$  to the set of distributions with compact support denoted by  $\mathcal{E}'(\mathbb{R}_+^3)$ . For this reason, we take advantage of the fact that  $F$  and  $F^*$  are Fourier integral operators. By page 371 in [GS77] the operators  $F$  as well as  $F^*$  are Fourier integral operators of order  $-1$  since they are generalised Radon transforms. Nevertheless, we need the representations of both later on. In order to get these, we reformulate both operators and verify that the obtained representations satisfy the assumptions for a Fourier integral operator. For  $f \in C_c^\infty(\mathbb{R}_+^3)$  we obtain

$$\begin{aligned}
Ff(s, t) &= \int_{\mathbb{R}_+^3} f(x) \delta(t - \varphi(s, x)) A(s, x) dx \\
&= \int_{\mathbb{R}_+^3} f(x) A(s, x) \mathcal{F}_t^{-1}(\mathcal{F}_t(t \mapsto \delta(t - \varphi(s, x)))) dx \\
&= \int_{\mathbb{R}_+^3} f(x) A(s, x) \mathcal{F}_t^{-1}(t \mapsto \frac{1}{\sqrt{2\pi}} e^{-i\varphi(s, x)t}) dx \\
&= \frac{1}{2\pi} \int_{\mathbb{R}_+^3} \int_{\mathbb{R}} f(x) A(s, x) e^{i\omega(t - \varphi(s, x))} d\omega dx \\
&= \frac{1}{2\pi} \int_{\mathbb{R}} \int_{\mathbb{R}_+^3} f(x) A(s, x) e^{i\omega(t - \varphi(s, x))} dx d\omega
\end{aligned} \tag{3.9}$$

for  $(s, t) \in S_0 \times (2\alpha, \infty)$ . Here,  $\mathcal{F}_t$  denotes the one dimensional Fourier transform with respect to  $t$  and  $\mathcal{F}_t^{-1}$  its inverse. We note that  $\mathcal{F}_t$  is invertible on  $L^2$ , on the Schwartz space and on its dual, the space of tempered distributions.

First, we verify that  $p: S_0 \times (2\alpha, \infty) \times \mathbb{R}_+^3 \times \mathbb{R} \rightarrow \mathbb{R}$  defined by  $p(s, t, x, \omega) := \frac{1}{2\pi} A(s, x) = \frac{1}{2\pi} \frac{1}{|\mathbf{x}_s(s) - x|} \frac{1}{|x - \mathbf{x}_r(s)|}$  is a symbol of order 0. Since for all  $s \in S_0$  the points  $\mathbf{x}_s(s)$  and  $\mathbf{x}_r(s)$  are no elements of  $\mathbb{R}_+^3$ , we have  $p \in C^\infty(S_0 \times (2\alpha, \infty) \times \mathbb{R}_+^3 \times \mathbb{R})$ . The function  $p$  is positive homogeneous of degree 0 and so, according to Lemma 2.2,  $p$  is a symbol of order 0. Further, we define  $\phi: S_0 \times (2\alpha, \infty) \times \mathbb{R}_+^3 \times \mathbb{R} \setminus \{0\} \rightarrow \mathbb{R}$  by  $\phi(s, t, x, \omega) := \omega(t - \varphi(s, x))$ . Then,  $\phi \in C^\infty(S_0 \times (2\alpha, \infty) \times \mathbb{R}_+^3 \times \mathbb{R} \setminus \{0\})$  is satisfied as  $\varphi$  is in  $C^\infty(S_0 \times \mathbb{R}_+^3)$  and we get

$$\phi(s, t, x, \lambda\omega) = \lambda\omega(t - \varphi(s, x)) = \lambda\phi(s, t, x, \omega)$$

for  $\lambda > 0$  and  $(s, t, x, \omega) \in S_0 \times (2\alpha, \infty) \times \mathbb{R}_+^3 \times \mathbb{R} \setminus \{0\}$ . Hence,  $\phi$  is positive homogeneous of degree 1 in the last variable. Further, we have

$$\begin{aligned}
\nabla_{(s,t)} \phi(s, t, x, \omega) &= \left( \omega \left( \frac{x_1 - s_1}{|\mathbf{x}_s(s) - x|} + \frac{x_1 - s_1}{|x - \mathbf{x}_r(s)|}, \frac{x_2 - (s_2 - \alpha)}{|\mathbf{x}_s(s) - x|} + \frac{x_2 - (s_2 + \alpha)}{|x - \mathbf{x}_r(s)|} \right), \omega \right)^\top, \\
\nabla_x \phi(s, t, x, \omega) &= -\omega \left( \frac{x_1 - s_1}{|\mathbf{x}_s(s) - x|} + \frac{x_1 - s_1}{|x - \mathbf{x}_r(s)|}, \frac{x_2 - (s_2 - \alpha)}{|\mathbf{x}_s(s) - x|} + \frac{x_2 - (s_2 + \alpha)}{|x - \mathbf{x}_r(s)|}, \frac{x_3}{|\mathbf{x}_s(s) - x|} + \frac{x_3}{|x - \mathbf{x}_r(s)|} \right)^\top \\
&= -\omega \nabla_x \varphi(s, x), \\
\partial_\omega \phi(s, t, x, \omega) &= t - (|\mathbf{x}_s(s) - x| + |x - \mathbf{x}_r(s)|) = t - \varphi(s, x).
\end{aligned} \tag{3.10}$$

Since  $x_3 > 0$  is satisfied, the gradients  $\nabla_{(s,t)} \phi$  and  $\nabla_x \phi$  are nowhere zero on  $S_0 \times (2\alpha, \infty) \times \mathbb{R}_+^3 \times \mathbb{R} \setminus \{0\}$ . For this reason,  $(\nabla_{(s,t)} \phi, \partial_\omega \phi)$  and  $(\nabla_x \phi, \partial_\omega \phi)$  do not vanish on  $S_0 \times (2\alpha, \infty) \times \mathbb{R}_+^3 \times \mathbb{R} \setminus \{0\}$ . Hence,  $\phi$  is a phase function.

Next, we consider the matrix given by

$$\begin{pmatrix} \partial_{(s,t)} \partial_\omega \phi(s, t, x, \omega) & \partial_x \partial_\omega \phi(s, t, x, \omega) & \partial_\omega^2 \phi(s, t, x, \omega) \end{pmatrix}.$$

Again, the derivatives  $\partial_x \partial_\omega \phi(s, t, x, \omega) = -\partial_x \varphi(s, x)$  do not vanish for  $(s, t, x, \omega) \in S_0 \times (2\alpha, \infty) \times \mathbb{R}_+^3 \times \mathbb{R} \setminus \{0\}$  because  $x_3$  is strictly positive. Thus, the rank of the matrix above is 1 and the phase function  $\phi$  is non-degenerate. With the formula for the order  $k$  of a Fourier integral operator we obtain  $k = 0 - (\frac{3+3}{4} - \frac{1}{2}) = -1$  for the order of  $F$ . Altogether, the above expression for  $F$  satisfies the assumption on a Fourier integral operator of order  $-1$ . Analogously, we have

$$\begin{aligned} F^* g(x) &= \int_{S_0 \times (2\alpha, \infty)} g(s, t) \delta(t - \varphi(s, x)) A(s, x) d(s, t) \\ &= \int_{S_0 \times (2\alpha, \infty)} g(s, t) A(s, x) \mathcal{F}_t^{-1}(\mathcal{F}_t(t \mapsto \delta(t - \varphi(s, x)))) d(s, t) \\ &= \int_{S_0 \times (2\alpha, \infty)} g(s, t) A(s, x) \mathcal{F}_t^{-1}(t \mapsto \frac{1}{\sqrt{2\pi}} e^{-i\varphi(s, x)t}) d(s, t) \\ &= \frac{1}{2\pi} \int_{S_0 \times (2\alpha, \infty)} \int_{\mathbb{R}} g(s, t) A(s, x) e^{i\omega(t - \varphi(s, x))} d\omega d(s, t) \\ &= \frac{1}{2\pi} \int_{\mathbb{R}} \int_{S_0 \times (2\alpha, \infty)} g(s, t) A(s, x) e^{i\omega(t - \varphi(s, x))} d(s, t) d\omega \end{aligned} \quad (3.11)$$

for  $g \in C_c^\infty(S_0 \times (2\alpha, \infty))$  and  $x \in \mathbb{R}_+^3$ .

With the functions  $p^*(x, s, t, \omega) = \frac{1}{2\pi} A(s, x) = p(s, t, x, \omega)$  and analogously  $\phi^*(x, s, t, \omega) = \omega(t - \varphi(s, x)) = \phi(s, t, x, \omega)$  we also have a representation for  $F^*$  as a Fourier integral operator of order  $-1$ , which confirms that it is the dual operator to  $F$ .

By the above observations,  $F|_{C_c^\infty(\mathbb{R}_+^3)} : C_c^\infty(\mathbb{R}_+^3) \rightarrow C^\infty(S_0 \times (2\alpha, \infty))$  and  $F^* : C_c^\infty(S_0 \times (2\alpha, \infty)) \rightarrow C_c^\infty(\mathbb{R}_+^3)$  are Fourier integral operators. Thus, there exist the continuous extensions  $F : \mathcal{E}'(\mathbb{R}_+^3) \rightarrow \mathcal{D}'(S_0 \times (2\alpha, \infty))$  and  $F^* : \mathcal{E}'(S_0 \times (2\alpha, \infty)) \rightarrow \mathcal{D}'(\mathbb{R}_+^3)$ .

In Section 2.1 we have seen that there are two sets, the canonical relation  $C$  and the set  $\Sigma_\phi$ , related to a Fourier integral operator. We need these later on to describe the microlocal behaviour of a composed operator consisting of  $F$  and its dual  $F^*$ . As a preparation we calculate both sets for  $F$  and  $F^*$  in the following.

With the identities in (3.10) we obtain the set

$$\Sigma_\phi = \{(s, t, x, \omega) \in S_0 \times (2\alpha, \infty) \times \mathbb{R}_+^3 \times \mathbb{R} \setminus \{0\} \mid \varphi(s, x) = t\}$$

and the canonical relation  $C \subseteq ((S_0 \times (2\alpha, \infty)) \times \mathbb{R}^3 \setminus \{0\}) \times (\mathbb{R}_+^3 \times \mathbb{R}^3 \setminus \{0\})$ , which is given

by

$$\begin{aligned}
C &= \{(s, t, \nabla_{(s,t)}\phi(s, t, x, \omega); x, -\nabla_x\phi(s, t, x, \omega)) \mid (s, t, x, \omega) \in \Sigma_\phi\} \\
&= \{(s, t, (-\omega\nabla_s\varphi(s, x), \omega)^\top; x, \omega\nabla_x\varphi(s, x)) \mid \varphi(s, x) = t, \omega \neq 0\} \\
&= \left\{ \left( s, t, \left( \omega \left( \frac{x_1-s_1}{|\mathbf{x}_s(s)-x|} + \frac{x_1-s_1}{|x-\mathbf{x}_r(s)|} \right), \omega \left( \frac{x_2-(s_2-\alpha)}{|\mathbf{x}_s(s)-x|} + \frac{x_2-(s_2+\alpha)}{|x-\mathbf{x}_r(s)|} \right), \omega \right)^\top; x, \right. \right. \\
&\quad \left. \left( \omega \left( \frac{x_1-s_1}{|\mathbf{x}_s(s)-x|} + \frac{x_1-s_1}{|x-\mathbf{x}_r(s)|} \right), \omega \left( \frac{x_2-(s_2-\alpha)}{|\mathbf{x}_s(s)-x|} + \frac{x_2-(s_2+\alpha)}{|x-\mathbf{x}_r(s)|} \right), \omega \left( \frac{x_3}{|\mathbf{x}_s(s)-x|} + \frac{x_3}{|x-\mathbf{x}_r(s)|} \right) \right)^\top \right. \\
&\quad \left. \mid |\mathbf{x}_s(s) - x| + |x - \mathbf{x}_r(s)| = t, \omega \neq 0 \right\} \\
&= \left\{ \left( s, \varphi(s, x), \left( \omega \left( \frac{x_1-s_1}{|\mathbf{x}_s(s)-x|} + \frac{x_1-s_1}{|x-\mathbf{x}_r(s)|} \right), \omega \left( \frac{x_2-(s_2-\alpha)}{|\mathbf{x}_s(s)-x|} + \frac{x_2-(s_2+\alpha)}{|x-\mathbf{x}_r(s)|} \right), \omega \right)^\top; x, \right. \right. \\
&\quad \left. \left( \omega \left( \frac{x_1-s_1}{|\mathbf{x}_s(s)-x|} + \frac{x_1-s_1}{|x-\mathbf{x}_r(s)|} \right), \omega \left( \frac{x_2-(s_2-\alpha)}{|\mathbf{x}_s(s)-x|} + \frac{x_2-(s_2+\alpha)}{|x-\mathbf{x}_r(s)|} \right), \omega \left( \frac{x_3}{|\mathbf{x}_s(s)-x|} + \frac{x_3}{|x-\mathbf{x}_r(s)|} \right) \right)^\top \right. \\
&\quad \left. \mid \omega \neq 0 \right\}. \tag{3.12}
\end{aligned}$$

For the canonical relation of the dual  $F^*$  we further get

$$\begin{aligned}
C^\top &= \{(x, -\nabla_x\phi(s, t, x, \omega); s, t, \nabla_{(s,t)}\phi(s, t, x, \omega)) \mid \varphi(s, x) = t, \omega \neq 0\} \\
&= \left\{ \left( x, \left( \omega \left( \frac{x_1-s_1}{|\mathbf{x}_s(s)-x|} + \frac{x_1-s_1}{|x-\mathbf{x}_r(s)|} \right), \omega \left( \frac{x_2-s_2+\alpha}{|\mathbf{x}_s(s)-x|} + \frac{x_2-s_2+\alpha}{|x-\mathbf{x}_r(s)|} \right), \omega \left( \frac{x_3}{|\mathbf{x}_s(s)-x|} + \frac{x_3}{|x-\mathbf{x}_r(s)|} \right) \right)^\top; \right. \\
&\quad \left. s, t, \left( \omega \left( \frac{x_1-s_1}{|\mathbf{x}_s(s)-x|} + \frac{x_1-s_1}{|x-\mathbf{x}_r(s)|} \right), \omega \left( \frac{x_2-s_2+\alpha}{|\mathbf{x}_s(s)-x|} + \frac{x_2-s_2+\alpha}{|x-\mathbf{x}_r(s)|} \right), \omega \right)^\top \right. \\
&\quad \left. \mid |\mathbf{x}_s(s) - x| + |x - \mathbf{x}_r(s)| = t, \omega \neq 0 \right\} \tag{3.13}
\end{aligned}$$

following the definition in identity (2.6).

In direct connection with the canonical relation are the two canonical projections illustrated in Figure 2.1. In our case these are given by  $\Pi_{S_0 \times (2\alpha, \infty)} : C \rightarrow S_0 \times (2\alpha, \infty) \times \mathbb{R}^3 \setminus \{0\}$  and  $\Pi_{\mathbb{R}_+^3} : C \rightarrow \mathbb{R}_+^3 \times \mathbb{R}^3 \setminus \{0\}$ , i.e. they project on the first and the second component of the canonical relation, respectively.

$$\begin{array}{ccc}
& C \subseteq ((S_0 \times (2\alpha, \infty)) \times \mathbb{R}^3 \setminus \{0\}) \times (\mathbb{R}_+^3 \times \mathbb{R}^3 \setminus \{0\}) & \\
& \swarrow \Pi_{S_0 \times (2\alpha, \infty)} & \searrow \Pi_{\mathbb{R}_+^3} \\
S_0 \times (2\alpha, \infty) \times \mathbb{R}^3 \setminus \{0\} & & \mathbb{R}_+^3 \times \mathbb{R}^3 \setminus \{0\}
\end{array}$$

### 3.2.2. The normal operator and its wave front set

In the smooth situation  $F$  maps  $C_c^\infty(\mathbb{R}_+^3)$  into  $C^\infty(S_0 \times (2\alpha, \infty))$  but in general the image does not have compact support. Thus, also in the distributional setting the operator  $F$  maps  $\mathcal{E}'(\mathbb{R}_+^3)$  into  $\mathcal{D}'(S_0 \times (2\alpha, \infty))$  in place of  $\mathcal{E}'(S_0 \times (2\alpha, \infty))$ . For this reason, we are not able to compose  $F^*$  with  $F$  in general.

However, there is still a way to use the claim that  $R^*R$  is an elliptic pseudodifferential operator according to page 371 in [GS77] for a generalised Radon transform  $R$ . We introduce a cut-off function  $\psi \in C_c^\infty(S_0 \times (2\alpha, \infty))$  and have  $\psi F : \mathcal{E}'(\mathbb{R}_+^3) \rightarrow \mathcal{E}'(S_0 \times (2\alpha, \infty))$ . Hence,

we are able to compose  $F^*: \mathcal{E}'(S_0 \times (2\alpha, \infty)) \rightarrow \mathcal{D}'(\mathbb{R}_+^3)$  with  $\psi F$ . This yields an operator  $F^*\psi F: \mathcal{E}'(\mathbb{R}_+^3) \rightarrow \mathcal{D}'(\mathbb{R}_+^3)$ .

In this subsection, we first show that  $F^*\psi F$  is a pseudodifferential operator. Afterwards we analyse the wave front set of  $F^*\psi F$  using the representations of the canonical relations of  $F$  and  $F^*$  we calculated in the last subsection.

**3.12 Theorem.** *The operator  $F^*\psi F: \mathcal{E}'(\mathbb{R}_+^3) \rightarrow \mathcal{D}'(\mathbb{R}_+^3)$  is a pseudodifferential operator of order  $-2$ .*

*Proof.* In Subsection 3.2.1 we have seen that the generalised Radon transform  $F$  and its dual  $F^*$  are Fourier integral operators of order  $-1$ . As we have outlined above this theorem we insert the cut-off function  $\psi$  since without it we are not able to compose  $F^*$  and  $F$ . By the mapping properties of  $F$  and  $F^*$  we obtain  $F^*\psi F: \mathcal{E}'(\mathbb{R}_+^3) \rightarrow \mathcal{D}'(\mathbb{R}_+^3)$ . Moreover, the Bolker condition for  $F$  is satisfied. This means, that the projection  $\Pi_{S_0 \times (2\alpha, \infty)}: C \rightarrow S_0 \times (2\alpha, \infty) \times \mathbb{R}^3 \setminus \{0\}$  from the canonical relation  $C$  onto its first three components is an injective immersion, i.e.  $\Pi_{S_0 \times (2\alpha, \infty)}$  and its derivative are injective. A proof of this is given in Section 3.2 in [FKNQ16]. Since this condition is fulfilled by  $F$ , the operator  $F^*\psi F$  is a pseudodifferential operator of order  $-2$  according to page 371 in [GS77] (see also page 331 and 335 in [Quin80]). We note that the symbol of  $\psi F$  is given by  $\psi(s, t)p(s, t, x, \omega)$  for  $(s, t, x, \omega) \in S_0 \times (2\alpha, \infty) \times \mathbb{R}_+^3 \times \mathbb{R} \setminus \{0\}$ . Since  $\psi$  does not depend on the phase variable  $\omega$ , the order and the canonical relation of  $\psi F$  do not change in comparison to  $F$ . For more details we refer to the proof of Theorem 3.15 below.  $\square$

The assertion on page 371 in [GS77] is that for a generalised Radon transform  $R$  the operator  $R^*R$  is an elliptic pseudodifferential operator. In Theorem 3.12 we applied this result to show that  $F^*\psi F$  is a pseudodifferential operator. However, we do not obtain that  $F^*\psi F$  is an elliptic pseudodifferential operator. The reason for this is the cut-off function  $\psi$ . At points in which the cut-off function  $\psi$  vanishes it is not possible to show the estimate required for ellipticity.

For the proof of the next theorem we need the following lemma. This assertion is already published as Lemma 3.4 in [GKQR18b]. We include the proof for convenience of the reader.

**3.13 Lemma.** *Let  $(x, \xi) \in \mathbb{R}_+^3 \times \mathbb{R}^3$  with  $\xi_3 \neq 0$ . The equation  $\xi = \omega \nabla_x \varphi(s, x)$  determines uniquely  $s \in \mathbb{R}^2$  and  $\omega \in \mathbb{R} \setminus \{0\}$  depending on  $x$  and  $\xi$ . Explicitly, we have*

$$w(x, \xi) = \frac{\xi_3}{x_3 \left( \frac{1}{|x - \mathbf{x}_s(s)|} + \frac{1}{|x - \mathbf{x}_r(s)|} \right)}$$

and  $s(x, \xi) = (s_1(x, \xi), s_2(x, \xi))$  where

$$s_1(x, \xi) = x_1 - \frac{\xi_1}{\xi_3} x_3,$$

$$s_2(x, \xi) = \begin{cases} x_2 - \frac{1}{2} \frac{\xi_3}{\xi_2} \left( \left( \frac{\xi_2^2 - \xi_1^2}{\xi_3^2} - 1 \right) x_3 + \sqrt{x_3^2 \left( \frac{\xi_1^2 + \xi_2^2}{\xi_3^2} + 1 \right)^2 + 4\alpha^2 \frac{\xi_2^2}{\xi_3^2}} \right), & \text{for } \xi_2 \neq 0, \\ x_2, & \text{for } \xi_2 = 0, \end{cases}$$

and thus

$$\omega(x, \xi) = \frac{\xi_3}{x_3} \frac{\sqrt{(x_1 - s_1(x, \xi))^2 + (x_2 - (s_2(x, \xi) - \alpha))^2 + x_3^2} \sqrt{(x_1 - s_1(x, \xi))^2 + (x_2 - (s_2(x, \xi) + \alpha))^2 + x_3^2}}{\sqrt{(x_1 - s_1(x, \xi))^2 + (x_2 - (s_2(x, \xi) - \alpha))^2 + x_3^2} + \sqrt{(x_1 - s_1(x, \xi))^2 + (x_2 - (s_2(x, \xi) + \alpha))^2 + x_3^2}}.$$

Before we prove the lemma, we focus on the representation of  $s_2$  depending on  $(x, \xi) \in \mathbb{R}_+^3 \times \mathbb{R}^3$  with  $\xi_3 \neq 0$ .

**3.14 Remark.** Although at first glance it is not clear whether the representation of  $s_2$  depending on  $(x, \xi) \in \mathbb{R}_+^3 \times \mathbb{R}^3$  with  $\xi_3 \neq 0$  is continuous, it is even smooth. In order to show this, we rewrite  $s_2$ . For  $(x, \xi) \in \mathbb{R}_+^3 \times \mathbb{R}^3$  with  $\xi_2 \neq 0$  and  $\xi_3 \neq 0$  we have

$$\begin{aligned}
s_2(x, \xi) &= x_2 - \frac{1}{2} \frac{\xi_3}{\xi_2} x_3 \left( \frac{\xi_2^2}{\xi_3^2} + \frac{\left( \frac{\xi_1^2}{\xi_3^2} + \frac{\xi_2^2}{\xi_3^2} + 1 \right)^2 + 4 \frac{\alpha^2}{x_3^2} \frac{\xi_2^2}{\xi_3^2} - \left( \frac{\xi_1^2}{\xi_3^2} + 1 \right)^2}{\sqrt{\left( \frac{\xi_1^2}{\xi_3^2} + \frac{\xi_2^2}{\xi_3^2} + 1 \right)^2 + 4 \frac{\alpha^2}{x_3^2} \frac{\xi_2^2}{\xi_3^2} + \left( \frac{\xi_1^2}{\xi_3^2} + 1 \right)^2}} \right) \\
&= x_2 - \frac{1}{2} \frac{\xi_3}{\xi_2} x_3 \left( \frac{\xi_2^2}{\xi_3^2} + \frac{\frac{\xi_1^4}{\xi_3^4} + 2 \frac{\xi_1^2 \xi_2^2}{\xi_3^2} \left( \frac{\xi_1^2}{\xi_3^2} + 1 \right) + 4 \frac{\alpha^2}{x_3^2} \frac{\xi_2^2}{\xi_3^2}}{\sqrt{\left( \frac{\xi_1^2}{\xi_3^2} + \frac{\xi_2^2}{\xi_3^2} + 1 \right)^2 + 4 \frac{\alpha^2}{x_3^2} \frac{\xi_2^2}{\xi_3^2} + \left( \frac{\xi_1^2}{\xi_3^2} + 1 \right)^2}} \right) \\
&= x_2 - \frac{1}{2} \frac{\xi_2}{\xi_3} x_3 - x_3 \frac{\frac{1}{2} \frac{\xi_3^3}{\xi_3^2} + \frac{\xi_2}{\xi_3} \left( \frac{\xi_1^2}{\xi_3^2} + 1 \right) + 2 \frac{\alpha^2}{x_3^2} \frac{\xi_2}{\xi_3}}{\sqrt{\left( \frac{\xi_1^2}{\xi_3^2} + \frac{\xi_2^2}{\xi_3^2} + 1 \right)^2 + 4 \frac{\alpha^2}{x_3^2} \frac{\xi_2^2}{\xi_3^2} + \left( \frac{\xi_1^2}{\xi_3^2} + 1 \right)^2}} \\
&\rightarrow x_2 - 0 - x_3 \frac{0 + 0 + 0}{\sqrt{\left( \frac{\xi_1^2}{\xi_3^2} + 0 + 1 \right)^2 + 0 + \left( \frac{\xi_1^2}{\xi_3^2} + 1 \right)}} = x_2
\end{aligned}$$

for  $\xi_2 \rightarrow 0$ . Hence,  $s_2$  is continuous in  $\xi_2 = 0$ . We observe further that this representation of  $s_2$  is smooth on  $\mathbb{R}_+^3 \times \mathbb{R}^3$  with  $\xi_3 \neq 0$ .

*Proof of Lemma 3.13.* We explicitly solve the equation

$$\xi = \omega \nabla_x \varphi(s, x) \quad (3.14)$$

for  $s \in \mathbb{R}^2$  and  $\omega \in \mathbb{R} \setminus \{0\}$ . With

$$\nabla_x \varphi(s, x) = \left( \frac{x_1 - s_1}{|\mathbf{x}_s(s) - x|} + \frac{x_1 - s_1}{|x - \mathbf{x}_r(s)|}, \frac{x_2 - (s_2 - \alpha)}{|\mathbf{x}_s(s) - x|} + \frac{x_2 - (s_2 + \alpha)}{|x - \mathbf{x}_r(s)|}, \frac{x_3}{|\mathbf{x}_s(s) - x|} + \frac{x_3}{|x - \mathbf{x}_r(s)|} \right)^\top$$

we obtain the following three equations

$$\xi_1 = \omega \left( \frac{x_1 - s_1}{|\mathbf{x}_s(s) - x|} + \frac{x_1 - s_1}{|x - \mathbf{x}_r(s)|} \right), \quad (3.15)$$

$$\xi_2 = \omega \left( \frac{x_2 - (s_2 - \alpha)}{|\mathbf{x}_s(s) - x|} + \frac{x_2 - (s_2 + \alpha)}{|x - \mathbf{x}_r(s)|} \right), \quad (3.16)$$

$$\xi_3 = \omega \left( \frac{x_3}{|\mathbf{x}_s(s) - x|} + \frac{x_3}{|x - \mathbf{x}_r(s)|} \right) \quad (3.17)$$

from identity (3.14). Further, we rearrange the last one (3.17) and deduce

$$\omega = \frac{\xi_3}{x_3 \left( \frac{1}{|\mathbf{x}_s(s) - x|} + \frac{1}{|x - \mathbf{x}_r(s)|} \right)} = \frac{\xi_3 |\mathbf{x}_s(s) - x| |x - \mathbf{x}_r(s)|}{x_3 (|\mathbf{x}_s(s) - x| + |x - \mathbf{x}_r(s)|)}. \quad (3.18)$$

Inserting representation (3.18) in (3.15) yields  $\xi_1 = \frac{\xi_3 (x_1 - s_1)}{x_3}$  and so

$$s_1 = s_1(x, \xi) = x_1 - \frac{\xi_1}{\xi_3} x_3.$$

Further, we insert (3.18) in (3.16) and have

$$\xi_2 = \frac{\xi_3}{x_3} \frac{(x_2 - (s_2 - \alpha)) |x - \mathbf{x}_r(s)| + (x_2 - (s_2 + \alpha)) |\mathbf{x}_s(s) - x|}{|\mathbf{x}_s(s) - x| + |x - \mathbf{x}_r(s)|}.$$

Solving for  $s_2$  we obtain

$$\begin{aligned} s_2 &= s_2(x, \xi) = x_2 - \frac{\xi_2}{\xi_3} x_3 - \alpha \frac{|\mathbf{x}_s(s) - x| - |x - \mathbf{x}_r(s)|}{|\mathbf{x}_s(s) - x| + |x - \mathbf{x}_r(s)|} \\ &= x_2 - \frac{\xi_2}{\xi_3} x_3 - \alpha \frac{\sqrt{(x_1 - s_1)^2 + (x_2 - (s_2 - \alpha))^2 + x_3^2} - \sqrt{(x_1 - s_1)^2 + (x_2 - (s_2 + \alpha))^2 + x_3^2}}{\sqrt{(x_1 - s_1)^2 + (x_2 - (s_2 - \alpha))^2 + x_3^2} + \sqrt{(x_1 - s_1)^2 + (x_2 - (s_2 + \alpha))^2 + x_3^2}}. \end{aligned} \quad (3.19)$$

Now, we introduce the abbreviations  $c := x_1 - s_1$  and  $d := x_2 - s_2$  to simplify the terms in the following. Using these we reformulate the above identity (3.19) for  $s_2$  to

$$\frac{\xi_2}{\xi_3} x_3 = g(d)$$

where  $g: \mathbb{R} \rightarrow \mathbb{R}$  is defined by

$$g(d) = d - \alpha \frac{\sqrt{c^2 + (d + \alpha)^2 + x_3^2} - \sqrt{c^2 + (d - \alpha)^2 + x_3^2}}{\sqrt{c^2 + (d + \alpha)^2 + x_3^2} + \sqrt{c^2 + (d - \alpha)^2 + x_3^2}} = \frac{(d - \alpha) \sqrt{c^2 + (d + \alpha)^2 + x_3^2} + (d + \alpha) \sqrt{c^2 + (d - \alpha)^2 + x_3^2}}{\sqrt{c^2 + (d + \alpha)^2 + x_3^2} + \sqrt{c^2 + (d - \alpha)^2 + x_3^2}}. \quad (3.20)$$

So, if we are able to show that  $g$  is invertible, we solve equation (3.20) for  $d$  using  $d = x_2 - s_2$  and obtain a representation of  $s_2$  in terms of  $x$  and  $\xi$ .

First, we show that  $g$  is injective. Therefore, we consider its derivative given by

$$g'(d) = \frac{2(c^2 + d^2 + \alpha^2 + x_3^2)(\sqrt{c^2 + (d + \alpha)^2 + x_3^2} \sqrt{c^2 + (d - \alpha)^2 + x_3^2} + c^2 + d^2 - \alpha^2 + x_3^2)}{\sqrt{c^2 + (d - \alpha)^2 + x_3^2} \sqrt{c^2 + (d + \alpha)^2 + x_3^2} \left( \sqrt{c^2 + (d + \alpha)^2 + x_3^2} + \sqrt{c^2 + (d - \alpha)^2 + x_3^2} \right)^2}$$

for  $d \in \mathbb{R}$  and analyse its monotonicity. Since it holds

$$\begin{aligned} &\sqrt{c^2 + (d + \alpha)^2 + x_3^2} \sqrt{c^2 + (d - \alpha)^2 + x_3^2} + c^2 + d^2 - \alpha^2 + x_3^2 \\ &\geq \sqrt{(d + \alpha)^2} \sqrt{(d - \alpha)^2} + c^2 + d^2 - \alpha^2 + x_3^2 = |d^2 - \alpha^2| + c^2 + d^2 - \alpha^2 + x_3^2 \\ &\geq c^2 + x_3^2 \geq x_3^2 > 0 \end{aligned}$$

for  $d \in \mathbb{R}$ , the numerator of  $g'(d)$  is greater than zero and so  $g'(d) > 0$  for all  $d \in \mathbb{R}$ . Hence,  $g$  is strictly monotone increasing and therefore injective. For surjectivity we rearrange

$$\begin{aligned} g(d) &= d - \alpha \frac{c^2 + (d + \alpha)^2 + x_3^2 - (c^2 + (d - \alpha)^2 + x_3^2)}{(\sqrt{c^2 + (d + \alpha)^2 + x_3^2} + \sqrt{c^2 + (d - \alpha)^2 + x_3^2})^2} = d - \frac{4\alpha^2 d}{(\sqrt{c^2 + (d + \alpha)^2 + x_3^2} + \sqrt{c^2 + (d - \alpha)^2 + x_3^2})^2} \\ &= d \left( 1 - \frac{2\alpha^2}{c^2 + d^2 + \alpha^2 + x_3^2 + \sqrt{c^2 + (d + \alpha)^2 + x_3^2} \sqrt{c^2 + (d - \alpha)^2 + x_3^2}} \right) \\ &= d \frac{c^2 + d^2 - \alpha^2 + x_3^2 + \sqrt{c^2 + (d + \alpha)^2 + x_3^2} \sqrt{c^2 + (d - \alpha)^2 + x_3^2}}{c^2 + d^2 + \alpha^2 + x_3^2 + \sqrt{c^2 + (d + \alpha)^2 + x_3^2} \sqrt{c^2 + (d - \alpha)^2 + x_3^2}} \end{aligned} \quad (3.21)$$

for  $d \in \mathbb{R}$ . Hence, we see

$$\lim_{d \rightarrow \infty} \frac{g(d)}{d} = 1 \quad \text{and} \quad \lim_{d \rightarrow -\infty} \frac{g(d)}{d} = 1$$

and so  $g(\mathbb{R}) = \mathbb{R}$ . Thus,  $g$  is surjective. In order to determine the inverse of  $g$  we consider  $g(d) = \delta$  for fixed  $\delta \in \mathbb{R}$  and search for  $d$ . In case of  $\delta = 0$  we deduce  $d = 0$  as  $g(0) = 0$  holds. If we have  $\delta \neq 0$ , we achieve

$$\begin{aligned} &d \left( c^2 + d^2 - \alpha^2 + x_3^2 + \sqrt{c^2 + (d + \alpha)^2 + x_3^2} \sqrt{c^2 + (d - \alpha)^2 + x_3^2} \right) \\ &= \delta \left( c^2 + d^2 + \alpha^2 + x_3^2 + \sqrt{c^2 + (d + \alpha)^2 + x_3^2} \sqrt{c^2 + (d - \alpha)^2 + x_3^2} \right) \end{aligned}$$

by using (3.21). This is equivalent to

$$d(c^2 + d^2 - \alpha^2 + x_3^2) - \delta(c^2 + d^2 + \alpha^2 + x_3^2) = (\delta - d)\sqrt{c^2 + (d + \alpha)^2 + x_3^2}\sqrt{c^2 + (d - \alpha)^2 + x_3^2}.$$

Now, we square both sides, rearrange and divide by  $\alpha$  and  $d$  what leads to

$$-\delta d^2 + (\delta^2 - x_3^2 - c^2)d + (\alpha^2 + x_3^2 + c^2)\delta = 0.$$

We notice that  $d \neq 0$  holds for  $\delta \neq 0$  as  $g(0) = 0$  and  $g$  is injective. Further, we observe that we introduced a second solution when we squared both sides. Solving this quadratic equation and keeping in mind that  $d$  and  $\delta$  have the same signs yields the unique solution

$$d = \frac{\delta^2 - x_3^2 - c^2 + \sqrt{(\delta^2 + x_3^2 + c^2)^2 + 4\alpha^2\delta^2}}{2\delta}.$$

So, we find to given  $\delta$  a unique  $d$  such that  $g(d) = \delta$  and conclude

$$\begin{aligned} s_2 &= s_2(x, \xi) = x_2 - d(x, \xi) = x_2 - g^{-1}\left(\frac{\xi_2}{\xi_3}x_3\right) \\ &= x_2 - \frac{1}{2} \frac{\xi_3}{\xi_2} \left( \left( \frac{\xi_2^2 - \xi_1^2}{\xi_3^2} - 1 \right) x_3 + \sqrt{x_3^2 \left( \frac{\xi_1^2 + \xi_2^2}{\xi_3^2} + 1 \right)^2 + 4\alpha^2 \frac{\xi_2^2}{\xi_3^2}} \right) \end{aligned}$$

for  $x \in \mathbb{R}_+^3$  and  $\xi \in \mathbb{R}^3$  with  $\xi_2 \neq 0$  and  $\xi_3 \neq 0$ . Moreover, for  $x \in \mathbb{R}_+^3$  and  $\xi \in \mathbb{R}^3$  with  $\xi_2 = 0$  and  $\xi_3 \neq 0$  we obtain

$$s_2 = s_2(x, \xi) = x_2 - d(x, \xi) = x_2 - g^{-1}\left(\frac{\xi_2}{\xi_3}x_3\right) = x_2 - g^{-1}(0) = x_2$$

using  $g^{-1}(0) = 0$ . Hence, we have explicit expressions for  $s_1$  and  $s_2$  in terms of  $x$  and  $\xi$  and thus, for  $\omega$  by (3.18).  $\square$

In the following theorem, we calculate the wave front set of the operator  $F^*\psi F$  modified by the cut-off function  $\psi$ . If we consider its wave front set, we see that singularities related to one special direction are no part of it. Hence, using the operator  $F^*\psi F$  as reconstruction operator, we are not able to reconstruct all singularities as it does not preserve all singularities of an element  $n \in \mathcal{E}'(\mathbb{R}_+^3)$ .

In the theorem the wave front set of an operator appears. This is a notion we mentioned in Theorem 2.18.

**3.15 Theorem.** *The wave front set  $\text{WF}(F^*\psi F) \subseteq (\mathbb{R}_+^3 \times \mathbb{R}^3 \setminus \{0\}) \times (\mathbb{R}_+^3 \times \mathbb{R}^3 \setminus \{0\})$  of  $F^*\psi F$  satisfies*

$$\text{WF}(F^*\psi F) \subseteq \{(x, \xi; x, \xi) \mid \text{there exists } s \in S_0 \text{ and } \omega \neq 0 \text{ such that } \xi = \omega \nabla_x \varphi(s, x)\}.$$

So, the direction  $\xi$  to a point  $x$  consists of all non-zero multiples of

$$\nabla_x \varphi(s, x) = \nabla_x (|\mathbf{x}_s(s) - x| + |x - \mathbf{x}_r(s)|)$$

with  $s \in S_0$ .

The condition  $\xi = \omega \nabla_x \varphi(s, x)$  for  $\xi \in \mathbb{R}^3 \setminus \{0\}$  yields  $\xi_3 \neq 0$  by Lemma 3.13.

At this point, we observe that if we assume  $s$  to be in  $\mathbb{R}^2$  instead of just in  $S_0$ , we obtain

$$\text{WF}(F^*\psi F) \subseteq \{(x, \xi; x, \xi) \mid \xi_3 \neq 0\}.$$

This follows because we obtain for each  $x \in \mathbb{R}_+^3$  and  $\xi \in \mathbb{R}^3$  with  $\xi_3 \neq 0$  unique  $s \in \mathbb{R}^2$  and  $\omega \in \mathbb{R} \setminus \{0\}$  such that  $\xi = \omega \nabla_x \varphi(s, x)$  is satisfied by Lemma 3.13. Except of the boundedness,  $\mathbb{R}^2$  fulfils all assumptions made on  $S_0$  as  $\mathbb{R}^2$  is open and connected. Nevertheless, in case of applications it is natural to assume the set of sources and receivers to be bounded, even more, to be finite.

Before we prove the theorem stated above, we give some remarks how the result changes if we consider the full space  $\mathbb{R}^3$  in place of only  $\mathbb{R}_+^3$ . In this case, we obtain additionally the mirror points described in Remark 3.3. If we choose  $s$  in  $\mathbb{R}^2$ , this yields

$$\text{WF}(F^* \psi F) \subseteq \{(\tilde{x}, \xi; \tilde{x}, \xi) \mid \xi \neq 0\} \cup \{(\tilde{x}, \xi; \tilde{x}, \bar{\xi}) \mid \xi \neq 0\},$$

with  $\bar{\xi} = (\xi_1, \xi_2, -\xi_3)^\top$  for  $\xi = (\xi_1, \xi_2, \xi_3)^\top$  and  $(\xi_1, \xi_2, \xi_3)^\top = -\omega \nabla_x \varphi(s, \tilde{x})$  as before for points  $\tilde{x}$  in the full space  $\mathbb{R}^3$ . In reconstructions the above result is visible in the fact that all objects are mirrored at the  $x_1$ - $x_2$ -plane (see also figures 2-4 in [KLQ12]). These considerations are consistent with Theorem 4 in [KLQ12]. Here, the authors consider the two-dimensional case with points in the full space  $\mathbb{R}^2$ . Also, the proof of Theorem 3.15 is analogue to the one of Theorem 4 in [KLQ12]. In [KQ11] a similar result concerning a different geometry is shown.

However, if we consider the full space it is not clear whether we work still with generalised Radon transforms. Our proof which shows that we have the required fibre maps in Lemma 3.6 takes advantage of the fact that we consider just the half-space. Then, the function  $\zeta$  (see Lemma 3.5) yields exactly one value for  $x_3$ . In case of the full space, we have two possible values when taking the square root. Thus, the function  $\Psi$  defined in Lemma 3.6 is no longer a homeomorphism.

In contrast, the assumptions we verified for the generalised Radon transform do not get violated if we assume the parameter  $s$ , which determines the foci of the open half-ellipsoid, to be in  $\mathbb{R}^2$  instead of the bounded set  $S_0$ .

*Proof of Theorem 3.15.* First, we observe that  $\psi F$  is again a Fourier integral operator with symbol  $\tilde{p}(s, t, x, \omega) = \psi(s, t) p(s, t, x, \omega)$  for  $(s, t, x, \omega) \in S_0 \times (2\alpha, \infty) \times \mathbb{R}_+^3 \times \mathbb{R} \setminus \{0\}$  as  $\psi \in C_c^\infty(S_0 \times (2\alpha, \infty))$  holds. Since the canonical relation (2.5) only depends on the phase function and not on the symbol, the associated canonical relation of the operator  $\psi F$  is also the set  $C$  given in (3.12). Thus, the Hörmander-Sato Lemma (Theorem 2.18) yields

$$\text{WF}(F^* \psi F) \subseteq C^\top \circ C.$$

Of course, the points which are not in the support of  $\psi$  yield no elements of the wave front set. But as we only make a point about the inclusion, there is no difference between with or without the cut-off function  $\psi$ .

The canonical relations  $C$  and  $C^\top$  are given by (3.12) and (3.13), so that we calculate  $C^\top \circ C$  using Definition 2.7. In this way, we obtain

$$\begin{aligned} & C^\top \circ C \\ &= \{(y, -\nabla_y \phi(s, t, y, \omega); x, -\nabla_x \phi(s, t, x, \omega)) \mid \\ & \quad \text{there exists } (s, \varphi(s, x), \nabla_{(s,t)} \phi(s, t, x, \omega)) \\ & \quad \text{such that } (y, -\partial_y \phi(s, t, y, \omega); s, \varphi(s, x), \nabla_{(s,t)} \phi(s, t, x, \omega)) \in C^\top \text{ and} \\ & \quad (s, \varphi(s, x), \nabla_{(s,t)} \phi(s, t, x, \omega); x, -\nabla_x \phi(s, t, x, \omega)) \in C\} \\ &= \{(y, -\nabla_y \phi(s, t, y, \omega); x, -\nabla_x \phi(s, t, x, \omega)) \mid \text{there exists } s \in S_0 \text{ and } \omega \neq 0 \text{ such that} \\ & \quad \varphi(s, x) = \varphi(s, y), \nabla_s \phi(s, t, x, \omega) = \nabla_s \phi(s, t, y, \omega)\}. \end{aligned}$$

Here, the three required conditions on  $x \in \mathbb{R}_+^3$  and  $y \in \mathbb{R}_+^3$  are

$$\begin{aligned} |\mathbf{x}_s(s) - x| + |x - \mathbf{x}_r(s)| &= |\mathbf{x}_s(s) - y| + |y - \mathbf{x}_r(s)|, \\ \frac{x_1 - s_1}{|\mathbf{x}_s(s) - x|} + \frac{x_1 - s_1}{|x - \mathbf{x}_r(s)|} &= \frac{y_1 - s_1}{|\mathbf{x}_s(s) - y|} + \frac{y_1 - s_1}{|y - \mathbf{x}_r(s)|}, \\ \frac{x_2 - (s_2 - \alpha)}{|\mathbf{x}_s(s) - x|} + \frac{x_2 - (s_2 + \alpha)}{|x - \mathbf{x}_r(s)|} &= \frac{y_2 - (s_2 - \alpha)}{|\mathbf{x}_s(s) - y|} + \frac{y_2 - (s_2 + \alpha)}{|y - \mathbf{x}_r(s)|}. \end{aligned}$$

These are exactly the three equations of Lemma 3.2 which yields necessarily  $x = y$ . Moreover, we have  $\nabla_x \phi(s, t, x, \omega) = -\omega \nabla_x \varphi(s, x)$ . Hence, we have

$$C^\top \circ C = \{(x, \xi; x, \xi) \mid \text{there exists } s \in S_0 \text{ and } \omega \neq 0 \text{ such that } \xi = \omega \nabla_x \varphi(s, x)\}$$

by Lemma 3.13 and so the assertion is shown.  $\square$

**3.16 Remark.** In this remark, we consider again what happens if we replace the bounded set  $S_0 \subseteq \mathbb{R}^2$  by the full space  $\mathbb{R}^2$ . We define

$$\begin{aligned} \Delta_0 = \{(x, \xi; x, \xi) \in (\mathbb{R}_+^3 \times \mathbb{R}^3 \setminus \{0\}) \times (\mathbb{R}_+^3 \times \mathbb{R}^3 \setminus \{0\}) \mid \text{there exists } s \in S_0 \text{ and } \omega \neq 0 \\ \text{such that } \xi = \omega \nabla_x \varphi(s, x)\}. \end{aligned}$$

For a set  $A \subseteq \mathbb{R}_+^3 \times \mathbb{R}^3 \setminus \{0\}$  we get

$$\begin{aligned} \Delta_0 \circ A &= \{(x, \xi) \in \mathbb{R}_+^3 \times \mathbb{R}^3 \setminus \{0\} \mid \text{there exists } (y, \eta) \in A \text{ such that } (x, \xi; y, \eta) \in \Delta_0\} \\ &= \{(x, \xi) \in \mathbb{R}_+^3 \times \mathbb{R}^3 \setminus \{0\} \mid \text{there exists } s \in S_0 \text{ and } \omega \neq 0 \text{ such that } \xi = \omega \nabla_x \varphi(s, x) \\ &\quad \text{and } (x, \xi) \in A\} \subseteq A \end{aligned}$$

by Definition 2.7. Moreover, the Hörmander-Sato Lemma (see Theorem 2.18) yields

$$\begin{aligned} \text{WF}(F^* \psi F n) &\subseteq \Delta_0 \circ \text{WF}(n) \\ &= \{(x, \xi) \in \mathbb{R}_+^3 \times \mathbb{R}^3 \setminus \{0\} \mid \text{there exists } s \in S_0 \text{ and } \omega \neq 0 \text{ such that} \\ &\quad \xi = \omega \nabla_x \varphi(s, x) \text{ and } (x, \xi) \in \text{WF}(n)\} \subseteq \text{WF}(n) \end{aligned}$$

for  $n \in \mathcal{E}'(\mathbb{R}_+^3)$ . In case of  $s \in \mathbb{R}^2$ , this inclusion simplifies to

$$\text{WF}(F^* \psi F n) \subseteq \{(x, \xi) \in \mathbb{R}_+^3 \times \mathbb{R}^3 \setminus \{0\} \mid \xi_3 \neq 0 \text{ and } (x, \xi) \in \text{WF}(n)\} \subseteq \text{WF}(n)$$

by Lemma 3.13. Thus, even if we have sources and receivers at every point of  $\mathbb{R}^2$ , we cannot reconstruct singularities related to directions with vanishing third component.

### 3.3. The reconstruction operator $\Lambda$

In this section, we choose the reconstruction operator  $\Lambda$  containing the normal operator  $F^* \psi F$  and explain our choice. Afterwards, we state the explicit top order symbol of  $\Lambda$  for which we refer to our publication [GKQR18b] which is joint work with Kunstmann, Quinto and Rieder. However, we do not repeat the calculation presented therein. Instead, we give another approach to obtain the top order symbol of  $F^* \psi F$  and thus of  $\Lambda$ . We use this expression to analyse the behaviour of  $\Lambda$ . Based on these results, we define other modified reconstruction operators.

### 3.3.1. The choice of $\Lambda$

In Subsection 3.2.2 we have shown that  $F^*\psi F$  is a pseudodifferential operator of order  $-2$ . However, operators of negative order are smoothing. But it also works the other way round. At points in which a pseudodifferential operator of positive order is microlocally elliptic it emphasises the related singularities.

For this reason, we augment  $F^*\psi F$  by two differential operators which increase the order by 3. These are the Laplace operator  $\Delta$  and the derivative in third direction  $\partial_3$ . We note that these differential operators are pseudodifferential operators according to Example 2.4, which map  $\mathcal{D}'(\mathbb{R}_+^3)$  into  $\mathcal{D}'(\mathbb{R}_+^3)$  since they map  $C_c^\infty(\mathbb{R}_+^3)$  into  $C_c^\infty(\mathbb{R}_+^3)$ .

The choice of the derivative in third direction is motivated by an inversion formula for the spherical Radon transform of Klein, in which this derivative appears (see [Klei04]). The spherical Radon transform integrates over spheres instead of ellipsoids as its name suggests. In the publication [QRS11], the authors use a reconstruction operator with these two derivatives inspired by [Klei04], too. However, we notice that the choice of the derivative in third direction yields that the operator  $\Lambda$  is microlocally elliptic on the largest possible set. Hence, if we choose the derivative in first or second direction, the set on which the operator is microlocally elliptic, can be the same one or even smaller. Since there are no cancellation effects (see Remark 3.25), the latter one is more probable.

There are also some other ideas for reconstruction operators we should mention at this point. In classical Kirchhoff migration the reconstruction operator is given by  $R^\sharp K R$  where  $K$  is a one-dimensional convolution operator,  $R$  a generalised Radon transform and  $R^\sharp$  a kind of dual transform. In [Beyl85] Beylkin shows the identity  $R^\sharp K R = I_{\text{partial}} + S$ . Here,  $I_{\text{partial}}$  is an operator of partial reconstruction and  $S$  a smoothing operator. In  $R^\sharp$  Beylkin uses the reciprocal of the weight in  $R$  as weight in  $R^\sharp$ . As a consequence, this yields a partial reconstruction with smooth artifacts.

In order to analyse the microlocal behaviour of  $\Lambda$  we have to calculate its top order symbol. We refer to our joint work [GKQR18b] with Kunstmann, Quinto and Rieder and state the top order symbol we obtained there using methods of [Quin80]. Here, we explain why we are able to apply Theorem 2.1 in [Quin80] which yields the top order symbol of  $R^* R$  if  $R$  is a generalised Radon transform. Afterwards we present a more straightforward approach to obtain the top order symbol of  $\Lambda$ . Our approach uses elementary calculations and take advantage of the structure of  $F^*\psi F$ . Further, we have to apply transformations and introduce various cut-off functions to continue the phase function smoothly to  $\mathbb{R}_+^3 \times \mathbb{R}_+^3 \setminus \{0\}$ . This is necessary to be able to apply a theorem of [Shu87].

**3.17 Theorem.** *The operator  $\Lambda: \mathcal{E}'(\mathbb{R}_+^3) \rightarrow \mathcal{D}'(\mathbb{R}_+^3)$  given by*

$$\Lambda := -\Delta \partial_3 F^* \psi F$$

*is a pseudodifferential operator of order 1.*

*Proof.* According to Theorem 3.12, the operator  $F^*\psi F$  is a pseudodifferential operator of order  $-2$  which maps from  $\mathcal{E}'(\mathbb{R}_+^3)$  into  $\mathcal{D}'(\mathbb{R}_+^3)$ . The differential operators  $\Delta$  and  $\partial_3$  map both from  $C_c^\infty(\mathbb{R}_+^3)$  into  $C_c^\infty(\mathbb{R}_+^3)$  and thus  $\mathcal{D}'(\mathbb{R}_+^3)$  into  $\mathcal{D}'(\mathbb{R}_+^3)$ . As a consequence, the reconstruction operator  $\Lambda$  maps  $\mathcal{E}'(\mathbb{R}_+^3)$  into  $\mathcal{D}'(\mathbb{R}_+^3)$ . We denote the pseudodifferential operator  $F^*\psi F$  by  $P$  and assume the following representation

$$Pu(x) = \frac{1}{(2\pi)^3} \int_{\mathbb{R}^3} \int_{\mathbb{R}_+^3} a(x, \xi) u(y) e^{i(x-y) \cdot \xi} dy d\xi$$

for  $u \in C_c^\infty(\mathbb{R}_+^3)$  with symbol  $a \in S^{-2}(\mathbb{R}_+^3 \times \mathbb{R}^3)$ . Then, we obtain

$$\begin{aligned} \Delta \partial_3 P u(x) &= \Delta \partial_3 \frac{1}{(2\pi)^3} \int_{\mathbb{R}^3} \int_{\mathbb{R}_+^3} a(x, \xi) u(y) e^{i(x-y) \cdot \xi} dy d\xi \\ &= \frac{1}{(2\pi)^3} \int_{\mathbb{R}^3} \int_{\mathbb{R}_+^3} \Delta \partial_3 \left( a(x, \xi) u(y) e^{i(x-y) \cdot \xi} \right) dy d\xi \\ &= \frac{1}{(2\pi)^3} \int_{\mathbb{R}^3} \int_{\mathbb{R}_+^3} \Delta \left( \left( \partial_{x_3} a(x, \xi) + i \xi_3 a(x, \xi) \right) u(y) e^{i(x-y) \cdot \xi} \right) dy d\xi \\ &= \frac{1}{(2\pi)^3} \int_{\mathbb{R}^3} \int_{\mathbb{R}_+^3} \left( -i \xi_3 |\xi|^2 a(x, \xi) - |\xi|^2 \partial_{x_3} a(x, \xi) + (2i - 2)(\xi_1 \partial_{x_1} + \xi_2 \partial_{x_2} + \xi_3 \partial_{x_3}) a(x, \xi) \right. \\ &\quad \left. + i \xi_3 \Delta a(x, \xi) + \Delta \partial_{x_3} a(x, \xi) u(y) \right) u(y) e^{i(x-y) \cdot \xi} dy d\xi \end{aligned}$$

Hence, the operator  $\Lambda$  is again a pseudodifferential operator with top order symbol  $(x, \xi) \mapsto i \xi_3 |\xi|^2 a(x, \xi)$  for  $(x, \xi) \in \mathbb{R}_+^3 \times \mathbb{R}^3 \setminus \{0\}$ . It is of order 1 since  $a \in S^{-2}(\mathbb{R}_+^3 \times \mathbb{R}^3)$  holds. Further, we extend  $\Lambda$  to  $\mathcal{E}'(\mathbb{R}_+^3)$  as  $\Lambda$  maps  $C_c^\infty(\mathbb{R}_+^3)$  into  $C^\infty(\mathbb{R}_+^3)$ . Then,  $\Lambda$  maps  $\mathcal{E}'(\mathbb{R}_+^3)$  into  $\mathcal{D}'(\mathbb{R}_+^3)$ , which finishes the proof.  $\square$

The next theorem states the explicit top order symbol of our reconstruction operator. In order to determine the top order symbol, we apply Theorem 2.1 in [Quin80]. In the proof given below we verify the assumptions needed in detail. For the explicit calculation of its expression we refer to [GKQR18b].

**3.18 Theorem.** *Let  $(x, \xi) \in \mathbb{R}_+^3 \times \mathbb{R}^3$  with  $\xi_3 \neq 0$ . If there exist  $s \in S_0$  and  $\omega \in \mathbb{R}$  such that  $\xi = \omega \nabla_x \varphi(s, x)$  is satisfied, the top order symbol of  $\Lambda$  as a pseudodifferential operator is*

$$\sigma(\Lambda)(x, \xi) = (2\pi)^5 i \xi_3 |\xi|^2 \frac{\psi(s(x, \xi), \varphi(s(x, \xi), x)) A^2(s(x, \xi), x)}{|\omega(s(x, \xi), x)|^2 |B(s(x, \xi), x)|} \quad (3.22)$$

with

$$B(s(x, \xi), x) = \det \begin{pmatrix} [\nabla_x \varphi](s(x, \xi), x)^\top \\ [\partial_{s_1} \nabla_x \varphi](s(x, \xi), x)^\top \\ [\partial_{s_2} \nabla_x \varphi](s(x, \xi), x)^\top \end{pmatrix}. \quad (3.23)$$

In this case,  $s$  and  $\omega$  are explicitly given by

$$\omega(x, \xi) = \frac{\xi_3}{x_3 \left( \frac{1}{|\mathbf{x}_s(s(x, \xi)) - x|} + \frac{1}{|x - \mathbf{x}_r(s(x, \xi))|} \right)} = \frac{\xi_3 |\mathbf{x}_s(s(x, \xi)) - x| |x - \mathbf{x}_r(s(x, \xi))|}{x_3 (|\mathbf{x}_s(s(x, \xi)) - x| + |x - \mathbf{x}_r(s(x, \xi))|)}$$

and  $s(x, \xi) = (s_1(x, \xi), s_2(x, \xi))$  where

$$\begin{aligned} s_1(x, \xi) &= x_1 - \frac{\xi_1}{\xi_3} x_3, \\ s_2(x, \xi) &= \begin{cases} x_2 - \frac{1}{2} \frac{\xi_3}{\xi_2} \left( \left( \frac{\xi_2^2 - \xi_1^2}{\xi_3^2} - 1 \right) x_3 + \sqrt{x_3^2 \left( \frac{\xi_1^2 + \xi_2^2}{\xi_3^2} + 1 \right)^2 + 4\alpha^2 \frac{\xi_2^2}{\xi_3^2}} \right), & \text{for } \xi_2 \neq 0, \\ x_2, & \text{for } \xi_2 = 0, \end{cases} \end{aligned}$$

and thus

$$\omega(x, \xi) = \frac{\xi_3}{x_3} \frac{\sqrt{(x_1 - s_1(x, \xi))^2 + (x_2 - (s_2(x, \xi) - \alpha))^2 + x_3^2} \sqrt{(x_1 - s_1(x, \xi))^2 + (x_2 - (s_2(x, \xi) + \alpha))^2 + x_3^2}}{\sqrt{(x_1 - s_1(x, \xi))^2 + (x_2 - (s_2(x, \xi) - \alpha))^2 + x_3^2} + \sqrt{(x_1 - s_1(x, \xi))^2 + (x_2 - (s_2(x, \xi) + \alpha))^2 + x_3^2}}.$$

If there is no  $s \in S_0$  satisfying  $\xi = \omega \nabla_x \varphi(s, x)$  for some  $\omega \in \mathbb{R} \setminus \{0\}$ , we have  $\sigma(\Lambda) = 0$ . Moreover, for  $(x, \xi) \in \mathbb{R}_+^3 \times \mathbb{R}^3$  with  $\xi_3 = 0$  the top order symbol  $\sigma(\Lambda)$  vanishes.

In the following remark, we observe that  $\sigma(\Lambda)$  is well defined as the determinant  $B$  does not vanish. The determinant  $B$  is called Beylkin determinant. Beylkin considers similar transforms in his two publications [Beyl84] and [Beyl85]. In contrast to our transform  $\xi = \omega \nabla_x \varphi(s, x)$  his transforms are simpler in the following way. In [Beyl84] there is no factor  $\omega$  and in [Beyl85] the explicit expression of  $\omega$  only depends on  $\xi$  and not on  $x$ . Thus, the results given in these two publications are not applicable in our situation.

**3.19 Remark.** The explicit representation of  $B$  is given by

$$\begin{aligned} B(s, x) &= \det \begin{pmatrix} \nabla_x \varphi(s, x)^\top \\ \partial_{s_1} \nabla_x \varphi(s, x)^\top \\ \partial_{s_2} \nabla_x \varphi(s, x)^\top \end{pmatrix} \\ &= x_3 \left( \frac{1}{|\mathbf{x}_s(s) - x|} + \frac{1}{|x - \mathbf{x}_r(s)|} \right) \left( \frac{1}{|\mathbf{x}_s(s) - x|^2} + \frac{1}{|x - \mathbf{x}_r(s)|^2} \right) \left( 1 + \frac{(x_1 - s_1)^2 + (x_2 - (s_2 - \alpha))(x_2 - (s_2 + \alpha)) + x_3^2}{|\mathbf{x}_s(s) - x| |x - \mathbf{x}_r(s)|} \right) \\ &= x_3 \left( \frac{1}{|\mathbf{x}_s(s) - x|} + \frac{1}{|x - \mathbf{x}_r(s)|} \right) \left( \frac{1}{|\mathbf{x}_s(s) - x|^2} + \frac{1}{|x - \mathbf{x}_r(s)|^2} \right) \left( 1 + \frac{x - \mathbf{x}_s(s)}{|\mathbf{x}_s(s) - x|} \cdot \frac{x - \mathbf{x}_r(s)}{|x - \mathbf{x}_r(s)|} \right) \end{aligned}$$

for  $s \in S_0$  and  $x \in \mathbb{R}_+^3$ . The detailed calculation is presented in Appendix A.1. We observe that the determinant  $B$  does not vanish using the factorisation of  $B$ . The first three factors are not zero since  $x_3$  is strictly positive and due to the absolute values. The last factor only vanishes if the two unit vectors  $u := \frac{x - \mathbf{x}_s(s)}{|\mathbf{x}_s(s) - x|}$  and  $v := \frac{x - \mathbf{x}_r(s)}{|x - \mathbf{x}_r(s)|}$  point in opposite directions, so  $u = -v$ . This is not the case as the third component of both is  $x_3$  divided by a distance and so strictly positive. Hence, the determinant  $B$  is nowhere zero.

For the explicit expression of the top order symbol in Theorem 3.18 we have to evaluate a function at the point  $\Pi_{\mathbb{R}_+^3}^{-1}(x, \xi)$  for  $(x, \xi) \in \mathbb{R}_+^3 \times \mathbb{R}^3 \setminus \{0\}$ . If  $\Pi_{\mathbb{R}_+^3}$  is injective, this expression naturally simplifies. Indeed, this is the case as we see in the next corollary.

**3.20 Corollary.** *The projection  $\Pi_{\mathbb{R}_+^3} : C \rightarrow \mathbb{R}_+^3 \times \mathbb{R}^3 \setminus \{0\}$  is injective.*

*Proof.* First, we define

$$c(s, x, \omega) := (s, \varphi(s, x), \omega \nabla_x \varphi(s, x), \omega; x, \omega \nabla_x \varphi(s, x))$$

for  $(s, x, \omega) \in S_0 \times \mathbb{R}_+^3 \times \mathbb{R} \setminus \{0\}$  referring to the canonical relation  $C$  of  $F$  given in (3.12). Let  $(x, \omega \nabla_x \varphi(s, x)), (\tilde{x}, \tilde{\omega} \nabla_x \varphi(\tilde{s}, \tilde{x})) \in \Pi_{\mathbb{R}_+^3}(C)$ , i.e.  $x, \tilde{x} \in \mathbb{R}_+^3, \omega, \tilde{\omega} \in \mathbb{R} \setminus \{0\}$  and  $s, \tilde{s} \in S_0$ , with  $x = \tilde{x}$  and  $\omega \nabla_x \varphi(s, x) = \tilde{\omega} \nabla_x \varphi(\tilde{s}, \tilde{x})$ . According to Lemma 3.13, we obtain for given  $x$  and  $\xi := \omega \nabla_x \varphi(s, x)$  unique elements  $s$  and  $\omega$ . We note that we obtain  $s \in S_0$  and  $\omega \neq 0$  as otherwise the image  $(x, \omega \nabla_x \varphi(s, x))$  is not in  $\Pi_{\mathbb{R}_+^3}(C)$ . By assumption, we have  $x = \tilde{x}$  and  $\xi = \tilde{\omega} \nabla_x \varphi(\tilde{s}, \tilde{x}) = \tilde{\omega} \nabla_x \varphi(\tilde{s}, x)$ , so Lemma 3.13 yields  $s = \tilde{s}$  and  $\omega = \tilde{\omega}$ . Thus, both times the preimage is  $c(s, x, \omega)$ , which yields a unique element of  $C$ , and so  $\Pi_{\mathbb{R}_+^3}$  is injective.  $\square$

*Proof of Theorem 3.18.* For the determination of the top order symbol of  $\Lambda$  we first consider the top order symbol of  $F^* \psi F$ . We apply Theorem 2.1 in [Quin80] which yields the top order symbol of  $R^* R$  for a generalised Radon transform  $R$  if the composition is well defined. As argued before, the cut-off function  $\psi$ , which we introduced for reasons of well-definedness, has not much influence on the assertion. It just appears as a factor in the top order symbol.

Before we apply this theorem, we have to verify the two required assumptions. Setting 3.4, Lemma 3.6 and Lemma 3.7 yield the assertions made in Assumption 2.27 and Assumption 2.28. So, in our situation the first assumption of the theorem is valid. As stated in Definition 3.10, we define the generalised Radon transform in our setting using that  $\pi_{S_0 \times (2\alpha, \infty)}$  is proper by Lemma 3.8.

The second assumption in [Quin80] is that the Bolker condition holds. This means, that the projection  $\Pi_{S_0 \times (2\alpha, \infty)}: C \rightarrow S_0 \times (2\alpha, \infty) \times \mathbb{R}^3 \setminus \{0\}$  from the canonical relation  $C$  onto the first three components is an injective immersion, i.e.  $\Pi_{S_0 \times (2\alpha, \infty)}$  itself and its derivative are injective. This is verified in Section 3.2 in [FKNQ16].

Hence, Theorem 2.1 in [Quin80] yields a formula for the top order symbol of  $F^*\psi F$  evaluated at the preimage of  $(x, \xi) \in \mathbb{R}_+^3 \times \mathbb{R}^3 \setminus \{0\}$  under  $\Pi_{\mathbb{R}_+^3}$ .

In our case, the evaluation of the term given by this formula at  $\Pi_{\mathbb{R}_+^3}^{-1}(x, \xi)$  for given  $(x, \xi) \in \mathbb{R}_+^3 \times \mathbb{R}^3$  with  $\xi_3 \neq 0$  is unique because  $\Pi_{\mathbb{R}_+^3}$  is injective on this set by Corollary 3.20. For the calculation of the term which yields the top order symbol, we refer to Section 5.2 in [GKQR18b] where it is shown that

$$\sigma(F^*\psi F)(x, \xi) = \frac{(2\pi)^5 \psi(s(x, \xi), \varphi(s(x, \xi), x)) A^2(s(x, \xi), x)}{|\omega(s(x, \xi), x)|^2 |B(s(x, \xi), x)|} \quad (3.24)$$

for  $(x, \xi) \in \mathbb{R}_+^3 \times \mathbb{R}^3 \setminus \{0\}$  with  $\xi_3 \neq 0$  in case there exists  $s \in S_0$  such that  $\xi = \omega \nabla_x \varphi(s, x)$  is satisfied for some  $\omega \in \mathbb{R} \setminus \{0\}$ . In this case,  $s$  and  $\omega$  are explicitly given by Lemma 3.13. If there is no  $s \in S_0$  which fulfils this condition for some  $\omega \in \mathbb{R} \setminus \{0\}$ , we set the top order symbol  $\sigma(\Lambda)$  to be zero at this point  $(x, \xi)$ . We remark that in the definition of a pseudodifferential operator in this thesis there is an additional factor  $\frac{1}{(2\pi)^3}$  in comparison to the one in [GKQR18b]. We took this into account when stating the top order symbol.

In order to obtain the top order symbol of  $\Lambda$  we have to multiply with the symbol of  $-\Delta \partial_3$  given by  $(x, \xi) \mapsto i\xi_3 |\xi|^2$  according to Theorem 3.17. This finishes the first part of Theorem 3.18.

Now, we consider  $(x, \xi) \in \mathbb{R}_+^3 \times \mathbb{R}^3 \setminus \{0\}$  with  $\xi_3 = 0$ . The third component  $\xi_3$  of the direction in the canonical relation  $C$  in (3.12) is given by

$$\omega \left( \frac{x_3}{|\mathbf{x}_s(s) - x|} + \frac{x_3}{|x - \mathbf{x}_r(s)|} \right)$$

for  $\omega \neq 0$  and  $x_3$  is strictly positive by assumption. For this reason, we have

$$\Pi_{\mathbb{R}_+^3}^{-1}(x, \xi) = \emptyset. \quad (3.25)$$

The above representation (3.24) of the top order symbol does not hold for  $\xi_3 = 0$ . In particular, it is not defined since we divide in (3.24) by  $\omega$  and so, according to the explicit representation of  $\omega$  given in Lemma 3.13, we divide by  $\xi_3$ . Further, we observe that for  $\xi_3$  near to zero the first variable  $s_1 = s_1(x, \xi) = x_2 - \frac{\xi_1}{\xi_3}$  of the cut-off function  $\psi$  is outside the compact support of  $\psi$ . For this reason, the cut-off function  $\psi$  vanishes and the top order symbol  $\sigma(\Lambda)$  is zero for  $(x, \xi) \in \mathbb{R}_+^3 \times \mathbb{R}^3$  with  $\xi_3 = 0$ . This finishes the proof.  $\square$

In the following, we present a more elementary approach to obtain the top order symbol of  $F^*\psi F$  and thus of the operator  $\Lambda$ . Beylkin uses a comparable method in his publication [Beyl84]. However, he assumes that the argument of the exponential function is a phase function. In our case this assumption is not satisfied. For this reason, we have to carry out a similar transformation which causes additional difficulties and dependencies compared to Beylkin.

For this different approach we have to manipulate the operator  $F^*\psi F$  for technical reasons. Instead of  $F^*\psi F$  we consider the operator  $F^*\psi F_\delta$  for  $\delta > 0$  given by

$$F^*\psi F_\delta n := F^*\psi F \zeta_\delta n$$

for  $n \in \mathcal{E}'(\mathbb{R}_+^3)$ , where  $\zeta_\delta: \mathbb{R}_+^3 \rightarrow \mathbb{R}$  such that  $\zeta_\delta \in C^\infty(\mathbb{R}_+^3)$  with

$$\zeta_\delta(y) = 1 \quad \text{if } y_3 \geq 2\delta \quad \text{and} \quad \zeta_\delta(y) = 0 \quad \text{if } y_3 < \delta$$

for  $y \in \mathbb{R}_+^3$ . Then, we have  $F^*\psi F_\delta n = F^*\psi F n$  for  $\delta$  sufficiently small. Analogue to  $\Lambda$  we define  $\Lambda^\delta n := -\Delta \partial_3 F^*\psi F_\delta n$  and deduce  $\Lambda n = \Lambda^\delta n$  for  $\delta$  sufficiently small. We note that  $\delta$  depends on  $n$ .

As a consequence, there is no difference between the two operators in application if we stay a small fixed distance away from the surface.

In the numerical examples in Chapter 5 we only consider functions with compact support like the characteristic function of a ball or functions having a fixed distance to the surface like the characteristic function of a half-space in the third direction. Hence, we do not distinguish between the operators  $F^*\psi F$  and  $F^*\psi F_\delta$  after we present and discuss the following theorem.

**3.21 Theorem.** *The operator  $F^*\psi F_\delta$  is a sum of a pseudodifferential operator and a smoothing operator.*

Further, let  $(x, \xi) \in \mathbb{R}_+^3 \times \mathbb{R}^3$  with  $\xi_3 \neq 0$ . If there exist  $s \in S_0$  and  $\omega \in \mathbb{R} \setminus \{0\}$  such that  $\xi = \omega \nabla_x \varphi(s, x)$  is satisfied, the top order symbol of  $F^*\psi F_\delta$  as a pseudodifferential operator is given by

$$\sigma(F^*\psi F_\delta)(x, \xi) = \frac{(2\pi)^5 \psi(s(x, \xi), \varphi(s(x, \xi), x)) A(s(x, \xi), x)^2 \zeta_\delta(x)}{|\omega(x, \xi)|^2 |B(s(x, \xi), x)|}$$

and the top order symbol of  $\Lambda_\delta$  by

$$\sigma(\Lambda_\delta)(x, \xi) = (2\pi)^5 i \xi_3 |\xi|^2 \frac{\psi(s(x, \xi), \varphi(s(x, \xi), x)) A(s(x, \xi), x)^2 \zeta_\delta(x)}{|\omega(x, \xi)|^2 |B(s(x, \xi), x)|}$$

where  $s$  and  $\omega$  are as in Theorem 3.18.

If there is no  $s \in S_0$  satisfying  $\xi = \omega \nabla_x \varphi(s, x)$  for some  $\omega \in \mathbb{R} \setminus \{0\}$ , it holds  $\sigma(\Lambda_\delta)(x, \xi) = \sigma(F^*\psi F_\delta)(x, \xi) = 0$ .

Moreover, the top order symbols  $\sigma(\Lambda_\delta)$  and  $\sigma(F^*\psi F_\delta)$  vanish for  $(x, \xi) \in \mathbb{R}_+^3 \times \mathbb{R}^3$  with  $\xi_3 = 0$ .

For the proof of Theorem 3.21 we need the following lemma.

**3.22 Lemma.** *Let  $\delta > 0$  be given. Further, let  $K \subseteq \mathbb{R}_+^3$  be compact with  $x_3 \geq \delta$  for  $x \in K$ . Then, there exist  $M_{1,\delta} > 0$  and  $M_{2,\delta} > 0$  such that*

$$\psi(s(x, \xi), \varphi(s(x, \xi), x)) = 0$$

for  $x \in K$  if  $|\frac{\xi_1}{\xi_3}| \geq M_{1,\delta}$  or  $|\frac{\xi_2}{\xi_3}| \geq M_{2,\delta}$  is satisfied. Here,  $s$  is given by the transformation  $\xi = \omega \nabla_x \varphi(s, x)$  we described in Lemma 3.13.

Moreover, let  $M := \max\{M_{1,\delta}, M_{2,\delta}\}$ . If  $\sqrt{\frac{\xi_1^2}{\xi_3^2} + \frac{\xi_2^2}{\xi_3^2}} \geq 2M$  is satisfied, we have

$$\psi(s(x, \xi), \varphi(s(x, \xi), x)) = 0$$

for  $x \in K$ .

For the proof of this lemma we refer to Appendix A.2. We go on with the proof of Theorem 3.21.

*Proof of Theorem 3.21. STEP 1: Representation of  $F^*\psi F_\delta$  as a Fourier integral operator and transformation  $\tilde{s} := s\omega$ .* We start with rewriting  $F^*\psi F_\delta$  in order to determine the representation of  $F^*\psi F_\delta$  as a Fourier integral operator. For this purpose, we take the representations of  $F$  and  $F^*$  as Fourier integral operators which we derived in (3.9) and (3.11). We have

$$\begin{aligned} & (F^*\psi F_\delta n)(x) \\ &= \frac{1}{2\pi} \int_{S_0} A(s, x) \psi(s, \varphi(s, x)) \int_{\mathbb{R}_+^3} \int_{\mathbb{R}} A(s, y) \zeta_\delta(y) n(y) e^{i\omega(\varphi(s, x) - \varphi(s, y))} d\omega dy ds \\ &= \frac{1}{2\pi} \int_{\mathbb{R}_+^3} \int_{\mathbb{R}} \int_{\mathbb{R}^2} \psi(s, \varphi(s, x)) A(s, x) A(s, y) \zeta_\delta(y) n(y) e^{i\omega(\varphi(s, x) - \varphi(s, y))} ds d\omega dy \\ &= \frac{1}{2\pi} \int_{\mathbb{R}_+^3} \int_{\mathbb{R} \setminus \{0\}} \int_{\mathbb{R}^2} \psi(s, \varphi(s, x)) A(s, x) A(s, y) \zeta_\delta(y) n(y) e^{i\omega(\varphi(s, x) - \varphi(s, y))} ds d\omega dy \end{aligned}$$

for  $n \in C_c^\infty(\mathbb{R}_+^3)$ . The second equality holds since  $\text{supp}(\psi) \subseteq S_0 \times (2\alpha, \infty)$ .

The function  $(s, \omega) \mapsto \omega(\varphi(s, x) - \varphi(s, y))$  is not homogeneous in  $(s, \omega)$  and so not a phase function. In order to get homogeneity, we have to transform the inner integral. Before we apply the transformation given by  $\tilde{s} := s\omega$  for  $s \in \mathbb{R}^2$  and  $\omega \in \mathbb{R} \setminus \{0\}$ , we introduce some notations. We use the following abbreviations

$$A(\tilde{s}, \omega, x) := A\left(\frac{\tilde{s}}{\omega}, x\right), \quad \varphi(\tilde{s}, \omega, x) := \varphi\left(\frac{\tilde{s}}{\omega}, x\right), \quad (3.26)$$

and

$$\psi(\tilde{s}, \omega, \varphi(\tilde{s}, \omega, x)) := \psi\left(\frac{\tilde{s}}{\omega}, \varphi\left(\frac{\tilde{s}}{\omega}, x\right)\right) = \psi\left(\frac{\tilde{s}}{\omega}, \varphi(\tilde{s}, \omega, x)\right)$$

for  $\tilde{s} \in \{s\omega \mid s \in \mathbb{R}^2, \omega \in \mathbb{R} \setminus \{0\}\} = \mathbb{R}^2$  to get rid off the fractions. With these definitions we obtain

$$\begin{aligned} & (F^*\psi F_\delta n)(x) \\ &= \frac{1}{2\pi} \int_{\mathbb{R}_+^3} \int_{\mathbb{R} \setminus \{0\}} \int_{\mathbb{R}^2} \frac{\psi(\tilde{s}, \omega, \varphi(\tilde{s}, \omega, x)) A(\tilde{s}, \omega, x) A(\tilde{s}, \omega, y)}{|\omega|^2} \zeta_\delta(y) n(y) \\ & \quad e^{i\omega(\varphi(\tilde{s}, \omega, x) - \varphi(\tilde{s}, \omega, y))} d\tilde{s} d\omega dy. \end{aligned}$$

Next, we define  $\Phi: \mathbb{R}_+^3 \times \mathbb{R}_+^3 \times (\mathbb{R}^2 \times \mathbb{R} \setminus \{0\}) \rightarrow \mathbb{R}$  by

$$(x, y, (\tilde{s}, \omega)) \mapsto \omega(\varphi(\tilde{s}, \omega, x) - \varphi(\tilde{s}, \omega, y)) = \omega(\varphi\left(\frac{\tilde{s}}{\omega}, x\right) - \varphi\left(\frac{\tilde{s}}{\omega}, y\right)).$$

For  $\lambda > 0$  we easily get

$$\Phi(x, y, \lambda(\tilde{s}, \omega)) = \lambda\omega(\varphi\left(\frac{\lambda\tilde{s}}{\lambda\omega}, x\right) - \varphi\left(\frac{\lambda\tilde{s}}{\lambda\omega}, y\right)) = \lambda\Phi(x, y, (\tilde{s}, \omega))$$

for  $(x, y, (\tilde{s}, \omega)) \in \mathbb{R}_+^3 \times \mathbb{R}_+^3 \times (\mathbb{R}^2 \times \mathbb{R} \setminus \{0\})$ . Hence,  $\Phi$  is homogeneous of degree 1 in  $(\tilde{s}, \omega)$ . Moreover, we have

$$\nabla_x \Phi(x, y, (\tilde{s}, \omega)) = \omega \partial_x \varphi\left(\frac{\tilde{s}}{\omega}, x\right) - \omega \partial_x \varphi\left(\frac{\tilde{s}}{\omega}, y\right) = \omega \nabla_x \varphi\left(\frac{\tilde{s}}{\omega}, x\right)$$

and

$$\nabla_y \Phi(x, y, (\tilde{s}, \omega)) = -\omega \nabla_y \varphi\left(\frac{\tilde{s}}{\omega}, y\right)$$

for  $(x, y, (\tilde{s}, \omega)) \in \mathbb{R}_+^3 \times \mathbb{R}_+^3 \times (\mathbb{R}^2 \times \mathbb{R} \setminus \{0\})$ . Since  $x_3, y_3 > 0$  is satisfied, the gradients  $\nabla_x \Phi$  and  $\nabla_y \Phi$  are nowhere zero on  $\mathbb{R}_+^3 \times \mathbb{R}_+^3 \times (\mathbb{R}^2 \times \mathbb{R} \setminus \{0\})$  (see (1.16) for the calculation).

Consequently,  $(\nabla_x \Phi, \nabla_{(\tilde{s}, \omega)} \Phi)$  and  $(\nabla_y \Phi, \nabla_{(\tilde{s}, \omega)} \Phi)$  do not vanish on  $\mathbb{R}_+^3 \times \mathbb{R}_+^3 \times (\mathbb{R}^2 \times \mathbb{R} \setminus \{0\})$ . Hence,  $\Phi$  is phase function.

Further, we define  $p(x, y, (\tilde{s}, \omega)) = \frac{1}{2\pi} \frac{\psi(\tilde{s}, \omega, \varphi(\tilde{s}, \omega, x)) A(\tilde{s}, \omega, x) A(\tilde{s}, \omega, y) \zeta_\delta(y)}{|\omega|^2}$  for  $(x, y, (\tilde{s}, \omega)) \in \mathbb{R}_+^3 \times \mathbb{R}_+^3 \times (\mathbb{R}^2 \times \mathbb{R} \setminus \{0\})$ . Due to

$$A(\lambda \tilde{s}, \lambda \omega, x) = A\left(\frac{\lambda \tilde{s}}{\lambda \omega}, x\right) = A\left(\frac{\tilde{s}}{\omega}, x\right)$$

for  $(x, y, (\tilde{s}, \omega)) \in \mathbb{R}_+^3 \times \mathbb{R}_+^3 \times (\mathbb{R}^2 \times \mathbb{R} \setminus \{0\})$  and  $\lambda > 0$  the function  $A$  is homogeneous of degree 0 in  $(\tilde{s}, \omega)$ . Moreover, we have

$$\psi(\lambda \tilde{s}, \lambda \omega, \varphi(\tilde{s}, \omega, x)) = \psi\left(\frac{\lambda \tilde{s}}{\lambda \omega}, \varphi\left(\frac{\lambda \tilde{s}}{\lambda \omega}, x\right)\right) = \psi\left(\frac{\tilde{s}}{\omega}, \varphi\left(\frac{\tilde{s}}{\omega}, x\right)\right)$$

for  $\lambda > 0$  and  $(\tilde{s}, \omega) \in \mathbb{R}^2 \times \mathbb{R} \setminus \{0\}$ , i.e. the function  $\psi$  is homogeneous of degree 0 in  $(\tilde{s}, \omega)$ . As a consequence, the function  $p$  is homogeneous of degree  $-2$  in  $(\tilde{s}, \omega)$ . By Lemma 2.2 and the explanation before Lemma 2.1 we obtain that  $p \in C_c^\infty(\mathbb{R}_+^3 \times \mathbb{R}_+^3 \times (\mathbb{R}^2 \times \mathbb{R} \setminus \{0\}))$  is a symbol of order  $-2$ . All in all,  $F^* \psi F_\delta$  is a Fourier integral operator with phase function  $\Phi$  and symbol  $p$ .

**STEP 2: Simplification of the set  $\Sigma_\Phi$  of  $F^* \psi F_\delta$ .** We have

$$\Sigma_\Phi = \{(x, y, (\tilde{s}, \omega)) \in \mathbb{R}_+^3 \times \mathbb{R}_+^3 \times (\mathbb{R}^2 \times \mathbb{R} \setminus \{0\}) \mid \nabla_{(\tilde{s}, \omega)} \Phi(x, y, (\tilde{s}, \omega)) = 0\}$$

and

$$\partial_{s_1} \Phi(x, y, (\tilde{s}, \omega)) = \partial_{s_1}(\omega \varphi\left(\frac{\tilde{s}}{\omega}, x\right)) - \partial_{s_1}(\omega \varphi\left(\frac{\tilde{s}}{\omega}, y\right)) = 0,$$

$$\partial_{s_2} \Phi(x, y, (\tilde{s}, \omega)) = \partial_{s_2}(\omega \varphi\left(\frac{\tilde{s}}{\omega}, x\right)) - \partial_{s_2}(\omega \varphi\left(\frac{\tilde{s}}{\omega}, y\right)) = 0,$$

$$\partial_\omega \Phi(x, y, (\tilde{s}, \omega)) = \partial_\omega(\omega \varphi\left(\frac{\tilde{s}}{\omega}, x\right)) - \partial_\omega(\omega \varphi\left(\frac{\tilde{s}}{\omega}, y\right)) = 0$$

for  $(x, y, (\tilde{s}, \omega)) \in \mathbb{R}_+^3 \times \mathbb{R}_+^3 \times (\mathbb{R}^2 \times \mathbb{R} \setminus \{0\})$ . Hence, for fixed  $(\tilde{s}, \omega) \in \mathbb{R}^2 \times \mathbb{R} \setminus \{0\}$  the condition in  $\Sigma_\Phi$  is equivalent to the three equations

$$\partial_\omega(\omega \varphi\left(\frac{\tilde{s}}{\omega}, x\right)) = \partial_\omega(\omega \varphi\left(\frac{\tilde{s}}{\omega}, y\right)), \quad (3.27)$$

$$\partial_{s_2}(\omega \varphi\left(\frac{\tilde{s}}{\omega}, x\right)) = \partial_{s_2}(\omega \varphi\left(\frac{\tilde{s}}{\omega}, y\right)), \quad (3.28)$$

$$\partial_{s_1}(\omega \varphi\left(\frac{\tilde{s}}{\omega}, x\right)) = \partial_{s_1}(\omega \varphi\left(\frac{\tilde{s}}{\omega}, y\right)) \quad (3.29)$$

for  $x, y \in \mathbb{R}_+^3$ . We show that the three conditions are fulfilled if and only if  $x = y$  is satisfied.

Let  $x, y \in \mathbb{R}_+^3$  satisfying the conditions (3.27)–(3.29) be given. We calculate

$$\begin{aligned} \partial_\omega(\omega \varphi\left(\frac{\tilde{s}}{\omega}, z\right)) &= \varphi\left(\frac{\tilde{s}}{\omega}, z\right) + \omega \partial_\omega \varphi\left(\frac{\tilde{s}}{\omega}, z\right) = \varphi\left(\frac{\tilde{s}}{\omega}, z\right) + \omega [\nabla_s \varphi]\left(\frac{\tilde{s}}{\omega}, z\right) \cdot \left(-\frac{\tilde{s}}{\omega^2}\right) \\ &= \varphi\left(\frac{\tilde{s}}{\omega}, z\right) - \omega \frac{s_1}{\omega} [\partial_{s_1} \varphi]\left(\frac{\tilde{s}}{\omega}, z\right) - \omega \frac{s_2}{\omega} [\partial_{s_2} \varphi]\left(\frac{\tilde{s}}{\omega}, z\right) \\ &= \varphi\left(\frac{\tilde{s}}{\omega}, z\right) - s_1 [\partial_{s_1} \varphi]\left(\frac{\tilde{s}}{\omega}, z\right) - s_2 [\partial_{s_2} \varphi]\left(\frac{\tilde{s}}{\omega}, z\right) \end{aligned}$$

and

$$\partial_{s_2}(\omega \varphi\left(\frac{\tilde{s}}{\omega}, z\right)) = [\partial_{s_2} \varphi]\left(\frac{\tilde{s}}{\omega}, z\right)$$

for  $z \in \mathbb{R}_+^3$ . As a consequence, the equations (3.27)–(3.29) are equivalent to

$$\begin{aligned} \varphi\left(\frac{\tilde{s}}{\omega}, x\right) - s_1 [\partial_{s_1} \varphi]\left(\frac{\tilde{s}}{\omega}, x\right) - s_2 [\partial_{s_2} \varphi]\left(\frac{\tilde{s}}{\omega}, x\right) &= \varphi\left(\frac{\tilde{s}}{\omega}, y\right) - s_1 [\partial_{s_1} \varphi]\left(\frac{\tilde{s}}{\omega}, y\right) - s_2 [\partial_{s_2} \varphi]\left(\frac{\tilde{s}}{\omega}, y\right), \\ [\partial_{s_1} \varphi]\left(\frac{\tilde{s}}{\omega}, x\right) &= [\partial_{s_1} \varphi]\left(\frac{\tilde{s}}{\omega}, y\right), \\ [\partial_{s_2} \varphi]\left(\frac{\tilde{s}}{\omega}, x\right) &= [\partial_{s_2} \varphi]\left(\frac{\tilde{s}}{\omega}, y\right). \end{aligned} \quad (3.30)$$

Now, we add to the first equation of (3.30) the term

$$s_1[\partial_{s_1}\varphi](\frac{\tilde{s}}{\omega}, x) + s_2[\partial_{s_2}\varphi](\frac{\tilde{s}}{\omega}, x)$$

on both sides. According to the last two identities in (3.30) this term is equal to

$$s_1[\partial_{s_1}\varphi](\frac{\tilde{s}}{\omega}, y) + s_2[\partial_{s_2}\varphi](\frac{\tilde{s}}{\omega}, y).$$

Then, the equations (3.30) simplify to

$$\begin{aligned}\varphi(\frac{\tilde{s}}{\omega}, x) &= \varphi(\frac{\tilde{s}}{\omega}, y) \\ [\partial_{s_2}\varphi](\frac{\tilde{s}}{\omega}, x) &= [\partial_{s_2}\varphi](\frac{\tilde{s}}{\omega}, y) \\ [\partial_{s_1}\varphi](\frac{\tilde{s}}{\omega}, x) &= [\partial_{s_1}\varphi](\frac{\tilde{s}}{\omega}, y).\end{aligned}$$

By Lemma 3.2 we obtain  $x = y$  since  $[\partial_{s_1}\varphi](\frac{\tilde{s}}{\omega}, z) = \partial_{z_1}\varphi(\frac{\tilde{s}}{\omega}, z)$  and  $[\partial_{s_2}\varphi](\frac{\tilde{s}}{\omega}, z) = \partial_{z_2}\varphi(\frac{\tilde{s}}{\omega}, z)$  for  $z \in \mathbb{R}_+^3$ . For  $x = y$  the conditions (3.27)–(3.29) are clearly satisfied. This leads to

$$\Sigma_\Phi = \{(x, x, (\tilde{s}, \omega)) \mid x \in \mathbb{R}_+^3, \tilde{s} \in \mathbb{R}^2, \omega \in \mathbb{R} \setminus \{0\}\}. \quad (3.31)$$

We need this set later on in order to show that one part of the operator  $F^*\psi F_\delta$  is smoothing.

**STEP 3: Preparations for the splitting of the operator  $F^*\psi F_\delta$ .** In the next step, we split the operator  $F^*\psi F_\delta$  in two operators. One is the candidate to be a pseudodifferential operator and the other one will be smoothing. In order to obtain that the first one is a pseudodifferential operator we use a cut-off function depending on  $|x - y|$  which ensures that the integrand of the operator vanishes if  $x$  is not sufficiently near to  $y$ . Before we go more into details, we analyse how the symbol of  $F^*\psi F_\delta$  behaves for values of  $x, y \in \mathbb{R}_+^3$  with  $|x - y| < 2\varepsilon_1$  for  $\varepsilon_1 < \frac{1}{16}\delta$ .

By definition the support of the cut-off function  $\psi$  is compact. Thus, we assume

$$\text{supp}(\psi) \subseteq [-s_{\max}, s_{\max}] \times [-s_{\max}, s_{\max}] \times [t_{\min}, t_{\max}] \subseteq S_0 \times (2\alpha, \infty)$$

for  $s_{\max} > 0$  and  $t_{\min}, t_{\max} \in (2\alpha, \infty)$  with  $t_{\min} < t_{\max}$ . Further, we have

$$\psi(\tilde{s}, \omega, \varphi(\tilde{s}, \omega, x)) = \psi(\frac{\tilde{s}}{\omega}, \varphi(\frac{\tilde{s}}{\omega}, x))$$

for  $\tilde{s} \in \mathbb{R}^2, \omega \in \mathbb{R} \setminus \{0\}$  and  $x \in \mathbb{R}_+^3$  and consequently  $\psi$  vanishes outside the set

$$B := \{x \in \mathbb{R}_+^3 \mid t_{\min} \leq \varphi(\frac{\tilde{s}}{\omega}, x) \leq t_{\max}, -s_{\max} \leq \frac{\tilde{s}_1}{\omega}, \frac{\tilde{s}_2}{\omega} \leq s_{\max}\}.$$

The set  $B$  is bounded but not compact since we consider  $\mathbb{R}_+^3$ . However, we obtain a compact set if we only consider  $x$  near to  $y$ . Due to the function  $\zeta_\delta$  the symbol of  $F^*\psi F_\delta$  vanishes for  $y_3 < \delta$ . Moreover, for  $x \in B_x$  with  $|x - y| < 2\varepsilon_1$  and  $\varepsilon_1 < \frac{1}{16}\delta$  the inequality  $x_3 \geq \frac{7}{8}\delta$  is satisfied. Consequently, we define

$$K_\delta := \{x \in \mathbb{R}_+^3 \mid t_{\min} \leq \varphi(\frac{\tilde{s}}{\omega}, x) \leq t_{\max}, -s_{\max} \leq \frac{\tilde{s}_1}{\omega}, \frac{\tilde{s}_2}{\omega} \leq s_{\max}, x_3 \geq \frac{7}{8}\delta\}$$

which is compact. Hence, there exists  $R > 0$  such that

$$K_\delta \subseteq B_R(0) \subseteq \mathbb{R}^3$$

is satisfied. Based on this set we define the sets

$$K_{R,\delta} := \overline{B_{R+1}(0)} \cap \{x \in \mathbb{R}_+^3 \mid x_3 \geq \frac{1}{2}\delta\}$$

and

$$\begin{aligned}\tilde{K}_{R,\delta} &:= \{z \in \mathbb{R}_+^3 \mid |z - x| \leq \frac{1}{4}\delta, x \in K_{R,\delta}\} \\ &= \overline{B_{R+1+\frac{\delta}{4}}(0)} \cap \{x \in \mathbb{R}_+^3 \mid x_3 \geq \frac{1}{4}\delta\}\end{aligned}$$

which we need later on.

**STEP 4: Splitting  $F^*\psi F_\delta$  in a smoothing and a non-smoothing operator.** Now, we apply Lemma 3.22. We choose  $K_\delta$  as the compact set and consider elements  $x \in K_\delta$  satisfying  $x_3 \geq \frac{\delta}{2}$ . Then, we get a constant  $M$  such that

$$\psi(s(x, \xi), \varphi(s(x, \xi), x)) = 0$$

for  $\sqrt{\frac{\xi_1^2}{\xi_3^2} + \frac{\xi_2^2}{\xi_3^2}} \geq 2M$  and  $x \in K_\delta$  is satisfied. As in the lemma  $s(x, \xi)$  is given by the transformation  $\xi = \omega \nabla_x \varphi(s, x)$ . An explicit expression of  $s$  depending on  $x$  and  $\xi$  is derived in Lemma 3.13.

We define the function  $\nu_M : \mathbb{R} \rightarrow \mathbb{R}$  such that  $\nu_M \in C_c^\infty(\mathbb{R})$  and  $0 \leq \nu_M \leq 1$  with

$$\nu_M(r) = 1 \quad \text{if } |r| \leq 2M \quad \text{and} \quad \nu_M(r) = 0 \quad \text{if } |r| > 2M + 1$$

for  $r \in \mathbb{R}$ . Then, the function  $\zeta_{M_0}^* : \mathbb{R}^3 \setminus \{0\} \rightarrow \mathbb{R}$  defined by

$$\zeta_{M_0}^*(\xi) := \begin{cases} \nu_M\left(\sqrt{\frac{\xi_1^2}{\xi_3^2} + \frac{\xi_2^2}{\xi_3^2}}\right), & \text{for } \xi_3 \neq 0, \\ 0, & \text{for } \xi_3 = 0, \end{cases}$$

is in  $C^\infty(\mathbb{R}^3 \setminus \{0\})$ .

Now, let  $\varepsilon > 0$  be given such that

$$\varepsilon := \min \left\{ \varepsilon_1, \frac{1}{8 \max_{x \in K_{R,\delta}, y \in \tilde{K}_{R,\delta}, |\xi|=1} \left| \nabla_\xi \left( \zeta_{M_0}^*(\xi) \omega(x, \xi) \sum_{|\alpha|=2} \frac{1}{\alpha!} D_x^\alpha \varphi(\tilde{s}(x, \xi), \omega(x, \xi), y) \right) \right|} \right\}.$$

We note that the appearing maximum is finite since we stay away from  $x_3 = 0$  by the choice of the set  $K_{R,\delta}$ .

We find a function  $\hat{\zeta}_\varepsilon : \mathbb{R}_+^3 \times \mathbb{R}_+^3 \rightarrow \mathbb{R}$  such that  $\hat{\zeta}_\varepsilon \in C^\infty(\mathbb{R}_+^3 \times \mathbb{R}_+^3)$ ,  $0 \leq \hat{\zeta}_\varepsilon \leq 1$  and with

$$\hat{\zeta}_\varepsilon(x, y) = 1 \quad \text{if } |x - y| < \varepsilon \quad \text{and} \quad \hat{\zeta}_\varepsilon(x, y) = 0 \quad \text{if } |x - y| > 2\varepsilon$$

for  $(x, y) \in \mathbb{R}_+^3 \times \mathbb{R}_+^3$ . We use this function  $\hat{\zeta}_\varepsilon$  to split the operator  $F^*\psi F_\delta$  into two operators  $F^*\psi F_\delta = P_\delta^{0,\varepsilon} + P_\delta^\varepsilon$  where

$$\begin{aligned}(P_\delta^{0,\varepsilon} n)(x) &= \frac{1}{2\pi} \int_{\mathbb{R}_+^3} \int_{\mathbb{R} \setminus \{0\}} \int_{\mathbb{R}^2} \frac{\psi(\tilde{s}, \omega, \varphi(\tilde{s}, \omega, x)) A(\tilde{s}, \omega, x) A(\tilde{s}, \omega, y)}{|\omega|^2} (1 - \hat{\zeta}_\varepsilon(x, y)) \zeta_\delta(y) n(y) \\ &\quad e^{i\omega(\varphi(\tilde{s}, \omega, x) - \varphi(\tilde{s}, \omega, y))} d\tilde{s} d\omega dy.\end{aligned}$$

and

$$\begin{aligned}(P_\delta^\varepsilon n)(x) &= \frac{1}{2\pi} \int_{\mathbb{R}_+^3} \int_{\mathbb{R} \setminus \{0\}} \int_{\mathbb{R}^2} \frac{\psi(\tilde{s}, \omega, \varphi(\tilde{s}, \omega, x)) A(\tilde{s}, \omega, x) A(\tilde{s}, \omega, y)}{|\omega|^2} \hat{\zeta}_\varepsilon(x, y) \zeta_\delta(y) n(y) \\ &\quad e^{i\omega(\varphi(\tilde{s}, \omega, x) - \varphi(\tilde{s}, \omega, y))} d\tilde{s} d\omega dy\end{aligned}$$

for  $x \in \mathbb{R}_+^3$ . Here,  $P_\delta^\varepsilon$  is the candidate to be a pseudodifferential operator. Now, we show that  $P_\delta^{0,\varepsilon}$  is smoothing.

For this purpose, we recall the set  $\Sigma_\Phi$  given in (3.31) by

$$\Sigma_\Phi = \{(x, x, (\tilde{s}, \omega)) \mid x \in \mathbb{R}_+^3, \tilde{s} \in \mathbb{R}^2, \omega \in \mathbb{R} \setminus \{0\}\}.$$

A conic neighbourhood of  $\Sigma_\Phi$  is given by

$$V_\varepsilon := \{(x, y, \lambda(\tilde{s}, \omega)) \mid x \in \mathbb{R}_+^3, y \in B_\varepsilon(x), \lambda \geq 0, (\tilde{s}, \omega) \in \mathbb{R}^2 \times \mathbb{R} \setminus \{0\}\}.$$

For each element of  $\Sigma_\Phi$  we get  $(x, x, (\tilde{s}, \omega)) \in V_\varepsilon$  by choosing  $y = x$  and  $\lambda = 1$ . Moreover, for  $(x, y, \lambda(\tilde{s}, \omega)) \in V_\varepsilon$  we have  $(x, y, \tilde{\lambda}\lambda(\tilde{s}, \omega)) \in V_\varepsilon$  for  $\tilde{\lambda} \geq 0$ .

With this definition and the function  $\widehat{\zeta}_\varepsilon$  we get

$$\frac{\psi(\tilde{s}, \omega, \varphi(\tilde{s}, \omega, x))A(\tilde{s}, \omega, x)A(\tilde{s}, \omega, y)}{|\omega|^2} (1 - \widehat{\zeta}_\varepsilon(x, y))\zeta_\delta(y) = 0$$

for  $(x, y, \xi) \in V_\varepsilon$ . Hence, the operator  $P_\delta^{0,\varepsilon}$  vanishes on the conic neighbourhood  $V_\varepsilon$  of  $\Sigma_\Phi$  and is consequently smoothing according to Proposition 2.1 b) in [Shu87]. So, in the following we concentrate on  $P_\delta^\varepsilon$ .

**STEP 5: Expansion of the phase function.** In this step we expand the phase function in a Taylor series with a remainder. Since the function  $\varphi$  is smooth, we obtain

$$\begin{aligned} \Phi(x, y, (\tilde{s}, \omega)) &= \omega(\varphi(\tilde{s}, \omega, x) - \varphi(\tilde{s}, \omega, y)) \\ &= \omega \left( \varphi(\tilde{s}, \omega, x) - \left( \varphi(\tilde{s}, \omega, x) + \nabla_x \varphi(\tilde{s}, \omega, x) \cdot (y - x) \right. \right. \\ &\quad \left. \left. + \int_0^1 \sum_{|\alpha|=2} \frac{(1-t)^2 (y-x)^\alpha}{\alpha!} D_x^\alpha \varphi(\tilde{s}, \omega, x + t(y-x)) dt \right) \right) \\ &= \omega \nabla_x \varphi(\tilde{s}, \omega, x) \cdot (x - y) - \omega \int_0^1 \sum_{|\alpha|=2} \frac{(1-t)^2 (y-x)^\alpha}{\alpha!} D_x^\alpha \varphi(\tilde{s}, \omega, x + t(y-x)) dt \end{aligned}$$

for  $(x, y, (\tilde{s}, \omega)) \in \mathbb{R}_+^3 \times \mathbb{R}_+^3 \times (\mathbb{R}^2 \times \mathbb{R} \setminus \{0\})$ , where  $\alpha = (\alpha_1, \alpha_2, \alpha_3)^\top$  is a three-dimensional multi-index. This yields

$$\begin{aligned} (P_\delta^\varepsilon n)(x) &= \frac{1}{2\pi} \int_{\mathbb{R}_+^3} \int_{\mathbb{R} \setminus \{0\}} \int_{\mathbb{R}^2} \frac{\psi(\tilde{s}, \omega, \varphi(\tilde{s}, \omega, x))A(\tilde{s}, \omega, x)A(\tilde{s}, \omega, y)}{|\omega|^2} \widehat{\zeta}_\varepsilon(x, y)\zeta_\delta(y)n(y) \\ &\quad e^{i\Phi(x, y, (\tilde{s}, \omega))} d\tilde{s} d\omega dy \\ &= \frac{1}{2\pi} \int_{\mathbb{R}_+^3} \int_{\mathbb{R} \setminus \{0\}} \int_{\mathbb{R}^2} \frac{\psi(\tilde{s}, \omega, \varphi(\tilde{s}, \omega, x))A(\tilde{s}, \omega, x)A(\tilde{s}, \omega, y)}{|\omega|^2} \widehat{\zeta}_\varepsilon(x, y)\zeta_\delta(y)n(y) \\ &\quad e^{i\omega \nabla_x \varphi(\tilde{s}, \omega, y) \cdot (x-y) - i\omega \int_0^1 \sum_{|\alpha|=2} \frac{(1-t)^2 (y-x)^\alpha}{\alpha!} D_x^\alpha \varphi(\tilde{s}, \omega, x + t(y-x)) dt} d\tilde{s} d\omega dy. \end{aligned}$$

**STEP 6: Transformation  $\xi = \omega \nabla_x \varphi(\tilde{s}, \omega, x)$ .** Next, we transform the integral once again. Therefore, we use the Transformation  $\xi = \omega \nabla_x \varphi(\tilde{s}, \omega, x)$  which yields by Lemma 3.13 unique  $\tilde{s} = \tilde{s}(x, \xi) \in \mathbb{R}^2$  and  $\omega = \omega(x, \xi) \in \mathbb{R} \setminus \{0\}$  for given  $x \in \mathbb{R}_+^3$  and  $\xi \in \mathbb{R}^3 \setminus \{0\}$  with  $\xi_3 \neq 0$ , so

$$\xi = \omega(x, \xi) [\nabla_x \varphi](\tilde{s}(x, \xi), \omega(x, \xi), x). \quad (3.32)$$

For the determinant of the Jacobian we get

$$\tilde{B}(\tilde{s}, \omega, x) = \det \begin{pmatrix} \partial_\omega \left( \omega [\nabla_x \varphi](\tilde{s}, \omega, x)^\top \right) \\ \partial_{s_1} \left( \omega [\nabla_x \varphi](\tilde{s}, \omega, x)^\top \right) \\ \partial_{s_2} \left( \omega [\nabla_x \varphi](\tilde{s}, \omega, x)^\top \right) \end{pmatrix}$$

for  $(\tilde{s}, \omega, x) \in \mathbb{R}^2 \times \mathbb{R} \setminus \{0\} \times \mathbb{R}_+^3$ . To show that  $\tilde{B}$  does not vanish we reformulate it into the function  $B$  given in (3.23) which does not vanish. We calculate

$$\begin{aligned} \tilde{B}(\tilde{s}, \omega, x) &= \det \begin{pmatrix} \partial_\omega \left( \omega \nabla_x \varphi(\frac{\tilde{s}}{\omega}, x)^\top \right) \\ \partial_{s_1} \left( \omega \nabla_x \varphi(\frac{\tilde{s}}{\omega}, x)^\top \right) \\ \partial_{s_2} \left( \omega \nabla_x \varphi(\frac{\tilde{s}}{\omega}, x)^\top \right) \end{pmatrix} = \det \begin{pmatrix} \nabla_x \varphi(\frac{\tilde{s}}{\omega}, x)^\top + \omega \partial_\omega \nabla_x \varphi(\frac{\tilde{s}}{\omega}, x)^\top \\ \omega [\partial_{s_1} \nabla_x \varphi](\frac{\tilde{s}}{\omega}, x)^\top \frac{1}{\omega} \\ \omega [\partial_{s_2} \nabla_x \varphi](\frac{\tilde{s}}{\omega}, x)^\top \frac{1}{\omega} \end{pmatrix} \\ &= \det \begin{pmatrix} \nabla_x \varphi(\frac{\tilde{s}}{\omega}, x)^\top + \omega [\nabla_s \nabla_x \varphi](\frac{\tilde{s}}{\omega}, x)^\top \cdot \left(-\frac{s}{\omega^2}\right) \\ [\partial_{s_1} \nabla_x \varphi](\frac{\tilde{s}}{\omega}, x)^\top \\ [\partial_{s_2} \nabla_x \varphi](\frac{\tilde{s}}{\omega}, x)^\top \end{pmatrix} \\ &= \det \begin{pmatrix} \nabla_x \varphi(\frac{\tilde{s}}{\omega}, x)^\top - \frac{s_1}{\omega} [\partial_{s_1} \nabla_x \varphi](\frac{\tilde{s}}{\omega}, x)^\top - \frac{s_2}{\omega} [\partial_{s_2} \nabla_x \varphi](\frac{\tilde{s}}{\omega}, x)^\top \\ [\partial_{s_1} \nabla_x \varphi](\frac{\tilde{s}}{\omega}, x)^\top \\ [\partial_{s_2} \nabla_x \varphi](\frac{\tilde{s}}{\omega}, x)^\top \end{pmatrix} \\ &= \det \begin{pmatrix} [\nabla_x \varphi](\frac{\tilde{s}}{\omega}, x)^\top \\ [\partial_{s_1} \nabla_x \varphi](\frac{\tilde{s}}{\omega}, x)^\top \\ [\partial_{s_2} \nabla_x \varphi](\frac{\tilde{s}}{\omega}, x)^\top \end{pmatrix} = B(\frac{\tilde{s}}{\omega}, x) \end{aligned}$$

for  $s \in \mathbb{R}^2$ ,  $\omega \in \mathbb{R} \setminus \{0\}$  and  $x \in \mathbb{R}_+^3$ . Here, the determinants of the last two written matrices are equal since the second can be achieved from the first by adding  $\frac{s_1}{\omega}$  times the second line and  $\frac{s_2}{\omega}$  times the third onto the first one. As  $B$  is not zero and even strictly positive by Remark 3.19, the calculation above yields that also  $\tilde{B}$  is strictly positive. After inserting this we have

$$\begin{aligned} &(P_\delta^\varepsilon n)(x) \\ &= \frac{1}{2\pi} \int_{\mathbb{R}_+^3} \int_{\mathbb{R}^3 \setminus \{\xi \in \mathbb{R}^3 \mid \xi_3 = 0\}} \frac{\psi(\tilde{s}(x, \xi), \omega(x, \xi), \varphi(\tilde{s}, \omega, x)) A(\tilde{s}(x, \xi), \omega(x, \xi), x) A(\tilde{s}(x, \xi), \omega(x, \xi), y)}{|\omega(x, \xi)|^2 |\tilde{B}(\tilde{s}(x, \xi), \omega(x, \xi), x)|} \\ &\quad \widehat{\zeta}_\varepsilon(x, y) \zeta_\delta(y) n(y) e^{i(x-y) \cdot \xi - i\omega(x, \xi)} \int_0^1 \sum_{|\alpha|=2} \frac{(1-t)^2 (y-x)^\alpha}{\alpha!} \partial_x^\alpha \varphi(\tilde{s}(x, \xi), \omega(x, \xi), x+t(y-x)) dt \, d\xi \, dy. \end{aligned}$$

First, we remark that the cut-off function  $\psi$  vanishes for  $\xi_3$  near to zero. Consequently, we have

$$\begin{aligned} &(P_\delta^\varepsilon n)(x) \\ &= \frac{1}{2\pi} \int_{\mathbb{R}_+^3} \int_{\mathbb{R}^3} \frac{\psi(\tilde{s}(x, \xi), \omega(x, \xi), \varphi(\tilde{s}, \omega, x)) A(\tilde{s}(x, \xi), \omega(x, \xi), x) A(\tilde{s}(x, \xi), \omega(x, \xi), y)}{|\omega(x, \xi)|^2 |\tilde{B}(\tilde{s}(x, \xi), \omega(x, \xi), x)|} \\ &\quad \widehat{\zeta}_\varepsilon(x, y) \zeta_\delta(y) n(y) e^{i(x-y) \cdot \xi - i\omega(x, \xi)} \int_0^1 \sum_{|\alpha|=2} \frac{(1-t)^2 (y-x)^\alpha}{\alpha!} \partial_x^\alpha \varphi(\tilde{s}(x, \xi), \omega(x, \xi), x+t(y-x)) dt \, d\xi \, dy. \end{aligned}$$

Moreover, we notice that  $\tilde{s}$  and  $\omega$  depending on  $x$  and  $\xi$  are smooth. At this point, it is crucial that the integrand of  $P_\delta^\varepsilon n$  vanishes for  $x \notin K_\delta$  due to the cut-off functions  $\psi$ ,  $\widehat{\zeta}_\varepsilon$  and  $\zeta_\delta$ . This means that the value of  $x_3$  stays away from zero. After observing this, we obtain the smoothness of the symbol by the representations given in Lemma 3.13 and Remark 3.14.

**STEP 7:**  $P_\delta^\varepsilon$  is a Fourier integral operator. In order to show that  $P_\delta^\varepsilon$  is a pseudodifferential operator we aim to apply Theorem 19.1 in [Shu87]. For this purpose, we have to verify that  $P_\delta^\varepsilon$  is a Fourier integral operator first.

Actually, we would like to take  $\Phi$  as the phase function of  $P_\delta^\varepsilon$ . However, a suitable phase function has to be an element of  $C^\infty(\mathbb{R}_+^3 \times \mathbb{R}_+^3 \times \mathbb{R}^3 \setminus \{0\})$  and  $\Phi$  is not smooth for  $(x, y, \xi) \in \mathbb{R}_+^3 \times \mathbb{R}_+^3 \times \mathbb{R}^3 \setminus \{0\}$  with  $\xi_3 = 0$ . In order to obtain a smooth version of  $\Phi$  we have to modify it. The modification has to be in such a way that we do not change the operator  $P_\delta^\varepsilon$ . Moreover, we ensure that the modification vanishes for  $x, y \in \mathbb{R}_+^3$  outside of compact sets. Thus, we are able to show the needed assumptions stated in Theorem 19.1 in [Shu87]. We define  $\Psi$  by

$$\begin{aligned} \Psi(x, y, \xi) := & \xi \cdot (x - y) - \bar{\zeta}_R(x) \widehat{\zeta}_{2\varepsilon}(x, y) \zeta_{M_0}^*(\xi) \\ & \cdot \omega(x, \xi) \int_0^1 \sum_{|\alpha|=2} \frac{(1-t)^2 (y-x)^\alpha}{\alpha!} D_x^\alpha \varphi(\tilde{s}(x, \xi), \omega(x, \xi), x + t(y-x)) dt \end{aligned}$$

for  $(x, y, \xi) \in \mathbb{R}_+^3 \times \mathbb{R}_+^3 \times \mathbb{R}^3 \setminus \{0\}$ . Here, the functions  $\bar{\zeta}_R$  and  $\widehat{\zeta}_{2\varepsilon}$  are given as follows. We choose  $\bar{\zeta}_R: \mathbb{R}_+^3 \rightarrow \mathbb{R}$  such that  $\bar{\zeta}_R \in C_c^\infty(\mathbb{R}_+^3)$  and  $0 \leq \bar{\zeta}_R \leq 1$  with

$$\zeta_R(x) = 1, \quad \text{on } K_{R,\delta}^1 := \overline{B_R(0)} \cap \{x \in \mathbb{R}_+^3 \mid x_3 \geq \frac{3}{4}\delta\} \quad \text{and} \quad \zeta_R(x) = 0 \quad \text{on } \mathbb{R}_+^3 \setminus K_{R,\delta}$$

for  $x \in \mathbb{R}_+^3$ , where we recall that  $K_{R,\delta} = \overline{B_{R+1}(0)} \cap \{x \in \mathbb{R}_+^3 \mid x_3 \geq \frac{\delta}{2}\}$ . Moreover, we consider  $\widehat{\zeta}_{2\varepsilon}: \mathbb{R}_+^3 \times \mathbb{R}_+^3 \rightarrow \mathbb{R}$  such that  $\widehat{\zeta}_{2\varepsilon} \in C_c^\infty(\mathbb{R}_+^3 \times \mathbb{R}_+^3)$ ,  $0 \leq \widehat{\zeta}_{2\varepsilon} \leq 1$  with

$$\widehat{\zeta}_{2\varepsilon}(x, y) = 1, \quad \text{if } |x - y| < 2\varepsilon \quad \text{and} \quad \widehat{\zeta}_{2\varepsilon}(x, y) = 0 \quad \text{if } |x - y| > 4\varepsilon$$

for  $(x, y) \in \mathbb{R}_+^3 \times \mathbb{R}_+^3$ .

We notice that for  $\xi_3 = 0$  there exist no  $\tilde{s}$  and  $\omega$  depending on  $x$  and  $\xi$ . However,  $\zeta_{M_0}^*(\xi)$  for  $\xi \in \mathbb{R}^3 \setminus \{0\}$  with  $\xi_3 = 0$  is zero. Hence,  $\Psi$  is equal to  $\xi \cdot (x - y)$  for  $x, y \in \mathbb{R}_+^3$  and  $\xi \in \mathbb{R}^3 \setminus \{0\}$  with  $\xi_3 = 0$ .

The idea is to show that the function  $\Psi$  coincides with  $\Phi$  on the set on which the integrand of  $P_\delta^\varepsilon n$  does not vanish.

In the representation of  $\Psi$  are three cut-off functions we inserted for two different reasons. We truncate with  $\zeta_{M_0}^*$  with respect to the variable  $\xi$  to ensure that  $\Psi \in C^\infty(\mathbb{R}_+^3 \times \mathbb{R}_+^3 \times \mathbb{R}^3 \setminus \{0\})$  is satisfied as we argued above. The smoothness is needed to show that  $\Psi$  is a phase function. Moreover, we truncate with  $\bar{\zeta}_R$  with respect to the variable  $x$  in order to obtain that  $\Psi$  vanishes for  $x$  off the compact set  $K_{R,\delta}$ . The cut-off function  $\widehat{\zeta}_{2\varepsilon}$  ensures that the phase function vanishes if  $y$  is not in the compact set  $\widetilde{K}_{R,\delta}$ . We recall that

$$\begin{aligned} \widetilde{K}_{R,\delta} &= \{z \in \mathbb{R}_+^3 \mid |z - x| \leq \frac{1}{4}\delta, x \in K_{R,\delta}\} \\ &= \overline{B_{R+1+\frac{\delta}{4}}(0)} \cap \{x \in \mathbb{R}_+^3 \mid x_3 \geq \frac{1}{4}\delta\}. \end{aligned}$$

Finally, we analyse whether we have chosen the cut-off functions in such a way that  $\Psi$  is equal to  $\Phi$  if the integrand of  $F_\delta^\varepsilon n$  does not vanish. By the definition of  $\Psi$  we have

$$\Phi(x, y, (\tilde{s}(x, \xi), \omega(x, \xi))) = \Psi(x, y, \xi)$$

for  $|x - y| \leq 2\varepsilon$ ,  $\xi \in \mathbb{R}^3$  with  $\sqrt{\frac{\xi_1^2}{\xi_3^2} + \frac{\xi_2^2}{\xi_3^2}} < 2M$  and  $x \in K_{R,\delta}^1$ . In case of  $|x - y| > 2\varepsilon$  the function  $\widehat{\zeta}_{2\varepsilon}$  vanishes. If  $x \notin K_{R,\delta}^1$ , we have  $x \notin K_{R,\delta}$  and hence the cut-off function  $\psi$  vanishes. Last, for  $\xi \in \mathbb{R}^3$  with  $\sqrt{\frac{\xi_1^2}{\xi_3^2} + \frac{\xi_2^2}{\xi_3^2}} \geq 2M$  and  $x \in K_{\delta,x}$  the cut-off function  $\psi$  is zero

by Lemma 3.22. Consequently, the integrand of  $P_\delta^\varepsilon n$  is zero. Hence, we have

$$\begin{aligned}
& (P_\delta^\varepsilon n)(x) \\
&= \frac{1}{2\pi} \int_{\mathbb{R}_+^3} \int_{\mathbb{R}^3} \frac{\psi(\tilde{s}(x, \xi), \omega(x, \xi), \varphi(\tilde{s}(x, \xi), \omega(x, \xi), x))A(\tilde{s}(x, \xi), \omega(x, \xi), x)A(\tilde{s}(x, \xi), \omega(x, \xi), y))}{|\omega(x, \xi)|^2} \\
&\quad \widehat{\zeta}_\varepsilon(x, y)\zeta_\delta(y)n(y)e^{i\Phi(x, y, (\tilde{s}(x, \xi), \omega(x, \xi)))} d\xi dy \\
&= \frac{1}{2\pi} \int_{\mathbb{R}_+^3} \int_{\mathbb{R}^3} \frac{\psi(\tilde{s}(x, \xi), \omega(x, \xi), \varphi(\tilde{s}(x, \xi), \omega(x, \xi), x))A(\tilde{s}(x, \xi), \omega(x, \xi), x)A(\tilde{s}(x, \xi), \omega(x, \xi), y))}{|\omega(x, \xi)|^2} \\
&\quad \widehat{\zeta}_\varepsilon(x, y)\zeta_\delta(y)n(y)e^{i\Psi(x, y, \xi)} d\xi dy
\end{aligned}$$

for  $x \in \mathbb{R}_+^3$ . Next, we show that  $\Psi$  is a phase function on  $\mathbb{R}_+^3 \times \mathbb{R}_+^3 \times \mathbb{R}^3 \setminus \{0\}$ .

First, we start with homogeneity. So, let  $\lambda > 0$  be given. We have

$$\varphi(\lambda\tilde{s}, \lambda\omega, x) = \varphi\left(\frac{\lambda\tilde{s}}{\lambda\omega}, x\right) = \varphi(\tilde{s}, \omega, x)$$

for  $(\tilde{s}, \omega, x) \in \mathbb{R}^2 \times \mathbb{R} \setminus \{0\} \times \mathbb{R}_+^3$  and so  $\varphi$  and  $\nabla_x \varphi$  are homogeneous of degree 0 in  $(\tilde{s}, \omega)$ . If we insert  $\lambda\xi$  in transformation (3.32) instead of  $\xi$ , we get

$$\lambda\xi = \omega(x, \lambda\xi)\nabla_x \varphi(\tilde{s}(x, \lambda\xi), \omega(x, \lambda\xi), x) = \omega(x, \lambda\xi)\nabla_x \varphi\left(\frac{\tilde{s}(x, \lambda\xi)}{\omega(x, \lambda\xi)}, x\right)$$

and by multiplying equation (3.32) with  $\lambda$  we obtain

$$\lambda\xi = \lambda\omega(x, \xi)[\nabla_x \varphi](\tilde{s}(x, \xi), \omega(x, \xi), x) = \lambda\omega(x, \xi)[\nabla_x \varphi]\left(\frac{\tilde{s}(x, \xi)}{\omega(x, \xi)}, x\right).$$

From the last two equations we conclude

$$\omega(x, \lambda\xi)\nabla_x \varphi\left(\frac{\tilde{s}(x, \lambda\xi)}{\omega(x, \lambda\xi)}, x\right) = \lambda\omega(x, \xi)\nabla_x \varphi\left(\frac{\lambda\tilde{s}(x, \xi)}{\lambda\omega(x, \xi)}, x\right)$$

for  $x \in \mathbb{R}_+^3$  and  $\xi \in \mathbb{R}^3 \setminus \{0\} \times \mathbb{R}_+^3$  with  $\xi_3 \neq 0$ . Since the transformation  $\xi = \omega\nabla_x \varphi(s, x)$  stated in (3.32) yield unique  $(s, \omega) \in \mathbb{R}^2 \times \mathbb{R} \setminus \{0\}$  for  $x \in \mathbb{R}_+^3$  and  $\xi \in \mathbb{R}^3 \setminus \{0\} \times \mathbb{R}_+^3$  with  $\xi_3 \neq 0$ , we get  $\lambda\omega(x, \xi) = \omega(x, \lambda\xi)$  and  $\lambda\tilde{s}(x, \xi) = \tilde{s}(x, \lambda\xi)$  for  $x \in \mathbb{R}_+^3$  and  $\xi \in \mathbb{R}^3 \setminus \{0\} \times \mathbb{R}_+^3$  with  $\xi_3 \neq 0$  and so  $\omega$  and  $\tilde{s}$  are homogeneous of degree 1 in  $\xi$ .

Using this and that  $\zeta_{M_0}^*$  is homogeneous of order 0, we obtain

$$\begin{aligned}
& \Psi(x, y, \lambda\xi) \\
&= \lambda\xi \cdot (x - y) - \bar{\zeta}_R(x)\widehat{\zeta}_{2\varepsilon}(x, y)\zeta_{M_0}^*(\lambda\xi)\omega(x, \lambda\xi) \\
&\quad \int_0^1 \sum_{|\alpha|=2} \frac{(1-t)^2(y-x)^\alpha}{\alpha!} D_x^\alpha \varphi(\tilde{s}(x, \lambda\xi), \omega(x, \lambda\xi), x + t(y-x)) dt \\
&= \lambda(y-x) \cdot \xi - \bar{\zeta}_R(x)\widehat{\zeta}_{2\varepsilon}(x, y)\zeta_{M_0}^*(\xi)\lambda\omega(x, \xi) \\
&\quad \int_0^1 \sum_{|\alpha|=2} \frac{(1-t)^2(y-x)^\alpha}{\alpha!} D_x^\alpha \varphi(\lambda\tilde{s}(x, \xi), \lambda\omega(x, \xi), x + t(y-x)) dt \\
&= \lambda\xi \cdot (y-x) - \lambda\bar{\zeta}_R(x)\widehat{\zeta}_{2\varepsilon}(x, y)\zeta_{M_0}^*(\xi)\omega(x, \xi) \\
&\quad \int_0^1 \sum_{|\alpha|=2} \frac{(1-t)^2(y-x)^\alpha}{\alpha!} D_x^\alpha \varphi(\tilde{s}(x, \xi), \omega(x, \xi), x + t(y-x)) dt \\
&= \lambda\Psi(y, x, \xi)
\end{aligned}$$

for  $(x, y, \xi) \in \mathbb{R}_+^3 \times \mathbb{R}_+^3 \times \mathbb{R}^3 \setminus \{0\}$  since  $\varphi$  and consequently  $\partial_{x_i}^{\alpha_i} \varphi$  for  $i \in \{1, 2, 3\}$  are homogeneous of degree 0 in  $(\tilde{s}, \omega)$ . We shortly remark that this also holds for  $\xi \in \mathbb{R}^3$  with  $\xi_3 = 0$  as then  $\zeta_{M_0}^*(\xi)$  is zero. Moreover, we have

$$\begin{aligned} & \nabla_x \Psi(x, y, \xi) \\ &= \xi - \nabla_x \left( \bar{\zeta}_R(x) \widehat{\zeta}_{2\varepsilon}(x, y) \zeta_{M_0}^*(\xi) \omega(x, \xi) \right. \\ & \quad \left. \int_0^1 \sum_{|\alpha|=2} \frac{(1-t)^2 (y-x)^\alpha}{\alpha!} D_x^\alpha \varphi(\tilde{s}(x, \xi), \omega(x, \xi), x+t(y-x)) dt \right) \end{aligned}$$

for  $(x, y, \xi) \in \mathbb{R}_+^3 \times \mathbb{R}_+^3 \times \mathbb{R}^3 \setminus \{0\}$ ,

$$\begin{aligned} & \nabla_y \Psi(x, y, \xi) \\ &= -\xi - \nabla_y \left( \bar{\zeta}_R(x) \widehat{\zeta}_{2\varepsilon}(x, y) \zeta_{M_0}^*(\xi) \omega(x, \xi) \right. \\ & \quad \left. \int_0^1 \sum_{|\alpha|=2} \frac{(1-t)^2 (y-x)^\alpha}{\alpha!} D_x^\alpha \varphi(\tilde{s}(x, \xi), \omega(x, \xi), x+t(y-x)) dt \right) \end{aligned}$$

for  $(x, y, \xi) \in \mathbb{R}_+^3 \times \mathbb{R}_+^3 \times \mathbb{R}^3 \setminus \{0\}$  and

$$\begin{aligned} & \nabla_\xi \Psi(x, y, \xi) \\ &= x - y - \nabla_\xi \left( \bar{\zeta}_R(x) \widehat{\zeta}_{2\varepsilon}(x, y) \zeta_{M_0}^*(\xi) \omega(x, \xi) \right. \\ & \quad \left. \int_0^1 \sum_{|\alpha|=2} \frac{(1-t)^2 (y-x)^\alpha}{\alpha!} D_x^\alpha \varphi(\tilde{s}(x, \xi), \omega(x, \xi), x+t(y-x)) dt \right) \end{aligned}$$

for  $(x, y, \xi) \in \mathbb{R}_+^3 \times \mathbb{R}_+^3 \times \mathbb{R}^3 \setminus \{0\}$ . Since the phase function  $\Psi$  is homogeneous of degree 1 in the third variable, the function  $\nabla_\xi \Psi$  is homogeneous of order 0 in the third variable according to Lemma 2.1. Thus, we have

$$\nabla_\xi \Psi(x, y, \xi) = \nabla_\xi \Psi\left(x, y, |\xi| \frac{\xi}{|\xi|}\right) = \nabla_\xi \Psi\left(x, y, \frac{\xi}{|\xi|}\right)$$

for  $(x, y, \xi) \in \mathbb{R}_+^3 \times \mathbb{R}_+^3 \times \mathbb{R}^3 \setminus \{0\}$ . For  $\xi \in \mathbb{R}^3 \setminus \{0\}$  with  $|\xi| = 1$  we calculate

$$\begin{aligned} & |\nabla_\xi \Psi(x, y, \xi)| \\ & \geq |x - y| - |\bar{\zeta}_R(x) \widehat{\zeta}_{2\varepsilon}(x, y)| \\ & \quad \left| \nabla_\xi \left( \zeta_{M_0}^*(\xi) \omega(x, \xi) \int_0^1 \sum_{|\alpha|=2} \frac{(1-t)^2 (y-x)^\alpha}{\alpha!} D_x^\alpha \varphi(\tilde{s}(x, \xi), \omega(x, \xi), x+t(y-x)) dt \right) \right| \\ & \geq |x - y| - |x - y|^2 \max_{x \in K_{R,\delta}, y \in \tilde{K}_{R,\delta}, |\xi|=1} \left| \nabla_\xi \left( \zeta_{M_0}^*(\xi) \omega(x, \xi) \sum_{|\alpha|=2} \frac{1}{\alpha!} D_x^\alpha \varphi(\tilde{s}(x, \xi), \omega(x, \xi), y) \right) \right| \\ & \geq |x - y| - 4\varepsilon |x - y| \max_{x \in K_{R,\delta}, y \in \tilde{K}_{R,\delta}, |\xi|=1} \left| \nabla_\xi \left( \zeta_{M_0}^*(\xi) \omega(x, \xi) \sum_{|\alpha|=2} \frac{1}{\alpha!} D_x^\alpha \varphi(\tilde{s}(x, \xi), \omega(x, \xi), y) \right) \right| \\ & \geq |x - y| - \frac{1}{2} |x - y| = \frac{1}{2} |x - y| \end{aligned}$$

for  $(x, y) \in \mathbb{R}_+^3 \times \mathbb{R}_+^3$  since  $\widehat{\zeta}_{2\varepsilon}$  vanishes for  $|x - y| > 4\varepsilon$  and by the choice of  $\varepsilon$ . Moreover, we used that  $\Psi$  vanishes for  $x \notin K_{R,\delta}$  and  $y \notin \tilde{K}_{R,\delta}$ .

As a consequence, we have  $x = y$  if  $\nabla_\xi \Psi(x, y, \xi) = 0$  for  $(x, y, \xi) \in \mathbb{R}_+^3 \times \mathbb{R}_+^3 \times \mathbb{R}^3 \setminus \{0\}$  is satisfied. Since  $\nabla_\xi \Psi$  vanishes for  $y = x$ , we have consequently  $\nabla_\xi \Psi(x, y, \xi) = 0$  if and only

if  $x = y$  is fulfilled. Further, it holds  $\nabla_x \Psi(x, x, \xi) = \xi$  and  $\nabla_y \Psi(x, x, \xi) = -\xi$  for  $(x, y, \xi) \in \mathbb{R}_+^3 \times \mathbb{R}_+^3 \times \mathbb{R}^3 \setminus \{0\}$ . Thus,  $(\nabla_x \Psi, \nabla_\xi \Psi)$  and  $(\nabla_y \Psi, \nabla_\xi \Psi)$  do not vanish on  $\mathbb{R}_+^3 \times \mathbb{R}_+^3 \times \mathbb{R}^3 \setminus \{0\}$ . Altogether, we obtain that  $\Psi$  is a phase function.

In addition, we define

$$\begin{aligned} & \tilde{p}(x, y, \xi) \\ &= \frac{1}{2\pi} \frac{\psi(\tilde{s}(x, \xi), \omega(x, \xi), \varphi(\tilde{s}(x, \xi), \omega(x, \xi), x)) A(\tilde{s}(x, \xi), \omega(x, \xi), x) A(\tilde{s}(x, \xi), \omega(x, \xi), y))}{|\omega(x, \xi)|^2 |\tilde{B}(\tilde{s}(x, \xi), \omega(x, \xi), x)|} \cdot \widehat{\zeta}_{2\varepsilon}(x, y) \zeta_\delta(y) \\ &= \frac{1}{2\pi} \frac{\psi\left(\frac{\tilde{s}(x, \xi)}{\omega(x, \xi)}, \varphi\left(\frac{\tilde{s}(x, \xi)}{\omega(x, \xi)}, x\right)\right) A\left(\frac{\tilde{s}(x, \xi)}{\omega(x, \xi)}, x\right) A\left(\frac{\tilde{s}(x, \xi)}{\omega(x, \xi)}, y\right)}{|\omega(x, \xi)|^2 \left| \tilde{B}\left(\frac{\tilde{s}(x, \xi)}{\omega(x, \xi)}, x\right) \right|} \widehat{\zeta}_{2\varepsilon}(x, y) \zeta_\delta(y) \end{aligned}$$

for  $(x, y, \xi) \in \mathbb{R}_+^3 \times \mathbb{R}_+^3 \times \mathbb{R}^3 \setminus \{0\}$ . Since  $\tilde{s}$  and  $\omega$  are homogeneous of degree 1 in  $\xi$  and the functions  $A$ ,  $\varphi$  and  $\psi$  are homogeneous of degree 0 in  $(\tilde{s}, \omega)$ , the functions  $A$ ,  $\varphi$  and  $\psi$  are homogeneous of degree 0 in  $\xi$ . Moreover, every element of the matrix with determinant  $\tilde{B}$  is homogeneous of degree zero in  $\xi$  because it consists of  $\varphi$  or derivatives of  $\varphi$  with respect to  $x$  and  $s$ . Thus, also the determinant  $\tilde{B}$  is homogeneous of degree zero in  $\xi$ . However, we recall that  $\omega$  is homogeneous of degree 1 in  $\xi$ . Altogether, the function  $\tilde{p}$  is homogeneous of degree  $-2$  in  $\xi$  since the denominator contains  $\omega^2$  and all other appearing functions are homogeneous of degree 0 in  $\xi$ .

As aforementioned, the functions  $\tilde{s}$  and  $\omega$  are smooth due to the fact that we stay away from  $x_3 = 0$  because of the cut-off functions  $\widehat{\zeta}_\varepsilon$  and  $\zeta_\delta$ . The other appearing functions in  $\tilde{p}$  are smooth on  $\mathbb{R}_+^3 \times \mathbb{R}_+^3 \times \mathbb{R}^3 \setminus \{0\}$ , too. Further, the function  $\tilde{p}$  is locally integrable on compact subsets in  $\mathbb{R}_+^3 \times \mathbb{R}_+^3$  and around  $\xi = 0$ .

Altogether, the function  $\tilde{p}$  is smooth and homogeneous of degree  $-2$  in  $\xi$  and thus a symbol of order  $-2$  according to Lemma 2.2 and the explanation before Lemma 2.1. This yields that  $P_\delta^\varepsilon$  is a Fourier integral operator.

**STEP 8:**  $P_\delta^\varepsilon$  is a pseudodifferential operator. Finally, we show that  $P_\delta^\varepsilon$  is not only a Fourier integral operator but also a pseudodifferential operator. In order to obtain this result, we apply Theorem 19.1 in [Shu87]. In this theorem two conditions are given, which we have to verify. The first one is that  $\nabla_\xi \Psi(x, y, \xi) = 0$  is satisfied if and only if  $y = x$  holds for  $\xi \in \mathbb{R}^3 \setminus \{0\}$  with  $\xi_3 \neq 0$ . We showed this condition in STEP 7 in order to prove that  $\Psi$  is a phase function. For the second one we calculate  $\nabla_x \Psi(x, x, \xi)$  for  $x \in \mathbb{R}_+^3$  and  $\xi \in \mathbb{R}^3 \setminus \{0\}$ . We have

$$\nabla_x \Psi(x, x, \xi) = \xi$$

for  $x \in \mathbb{R}_+^3$  and  $\xi \in \mathbb{R}^3 \setminus \{0\}$ , which is the second condition.

Hence, the operator  $P_\delta^\varepsilon$  is a pseudodifferential operator of order  $-2$ . By equation (2.1.4) in [Hör71] the top order symbol of  $P_\delta^\varepsilon$  is given by

$$\begin{aligned} & \sigma(P_\delta^\varepsilon)(x, \xi) \\ &= (2\pi)^6 p(x, x, \xi) \\ &= \frac{(2\pi)^5 \psi(\tilde{s}(x, \xi), \omega(x, \xi), \varphi(\tilde{s}(x, \xi), \omega(x, \xi), x)) A(\tilde{s}(x, \xi), \omega(x, \xi), x) A(\tilde{s}(x, \xi), \omega(x, \xi), x))}{|\omega(x, \xi)|^2 |\tilde{B}(\tilde{s}(x, \xi), \omega(x, \xi), x)|} \cdot \widehat{\zeta}_\varepsilon(x, x) \zeta_\delta(x) \end{aligned}$$

$$= \frac{(2\pi)^5 \psi(\tilde{s}(x, \xi), \omega(x, \xi), \varphi(\tilde{s}, \omega, x)) A(\tilde{s}(x, \xi), \omega(x, \xi), x)^2 \zeta_\delta(x)}{|\omega(x, \xi)|^2 |\tilde{B}(\tilde{s}(x, \xi), \omega(x, \xi), x)|}$$

for  $x \in \mathbb{R}_+^3$  and  $\xi \in \mathbb{R}^3 \setminus \{0\}$ .

Last, we notice that the transformation  $\xi = \omega \nabla_x \varphi(s, x)$  is injective in  $s$  and  $\omega$  according to Lemma 3.13. Hence, we obtain for  $\omega$  and  $\frac{\tilde{s}}{\omega}$  the same values as for  $\omega$  and  $s$ . Using the identity  $\tilde{s}\omega = s$  we obtain

$$\begin{aligned} \sigma(P_\delta^\varepsilon)(x, \xi) &= \frac{(2\pi)^5 \psi\left(\frac{\tilde{s}(x, \xi)}{\omega(x, \xi)}, \varphi\left(\frac{\tilde{s}(x, \xi)}{\omega(x, \xi)}, x\right)\right) A\left(\frac{\tilde{s}(x, \xi)}{\omega(x, \xi)}, x\right)^2}{|\omega(x, \xi)|^2 |\tilde{B}\left(\frac{\tilde{s}(x, \xi)}{\omega(x, \xi)}, x\right)|} \zeta_\delta(x) \\ &= \frac{(2\pi)^5 \psi(s(x, \xi), \varphi(s(x, \xi), x)) A(s(x, \xi), x)^2}{|\omega(x, \xi)|^2 |B(s(x, \xi), x)|} \zeta_\delta(x) \end{aligned}$$

for  $x \in \mathbb{R}_+^3$  and  $\xi \in \mathbb{R}^3 \setminus \{0\}$  with  $\xi_3 \neq 0$  if there exist  $s \in S_0$  and  $\omega \in \mathbb{R} \setminus \{0\}$  such that  $\xi = \omega \nabla_x \varphi(s, x)$  is satisfied.

If we consider  $x \in \mathbb{R}_+^3$  and  $\xi \in \mathbb{R}^3 \setminus \{0\}$  with  $\xi_3 = 0$  the top order symbol vanishes due to the cut-off function  $\psi$ . Moreover, in case there exist no  $s \in S_0$  and  $\omega \in \mathbb{R} \setminus \{0\}$  such that  $\xi = \omega \nabla_x \varphi(s, x)$  holds, the top order symbol is given by zero. This is ensured by the cut-off function  $\psi$ . We refer also to the explanation given in Theorem 3.18.

In order to deduce the top order symbol of  $\Lambda_\delta$  we have to multiply  $\sigma(F^* \psi F_\delta)$  with the symbol of  $-\Delta \partial_3$  given by  $(x, \xi) \mapsto i\xi_3 |\xi|^2$  for  $(x, \xi) \in \mathbb{R}_+^3 \times \mathbb{R}^3$  according to Theorem 3.17.  $\square$

In the expression of the top order symbol of  $P_\delta^\varepsilon$ , we obtained in the proof of the theorem, we observe that the pseudodifferential operator  $P_\delta^\varepsilon$  is zero for  $x \in \mathbb{R}_+^3$  with  $x_3 < \delta$ . As a consequence the operator  $F^* \psi F_\delta$  only consists of the smoothing operator for  $x \in \mathbb{R}_+^3$  with  $x_3 < \delta$ . This yields that the operator  $F^* \psi F_\delta$  and consequently  $\Lambda_\delta$  has no singularities for  $x \in \mathbb{R}_+^3$  with  $x_3 < \delta$ . For application this means that we are not able to detect singularities very close to the surface. As mentioned before Theorem 3.21 this has no affect on our numerical examples in Chapter 5 since we are only interested in reconstructions of areas which have a small distance to the surface.

### 3.3.2. Microlocal properties of $\Lambda$

In order to investigate how  $\Lambda$  influences the singularities of an element of  $\mathcal{E}'(\mathbb{R}_+^3)$ , we use the results from microlocal analysis presented in Chapter 2. We analyse which singularities  $\Lambda$  preserves, which are not preserved and which are added. The last mentioned case does not arise. For an explanation we consider the wave front set of  $F^* \psi F$ . According to the explanation after Theorem 3.15, we have

$$\text{WF}(F^* \psi F) \subseteq \{(x, \xi; x, \xi) \mid \xi_3 \neq 0\}$$

in case we assume  $s \in \mathbb{R}^2$ . Since the set  $\{(x, \xi; x, \xi) \mid x \in \mathbb{R}_+^3, \xi \in \mathbb{R}^3 \setminus \{0\}\}$  corresponds to the identity in  $(\mathbb{R}_+^3 \times \mathbb{R}^3 \setminus \{0\}) \times (\mathbb{R}_+^3 \times \mathbb{R}^3 \setminus \{0\})$ , there are no singularities added. If we consider  $s \in S_0$ , the set on the right-hand side of the inclusion above can be restricted. Thus, also in this situation there are no added singularities. However, we notice that singularities with direction  $\xi \in \mathbb{R}^3 \setminus \{0\}$  and  $\xi_3 = 0$  are not preserved by  $F^* \psi F$  regardless whether we have  $s \in \mathbb{R}^2$  or  $s \in S_0$ .

By the pseudolocal property (see Theorem 2.17) and the fact that  $\Delta$  and  $\partial_3$  are pseudodifferential operators by Example 2.4 we have

$$\text{WF}(\Lambda) \subseteq \text{WF}(F^* \psi F).$$

Consequently, the operator  $\Lambda$  does not add singularities and does not preserve the ones with a direction  $\xi \in \mathbb{R}^3 \setminus \{0\}$  with  $\xi_3 = 0$ .

Nevertheless, to answer whether preserved singularities are emphasised, we analyse the reconstruction operator  $\Lambda$  in a more detailed way. The main result is given in Proposition 3.24. In the proof of this proposition, we see why augmenting  $F^* \psi F$  with the derivative in third direction was a good choice. A detailed explanation concerning this issue is given in Remark 3.25.

Before we show under which conditions the reconstruction operator  $\Lambda$  is microlocally elliptic, we introduce some abbreviations to simplify notations and to highlight dependencies on certain variables.

**3.23 Remark.** For further calculations we introduce

$$p := p(\xi) = \frac{\xi_1}{\xi_3} \quad \text{and} \quad q := q(\xi) = \frac{\xi_2}{\xi_3}$$

for  $\xi \in \mathbb{R}^3$  with  $\xi_3 \neq 0$  and show that all single parts of the top order symbol depend only directly on  $x, \xi_3$  and the two ratios  $p$  and  $q$  of the single components of  $\xi$ . For this reason, we define the set

$$P := \{(p, q) \in \mathbb{R} \times \mathbb{R} \mid \text{there exists } \xi \in \mathbb{R}^3, \xi_3 \neq 0, p = \frac{\xi_1}{\xi_3}, q = \frac{\xi_2}{\xi_3}\} = \mathbb{R}^2.$$

By Theorem 3.18 we get  $s(p, q, x) = (s_1(p, q, x), s_2(p, q, x))$  with

$$s_1(p, q, x) = x_1 - px_3 \quad \text{and} \quad s_2(p, q, x) = x_2 - x_3 Q(p, q, \frac{\alpha}{x_3})$$

for  $(p, q) \in P$  and  $x \in \mathbb{R}_+^3$  by defining

$$Q(p, q, \lambda) := \begin{cases} \frac{1}{2q} \left( q^2 - p^2 - 1 + \sqrt{(p^2 + q^2 + 1)^2 + 4\lambda^2 q^2} \right), & \text{for } q \neq 0, \\ 0, & \text{for } q = 0, \end{cases}$$

for  $(p, q) \in P$  and  $\lambda > 0$ . We recall that  $Q$  is smooth by Remark 3.14. Using this, we further have

$$\begin{aligned} D := D(p, q, x) &:= |x - \mathbf{x}_s(s(p, q, x))| = \sqrt{(x_1 - s_1(p, q, x))^2 + (x_2 - (s_2(p, q, x) - \alpha))^2 + x_3^2} \\ &= \sqrt{p^2 x_3^2 + (x_3 Q(p, q, \frac{\alpha}{x_3}) + \alpha)^2 + x_3^2} = x_3 \sqrt{(Q(p, q, \frac{\alpha}{x_3}) + \frac{\alpha}{x_3})^2 + p^2 + 1} \end{aligned}$$

and analogously

$$E := E(p, q, x) = x_3 \sqrt{(Q(p, q, \frac{\alpha}{x_3}) - \frac{\alpha}{x_3})^2 + p^2 + 1}$$

each for  $(p, q) \in P$  and  $x \in \mathbb{R}_+^3$ . With these abbreviations we have

$$A(p, q, x) := A(s(p, q, x), x) = \frac{1}{D(p, q, x)} \frac{1}{E(p, q, x)}$$

and

$$\psi(p, q, x) := \psi(s(p, q, x), \varphi(s(p, q, x), x)) = D(p, q, x) + E(p, q, x)$$

for  $(p, q) \in P$  and  $x \in \mathbb{R}_+^3$ . Moreover, by the representation of  $\omega$  in Theorem 3.18 it follows

$$\omega(p, q, x, \xi_3) = \frac{\xi_3}{x_3} \frac{D(p, q, x) + E(p, q, x)}{D(p, q, x)E(p, q, x)}.$$

Last, we have

$$B(p, q, x) = x_3 \left( \frac{1}{D(p, q, x)} + \frac{1}{E(p, q, x)} \right) \left( \frac{1}{D^2(p, q, x)} + \frac{1}{E^2(p, q, x)} \right) \\ \left( 1 + \frac{(px_3, x_3 Q(p, q, \frac{\alpha}{x_3}) + \alpha, x_3)^\top}{D(p, q, x)} \cdot \frac{(px_3, x_3 Q(p, q, \frac{\alpha}{x_3}) - \alpha, x_3)^\top}{E(p, q, x)} \right)$$

according to the representation given in Remark 3.19 and calculated in Appendix A.1.

**3.24 Proposition.** *Let  $(y, \eta) \in \mathbb{R}_+^3 \times \mathbb{R}^3 \setminus \{0\}$ . Further, let*

$$C(y) := \{\xi \in \mathbb{R}^3 \mid \xi_3 \neq 0, \psi(s(y, \xi), \varphi(s(y, \xi), y)) > 0\}.$$

*If  $\eta \in C(y)$  is satisfied, then  $\Lambda$  is microlocally elliptic of order 1 at  $(y, \eta)$ .*

By the explanation after Theorem 3.15, we have  $\text{WF}(F^* \psi F) \subseteq \{(x, \xi; x, \xi) \mid \xi_3 \neq 0\}$  in case we assume  $s \in \mathbb{R}^2$ . As a consequence, the singularities of  $\Lambda n$  for  $n \in \mathcal{E}'(\mathbb{R}_+^3)$  with direction  $\xi_3 = 0$  are not contained in the wave front set of  $\Lambda n$  and the condition  $\xi_3 \neq 0$  in the set  $C(y)$  is no further restriction. At the points where the cut-off function  $\psi$  vanishes  $\Lambda$  cannot be microlocally elliptic. So, there is no way to avoid the second condition in the set  $C(y)$ . For these two reasons, the set  $C(y)$  is the largest set on which  $\Lambda$  can be microlocally elliptic and Proposition 3.24 the best result we can obtain for  $\Lambda$ .

*Proof of Proposition 3.24:* Let  $\eta \in C(y)$ . We define  $\bar{m} := \frac{\eta_1}{\eta_3}$  and  $\bar{n} := \frac{\eta_2}{\eta_3}$  which is possible as  $\eta_3$  is non-zero. Further, the cut-off function  $\psi$  in the definition of the set  $C(y)$  is continuous. Thus, there exist  $\delta_1, \delta_2 > 0$  and  $r_1 > 0$  such that  $\psi(p, q, x) > 0$  is satisfied for all  $p \in B_{\delta_1}(\bar{m})$ ,  $q \in B_{\delta_2}(\bar{n})$  and  $x \in B_{r_1}(y)$ . Moreover, we find  $\tilde{\delta}_1, \tilde{\delta}_2, r > 0$  with  $\tilde{\delta}_1 < \delta_1, \tilde{\delta}_2 < \delta_2$  and  $r < r_1$  such that we have

$$\overline{B_r(y)} \subseteq \mathbb{R}_+^3 \quad \text{and} \quad \psi(p, q, x) > 0 \quad (3.33)$$

for  $p \in \overline{B_{\tilde{\delta}_1}(\bar{m})}$ ,  $q \in \overline{B_{\tilde{\delta}_2}(\bar{n})}$  and  $x \in \overline{B_r(y)}$ . Now, we choose  $\delta$  to be the minimum of  $\tilde{\delta}_1$  and  $\tilde{\delta}_2$  so

$$\delta := \min\{\tilde{\delta}_1, \tilde{\delta}_2\}. \quad (3.34)$$

First, we consider the case  $\eta_3 > 0$ . We define

$$V_\delta(\eta) := \{(\lambda m, \lambda n, \lambda)^\top \in \mathbb{R}^3 \mid \bar{m} - \delta \leq m \leq \bar{m} + \delta, \bar{n} - \delta \leq n \leq \bar{n} + \delta, \lambda \geq 0\}.$$

Then, by choosing  $m = \bar{m}$ ,  $n = \bar{n}$  and  $\lambda = \eta_3 > 0$  we have  $\eta \in V_\delta(\eta)$ . Also for  $\varepsilon > 0$  with  $\varepsilon < \min\{\eta_3, \delta\}$  we get  $B_\varepsilon(\eta) \subseteq V_\delta(\eta)$ . Further, for  $\xi = (\tilde{\lambda} m, \tilde{\lambda} n, \tilde{\lambda}) \in V_\delta(\eta)$  with some  $\tilde{\lambda} \geq 0$ ,  $m \in [\bar{m} - \delta, \bar{m} + \delta]$  and  $n \in [\bar{n} - \delta, \bar{n} + \delta]$  we get  $\lambda \xi \in V_\delta(\eta)$  for  $\lambda \geq 0$  as  $\tilde{\lambda} \geq 0$  holds, so  $V_\delta(\eta)$  is conic. Thus,  $V_\delta(\eta)$  is a conic neighbourhood of  $\eta$ .

In case we have  $\eta_3 < 0$ , we consider

$$V_\delta(\eta) := \{(-\lambda m, -\lambda n, -\lambda)^\top \in \mathbb{R}^3 \mid \bar{m} - \delta \leq m \leq \bar{m} + \delta, \bar{n} - \delta \leq n \leq \bar{n} + \delta, \lambda \geq 0\}.$$

With  $m = \bar{m}$ ,  $n = \bar{n}$  and  $\lambda = -\eta_3 > 0$  we get  $\eta \in V_\delta(\eta)$  and for  $\varepsilon > 0$  with  $\varepsilon < \min\{-\eta_3, \delta\}$  we have  $B_\varepsilon(\eta) \subseteq V_\delta(\eta)$ . As in the first case, we have  $\lambda \xi \in V_\delta(\eta)$  for  $\xi \in V_\delta(\eta)$  and all  $\lambda \geq 0$ . Hence, the set  $V_\delta(\eta)$  is a conic neighbourhood of  $\eta$ .

From now on, all considerations hold for both cases, independently whether  $\eta_3$  is strictly positive or strictly negative.

In Remark 3.23 we have seen that nearly all factors of the symbol depend only on the two ratios  $p$  and  $q$  of the second variable. Hence, we introduce the set

$$M := \{(p, q, x) \in \mathbb{R} \times \mathbb{R} \times \mathbb{R}_+^3 \mid \text{there exists } \xi \in V_\delta(\eta) \setminus \{0\}, p = \frac{\xi_1}{\xi_3}, q = \frac{\xi_2}{\xi_3} \text{ and } x \in \overline{B_r(y)}\}$$

as a subset of  $\mathbb{R}^5$ . For further steps we rewrite the set  $M$ . Let  $\xi$  be in  $V_\delta(\eta) \setminus \{0\}$ , i.e.  $\xi = (\lambda m, \lambda n, \lambda)^\top$  or  $\xi = (-\lambda m, -\lambda n, -\lambda)^\top$  for some  $\lambda > 0$ ,  $m \in [\bar{m} - \delta, \bar{m} + \delta]$  and  $n \in [\bar{n} - \delta, \bar{n} + \delta]$ . By observing

$$p = p(\xi) = \frac{\xi_1}{\xi_3} = m \quad \text{and} \quad q = q(\xi) = \frac{\xi_2}{\xi_3} = n$$

and therewith

$$\bar{m} - \delta \leq p = m \leq \bar{m} + \delta \quad \text{and} \quad \bar{n} - \delta \leq q = n \leq \bar{n} + \delta, \quad (3.35)$$

we obtain

$$M = \{(p, q, x) \in \mathbb{R} \times \mathbb{R} \times \mathbb{R}_+^3 \mid \bar{m} - \delta \leq p \leq \bar{m} + \delta, \bar{n} - \delta \leq q \leq \bar{n} + \delta, \text{ and } x \in \overline{B_r(y)}\}.$$

In this representation, we see that the set  $M$  is closed and bounded and thus a compact subset of  $\mathbb{R}^5$ .

Next, we take a closer look at the top order symbol of  $F^* \psi F$  given in (3.24). Using Remark 3.23, we have

$$\begin{aligned} \sigma(F^* \psi F)(p, q, x, \xi_3) &= \frac{(2\pi)^5 A^2(p, q, x) \psi(s(p, q, x), \varphi(s(p, q, x), x))}{|\omega(p, q, x, \xi_3)|^2 |B(p, q, x)|} \\ &= \frac{(2\pi)^5 \frac{1}{D(p, q, x)^2 E(p, q, x)^2} \psi(s(p, q, x), \varphi(s(p, q, x), x))}{\frac{|\xi_3|^2}{|x_3|^2} \frac{D(p, q, x)^2 E(p, q, x)^2}{(D(p, q, x) + E(p, q, x))^2} |B(p, q, x)|} \\ &= \frac{(2\pi)^5 (D(p, q, x) + E(p, q, x))^2 \psi(s(p, q, x), \varphi(s(p, q, x), x)) x_3^2}{D(p, q, x)^4 E(p, q, x)^4 |B(p, q, x)|} \frac{1}{\xi_3^2} \end{aligned}$$

for  $(p, q, x) \in M$  and  $\xi_3$  such that  $\xi \in V_\delta(\eta) \setminus \{0\}$  holds. The map  $G: M \rightarrow [0, \infty)$  given by

$$(p, q, x) \mapsto \left| \frac{(2\pi)^5 (D(p, q, x) + E(p, q, x))^2 \psi(s(p, q, x), \varphi(s(p, q, x), x)) x_3^2}{D(p, q, x)^4 E(p, q, x)^4 |B(p, q, x)|} \right| \quad (3.36)$$

is continuous as the denominator does not vanish and so the map attains its minimum on the compact set  $M$  given by

$$N_{V_\delta(\eta), r} := \min_{(p, q, x) \in M} G(p, q, x).$$

As the functions  $D$  and  $E$  are strictly positive, the term  $(D(p, q, x) + E(p, q, x))^2$  does not vanish for  $(p, q, x) \in M$ . Due to the conditions stated in (3.35), we have

$$p \in \overline{B_\delta(\bar{m})} \quad \text{and} \quad q \in \overline{B_\delta(\bar{n})}$$

for  $(p, q)$  with  $(p, q, x) \in M$ . Thus, it follows

$$\psi(p, q, x) > 0$$

for  $(p, q, x) \in M$  using (3.33) and (3.34). Moreover, we have  $x_3 > 0$  since  $(p, q, x) \in M$  holds. For these reasons, the minimum  $N_{V_\delta(\eta),r}$  is strictly positive. Further, we obtain for the top order symbol of  $F^*\psi F$  the estimate

$$|\sigma(F^*\psi F)(x, \xi)| = |\sigma(F^*\psi F)(p, q, x, \xi_3)| \geq N_{V_\delta(\eta),r} \frac{1}{\xi_3^2} \quad (3.37)$$

for  $x \in \overline{B_r(y)}$  and  $\xi \in V_\delta(\eta) \setminus \{0\}$ .

In the next step, we consider the top order symbol of the operator  $\Lambda$  given by  $\Lambda = -\Delta\partial_3 F^*\psi F$ . As the symbol of  $-\Delta\partial_3$  is  $\sigma(-\Delta\partial_3)(\xi, x) = i\xi_3|\xi|^2$  for  $x \in \mathbb{R}_+^3$  and  $\xi \in \mathbb{R}^3$  (see Example 2.4). The top order symbol of  $\Lambda$  is estimated by

$$\begin{aligned} |\sigma(\Lambda)(x, \xi)| &\geq N_{V_\delta(\eta),r} \frac{|\xi_3||\xi|^2}{\xi_3^2} = N_{V_\delta(\eta),r} |\xi| \sqrt{\frac{\xi_1^2}{\xi_3^2} + \frac{\xi_2^2}{\xi_3^2} + 1} \\ &\geq N_{V_\delta(\eta),r} |\xi| \end{aligned}$$

for  $x \in \overline{B_r(y)}$  and  $\xi \in V_\delta(\eta) \setminus \{0\}$  and thus for  $x \in B_r(y)$  and  $\xi \in V_\delta(\eta) \setminus \{0\}$ .

Last, we get

$$|\sigma(\Lambda)(x, \xi)| \geq N_{V_\delta(\eta),r} \frac{|\xi|}{1+|\xi|} (1+|\xi|) \geq \frac{1}{2} N_{V_\delta(\eta),r} (1+|\xi|) = C_{\delta,\eta,r} (1+|\xi|)$$

with  $C_{\delta,\eta,r} := \frac{1}{2} N_{V_\delta(\eta),r}$  for  $x \in B_r(y)$  and  $\xi \in V_\delta(\eta)$  with  $|\xi| \geq 1$  as  $z \mapsto \frac{z}{1+z}$  is monotone increasing for  $z > 0$ . Hence,  $\Lambda$  is microlocally elliptic of order 1 at  $(y, \eta)$ .  $\square$

**3.25 Remark.** In this remark, we give an explanation why this specific proof of the microlocal ellipticity stated in Proposition 3.24 does not work if we augment  $F^*\psi F$  by  $\Delta\partial_1$  or  $\Delta\partial_2$  instead of  $\Delta\partial_3$ . According to (3.37) in the proof of Proposition 3.24, we estimated

$$|\sigma(F^*\psi F)(x, \xi)| \geq N_{V_\delta(\eta),r} \frac{1}{\xi_3^2}$$

for  $x \in \overline{B_r(y)}$  and  $\xi \in V_\delta(\eta) \setminus \{0\}$ . Thus, we obtain

$$\begin{aligned} |\sigma(-\Delta\partial_1 F^*\psi F)(x, \xi)| &\geq N_{V_\delta(\eta),r} \frac{|\xi_1|}{\xi_3^2} |\xi|^2 = N_{V_\delta(\eta),r} \frac{|\xi_1|}{|\xi_3|} |\xi| \sqrt{\frac{\xi_1^2}{\xi_3^2} + \frac{\xi_2^2}{\xi_3^2} + 1} \\ &\geq N_{V_\delta(\eta),r} \frac{|\xi_1|}{|\xi_3|} |\xi| \end{aligned}$$

for  $x \in \overline{B_r(y)}$  and  $\xi \in V_\delta(\eta) \setminus \{0\}$ . Here, we are not able to find a strictly positive lower bound. Indeed,  $p = \frac{\xi_1}{\xi_3}$  is in  $M$  and so bounded but the lower bound is not necessarily strictly positive. Therefore, we do not obtain the estimate we need to show that this operator is microlocally elliptic at  $(y, \eta) \in \mathbb{R}_+^3 \times \mathbb{R}^3 \setminus \{0\}$  if  $\eta \in C(y)$  holds. The argumentation in case of  $\Delta\partial_2 F^*\psi F$  is analogous.

However, if we restrict the set  $C(y)$  further, an analogous proof with different neighbourhoods works when using the derivative in first or in second direction. In case of the first direction, we have  $\xi_1 \neq 0$  and in case of the second one  $\xi_2 \neq 0$  as additional restrictions in  $C(y)$ .

Proposition 3.24 yields the points  $(x, \xi) \in \mathbb{R}_+^3 \times \mathbb{R}^3 \setminus \{0\}$  in which  $\Lambda$  is microlocally elliptic. Using this we are able to apply Theorem 2.23 to the operator  $\Lambda$ .

**3.26 Corollary.** *Let  $n \in \mathcal{E}'(\mathbb{R}_+^3)$ ,  $r \in \mathbb{R}$  and  $(x, \xi) \in \mathbb{R}_+^3 \times \mathbb{R}^3 \setminus \{0\}$  with  $\xi \in C(x)$ . Then, we have  $(x, \xi) \in \text{WF}^r(n)$  if and only if  $(x, \xi) \in \text{WF}^{r-1}(\Lambda n)$  holds.*

*Further, let  $n$  be a finite sum of characteristic functions of balls and half-spaces in  $\mathbb{R}_+^3$ . In this case, it holds  $\text{WF}^{1/2-\varepsilon}(n) = \emptyset$  for  $\varepsilon > 0$  and  $\text{WF}^{1/2+\gamma}(n) = \text{WF}(n)$  for  $\gamma \geq 0$ . Thus, we obtain  $(x, \xi) \in \text{WF}^{-1/2}(\Lambda n)$  for all  $(x, \xi) \in \text{WF}(n)$ .*

So, roughly speaking, a distribution  $u$  is not  $H^r$  at  $x$  in direction  $\xi$  if and only if  $\Lambda u$  is not  $H^{r-1}$  at  $x$  in direction  $\xi$ .

*Proof of Corollary 3.26.* By Theorem 3.17 the reconstruction operator  $\Lambda$  is of order 1. For this reason, the first assertion follows by Theorem 2.23.

According to Example 2.24 the function  $n$  is in  $H_{\text{loc}}^{1/2-\varepsilon}(\mathbb{R}_+^3)$  for any  $\varepsilon > 0$ . Hence, the second assertion follows from the first one.  $\square$

By the definition of the set  $C(x)$  in Proposition 3.24, the top order symbol  $\sigma(\Lambda)$  is zero off  $C(x)$ . But as we only know that the top order symbol vanishes there, we just obtain that  $\Lambda$  smooths one degree more off the set  $C(x)$  than on the set  $C(x)$  and not directly that  $\Lambda$  is  $C^\infty$ -smoothing there. In the following remark, we argue why this is nevertheless true.

**3.27 Remark.** In [QRS11] the authors argue that the reconstruction operator used there is  $C^\infty$ -smoothing off the set, in which it is elliptic. With the same arguments we show that  $\Lambda$  is  $C^\infty$ -smoothing at  $(x, \xi) \in \mathbb{R}_+^3 \times \mathbb{R}^3 \setminus \{0\}$  with  $\xi \notin \overline{C(x)}$ .

Let  $x \in \mathbb{R}_+^3$  and  $\xi \in \mathbb{R}^3 \setminus \{0\}$  with  $\xi \notin \overline{C(x)}$ . We first consider the case that  $\xi_3 \neq 0$  holds. As the generalised Radon transform  $F$  is a Fourier integral operator (for the representation see (3.9)), we have  $\text{WF}(Ff) \subseteq C \circ \text{WF}(f) = \Pi_{S_0 \times (2\alpha, \infty)}(\Pi_{\mathbb{R}_+^3}^{-1}(\text{WF}(f)))$  for  $f \in \mathcal{E}'(\mathbb{R}_+^3)$  by Theorem 2.18 and Lemma 2.8. Here,  $C$  is the canonical relation of  $F$  explicitly given in (3.12). According to Corollary 3.20 the projection  $\Pi_{\mathbb{R}_+^3}$  is injective and so we obtain  $\Pi_{\mathbb{R}_+^3}^{-1}(x, \xi) = (s, t, \eta, x, \xi)$  for unique  $(s, t) = (s, \varphi(s, x)) \in S_0 \times (2\alpha, \infty)$  and an appropriate direction  $\eta = (\omega \nabla_s \varphi(s, x), \omega) \in \mathbb{R}^3$ . Further, we have

$$\Pi_{S_0 \times (2\alpha, \infty)}(\Pi_{\mathbb{R}_+^3}^{-1}(x, \xi)) = (s, t, \eta). \quad (3.38)$$

By assumption,  $\xi \notin \overline{C(x)}$  holds and thus  $(s, t) \notin \text{supp}(\psi)$  is satisfied. Since  $\psi$  is continuous, there exists a neighbourhood of  $(s, t)$  on which  $\psi$  vanishes. Hence,  $\psi Ff$  is zero in a neighbourhood of  $(s, t)$  and thus  $(s, t, \eta) \notin \text{WF}(\psi Ff)$ . Further, we have

$$\text{WF}(F^* \psi Ff) \subseteq C^\top \circ \text{WF}(\psi Ff) = \Pi_{\mathbb{R}_+^3}(\Pi_{S_0 \times (2\alpha, \infty)}^{-1}(\text{WF}(\psi Ff)))$$

again as  $F^*$  is a Fourier integral operator and by Theorem 2.18 and Lemma 2.8. With the injectivity of  $\Pi_{\mathbb{R}_+^3}$  and  $\Pi_{S_0 \times (2\alpha, \infty)}$  (see Corollary 3.20 and the proof of Theorem 3.18) we obtain

$$\Pi_{\mathbb{R}_+^3}(\Pi_{S_0 \times (2\alpha, \infty)}^{-1}(\Pi_{S_0 \times (2\alpha, \infty)}(\Pi_{\mathbb{R}_+^3}^{-1}(x, \xi)))) = (x, \xi).$$

For an easier understanding of this equality it helps to follow the diagram in Figure 3.2 from the right to the left.

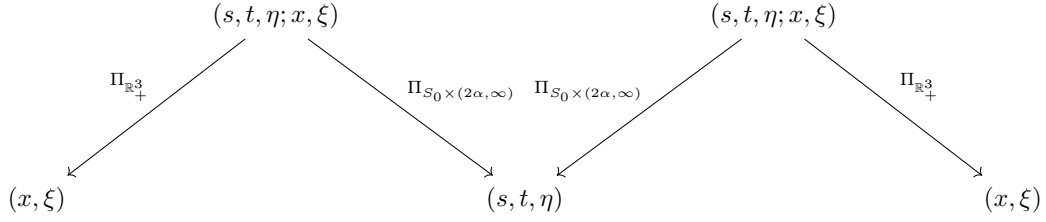


**Figure 3.2:** An illustration of the identities given in Remark 3.27.

As  $\Pi_{\mathbb{R}_+^3}$  is injective, we get the unique  $(s, t, \eta)$  as above such that  $\Pi_{\mathbb{R}_+^3}^{-1}(x, \xi) = (s, t, \eta; x, \xi)$  holds. By applying  $\Pi_{S_0 \times (2\alpha, \infty)}$  we then obtain  $(s, t, \eta)$ . Further, we get again  $(s, t, \eta; x, \xi)$  with  $(x, \xi)$  as before after taking the preimage under  $\Pi_{S_0 \times (2\alpha, \infty)}$ . This works because  $\Pi_{S_0 \times (2\alpha, \infty)}$  is injective and thus  $(s, t, \eta)$  has a unique preimage under  $\Pi_{S_0 \times (2\alpha, \infty)}$ . Last, we apply the projection  $\Pi_{\mathbb{R}_+^3}$  and end up with  $(x, \xi)$ .

Next, due to the equality given in (3.38), we have

$$(x, \xi) = \Pi_{\mathbb{R}_+^3}(\Pi_{S_0 \times (2\alpha, \infty)}^{-1}(\Pi_{S_0 \times (2\alpha, \infty)}(\Pi_{\mathbb{R}_+^3}^{-1}(x, \xi)))) = \Pi_{\mathbb{R}_+^3}(\Pi_{S_0 \times (2\alpha, \infty)}^{-1}(s, t, \eta)).$$

Therefore,  $(x, \xi) \notin \text{WF}(F^*\psi Ff)$  as  $(s, t, \eta) \notin \text{WF}(\psi Ff)$  holds and  $F^*\psi F$  is smoothing at  $x$  in direction  $\xi$ . Moreover, by Example 2.4 the differential operators  $\Delta$  and  $\partial_3$  are pseudodifferential operators and by the pseudolocal property (see Theorem 2.17) we obtain that  $\Lambda$  is smoothing at  $x$  in direction  $\xi$ .

In the second case, we consider  $\xi_3 = 0$ . As before we have  $\text{WF}(Ff) \subseteq C \circ \text{WF}(f) = \Pi_{S_0 \times (2\alpha, \infty)}(\Pi_{\mathbb{R}_+^3}^{-1}(\text{WF}(f)))$  for  $f \in \mathcal{E}'(\mathbb{R}_+^3)$ . Thus, let  $(x, \xi) \in \text{WF}(f)$ . According to identity (3.25), we have  $\Pi_{\mathbb{R}_+^3}^{-1}(x, \xi) = \emptyset$  and so  $\text{WF}(F^*\psi Ff) \subseteq \emptyset$ . As a consequence,  $F^*\psi F$  is  $C^\infty$ -smoothing at  $x$  in direction  $\xi$ . With the same arguments as in the first case, we get that  $\Lambda$  is  $C^\infty$ -smoothing at  $x$  in direction  $\xi$ .

### 3.3.3. Modification of the reconstruction operator $\Lambda$

The top order symbol of  $\Lambda$  depends on the distance to the surface, i.e. the value of  $x_3$  and the offset  $\alpha$  of source and receiver via the two foci  $\mathbf{x}_s(s)$  and  $\mathbf{x}_r(s)$  for fixed  $s \in S_0$ . However, we want to obtain reconstructions largely independent of the impact of these two parameters.

For this reason, we take a closer look at the behaviour of the top order symbol. In case the value of  $x_3$  is large in comparison to the offset  $\alpha$ , the open half-ellipsoids look like open half-spheres. Due to this fact, we evaluate the top order symbol  $\sigma(\Lambda)$  of  $\Lambda$  for the offset  $\alpha = 0$ . In order to cover large values of the offset  $\alpha$ , we observe what happens if  $\alpha$  goes to infinity in the expression for  $\sigma(\Lambda)$ .

We start with the first case, which is given by  $\alpha = 0$ . With  $\Lambda_0$  we denote the operator  $\Lambda$  in case  $\alpha = 0$  is satisfied.

**3.28 Corollary.** *If we assume  $\alpha = 0$ , so  $\mathbf{x}_s(s) = \mathbf{x}_r(s)$  for  $s \in S_0$  is satisfied, the top order symbol of  $\Lambda_0$  as a pseudodifferential operator is given by*

$$\sigma(\Lambda_0)(x, \xi) = \frac{16\pi^5 \xi_3 |\xi_3| \psi\left(x_1 - \frac{\xi_1}{\xi_3} x_3, x_2 - \frac{\xi_2}{\xi_3} x_3, 2|\xi| \frac{x_3}{\xi_3}\right)}{x_3^2 |\xi|}$$

for  $x \in \mathbb{R}_+^3$  and  $\xi \in \mathbb{R}^3 \setminus \{0\}$  with  $\xi_3 \neq 0$ . Further, we have  $\sigma(\Lambda_0)(x, \xi) = 0$  for  $x \in \mathbb{R}_+^3$  and  $\xi \in \mathbb{R}^3 \setminus \{0\}$  with  $\xi_3 = 0$ .

*Proof.* First, we define  $\widehat{s} := \mathbf{x}_s(s) = \mathbf{x}_r(s) = (s_1, s_2, 0)^\top$  where the equality holds as  $\alpha = 0$  by assumption. Since the representations of  $\omega$  in Lemma 3.13 and  $B$  in Remark 3.19 are rather complicated, we consider once again the condition  $\xi = \omega \nabla \varphi(s, x)$  to get the explicit expressions for  $s_1, s_2$  and  $\omega$  which is less involved. For  $\alpha = 0$  the three equations (3.15), (3.16) and (3.17) are

$$\xi_1 = 2\omega \frac{x_1 - s_1}{|x - \widehat{s}|}, \quad \xi_2 = 2\omega \frac{x_2 - s_2}{|x - \widehat{s}|}, \quad \xi_3 = 2\omega \frac{x_3}{|x - \widehat{s}|}.$$

Rearranging the last equation yields

$$\omega(\widehat{s}(x, \xi), x) = \frac{\xi_3}{2x_3} |x - \widehat{s}(x, \xi)| \quad (3.39)$$

and inserting in the first two equations we obtain

$$s_1(x, \xi) = x_1 - \frac{\xi_1}{\xi_3} x_3 \quad \text{and} \quad s_2(x, \xi) = x_2 - \frac{\xi_2}{\xi_3} x_3.$$

At this point, we observe that we do not distinguish two cases for  $s_2$  depending on  $\xi$  as before. Thus, we have

$$|x - \widehat{s}(x, \xi)| = \frac{x_3}{\xi_3} |\xi| \quad (3.40)$$

and therefore  $\varphi(s(x, \xi), x) = 2|x - \widehat{s}(x, \xi)| = 2\frac{x_3}{\xi_3} |\xi|$ . Further, using the representations in Appendix A.1 we calculate

$$[\nabla_x \varphi](\widehat{s}(x, \xi), x) = 2 \begin{pmatrix} \frac{x_1 - s_1(x, \xi)}{|x - \widehat{s}(x, \xi)|} \\ \frac{x_2 - s_2(x, \xi)}{|x - \widehat{s}(x, \xi)|} \\ \frac{x_3}{|x - \widehat{s}(x, \xi)|} \end{pmatrix} = \frac{2}{|\xi|} \begin{pmatrix} \xi_1 \\ \xi_2 \\ \xi_3 \end{pmatrix},$$

$$[\partial_{s_1} \nabla_x \varphi](\widehat{s}(x, \xi), x) = 2 \begin{pmatrix} -\frac{(x_2 - s_2(x, \xi))^2 + x_3^2}{|x - \widehat{s}(x, \xi)|^3} \\ \frac{(x_1 - s_1(x, \xi))(x_2 - s_2(x, \xi))}{|x - \widehat{s}(x, \xi)|^3} \\ \frac{x_3(x_1 - s_1(x, \xi))}{|x - \widehat{s}(x, \xi)|^3} \end{pmatrix} = \frac{2}{x_3 |\xi|^3} \begin{pmatrix} -(\xi_2^2 + \xi_3^2) \xi_3 \\ \xi_1 \xi_2 \xi_3 \\ \xi_1 \xi_3^2 \end{pmatrix}$$

and

$$[\partial_{s_2} \nabla_x \varphi](\widehat{s}(x, \xi), x) = 2 \begin{pmatrix} \frac{(x_1 - s_1(x, \xi))(x_2 - s_2(x, \xi))}{|x - \widehat{s}(x, \xi)|^3} \\ -\frac{(x_1 - s_1(x, \xi))^2 + x_3^2}{|x - \widehat{s}(x, \xi)|^3} \\ \frac{x_3(x_2 - s_2(x, \xi))}{|x - \widehat{s}(x, \xi)|^3} \end{pmatrix} = \frac{2}{x_3 |\xi|^3} \begin{pmatrix} \xi_1 \xi_2 \xi_3 \\ -(\xi_1^2 + \xi_3^2) \xi_3 \\ \xi_2 \xi_3^2 \end{pmatrix}.$$

Hence, by the definition of  $B$  given in (3.23) we get

$$B(\widehat{s}(x, \xi), x) = \frac{8\xi_3^2}{x_3^2|\xi|^7} \det \begin{pmatrix} \xi_1 & \xi_2 & \xi_3 \\ -(\xi_2^2 + \xi_3^2) & \xi_1\xi_2 & \xi_1\xi_3 \\ \xi_1\xi_2 & -(\xi_1^2 + \xi_3^2) & \xi_2\xi_3 \end{pmatrix} = \frac{8\xi_3^3}{x_3^2|\xi|^3}.$$

Moreover, using identity (3.40) we obtain

$$\omega(\widehat{s}(x, \xi), x) = \frac{\xi_3|x - \widehat{s}(x, \xi)|}{2x_3} = \frac{|\xi|}{2}$$

by (3.39) and

$$A(\widehat{s}(x, \xi), x) = \frac{1}{|x - \widehat{s}(x, \xi)|^2} = \frac{\xi_3^2}{x_3^2|\xi|^2}.$$

All in all, inserting in the representation (3.22) of the top order symbol we have

$$\sigma(\Lambda)(x, \xi) = 16\pi^5 i \xi_3 |\xi_3| \frac{\psi(x_1 - \frac{\xi_1}{\xi_3}x_3, x_2 - \frac{\xi_2}{\xi_3}x_3, 2\frac{x_3}{\xi_3}|\xi|)}{x_3^2|\xi|},$$

so the first assertion holds. The second claim follows by the same argumentation as in Theorem 3.18.  $\square$

Using the result for the top order symbol in case of  $\alpha = 0$ , we define a modified reconstruction operator. This operator highlights the singularities for small values of  $\alpha$  or if  $\alpha$  is small in comparison to the distance to the surface.

**3.29 Corollary.** *We define the modified reconstruction operator  $\Lambda_{\text{mod},0}: \mathcal{E}'(\mathbb{R}_+^3) \rightarrow \mathcal{D}'(\mathbb{R}_+^3)$  by*

$$\Lambda_{\text{mod},0} := -\Delta \partial_3 M F^* \psi F,$$

where  $M$  is the extension to  $\mathcal{E}'(\mathbb{R}_+^3)$  of the multiplication operator  $Mu(x) = x_3^2 u(x)$  for a function  $u$  on  $\mathbb{R}_+^3$ . The top order symbol of  $\Lambda_{\text{mod},0}$  is

$$\sigma(\Lambda_{\text{mod},0})(x, \xi) = \frac{(2\pi)^5 x_3^2 \xi_3 |\xi|^2 \psi(s(x, \xi), \varphi(s(x, \xi), x)) A^2(s(x, \xi), x)}{|\omega(s(x, \xi), x)|^2 |B(s(x, \xi), x)|} \quad (3.41)$$

for  $(x, \xi) \in \mathbb{R}_+^3 \times \mathbb{R}^3$  with  $\xi_3 \neq 0$  and  $\sigma(\Lambda_{\text{mod},0})(x, \xi) = 0$  for  $(x, \xi) \in \mathbb{R}_+^3 \times \mathbb{R}^3$  with  $\xi_3 = 0$ . Further, let  $(y, \eta) \in \mathbb{R}_+^3 \times \mathbb{R}^3 \setminus \{0\}$  and

$$C(y) = \{\xi \in \mathbb{R}^3 \mid \xi_3 \neq 0, \psi(s(y, \xi), \varphi(s(y, \xi), y)) > 0\}$$

be as in Proposition 3.24. If  $\eta \in C(y)$  holds,  $\Lambda_{\text{mod},0}$  is microlocally elliptic of order 1 at  $(y, \eta)$ . Moreover, the operator  $\Lambda_{\text{mod},0}$  is  $C^\infty$ -smoothing at  $(y, \eta) \in \mathbb{R}_+^3 \times \mathbb{R}^3 \setminus \{0\}$  with  $\eta \notin \overline{C(y)}$ .

*Proof.* The reconstruction operator  $\Lambda_{\text{mod},0}$  differs from  $\Lambda$  by the multiplication operator  $M$ , which maps from  $\mathcal{D}'(\mathbb{R}_+^3)$  into  $\mathcal{D}'(\mathbb{R}_+^3)$ . This yields the claimed mapping property. Further, Theorem 3.18 yields the top order symbol of  $\Lambda$ . By augmenting with the factor  $x_3^2$ , we get the claimed top order symbol of  $\Lambda_{\text{mod},0}$ .

Concerning the second assertion we take a closer look at the proof of Proposition 3.24. In case of  $\Lambda_{\text{mod},0}$ , we modify the map  $G$  defined by (3.36). Here, we also insert the factor  $x_3^2$  such that we consider  $H: M \rightarrow [0, \infty)$  defined by

$$(p, q, x) \mapsto \left| \frac{(2\pi)^5 x_3^2 (D(p, q, x) + E(p, q, x))^2 \psi(s(p, q, x), \varphi(s(p, q, x), x)) x_3^2}{D(p, q, x)^4 E(p, q, x)^4 |B(p, q, x)|} \right| \quad (3.42)$$

for  $(p, q, x) \in M$ . Nevertheless, this modified version attains its minimum on the compact set  $M$ . This minimum is strictly positive since  $\min_{(p,q,x) \in M} G(p, q, x) > 0$  is satisfied by the proof of Proposition 3.24 and  $x_3 > 0$  holds by assumption. Hence, from now on, the argumentation follows the same lines as for the reconstruction operator  $\Lambda$  in there.

For the proof of the last assertion, we note that the multiplication operator  $M$  is a pseudodifferential operator according to Example 2.5. Together with the pseudolocal property (see Theorem 2.17) Remark 3.27 yields that  $\Lambda_{\text{mod},0}$  is  $C^\infty$ -smoothing at  $(y, \eta) \in \mathbb{R}_+^3 \times \mathbb{R}^3 \setminus \{0\}$  if  $\eta \notin \overline{C(y)}$ .  $\square$

The modified reconstruction operator  $\Lambda_{\text{mod},0}$  is defined in such a way that it damps the singularities at places where  $\alpha$  is large in comparison to  $x_3$ . Therefore, we investigate how the top order symbol  $\sigma(\Lambda)$  of  $\Lambda$  behaves for  $\alpha$  going to infinity.

**3.30 Corollary.** *Let  $(x, \xi) \in \mathbb{R}_+^3 \times \mathbb{R}^3$  with  $\xi_3 \neq 0$ . For the top order symbol  $\sigma(\Lambda)$  of  $\Lambda$  we have*

$$\begin{aligned} \sigma(\Lambda)(x, \xi) &\sim \frac{1}{\alpha^2}, & \text{for } \xi_2 \neq 0, \\ \sigma(\Lambda)(x, \xi) &\sim \frac{1}{\alpha}, & \text{for } \xi_2 = 0, \end{aligned}$$

for  $\alpha \rightarrow \infty$ , where “ $\sim$ ” means asymptotically equal. Hence,  $\sigma(\Lambda)$  behaves like  $\frac{1}{\alpha^2}$  if  $\xi_2 \neq 0$  and like  $\frac{1}{\alpha}$  if  $\xi_2 = 0$  is satisfied.

*Proof.* By Theorem 3.18 and Remark 3.19, the top order symbol  $\sigma(\Lambda)$  of  $\Lambda$  is given by

$$\begin{aligned} \sigma(\Lambda)(x, \xi) &= (2\pi)^5 i \xi_3 |\xi|^2 \frac{\psi(s(x, \xi), \varphi(s(x, \xi), x)) A^2(s(x, \xi), x)}{|\omega(s(x, \xi), x)|^2 |B(s(x, \xi), x)|} \\ &= (2\pi)^5 i \xi_3 |\xi|^2 \frac{\psi(s(x, \xi), \varphi(s(x, \xi), x)) \frac{1}{D^2 E^2}}{\left| \frac{\xi_3}{x_3} \frac{DE}{D+E} \right|^2 x_3 \left( \frac{1}{D} + \frac{1}{E} \right) \left( \frac{1}{D^2} + \frac{1}{E^2} \right) \left( 1 + \frac{x - \mathbf{x}_s(s)}{D} \cdot \frac{x - \mathbf{x}_r(s)}{E} \right)} \end{aligned}$$

with the abbreviations  $D$  and  $E$  as in Remark 3.23. Here, we think of  $D$  and  $E$  depending on  $x$  and  $\xi$ , so

$$D = D(s(x, \xi), x) := \sqrt{(s_1(x, \xi) - x_1)^2 + (s_2(x, \xi) - \alpha - x_2)^2 + x_3^2}$$

and

$$E = E(s(x, \xi), x) := \sqrt{(x_1 - s_1(x, \xi))^2 + (x_2 - s_2(x, \xi) - \alpha)^2 + x_3^2}.$$

First, we consider  $\xi_2 \neq 0$ . We start with the two cases in which  $\xi_2$  and  $\xi_3$  have the same sign, i.e.  $\xi_2 > 0$  and  $\xi_3 > 0$  or  $\xi_2 < 0$  and  $\xi_3 < 0$ . Then, we obtain the following limits

$$\omega(s(x, \xi), x) = \frac{\xi_3}{x_3} E \frac{1}{1 + \frac{E}{D}} \rightarrow \frac{\xi_3}{x_3} \frac{x_3}{2\xi_2\xi_3} |\xi|^2 \cdot 1 = \frac{1}{2\xi_2} |\xi|^2$$

for  $\alpha \rightarrow \infty$  and

$$\begin{aligned} B(s(x, \xi), x) &= x_3 \left( \frac{1}{D} + \frac{1}{E} \right) \left( \frac{1}{D^2} + \frac{1}{E^2} \right) \left( 1 + \frac{(x_1 - s_1)^2}{DE} + \left( \frac{x_2 - s_2}{D} + \frac{\alpha}{D} \right) \frac{x_2 - s_2 - \alpha}{E} + \frac{x_3^2}{DE} \right) \\ &\rightarrow x_3 \left( 0 + \frac{2\xi_2\xi_3}{x_3|\xi|^2} \right) \left( 0 + \frac{4\xi_2^2\xi_3^2}{x_3^2|\xi|^4} \right) \left( 1 + 0 + \left( \frac{1}{2} + \frac{1}{2} \right) \frac{x_3}{2\xi_2\xi_3} (\xi_2^2 - \xi_1^2 - \xi_3^2) \frac{2\xi_2\xi_3}{x_3(\xi_2^2 + \xi_1^2 + \xi_3^2)} + 0 \right) \\ &= \frac{8\xi_2^3\xi_3^3}{x_3^2|\xi|^6} \left( 1 + \frac{\xi_2^2 - \xi_1^2 - \xi_3^2}{\xi_1^2 + \xi_2^2 + \xi_3^2} \right) \end{aligned}$$

for  $\alpha \rightarrow \infty$  by using the single limits determined in Appendix A.3 (a). Moreover, we have

$$A = \frac{1}{DE} \longrightarrow 0$$

for  $\alpha \rightarrow \infty$  again by Appendix A.3 (a). However, by multiplying with  $\alpha$  the result in Appendix A.3 (a) yields

$$\alpha A = \frac{\alpha}{D} \frac{1}{E} \longrightarrow \frac{1}{2} \frac{2\xi_2\xi_3}{x_3|\xi|^2} = \frac{\xi_2\xi_3}{x_3|\xi|^2}$$

for  $\alpha \rightarrow \infty$ .

Next, we take a look at the cases when  $\xi_2$  and  $\xi_3$  have different signs, i.e.  $\xi_2 > 0$  and  $\xi_3 < 0$  or  $\xi_2 < 0$  and  $\xi_3 > 0$ . In comparison to the first cases, the roles of  $D$  and  $E$  are interchanged. Hence, we achieve in an analogous way

$$\omega(s(x, \xi), x) = \frac{\xi_3}{x_3} D \frac{1}{1 + \frac{D}{E}} \longrightarrow -\frac{\xi_3}{x_3} \frac{x_3}{2\xi_2\xi_3} |\xi|^2 \cdot 1 = -\frac{1}{2\xi_2} |\xi|^2$$

for  $\alpha \rightarrow \infty$  and

$$\begin{aligned} B(s(x, \xi), x) &= x_3 \left( \frac{1}{D} + \frac{1}{E} \right) \left( \frac{1}{D^2} + \frac{1}{E^2} \right) \left( 1 + \frac{(x_1 - s_1)^2}{DE} + \frac{x_2 - s_2 + \alpha}{D} \left( \frac{x_2 - s_2}{E} - \frac{\alpha}{E} \right) + \frac{x_3^2}{DE} \right) \\ &\longrightarrow x_3 \left( -\frac{2\xi_2\xi_3}{x_3|\xi|^2} + 0 \right) \left( \frac{4\xi_2^2\xi_3^2}{x_3^2|\xi|^4} + 0 \right) \\ &\quad \left( 1 + 0 + \frac{x_3}{2\xi_2\xi_3} (\xi_2^2 - \xi_1^2 - \xi_3^2) \left( -\frac{2\xi_2\xi_3}{x_3(\xi_2^2 + \xi_1^2 + \xi_3^2)} \right) \left( -\frac{1}{2} - \frac{1}{2} \right) + 0 \right) \\ &= -\frac{8\xi_2^3\xi_3^3}{x_3^2|\xi|^6} \left( 1 + \frac{\xi_2^2 - \xi_1^2 - \xi_3^2}{\xi_1^2 + \xi_2^2 + \xi_3^2} \right) \end{aligned}$$

for  $\alpha \rightarrow \infty$  with the single limits in Appendix A.3 (b). Still, we have

$$A = \frac{1}{DE} \longrightarrow 0$$

for  $\alpha \rightarrow \infty$  and also we achieve

$$\alpha A = \frac{1}{D} \frac{\alpha}{E} \longrightarrow -\frac{2\xi_2\xi_3}{x_3|\xi|^2} \frac{1}{2} = -\frac{\xi_2\xi_3}{x_3|\xi|^2}$$

for  $\alpha \rightarrow \infty$ .

So, except for the signs the limits of  $\omega$ ,  $B$  and  $\alpha A$  in both cases are the same. We obtain in both cases

$$\begin{aligned} \alpha^2 \sigma(\Lambda)(x, \xi) &= \frac{(2\pi)^5 \xi_3 |\xi|^2 \psi(s(x, \xi), \varphi(s(x, \xi), x)) (\alpha A(s(x, \xi), x))^2}{|\omega(s(x, \xi), x)|^2 |B(s(x, \xi), x)|} \\ &\longrightarrow \frac{(2\pi)^5 \xi_3 |\xi|^2 \psi(s(x, \xi), \varphi(s(x, \xi), x)) \frac{\xi_2^2 \xi_3^2}{x_3^2 |\xi|^4}}{\frac{|\xi|^4}{4\xi_2^2} \frac{8\xi_2^3 \xi_3^3}{x_3^2 |\xi|^6} \left( 1 + \frac{\xi_2^2 - \xi_1^2 - \xi_3^2}{\xi_1^2 + \xi_2^2 + \xi_3^2} \right)} = \frac{16\pi^5 \xi_2 \psi(s(x, \xi), \varphi(s(x, \xi), x))}{1 + \frac{\xi_2^2 - \xi_1^2 - \xi_3^2}{\xi_1^2 + \xi_2^2 + \xi_3^2}} \end{aligned}$$

for  $\alpha \rightarrow \infty$  since we only consider absolute values and squares of  $\omega$ ,  $B$  and  $\alpha A$ . This proves the assertion for  $\xi_2 \neq 0$ .

Second, let  $\xi_2$  be zero. Using the notations of Remark 3.23, we have  $q = 0$ , so  $Q(p, q, \lambda) = 0$  for  $p, q \in \mathbb{R}$  and  $\lambda > 0$  is satisfied. This leads to

$$D = x_3 \sqrt{(Q(p, q, \frac{\alpha}{x_3}) + \frac{\alpha}{x_3})^2 + p^2 + 1} = x_3 \sqrt{\frac{\alpha^2}{x_3^2} + p^2 + 1} = x_3 \sqrt{\frac{\alpha^2}{x_3^2} + \frac{\xi_1^2}{\xi_3^2} + 1}$$

and

$$E = x_3 \sqrt{\left(Q(p, q, \frac{\alpha}{x_3}) - \frac{\alpha}{x_3}\right)^2 + p^2 + 1} = x_3 \sqrt{\frac{\alpha^2}{x_3^2} + p^2 + 1} = x_3 \sqrt{\frac{\alpha^2}{x_3^2} + \frac{\xi_1^2}{\xi_3^2} + 1}.$$

Hence, we have  $D = E$ . Thus, we simplify

$$\omega(s(x, \xi), x) = \frac{\xi_3}{x_3} \frac{D^2}{2D} = \frac{\xi_3}{2x_3} D = \frac{\xi_3}{2} \sqrt{\frac{\alpha^2}{x_3^2} + \frac{\xi_1^2}{\xi_3^2} + 1}$$

and

$$A(s(x, \xi), x) = \frac{1}{D^2} = \frac{1}{x_3^2 \left(\frac{\alpha^2}{x_3^2} + \frac{\xi_1^2}{\xi_3^2} + 1\right)}.$$

Further, we obtain  $s_1(x, \xi) = x_1 - \frac{\xi_1}{\xi_3}$  and  $s_2(x, \xi) = x_2 - Q(p, q, \frac{\alpha}{x_3})x_3 = x_2$  again using Remark 3.23. Then, we have

$$\begin{aligned} B(s(x, \xi), x) &= x_3 \frac{2}{D} \frac{2}{D^2} \left(1 + \frac{(x_1 - s_1)^2 + (x_2 - (s_2 - \alpha))(x_2 - (s_2 + \alpha)) + x_3^2}{D^2}\right) \\ &= \frac{4x_3}{D^5} \left(D^2 + \frac{\xi_1^2}{\xi_3^2} x_3^2 - \alpha^2 + x_3^2\right) \\ &= \frac{4x_3}{x_3^5 \left(\sqrt{\frac{\alpha^2}{x_3^2} + \frac{\xi_1^2}{\xi_3^2} + 1}\right)^5} \left(x_3^2 \left(\frac{\alpha^2}{x_3^2} + \frac{\xi_1^2}{\xi_3^2} + 1\right) + \frac{\xi_1^2}{\xi_3^2} x_3^2 - \alpha^2 + x_3^2\right) \\ &= \frac{8 \left(\frac{\xi_1^2}{\xi_3^2} + 1\right)}{x_3^2 \left(\sqrt{\frac{\alpha^2}{x_3^2} + \frac{\xi_1^2}{\xi_3^2} + 1}\right)^5}. \end{aligned}$$

With these calculations we conclude

$$\begin{aligned} \sigma(\Lambda)(x, \xi) &= \frac{(2\pi)^5 \xi_3 |\xi|^2 \psi(s(x, \xi), \varphi(s(x, \xi), x)) A^2(s(x, \xi), x)}{|\omega(s(x, \xi), x)|^2 |B(s(x, \xi), x)|} \\ &= \frac{4}{\xi_3^2 \left(\frac{\alpha^2}{x_3^2} + \frac{\xi_1^2}{\xi_3^2} + 1\right)} \frac{(2\pi)^5 \xi_3 |\xi| \psi\left(x_1 - \frac{\xi_1}{\xi_3}, x_2, \varphi\left(x_1 - \frac{\xi_1}{\xi_3}, x_2, x\right)\right)}{x_3^4 \left(\frac{\alpha^2}{x_3^2} + \frac{\xi_1^2}{\xi_3^2} + 1\right)^2} \frac{x_3^2 \left(\sqrt{\frac{\alpha^2}{x_3^2} + \frac{\xi_1^2}{\xi_3^2} + 1}\right)^5}{8 \left(\frac{\xi_1^2}{\xi_3^2} + 1\right)} \\ &= \frac{16\pi^5 |\xi| \psi\left(x_1 - \frac{\xi_1}{\xi_3}, x_2, \varphi\left(x_1 - \frac{\xi_1}{\xi_3}, x_2, x\right)\right)}{x_3^2 \xi_3 \sqrt{\frac{\alpha^2}{x_3^2} + \frac{\xi_1^2}{\xi_3^2} + 1} \left(\frac{\xi_1^2}{\xi_3^2} + 1\right)} \end{aligned}$$

which yields that the top order symbol  $\sigma(\Lambda)$  behaves like  $\frac{1}{\alpha}$  for  $\xi_2 = 0$ . This finishes the proof.  $\square$

Since we want a reconstruction operator which is independent on how the offset  $\alpha$  relates to the value of  $x_3$ , we define a new reconstruction operator by a sum of two operators. Therefore, we take the first modified reconstruction operator  $\Lambda_{\text{mod},0}$  and add an operator which compensates the behaviour of  $\sigma(\Lambda)$  for  $\alpha$  going to infinity. This approach balances the two cases in such a way that none is highlighted.

**3.31 Corollary.** We define the modified reconstruction operators  $\Lambda_{\text{mod},1}: \mathcal{E}'(\mathbb{R}_+^3) \rightarrow \mathcal{D}'(\mathbb{R}_+^3)$  and  $\Lambda_{\text{mod},2}: \mathcal{E}'(\mathbb{R}_+^3) \rightarrow \mathcal{D}'(\mathbb{R}_+^3)$  by

$$\begin{aligned} \Lambda_{\text{mod},1} &= -\Delta \partial_3 (M + \alpha \text{Id}) F^* \psi F & \text{and} & & \Lambda_{\text{mod},2} &= -\Delta \partial_3 (M + \alpha^2 \text{Id}) F^* \psi F \\ &= \Lambda_{\text{mod},0} + \alpha \Lambda & & & &= \Lambda_{\text{mod},0} + \alpha^2 \Lambda. \end{aligned}$$

The corresponding symbols are given by

$$\sigma(\Lambda_{\text{mod},1})(x, \xi) = \frac{(2\pi)^5 (x_3^2 + \alpha) \xi_3 |\xi|^2 \psi(s(x, \xi), \varphi(s(x, \xi), x)) A^2(s(x, \xi), x)}{|\omega(s(x, \xi), x)|^2 |B(s(x, \xi), x)|}$$

and

$$\sigma(\Lambda_{\text{mod},2})(x, \xi) = \frac{(2\pi)^5 (x_3^2 + \alpha^2) \xi_3 |\xi|^2 \psi(s(x, \xi), \varphi(s(x, \xi), x)) A^2(s(x, \xi), x)}{|\omega(s(x, \xi), x)|^2 |B(s(x, \xi), x)|}$$

for  $(x, \xi) \in \mathbb{R}_+^3 \times \mathbb{R}^3$  with  $\xi_3 \neq 0$  and  $\sigma(\Lambda_{\text{mod},i})(x, \xi) = 0$  for  $i \in \{1, 2\}$  and  $(x, \xi) \in \mathbb{R}_+^3 \times \mathbb{R}^3 \setminus \{0\}$  with  $\xi_3 = 0$ . Moreover, let  $(y, \eta) \in \mathbb{R}_+^3 \times \mathbb{R}^3 \setminus \{0\}$  and

$$C(y) = \{\xi \in \mathbb{R}^3 \mid \xi_3 \neq 0, \psi(s(y, \xi), \varphi(s(y, \xi), y)) > 0\}$$

as in Proposition 3.24. If  $\eta \in C(y)$ , then  $\Lambda_{\text{mod},1}$  and  $\Lambda_{\text{mod},2}$  are microlocally elliptic of order 1 at  $(y, \eta)$ . Last, both operators are  $C^\infty$ -smoothing at  $(y, \eta) \in \mathbb{R}_+^3 \times \mathbb{R}^3 \setminus \{0\}$  if  $\eta \notin \overline{C(y)}$ .

Both reconstruction operators  $\Lambda_{\text{mod},1}$  or  $\Lambda_{\text{mod},2}$  consist of a sum of two operators. In both cases, the first operator dominates if  $x_3$  is large in comparison to  $\alpha$  and the second one if  $\alpha$  is large in comparison to  $x_3$ . In this way, we achieve a balance between the two cases.

*Proof of Corollary 3.31.* In comparison to  $\Lambda_{\text{mod},0}$ , the two reconstruction operators  $\Lambda_{\text{mod},1}$  and  $\Lambda_{\text{mod},2}$  are a sum of two operators. They consist of  $\Lambda_{\text{mod},0}$  plus a second operator. These second operators are given by  $\Lambda$  multiplied with the factor  $\alpha$  and  $\alpha^2$ , respectively. For the top order symbols of  $\Lambda_{\text{mod},1}$  and  $\Lambda_{\text{mod},2}$  we proceed analogously as in the proof of Corollary 3.29 where we considered the top order symbol of  $\Lambda_0$ . Then, using the top order symbol of  $\Lambda_{\text{mod},0}$  stated in Corollary 3.29 we get the two claimed representations of the top order symbols. Here, there are no cancellation effects since the terms  $x_3^2 + \alpha$  and  $x_3^2 + \alpha^2$  are strictly positive.

For the second part, we argue again analogously to the proof of Corollary 3.29. This time, we consider the maps

$$\begin{aligned} (p, q, x) &\mapsto \left| \frac{(2\pi)^5 (x_3^2 + \alpha) (D(p, q, x) + E(p, q, x))^2 \psi(s(p, q, x), \varphi(s(p, q, x), x)) x_3^2}{D(p, q, x)^4 E(p, q, x)^4 |B(p, q, x)|} \right| \\ &= H(p, q, x) + \alpha G(p, q, x) \end{aligned}$$

and

$$\begin{aligned} (p, q, x) &\mapsto \left| \frac{(2\pi)^5 (x_3^2 + \alpha^2) (D(p, q, x) + E(p, q, x))^2 \psi(s(p, q, x), \varphi(s(p, q, x), x)) x_3^2}{D(p, q, x)^4 E(p, q, x)^4 |B(p, q, x)|} \right| \\ &= H(p, q, x) + \alpha^2 G(p, q, x) \end{aligned}$$

where  $G$  and  $H$  are defined as in the proof of Proposition 3.24 and Corollary 3.29 for  $(p, q, x) \in M$  and  $M$  is as in the proof of Proposition 3.24. Both maps attain their minimum on the compact set  $M$ . Moreover, both minimums are positive. Since  $\alpha$  is strictly positive, we obtain  $\min_{(p,q,x) \in M} G(p, q, x) > 0$  by Proposition 3.24 as well as  $\min_{(p,q,x) \in M} H(p, q, x) > 0$  by Corollary 3.29. Further, we proceed as in the proof of Proposition 3.24. Finally, it follows by Remark 3.27 and Corollary 3.29 that both operators are  $C^\infty$ -smoothing at  $(y, \eta) \in \mathbb{R}_+^3 \times \mathbb{R}^3 \setminus \{0\}$  with  $\eta \notin \overline{C(y)}$ .  $\square$



---

## Numerical realisation

---

In this chapter, we consider the unmodified reconstruction operator  $\Lambda$ . The procedure described in the following works in the same way as in case of the modified reconstruction operators by replacing  $\Lambda$  with the considered modified operator. Further details concerning the modified operators are given in Chapter 5.

In the first section, we present how we approximate  $\Lambda n$  evaluated at  $p \in \mathbb{R}_+^3$  for  $n \in \mathcal{E}'(\mathbb{R}_+^3)$ . An approximation is necessary since it is not possible to evaluate distributions at a point.

One part of the numerical approximation is given by the elliptic Radon transform applied to  $n$ . In the numerical experiments we choose  $n$  to be a sum of characteristic functions of balls and a half-space. Thus, we reformulate the elliptic Radon transform applied to these functions. The reformulations simplify the computation and are presented in the following two sections.

### 4.1. Approximation of $\Lambda n$ by the concept of approximate inverse

For numerical experiments we have to evaluate the reconstruction operator  $\Lambda$  applied to  $n$  at a point  $p \in \mathbb{R}_+^3$ . Since a direct evaluation is not necessarily possible depending on which space  $n$  belongs to, we approximate the value sought after. By definition, the reconstruction operator  $\Lambda$  contains the operator  $F$  and its dual  $F^*$ . This structure is ideally suited to apply the method of the approximate inverse for a stable evaluation of an approximation of  $\Lambda n$  with  $n \in \mathcal{E}'(\mathbb{R}_+^3)$  at a point  $p \in \mathbb{R}_+^3$ . For the modified versions of  $\Lambda$  introduced in Subsection 3.3.3 this observation is also valid.

The method of the approximate inverse was first presented in [LM90] and introduced by name in [Lou96]. It is a method to solve problems of the form  $Af = g$  and is described as a solution operator which maps the data  $g$  to a stable approximation of the solution of  $Af = g$ , i.e. a regularised version of the solution.

Now, we fix a point  $p \in \mathbb{R}_+^3$ . In order to apply the method of the approximate inverse, let for  $\varepsilon > 0$  smooth functions  $e_{p,\varepsilon}$  with  $\text{supp}(e_{p,\varepsilon}) = \overline{B_\varepsilon(p)}$  and  $\int_{\mathbb{R}_+^3} e_{p,\varepsilon}(x) dx = 1$  be given. By these properties it follows that  $e_{p,\varepsilon}$  for  $\varepsilon > 0$  is a mollifier and  $(e_{p,\varepsilon})_{\varepsilon>0}$  approximates  $\delta(\cdot - p)$  for  $\varepsilon \rightarrow 0$ . The parameter  $\varepsilon$  is a scaling parameter. The smaller  $\varepsilon$ , the smaller is the support of  $e_{p,\varepsilon}$ . Another name for  $\varepsilon$  is regularisation parameter since it determines the size of the neighbourhood where the regularisation of the  $\delta$ -distribution does not vanish.

Instead of computing  $\Lambda n$  at a point  $p$  which is in general not possible for  $n \in \mathcal{E}'(\mathbb{R}_+^3)$ , we

fix a sufficiently small  $\varepsilon := \gamma > 0$  and obtain

$$\begin{aligned}\Lambda_\gamma n(p) &:= \langle \Lambda n, e_{p,\gamma} \rangle_{\mathcal{D}', \mathcal{D}} = \langle -\Delta \partial_3 F^* \psi F n, e_{p,\gamma} \rangle_{\mathcal{D}', \mathcal{D}} \\ &= \langle \psi F n, F \partial_3 \Delta e_{p,\gamma} \rangle_{\mathcal{E}', \mathcal{E}}\end{aligned}$$

for  $n \in \mathcal{E}'(\mathbb{R}_+^3)$ . Here, we denote by  $\langle \cdot, \cdot \rangle$  the dual pairing of the spaces  $\mathcal{D}(\mathbb{R}_+^3)$  and  $\mathcal{D}'(\mathbb{R}_+^3)$ . This approximation is motivated by the fact that for  $n \in C_c^\infty(\mathbb{R}_+^3)$  we have

$$\begin{aligned}\Lambda n(p) &= \langle \Lambda n, \delta(\cdot - p) \rangle_{\mathcal{E}, \mathcal{E}'} = \lim_{\varepsilon \rightarrow 0} \langle \Lambda n, e_{p,\varepsilon} \rangle_{\mathcal{E}, \mathcal{E}'} \\ &\approx \langle \Lambda n, e_{p,\gamma} \rangle_{\mathcal{E}, \mathcal{E}'}\end{aligned}$$

since  $\Lambda n$  is then an element of  $C^\infty(\mathbb{R}_+^3)$ . In this case,  $\langle \cdot, \cdot \rangle$  is the dual pairing of the spaces  $\mathcal{E}(\mathbb{R}_+^3)$  and  $\mathcal{E}'(\mathbb{R}_+^3)$ .

Further, the data  $y$  is given by  $y = F n$  according to (1.13). For this reason, the approximation simplifies to

$$\begin{aligned}\Lambda_\gamma n(p) &= \langle \Lambda n, e_{p,\gamma} \rangle_{\mathcal{D}', \mathcal{D}} = \langle \psi y, F \partial_3 \Delta e_{p,\gamma} \rangle_{\mathcal{E}', \mathcal{E}} \\ &= \int_{S_0 \times (2\alpha, \infty)} \psi(s, t) y(s, t) F \partial_3 \Delta e_{p,\gamma}(s, t) \, d(s, t)\end{aligned}\quad (4.1)$$

for  $n \in \mathcal{E}'(\mathbb{R}_+^3)$ . By this identity, we have to calculate the operator  $F$  applied to a function supported in a closed ball.

For the first considerations and investigations how our approach works, we generate synthetic data  $y$ . We compute the data by using the identity  $y = F n$ .

In the experiments later on, we choose  $n$  to be a sum of characteristic functions of balls and a half-space. The first mentioned ones come within functions supported in a closed ball. For the second one, we additionally consider  $F$  applied to the characteristic function of a half-space. These two cases are presented in the next two sections.

## 4.2. The operator $F$ applied to a function supported in a closed ball

The aim of this section is to calculate the elliptic Radon transform of a function  $n$  supported in a closed ball. More precisely, we assume  $n = \tilde{n} \chi_{B_r(P)}$  for an appropriate function  $\tilde{n} \in C^\infty(\mathbb{R}_+^3)$  and a ball  $B_r(P)$  with midpoint  $P$  and radius  $r > 0$ .

However, we first consider  $n \in C_c^\infty(\mathbb{R}_+^3)$  with  $\text{supp}(n) \subseteq \overline{B_r(P)}$ , i.e. we are also able to write  $n = \tilde{n} \chi_{B_r(P)}$ . In order to calculate  $F$  applied to  $n$ , we introduce a new coordinate system which simplifies the calculations. Using these observations, we transform the integral

$$F n(s, t) = \int_{\mathbb{R}_+^3} n(x) A(s, x) \delta(t - \varphi(s, x)) \, dx$$

for fixed  $(s, t) \in S_0 \times (2\alpha, \infty)$ . Afterwards, we calculate the limiting angles for  $\theta$  and  $\phi$  and analyse for which  $t \in (2\alpha, \infty)$  the value of  $F n(s, t)$  vanishes for fixed  $s \in S_0$ . Last, we argue why the obtained representation is also valid for the more general functions  $n$  mentioned above.

### 4.2.1. Change of the considered coordinate system

In Chapter 1 we derived the following expression

$$F n(s, t) = \frac{1}{2} \int_{\theta_{\min}}^{\theta_{\max}} \int_{\phi(\theta)_{\min}}^{\phi(\theta)_{\max}} n(x(s, t, \phi, \theta)) \sin(\phi) \, d\phi \, d\theta$$

for a function  $n \in C_c^\infty(\mathbb{R}_+^3)$  with

$$\begin{aligned} \theta_{\min} &= \theta_{\min}(s, t) = \min\{\theta \in (0, \pi) \mid x(s, t, \phi, \theta) \in \text{supp}(n)\}, \\ \theta_{\max} &= \theta_{\max}(s, t) = \max\{\theta \in (0, \pi) \mid x(s, t, \phi, \theta) \in \text{supp}(n)\}, \end{aligned}$$

and

$$\begin{aligned} \phi(\theta)_{\min} &= \phi(\theta)_{\min}(s, t) = \min\{\phi \in (0, \pi) \mid x(s, t, \phi, \theta) \in \text{supp}(n)\}, \\ \phi(\theta)_{\max} &= \phi(\theta)_{\max}(s, t) = \max\{\phi \in (0, \pi) \mid x(s, t, \phi, \theta) \in \text{supp}(n)\} \end{aligned}$$

according to (1.18). This means we have to determine the limiting angles for  $\theta$  and  $\phi = \phi(\theta)$

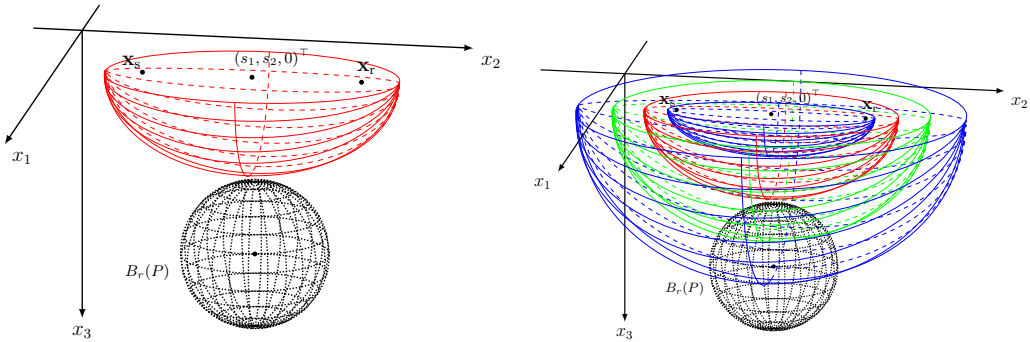


**Figure 4.1:** The given situation for one and several travel times  $t$ , respectively. Each travel time  $t$  is associated with one open half-ellipsoid for fixed  $s \in S_0$ .

where the open half-ellipsoid given by  $(s, t) \in S_0 \times (2\alpha, \infty)$  intersects the ball  $B_r(P)$ . An illustration is given in Figure 4.1. In order to determine the expression stated in (4.1), we have to calculate the value of  $F_n(s, t)$  for each  $(s, t) \in S_0 \times (2\alpha, \infty)$ . Since this is quite complicated in the considered coordinate system in Figure 4.1, we simplify the calculation of  $F_n$  by changing the coordinate system.

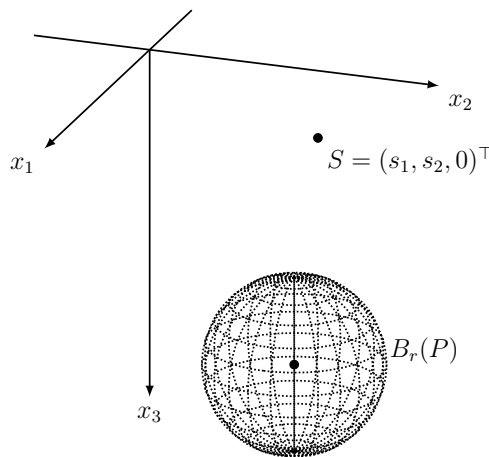


**Figure 4.2:** The situation at the beginning.

As we have mentioned in Chapter 1 and Lemma 3.1, the operator  $F$  integrates over an open half-ellipsoid with the two foci  $x_s(s)$  and  $x_r(s)$  for fixed  $s \in S_0$  and travel time

$t \in (2\alpha, \infty)$ . Thus, let  $s \in S_0$  and  $t \in (2\alpha, \infty)$  be fixed. In Figure 4.2 the situation in the original coordinate system given by  $(x_1, x_2, x_3)$  is illustrated. First, we shift the co-

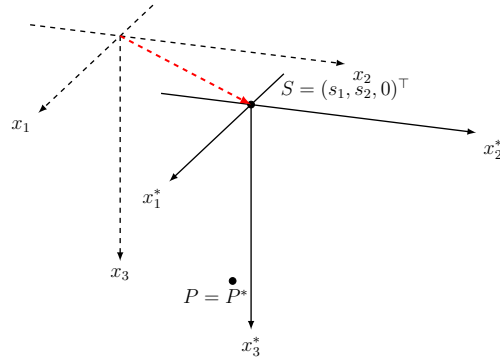


**Figure 4.3:** The Shift of the coordinate system.

ordinate system  $(x_1, x_2, x_3)$  such that the origin of the new coordinate system  $(x_1^*, x_2^*, x_3^*)$  is the midpoint  $(s_1, s_2, 0)^\top$  of the open half-ellipsoid we are integrating over. Hence, the two foci  $\mathbf{x}_s(s)$  and  $\mathbf{x}_r(s)$  lie on the  $x_2^*$ -axis, both with distance  $\alpha$  to the origin in the system  $(x_1^*, x_2^*, x_3^*)$ . The midpoint  $p$  of the ball in the coordinates of the system  $(x_1^*, x_2^*, x_3^*)$  is given by  $P^* = (p_1^*, p_2^*, p_3^*)^\top = (p_1 - s_1, p_2 - s_2, p_3)^\top$ . An illustration is given in Figure 4.3.

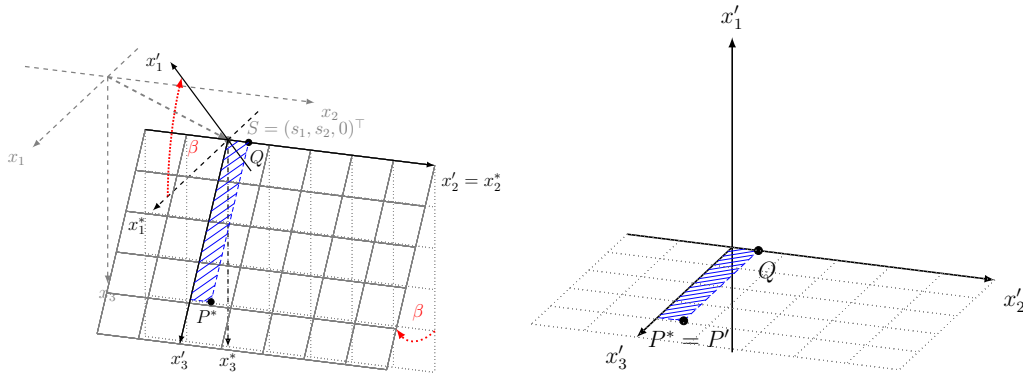


**Figure 4.4:** Rotation into the new coordinate system  $(x'_1, x'_2, x'_3)$  such that  $P^*$  lies in the  $x'_2$ - $x'_3$ -plane. Here, the point  $Q$  is given by  $(0, p'_2, 0)^\top$ .

Second, we transform the coordinate system  $(x_1^*, x_2^*, x_3^*)$  in such a way in a new coordinate system  $(x'_1, x'_2, x'_3)$  that the three points  $\mathbf{x}_s(s)$ ,  $\mathbf{x}_r(s)$  and  $P^* = (p_1 - s_1, p_2 - s_2, p_3)^\top$  are located in the same plane, to be more precise in the  $x'_2$ - $x'_3$ -plane. We denote the associated rotation angle by  $\beta$ . For an illustration we refer to Figure 4.4.

Next, we aim to get the coordinates of  $P'$  with respect to the original coordinate system  $(x_1, x_2, x_3)$ . From Figure 4.5 we get

$$\tan(\beta) = \frac{p_1^*}{p_3^*} = \frac{p_1 - s_1}{p_3} \quad \text{and} \quad \cos(\beta) = \frac{p_3^*}{p_3} = \frac{p_3}{p_3}.$$

Inserting the first equation into the second one we conclude

$$p'_3 = \frac{p_3}{\cos\left(\arctan\left(\frac{p_1 - s_1}{p_3}\right)\right)}.$$

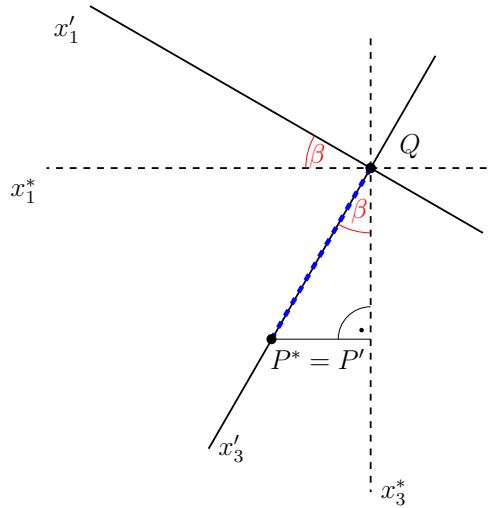


Figure 4.5: The situation in the  $x'_2 = p'_2 = p_2^*$ -plane.

Furthermore,  $p'_2$  does not change as we performed the rotation around the  $x_2^*$ -axis and  $p'_1$  is set to zero by the condition that  $P'$  lies in the  $x'_2$ - $x'_3$ -plane. Altogether, the coordinates of  $P'$  in the new coordinate system  $(x'_1, x'_2, x'_3)$  expressed by the given values from the beginning are

$$P' = \left( 0, p_2 - s_2, \frac{p_3}{\cos\left(\arctan\left(\frac{p_1 - s_1}{p_3}\right)\right)} \right)^\top.$$

The rotation of the coordinate system is described by

$$R = \begin{pmatrix} \cos(\beta) & 0 & -\sin(\beta) \\ 0 & 1 & 0 \\ \sin(\beta) & 0 & \cos(\beta) \end{pmatrix}$$

with  $\beta = \arctan((p_1 - s_1)/p_3)$ . Further, with the inverse  $R^{-1} = R^\top$  we have

$$\begin{aligned} R^{-1}P' + \begin{pmatrix} s_1 \\ s_2 \\ 0 \end{pmatrix} &= \begin{pmatrix} \cos(\beta) & 0 & \sin(\beta) \\ 0 & 1 & 0 \\ -\sin(\beta) & 0 & \cos(\beta) \end{pmatrix} \begin{pmatrix} 0 \\ p_2 - s_2 \\ \frac{p_3}{\cos(\beta)} \end{pmatrix} = \begin{pmatrix} \sin(\beta)\frac{p_3}{\cos(\beta)} \\ p_2 - s_2 \\ \cos(\beta)\frac{p_3}{\cos(\beta)} \end{pmatrix} \\ &= \begin{pmatrix} \tan(\arctan(\frac{p_1 - s_1}{p_3}))p_3 + s_1 \\ p_2 \\ p_3 \end{pmatrix} = \begin{pmatrix} p_1 \\ p_2 \\ p_3 \end{pmatrix} = P, \end{aligned}$$

where we used  $\beta = \arctan((p_1 - s_1)/p_3)$  in the second last step. Rearranging the above equation yields

$$R(P - (s_1, s_2, 0)^\top) = P'. \quad (4.2)$$

#### 4.2.2. Some geometrical considerations

In this subsection, we rewrite the integral representation of the elliptic Radon transform of  $n \in C_c^\infty(\mathbb{R}_+^3)$  with  $\text{supp}(n) \subseteq \overline{B_r(P)}$  using the new coordinates. Therefore, we use the considerations of the last subsection.

We assume  $(s, t) \in S_0 \times (2\alpha, \infty)$  to be fixed. Now, we apply the transformations we outlined in the subsection before to calculate the integral given by  $Fn$ . According to the transformation theorem and the argumentation in Appendix A.4, we obtain

$$\begin{aligned}
Fn(s, t) &= \int_{\mathbb{R}_+^3} n(x)A(s, x)\delta(t - \varphi(s, x)) dx \\
&= \int_{\mathbb{R}^3} \tilde{n}(x)A(s, x)\chi_{B_r(P)}(x)\delta(t - \varphi(s, x)) dx \\
&= \int_{\mathbb{R}^3} \tilde{n}(x + (s_1, s_2, 0)^\top)A(s, x + (s_1, s_2, 0)^\top)\chi_{B_r(P)}(x + (s_1, s_2, 0)^\top) \\
&\quad \delta(t - \varphi(s, x + (s_1, s_2, 0)^\top)) dx \\
&= \int_{\mathbb{R}^3} \tilde{n}(R^{-1}x + (s_1, s_2, 0)^\top)A(s, R^{-1}x + (s_1, s_2, 0)^\top)\chi_{B_r(P)}(R^{-1}x + (s_1, s_2, 0)^\top) \\
&\quad \delta(t - \varphi(s, R^{-1}x + (s_1, s_2, 0)^\top)) dx,
\end{aligned}$$

where  $R$  is the associated rotation matrix to the rotation we mentioned before given by

$$R = \begin{pmatrix} \cos(\beta) & 0 & -\sin(\beta) \\ 0 & 1 & 0 \\ \sin(\beta) & 0 & \cos(\beta) \end{pmatrix}$$

with

$$\beta = \arctan((p_1 - s_1)/p_3). \quad (4.3)$$

Further, we simplify

$$\begin{aligned}
&\varphi(s, R^{-1}x + (s_1, s_2, 0)^\top) \\
&= |\mathbf{x}_s(s) - (R^{-1}x + (s_1, s_2, 0)^\top)| + |R^{-1}x + (s_1, s_2, 0)^\top - \mathbf{x}_r(s)| \\
&= |(s_1, s_2 - \alpha, 0)^\top - R^{-1}x - (s_1, s_2, 0)^\top| + |R^{-1}x + (s_1, s_2, 0)^\top - (s_1, s_2 + \alpha, 0)^\top| \\
&= |(0, -\alpha, 0)^\top - R^{-1}x| + |R^{-1}x - (0, \alpha, 0)^\top| \\
&= |R^{-1}||R(0, -\alpha, 0)^\top - x| + |R^{-1}||x - R(0, \alpha, 0)^\top| \\
&= |(0, -\alpha, 0)^\top - x| + |x - (0, \alpha, 0)^\top| = \varphi((0, 0), x)
\end{aligned}$$

and

$$\begin{aligned}
A(s, R^{-1}x + (s_1, s_2, 0)^\top) &= \frac{1}{|\mathbf{x}_s(s) - (R^{-1}x + (s_1, s_2, 0)^\top)||R^{-1}x + (s_1, s_2, 0)^\top - \mathbf{x}_r(s)|} \\
&= \frac{1}{|(0, -\alpha, 0)^\top - x||x - (0, \alpha, 0)^\top|} = A((0, 0), x)
\end{aligned}$$

using the definition of the rotation matrix  $R$  for  $x \in \mathbb{R}^3$ .

Moreover, we have

$$R^{-1}x(t, \phi, \theta) = \begin{pmatrix} \sqrt{\frac{1}{4}t^2 - \alpha^2} \sin(\phi)(\cos(\beta) \cos(\theta) + \sin(\beta) \sin(\theta)) \\ \frac{1}{2}t \cos(\phi) \\ \sqrt{\frac{1}{4}t^2 - \alpha^2} \sin(\phi)(-\sin(\beta) \cos(\theta) + \cos(\beta) \sin(\theta)) \end{pmatrix} \quad (4.4)$$

by inserting the prolate spheroidal coordinates introduced in (1.15) with respect to  $(0, 0, 0)^\top$  on  $\mathbb{R}^3$  given by

$$\begin{aligned} x_1 &= \sqrt{\frac{1}{4}t^2 - \alpha^2} \sin(\phi) \cos(\theta), \\ x_2 &= \frac{1}{2}t \cos(\phi), \\ x_3 &= \sqrt{\frac{1}{4}t^2 - \alpha^2} \sin(\phi) \sin(\theta) \end{aligned} \quad (4.5)$$

for  $\phi \in [0, \pi)$  and  $\theta \in [0, 2\pi)$ . In addition, we obtain

$$\begin{aligned} &\chi_{B_r(P)}(R^{-1}x(t, \phi, \theta) + (s_1, s_2, 0)^\top) \\ &= \{x(t, \phi, \theta) \in \mathbb{R}^3 \mid |R^{-1}x(t, \phi, \theta) + (s_1, s_2, 0)^\top - P| < r\} \\ &= \{x(t, \phi, \theta) \in \mathbb{R}^3 \mid |R^{-1}|x(t, \phi, \theta) - R(P - (s_1, s_2, 0)^\top)| < r\} \\ &= \chi_{B_r(P')}(x(t, \phi, \theta)) \end{aligned}$$

by our choice of  $R$  as stated in (4.2). In particular, we have

$$|R^{-1}x(t, \phi, \theta) + (s_1, s_2, 0)^\top - P| = |x(t, \phi, \theta) - R(P - (s_1, s_2, 0)^\top)| = |x(t, \phi, \theta) - P'|. \quad (4.6)$$

Finally, we use the equality of the two integrals in identity (1.19). We notice that we are in case of  $(s_1, s_2) = (0, 0)$  when applying (1.19) and end up with

$$\begin{aligned} Fn(s, t) &= \int_{\mathbb{R}^3} \tilde{n}(R^{-1}x + (s_1, s_2, 0)^\top) A((0, 0), x) \chi_{B_r(P')}(x) \delta(t - \varphi((0, 0), x)) dx \\ &= \frac{1}{2} \int_{[0, \pi) \times [0, 2\pi)} \tilde{n}(R^{-1}x(t, \phi, \theta) + (s_1, s_2, 0)^\top) \chi_{B_r(P')}(x(t, \phi, \theta)) \sin(\phi) d(\phi, \theta) \\ &= \frac{1}{2} \int_{\theta_{\min}}^{\theta_{\max}} \int_{\phi(\theta)_{\min}}^{\phi(\theta)_{\max}} \tilde{n}(R^{-1}x(t, \phi, \theta) + (s_1, s_2, 0)^\top) \chi_{B_r(P')}(x(t, \phi, \theta)) \sin(\phi) d\phi d\theta \end{aligned} \quad (4.7)$$

where

$$\begin{aligned} \theta_{\min} &= \min\{\phi \in [0, 2\pi) \mid x(t, \phi, \theta) \in \overline{B_r(P')}\}, \\ \theta_{\max} &= \max\{\phi \in [0, 2\pi) \mid x(t, \phi, \theta) \in \overline{B_r(P')}\}, \\ \phi(\theta)_{\min} &= \min\{\phi \in [0, \pi) \mid x(t, \phi, \theta) \in \overline{B_r(P')}\}, \\ \phi(\theta)_{\max} &= \max\{\phi \in [0, \pi) \mid x(t, \phi, \theta) \in \overline{B_r(P')}\}. \end{aligned}$$

Here, the limiting angles  $\phi(\theta)_{\min}$  and  $\phi(\theta)_{\max}$  depend on  $\theta$ . Thus, if we are able to determine the angles  $\theta_{\min}$  and  $\theta_{\max}$  and afterwards  $\phi(\theta)_{\min}$  and  $\phi(\theta)_{\max}$ , we obtain the value of  $Fn(s, t)$  for  $(s, t) \in S_0 \times (2\alpha, \infty)$ .

In the same way as in Chapter 1, we argue that the representation (4.7) is also valid for  $n = \tilde{n} \chi_{B_r(P)}$  with  $\tilde{n} \in C^\infty(\mathbb{R}_+^3)$ . For fixed  $t \in (2\alpha, \infty)$  the function  $n$  is in  $L^1(\Psi_t((0, \pi) \times (0, 2\pi)))$ . Thus, representation (4.7) is well defined for  $n = \tilde{n} \chi_{B_r(P)}$ .

### 4.2.3. Calculation of the required angles

In the following, we determine the four angles  $\theta_{\min}$ ,  $\theta_{\max}$ ,  $\phi_{\min}(\theta)$  and  $\phi_{\max}(\theta)$  which we need to compute  $Fn$  evaluated at a fixed point  $(s, t) \in S_0 \times (2\alpha, \infty)$ . For this reason, we consider the ball given by  $B_r(P')$  in the coordinate system  $(x'_1, x'_2, x'_3)$  and locate the two angles of  $\theta$

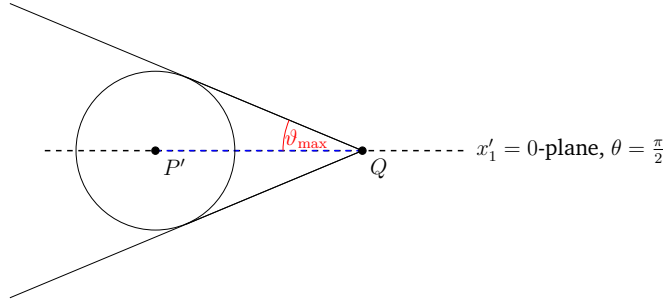


**Figure 4.6:** An illustration of the angle  $\vartheta_{\max}$  in the  $x'_2 = p'_2$ -plane.

and the two angles of  $\phi = \phi(\theta)$  depending on  $\theta$  which enclose the ball. For this purpose, we consider the prolate spheroidal coordinates with respect to  $(0, 0, 0)^\top$  stated in (4.5).

We start with the two limiting angles for  $\theta$  and determine the angle  $\vartheta_{\max}$  marked in Figure 4.6. In this figure, the  $x_2 = p'_2$ -plane is illustrated. A further look on Figure 4.4 might be helpful to understand where the cross section is taken. The prolate spheroidal coordinates are constructed in such a way that the half-line given by  $x'_2 = p'_2$  and  $x'_3 \geq 0$  corresponds to the angle  $\theta = \frac{\pi}{2}$ . Thus, the limiting angles for  $\theta$  which enclose the ball  $B_r(P')$  are given by  $\theta_{\min} = \frac{\pi}{2} - \vartheta_{\max}$  and  $\theta_{\max} = \frac{\pi}{2} + \vartheta_{\max}$ .

In order to get the value of  $\vartheta_{\max}$ , one possibility would be to construct the two half-planes drawn as half-lines in Figure 4.6. However, this is more complicated than considering the setting given in Figure 4.6 in two space dimensions. We analyse the situation in the  $x'_2 = p'_2$ -

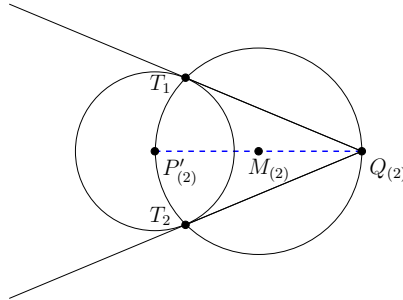


**Figure 4.7:** Constructing the two equations for the tangents on the circle around  $P'_{(2)}$  with the help of a circle around  $M_{(2)}$ .

plane and introduce the points  $P'_{(2)} = (0, p'_3)^\top$  and  $Q_{(2)} = (0, 0)^\top$ . Further, we intersect the circle having radius  $r$  around  $P'_{(2)}$  with the circle having radius  $\frac{1}{2}p'_3$  around  $M = (0, \frac{1}{2}p'_3)^\top$ , the midpoint of  $P'_{(2)}$  and  $Q_{(2)}$ , to get the equations of the two tangents. This approach is illustrated in Figure 4.7. The intersection points of the two circles are elements of the set given by

$$\begin{aligned} & \{x \in \mathbb{R}^2 \mid |M_{(2)} - x|^2 - (\tfrac{1}{2}p'_3)^2 = |P'_{(2)} - x|^2 - r^2\} \\ & = \{x \in \mathbb{R}^2 \mid x_1^2 + (x_3 - \tfrac{1}{2}p'_3)^2 - \tfrac{1}{4}(p'_3)^2 = x_1^2 + (x_3 - p'_3)^2 - r^2\} \\ & = \left\{x \in \mathbb{R}^2 \mid x_3 = \frac{(p'_3)^2 - r^2}{p'_3}\right\}. \end{aligned}$$

Next, we insert the defining condition of this set in the equation of the circle  $x_1^2 + (x_3 - p'_3)^2 = r^2$  and end up with the requirement  $x_1^2 = r^2 - \frac{r^4}{(p'_3)^2}$  for the first component. So, the two

intersection points are

$$T_1 = \left( r \sqrt{1 - \frac{r^2}{(p'_3)^2}}, \frac{(p'_3)^2 - r^2}{p'_3} \right) \quad \text{and} \quad T_2 = \left( -r \sqrt{1 - \frac{r^2}{(p'_3)^2}}, \frac{(p'_3)^2 - r^2}{p'_3} \right).$$

Without loss of generality we consider the point  $T_1$  and the associated right-angled triangle given by the three points  $P'_{(2)}$ ,  $Q_{(2)}$  and  $T_1$  illustrated in Figure 4.8. The angle at the point

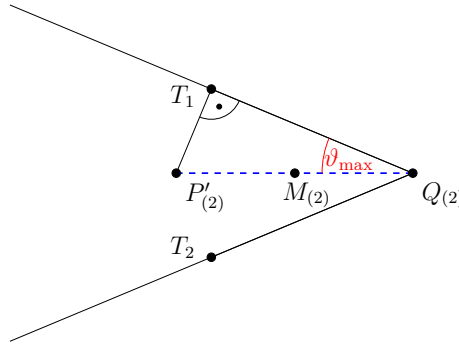


**Figure 4.8:** The intersection point  $T_1$  and the associated right-angled triangle.

$Q_{(2)}$  is the angle  $\vartheta_{\max}$  we are searching for. We read off the relation

$$\cos(\vartheta_{\max}) = \frac{|T_1 - Q_{(2)}|}{p'_3}.$$

By the identity

$$|T_1 - Q_{(2)}| = \sqrt{r^2 - \frac{r^4}{(p'_3)^2} + (p'_3)^2 - 2r^2 + \frac{r^4}{(p'_3)^2}} = \sqrt{(p'_3)^2 - r^2},$$

we obtain

$$\vartheta_{\max} = \arccos \left( \frac{\sqrt{(p'_3)^2 - r^2}}{p'_3} \right).$$

Finally, we conclude that

$$\theta_{\min} = \frac{\pi}{2} - \vartheta_{\max} \quad \text{and} \quad \theta_{\max} = \frac{\pi}{2} + \vartheta_{\max} \quad (4.8)$$

using the arguments stated at the beginning of this section.

At this point, we recall the representation of  $F$  given by

$$Fn(s, t) = \frac{1}{2} \int_{\theta_{\min}}^{\theta_{\max}} \int_{\phi(\theta)_{\min}}^{\phi(\theta)_{\max}} \tilde{n}(R^{-1}x + (s_1, s_2, 0)) \chi_{B_r(P')} (x(t, \phi, \theta)) \sin(\phi) \, d\phi \, d\theta$$

where the limits of the angles  $\phi = \phi(\theta)$  and  $\theta$  are defined as in (4.7). Since we know the limits of the angle  $\theta$ , we are able to fix  $\theta \in [\theta_{\min}, \theta_{\max}]$  to compute the angles  $\phi(\theta)_{\min}$  and  $\phi(\theta)_{\max}$ .

Thus, let  $\theta \in [\theta_{\min}, \theta_{\max}]$  be fixed. We determine the minimal and maximal angle of  $\phi = \phi(\theta)$  by looking for the the prolate spheroidal coordinates of the two points having distance  $r$  to  $P'$  for given  $\theta$ . We denote them by  $\phi(\theta)_{\min}$  and  $\phi(\theta)_{\max}$ . For this purpose, we consider the situation in the  $x'_1 = 0$ -plane which is illustrated in Figure 4.9.

In order to determine the two points mentioned, we solve the equation

$$r^2 = |(0, p'_2, p'_3)^\top - \mathbf{x}(t, \phi(\theta), \theta)|^2$$

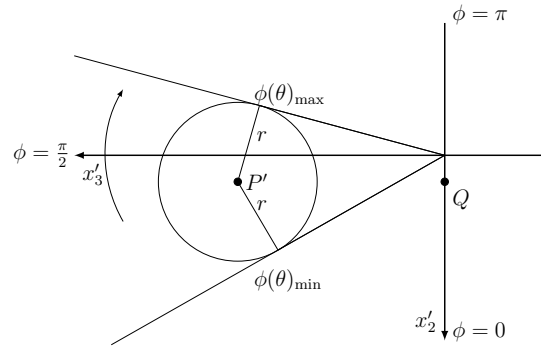


**Figure 4.9:** Here, the situation in the  $x'_1 = 0$ -plane is shown. So, we are looking from a bird's eye view on the given setting in the rotated coordinate system. A look at Figure 4.4 helps for understanding.

for  $\phi(\theta)$ . Here, we insert the prolate spheroidal coordinates with respect to  $(0, 0, 0)^\top$  stated in (4.5) and receive

$$r^2 = \left(\frac{1}{4}t^2 - \alpha^2\right) \sin^2(\phi(\theta)) \cos^2(\theta) + \left(p'_2 - \frac{1}{2}t \cos(\phi)\right)^2 + \left(p'_3 - \sqrt{\frac{1}{4}t^2 - \alpha^2} \sin(\phi(\theta)) \sin(\theta)\right)^2$$

which is equivalent to

$$r^2 = (p'_2)^2 + (p'_3)^2 + \frac{1}{4}t^2 - \alpha^2 \sin(\phi(\theta)) - p'_2 t \sin(\phi(\theta)) - p'_3 \sqrt{t^2 - 4\alpha^2} \sin(\phi(\theta)) \sin(\theta).$$

With the substitution  $z = \cos(\phi(\theta))$  we arrive at

$$r^2 = (p'_2)^2 + (p'_3)^2 + \frac{1}{4}t^2 - \alpha^2(1 - z^2) - p'_2 t z - p'_3 \sqrt{t^2 - 4\alpha^2} \sqrt{1 - z^2} \sin(\theta),$$

which we express by

$$c + bz + \alpha^2 z^2 = -d\sqrt{1 - z^2}$$

using the abbreviations

$$b = p'_2 t, \quad c = (p'_2)^2 + (p'_3)^2 + \frac{1}{4}t^2 - \alpha^2 - r^2, \quad d = -p'_3 \sqrt{t^2 - 4\alpha^2} \sin(\theta).$$

As illustrated in Figure 4.9 this equation has exactly two solutions  $z_1$  and  $z_2$  in  $[-1, 1]$  for fixed  $\theta \in (\theta_{\min}, \theta_{\max})$ . If we consider  $\theta = \theta_{\min}$  or  $\theta = \theta_{\max}$ , there is only one point with distance  $r$  to the midpoint  $P'$ . Hence, the integral over  $\phi$  vanishes in case of  $\theta = \theta_{\min}$  and  $\theta = \theta_{\max}$  such that we do not regard these cases later on. Without loss of generality we obtain

$$\phi(\theta)_{\min} = \arccos(z_1) \quad \text{and} \quad \phi(\theta)_{\max} = \arccos(z_2) \quad (4.9)$$

with  $\phi(\theta)_{\min} < \phi(\theta)_{\max}$ .

We remark that we have not calculated the explicit representations of  $z_1$  and  $z_2$  and consequently of  $\phi(\theta)_{\min}$  and  $\phi(\theta)_{\max}$  although they exist. In the numerical experiments we solve for  $z_1$  and  $z_2$  approximately by Newton's method.

#### 4.2.4. Determination of the limits for the travel time

Up to this point, we identified the limits for the angles of the prolate spheroidal coordinates between which the elliptic Radon transform does not vanish. Beside the restrictions of the two angles, we are also able to limit the values of the travel time. If we remember the original situation illustrated in Figure 4.1, there are open half-ellipsoids which do not intersect the ball  $B_r(P)$ . Also, in the transformed situation only ellipsoids with travel time  $t$  in a certain interval intersect the ball  $B_r(P')$ . In all other cases, the value of  $F\eta(s, t)$  for fixed  $s \in S_0$  is zero. In the following, we determine this interval for the travel time  $t$  given by  $(T_{\min}, T_{\max})$ , where  $T_{\min}$  and  $T_{\max}$  are the minimal and maximal travel time, respectively.

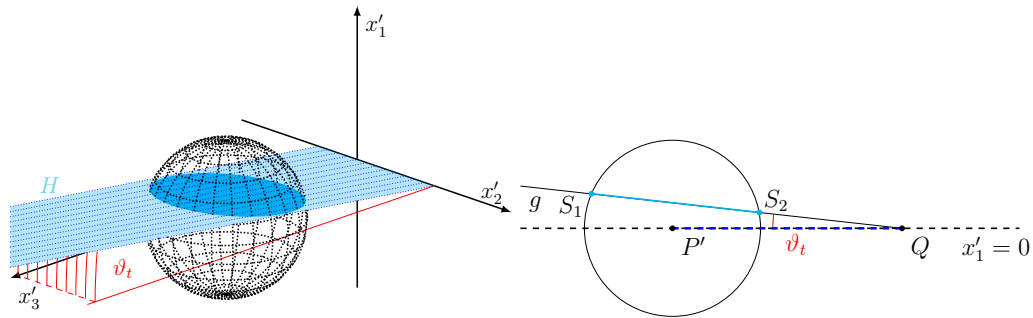


**Figure 4.10:** The intersection circle of the ball  $B_r(P')$  and the plane determined by  $\vartheta_t$  and a cross section of the situation in  $x'_2 = p'_2$ .

We consider the half-plane  $H$  which encloses the angle  $\vartheta_t$  together with the  $x'_2$ - $x'_3$ -plane and calculate the intersection circle of  $\partial B_r(P')$  with  $H$ . In the  $x'_2 = p'_2$ -plane the half-plane  $H$  and the boundary have two intersection points. We denote them by  $S_1$  and  $S_2$  as it is marked in Figure 4.10. Based on these two points, we determine the intersection circle.

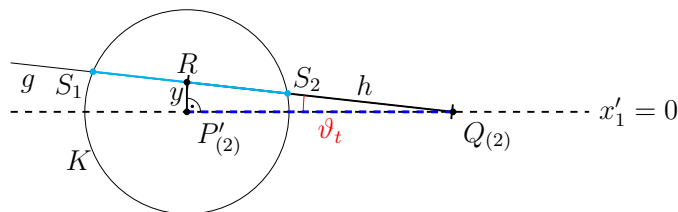


**Figure 4.11:** This figure illustrates the relations we consider.

Again, we consider the situation in the  $x'_2 = p'_2$ -plane and assume everything to be given in two dimensions. First, we want to formulate an equation for the half-line  $g$  starting at  $Q_{(2)}$  and lying in the half-plane  $H$ . Considering the right-angled triangle given by  $Q_{(2)}$ ,  $R = (y, p'_3)^\top$  for some unknown  $y > 0$  and  $P'_{(2)}$  we obtain the equations

$$\sin(\vartheta_t) = \frac{y}{h} \quad \text{and} \quad \cos(\vartheta_t) = \frac{p'_3}{h},$$

where  $\vartheta_t$  is the angle at the point  $Q_{(2)}$  and  $h$  the distance between  $R$  and  $Q_{(2)}$  as marked in Figure 4.11. Together, these two equations yield  $y = h \sin(\vartheta_t) = p'_3 \tan(\vartheta_t)$ . Then, the

half-line  $g$  is the following set of points

$$\left\{ x \in \mathbb{R}^2 \mid x = \lambda \begin{pmatrix} p'_3 \tan(\vartheta_t) \\ p'_3 \end{pmatrix} \text{ for } \lambda \in \mathbb{R} \right\}.$$

Next, we determine the two intersection points of  $g$  and the circle  $K$  given by  $x_1^2 + (x_3 - p'_3)^2 = r^2$ . Inserting the conditions on points lying on  $g$ , we get the quadratic equation

$$\lambda^2 ((p'_3)^2 \tan^2(\vartheta_t) + (p'_3)^2) - \lambda 2(p'_3)^2 + (p'_3)^2 - r^2 = 0,$$

which has the two solutions

$$\lambda_{1/2} = \frac{2(p'_3)^2 \pm \sqrt{4(p'_3)^4 - 4(p'_3)^2(\tan^2(\vartheta_t) + 1)((p'_3)^2 - r^2)}}{2(p'_3)^2(\tan^2(\vartheta_t) + 1)},$$

where we notice that  $\lambda_1 > \lambda_2$  holds. This yields the two intersection points

$$S_1 = \lambda_1 \begin{pmatrix} p'_3 \tan(\vartheta_t) \\ p'_3 \end{pmatrix} \quad \text{and} \quad S_2 = \lambda_2 \begin{pmatrix} p'_3 \tan(\vartheta_t) \\ p'_3 \end{pmatrix}.$$

We note that the midpoint  $\widetilde{M}_{(2)}$  of  $S_1$  and  $S_2$  is given by

$$\widetilde{M}_{(2)} = \begin{pmatrix} \frac{(\lambda_1 + \lambda_2)}{2} p'_3 \tan(\vartheta_t) \\ \frac{(\lambda_1 + \lambda_2)}{2} p'_3 \end{pmatrix}$$

and emphasise that this is not the point  $R$  although it looks like in Figure 4.11.

Before we end up with the equation of the intersection circle drawn in Figure 4.10, we compute another circle  $\widetilde{C}$  as an intermediate step. The circle  $\widetilde{C}$  is illustrated in Figure 4.12. It lies parallel to the  $x'_2$ - $x'_3$ -plane, its midpoint is  $\widetilde{M}$  given by

$$\widetilde{M} = \begin{pmatrix} \frac{(\lambda_1 + \lambda_2)}{2} p'_3 \tan(\vartheta_t) \\ p'_2 \\ \frac{(\lambda_1 + \lambda_2)}{2} p'_3 \end{pmatrix}$$

and its radius is half the distance from  $S_1$  to  $S_2$ , so this is  $\frac{(\lambda_1 - \lambda_2)p'_3}{2 \cos(\vartheta_t)}$ . We observe that the points  $S_1$  and  $S_2$  are not part of the circle  $\widetilde{C}$ . According to the stated properties, the circle  $\widetilde{C}$  is given by

$$\widetilde{C} = \left\{ x \in \mathbb{R}^3 \mid x = \begin{pmatrix} \frac{\lambda_1 + \lambda_2}{2} p'_3 \tan(\vartheta_t) \\ p'_2 \\ \frac{\lambda_1 + \lambda_2}{2} p'_3 \end{pmatrix} + \frac{(\lambda_1 - \lambda_2)p'_3}{2 \cos(\vartheta_t)} \begin{pmatrix} 0 \\ \cos(\tau) \\ \sin(\tau) \end{pmatrix} \text{ for } 0 \leq \tau \leq 2\pi \right\}.$$

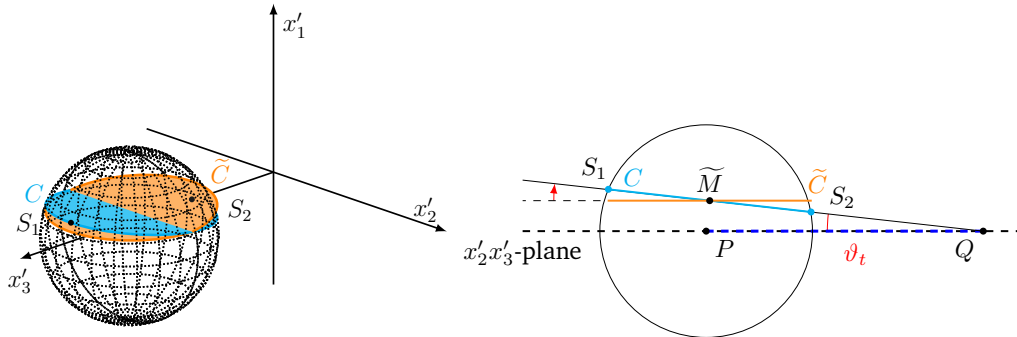


**Figure 4.12:** Both figures illustrate the locations of the searched circle  $C$  and the circle  $\widetilde{C}$ . We note that the circle  $\widetilde{C}$  is not contained in the ball around  $P$ .

In order to get the originally searched circle  $C$ , we have to rotate the circle  $\tilde{C}$ . The rotation matrix of a rotation around the  $x'_2$ -axis with angle  $\vartheta_t$  is given by

$$\begin{pmatrix} \cos(\vartheta_t) & 0 & \sin(\vartheta_t) \\ 0 & 1 & 0 \\ -\sin(\vartheta_t) & 0 & \cos(\vartheta_t) \end{pmatrix}.$$

Since we do not rotate around the  $x'_2$ -axis but around a line parallel to it, we have to shift the circle about the vector

$$\begin{pmatrix} -\frac{\lambda_1+\lambda_2}{2}p'_3 \tan(\vartheta_t) \\ 0 \\ -\frac{\lambda_1+\lambda_2}{2}p'_3 \end{pmatrix}$$

before we apply the rotation matrix from above. Afterwards, we have to shift back about the same vector with changed sign. Applying this on an arbitrary vector  $v = (v_1, v_2, v_3)^\top$  in  $\mathbb{R}^3$ , we arrive at

$$\begin{pmatrix} \cos(\vartheta_t) & 0 & \sin(\vartheta_t) \\ 0 & 1 & 0 \\ -\sin(\vartheta_t) & 0 & \cos(\vartheta_t) \end{pmatrix} \cdot \begin{pmatrix} v_1 - \frac{\lambda_1+\lambda_2}{2}p'_3 \tan(\vartheta_t) \\ v_2 \\ v_3 - \frac{\lambda_1+\lambda_2}{2}p'_3 \end{pmatrix} + \begin{pmatrix} \frac{\lambda_1+\lambda_2}{2}p'_3 \tan(\vartheta_t) \\ 0 \\ \frac{\lambda_1+\lambda_2}{2}p'_3 \end{pmatrix}.$$

If we apply this to an arbitrary point of the circle  $\tilde{C}$ , we obtain the condition

$$\begin{aligned} & \begin{pmatrix} \cos(\vartheta_t) & 0 & \sin(\vartheta_t) \\ 0 & 1 & 0 \\ -\sin(\vartheta_t) & 0 & \cos(\vartheta_t) \end{pmatrix} \cdot \begin{pmatrix} \frac{\lambda_1+\lambda_2}{2}p'_3 \tan(\vartheta_t) - \frac{\lambda_1+\lambda_2}{2}p'_3 \tan(\vartheta_t) \\ p'_2 + \frac{\lambda_1-\lambda_2}{2\cos(\vartheta_t)}p'_3 \cos(\tau) \\ \frac{\lambda_1+\lambda_2}{2}p'_3 + \frac{\lambda_1-\lambda_2}{2\cos(\vartheta_t)}p'_3 \sin(\tau) - \frac{\lambda_1+\lambda_2}{2}p'_3 \end{pmatrix} \\ & \quad + \begin{pmatrix} \frac{\lambda_1+\lambda_2}{2}p'_3 \tan(\vartheta_t) \\ 0 \\ \frac{\lambda_1+\lambda_2}{2}p'_3 \end{pmatrix} \\ & = \begin{pmatrix} \sin(\vartheta_t) \frac{(\lambda_1-\lambda_2)p'_3}{2\cos(\vartheta_t)} \sin(\tau) + \frac{\lambda_1+\lambda_2}{2}p'_3 \tan(\vartheta_t) \\ p'_2 + \frac{(\lambda_1-\lambda_2)p'_3 \cos(\tau)}{2\cos(\vartheta_t)} \\ \cos(\vartheta_t) \frac{(\lambda_1-\lambda_2)p'_3}{2\cos(\vartheta_t)} \sin(\tau) + \frac{\lambda_1+\lambda_2}{2}p'_3 \end{pmatrix} \end{aligned}$$

for  $0 \leq \tau \leq 2\pi$ . Thus, we end up with

$$C = \left\{ x \in \mathbb{R}^3 \mid x = \begin{pmatrix} R \sin(\vartheta_t) \sin(\tau) + \frac{\lambda_1+\lambda_2}{2}p'_3 \tan(\vartheta_t) \\ p'_2 + R \cos(\tau) \\ R \cos(\vartheta_t) \sin(\tau) + \frac{\lambda_1+\lambda_2}{2}p'_3 \end{pmatrix} \text{ for } 0 \leq \tau \leq 2\pi \right\},$$

where  $R = \frac{(\lambda_1-\lambda_2)p'_3}{2\cos(\vartheta_t)}$ .

Finally, for the computation of  $T_{\min}$  and  $T_{\max}$  we have to minimise and maximise the distance

$$|(0, -\alpha, 0)^\top - x| + |x - (0, \alpha, 0)^\top|$$

for  $x \in C$ . In short, we have

$$T_{\min} = \min_{x \in C} \left( |(0, -\alpha, 0)^\top - x| + |x - (0, \alpha, 0)^\top| \right)$$

and

$$T_{\max} = \max_{x \in C} \left( |(0, -\alpha, 0)^\top - x| + |x - (0, \alpha, 0)^\top| \right)$$

(4.10)

with  $C$  as above. Since there is only one intersection point with the ball for  $t = T_{\min}$  and  $t = T_{\max}$ , the value of  $F_n(s, t)$  is zero for these two values of  $t$  and  $s \in S_0$ . Altogether, for fixed  $s \in S_0$  we obtain

$$F_n(s, t) = \frac{1}{2} \int_{\theta_{\min}}^{\theta_{\max}} \int_{\phi(\theta)_{\min}}^{\phi(\theta)_{\max}} \tilde{n}(R^{-1}x + (s_1, s_2, 0)^\top) \chi_{B_r(P')} (x(t, \phi, \theta)) \sin(\phi) \, d\phi \, d\theta \quad (4.11)$$

in case of  $t \in (T_{\min}, T_{\max})$  and  $F_n(s, t) = 0$  if  $t \leq T_{\min}$  or  $t \geq T_{\max}$  is satisfied for  $n = \tilde{n} \chi_{B_r(P)}$  with  $\tilde{n} \in C^\infty(\mathbb{R}_+^3)$ .

### 4.3. The operator $F$ applied to the characteristic function of a half-space

In this section, we compute  $F_n(s, t)$  for fixed  $(s, t) \in S_0 \times (2\alpha, \infty)$  in case of  $n$  is the characteristic function of a half-space. Precisely, the half-space is given by  $\{x \in \mathbb{R}_+^3 \mid x_3 \geq l\}$  for some fixed  $l > 0$ , i.e.  $n = \chi_{\{x \in \mathbb{R}_+^3 \mid x_3 \geq l\}}$ . According to identity (1.18), we have

$$F_n(s, t) = \frac{1}{2} \int_{\theta_{\min}}^{\theta_{\max}} \int_{\phi(\theta)_{\min}}^{\phi(\theta)_{\max}} n(x(s, t, \phi, \theta)) \sin(\phi) \, d\phi \, d\theta$$

for  $(s, t) \in S_0 \times (2\alpha, \infty)$  with

$$\begin{aligned} \theta_{\min} &= \theta_{\min}(s, t) := \min\{\theta \in (0, \pi) \mid x(s, t, \phi, \theta) \in \text{supp}(n)\}, \\ \theta_{\max} &= \theta_{\max}(s, t) := \max\{\theta \in (0, \pi) \mid x(s, t, \phi, \theta) \in \text{supp}(n)\}, \end{aligned}$$

and

$$\begin{aligned} \phi(\theta)_{\min} &= \phi(\theta)_{\min}(s, t) := \min\{\phi \in (0, \pi) \mid x(s, t, \phi, \theta) \in \text{supp}(n)\}, \\ \phi(\theta)_{\max} &= \phi(\theta)_{\max}(s, t) := \max\{\phi \in (0, \pi) \mid x(s, t, \phi, \theta) \in \text{supp}(n)\} \end{aligned}$$

if  $n \in L^1(\Psi_t((0, \pi) \times (0, \pi)))$  for fixed  $t \in (2\alpha, \infty)$  holds.

In case of  $n = \chi_{\{x \in \mathbb{R}_+^3 \mid x_3 \geq l\}}$  for fixed  $(s, t) \in S_0 \times (2\alpha, \infty)$ , the value  $n(x(s, t, \phi, \theta))$  is equal to 1 if  $\theta \in (\theta_{\min}, \theta_{\max})$  and additionally  $\phi(\theta) \in (\phi(\theta)_{\min}, \phi(\theta)_{\max})$  is satisfied. Otherwise  $n(x(s, t, \phi, \theta))$  vanishes for fixed  $(s, t) \in S_0 \times (2\alpha, \infty)$ .

As a consequence, we deduce  $n \in L^1(\Psi_t((0, \pi) \times (0, \pi)))$  for fixed  $t \in (2\alpha, \infty)$  and

$$F_n(s, t) = \frac{1}{2} \int_{\theta_{\min}}^{\theta_{\max}} \int_{\phi(\theta)_{\min}}^{\phi(\theta)_{\max}} \sin(\phi) \, d\phi \, d\theta$$

for  $(s, t) \in S_0 \times (2\alpha, \infty)$  and the angles  $\theta_{\min}$ ,  $\theta_{\max}$ ,  $\phi(\theta)_{\min}$  and  $\phi(\theta)_{\max}$ .

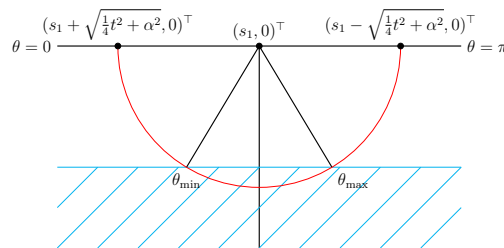


Figure 4.13: The minimal and maximal angle for  $\theta$  illustrated in the  $x_2 = s_2$ -plane.

In order to calculate the minimal and maximal angle for  $\theta$  where the open half-ellipsoid intersects the half-space, we consider the situation in the  $x_2 = s_2$ -plane. In Figure 4.13 the two angles are marked. We start to measure with  $\theta = 0$  at values with  $x_3 = 0$  and  $x_1$  larger than  $s_1$  in prolate spheroidal coordinates. This time we consider these coordinates with respect to  $(s_1, s_2, 0)^\top$  as stated in (1.15) on  $\mathbb{R}_+^3$  but now for fixed  $t \in (2\alpha, \infty)$ , so

$$\begin{aligned} x_1 &= s_1 + \sqrt{\frac{1}{4}t^2 - \alpha^2} \sin(\phi) \cos(\theta), \\ x_2 &= s_2 + \frac{1}{2}t \cos(\phi), \\ x_3 &= \sqrt{\frac{1}{4}t^2 - \alpha^2} \sin(\phi) \sin(\theta) \end{aligned} \quad (4.12)$$

for  $\phi, \theta \in (0, \pi)$ . If we intersect the open half-ellipsoid determined by  $s$  and  $t$  with the plane given by  $x_2 = s_2$ , we obtain a circle. We search now for the two points lying on this circle and the plane given by  $x_3 = l$ . For all points in the  $x_2 = s_2$ -plane we have  $\phi = \frac{1}{2}\pi$  in the prolate spheroid coordinates. An illustration is given in Figure 1.3. Thus, the possible points given in prolate spheroidal coordinates satisfy  $\phi = \frac{1}{2}\pi$  and  $x_3 = l$ . Then, the last component written in these coordinates is

$$l = x_3 = \sqrt{\frac{1}{4}t^2 - \alpha^2} \sin(\theta)$$

and we solve for one solution of  $\theta$  with the result

$$\theta = \arcsin\left(\frac{l}{\sqrt{\frac{1}{4}t^2 - \alpha^2}}\right).$$

Since

$$\arcsin\left(\frac{l}{\sqrt{\frac{1}{4}t^2 - \alpha^2}}\right) \in \left(0, \frac{\pi}{2}\right]$$

holds as  $l > 0$  is satisfied, we obtain

$$\theta_{\min} = \arcsin\left(\frac{l}{\sqrt{\frac{1}{4}t^2 - \alpha^2}}\right) \quad \text{and} \quad \theta_{\max} = \pi - \theta_{\min} = \pi - \arcsin\left(\frac{l}{\sqrt{\frac{1}{4}t^2 - \alpha^2}}\right). \quad (4.13)$$

In order to observe that this is true, see Figure 1.2. Since values with  $x_3 = 0$  and  $x_1 > s_1$  correspond to  $\theta = 0$  and values with  $x_3 = 0$  and  $x_1 < s_1$  to  $\theta = \pi$ , we obtain  $\theta_{\max}$  by subtracting  $\theta_{\min}$  from  $\pi$ .

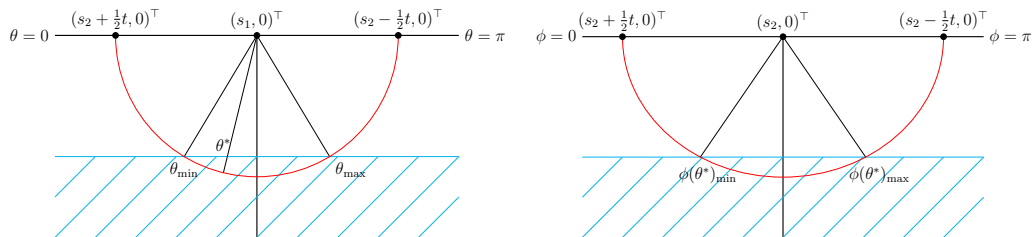


**Figure 4.14:** We fix a value  $\theta^* \in [\theta_{\min}, \theta_{\max}]$  and consider then the plane  $\theta = \theta^*$  which is given in the right image.

Also in case of the half-space we determine the angle  $\phi$  in dependence of  $\theta$ . Thus, let  $\theta^* \in [\theta_{\min}, \theta_{\max}]$  be fixed. We consider the situation in the half-plane given by  $\theta = \theta^*$  in radial direction to the point  $(s_1, s_2, 0)^\top$ . An illustration is given in Figure 4.14. For the fixed angle  $\theta^*$  we determine the limiting angles  $\phi(\theta^*)_{\min}$  and  $\phi(\theta^*)_{\max}$ . The searched angles for  $\phi$  are given by the condition where the open half-ellipsoid intersects the plane  $x_3 = l$ . Hence, using again the prolate spheroidal coordinates stated in (4.12) we deduce

$$l = x_3 = \sqrt{\frac{1}{4}t^2 - \alpha^2 \sin(\phi(\theta^*)) \sin(\theta^*)}.$$

Solving this equation for one possible  $\phi(\theta^*)$ , we obtain

$$\phi(\theta^*) = \arcsin\left(\frac{l}{\sqrt{\frac{1}{4}t^2 - \alpha^2 \sin(\theta^*)}}\right).$$

Since  $\theta^* \in (0, \pi)$  holds, we have that  $\sin(\theta^*) > 0$  is satisfied. This yields

$$\arcsin\left(\frac{l}{\sqrt{\frac{1}{4}t^2 - \alpha^2 \sin(\theta^*)}}\right) \in \left(0, \frac{\pi}{2}\right].$$

Similarly to the values of the angle  $\theta$  the values satisfying  $x_3 = 0$  and  $x_2$  smaller than  $s_2$  correspond to the angle  $\phi = \pi$  and those larger than  $s_2$  to the angle  $\phi = 0$ . This is confirmed by Figure 1.3. Consequently, it follows

$$\phi(\theta^*)_{\min} = \arcsin\left(\frac{l}{\sqrt{\frac{1}{4}t^2 - \alpha^2 \sin(\theta^*)}}\right)$$

and

(4.14)

$$\phi(\theta^*)_{\max} = \pi - \phi(\theta^*)_{\min} = \pi - \arcsin\left(\frac{l}{\sqrt{\frac{1}{4}t^2 - \alpha^2 \sin(\theta^*)}}\right).$$

As in the case we considered in Section 4.2, there are open half-ellipsoids which do not intersect the given half-space. The reason in case of the half-space is that the travel time of them is too small. Thus, we calculate the minimal travel time  $T_{\min}$ . This is the associated travel time to the open half-ellipsoid which intersects the half-space in exactly one point. The intersection point lies on the plane  $x_3 = l$  and is just below the midpoint  $(s_1, s_2, 0)^\top$  of the two foci  $\mathbf{x}_s(s)$  and  $\mathbf{x}_r(s)$ . Hence, it is given by  $(s_1, s_2, l)^\top$ . These deliberations yield

$$\begin{aligned} T_{\min} &= \min_{\{x \in \mathbb{R}_+^3 \mid \varphi(s, x) = t\}} \left( |\mathbf{x}_s(s) - x| + |x - \mathbf{x}_r(s)| \right) \\ &= |(s_1, s_2 - \alpha, 0)^\top - (s_1, s_2, l)^\top| + |(s_1, s_2, l)^\top - (s_1, s_2 + \alpha, 0)^\top| \\ &= |(0, -\alpha, -l)^\top| + |(0, -\alpha, l)^\top| = 2\sqrt{\alpha^2 + l^2}. \end{aligned}$$

For  $t = T_{\min}$  the integral also vanishes because there is only one intersection point of the half-space with the open half-ellipsoid.

Finally, for fixed  $s \in S_0$  we obtain

$$Fn(s, t) = \frac{1}{2} \int_{\theta_{\min}}^{\theta_{\max}} \int_{\phi(\theta)_{\min}}^{\phi(\theta)_{\max}} \sin(\phi) \, d\phi \, d\theta \quad (4.15)$$

in case of  $t \in (T_{\min}, \infty)$  and  $Fn(s, t) = 0$  if  $t \leq T_{\min}$  holds.

---

## Numerical experiments

---

In the last chapter of this thesis, we present the numerical results we achieve with the approach described in the previous chapters. But before we are in the position to realise numerical experiments, we have to explain how we obtain the numerical reconstructions in form of  $\tilde{\Lambda}_\gamma n$ , where  $\tilde{\Lambda}$  is one of the reconstruction operators we introduced. For that reason, we consider in a first section the reconstruction kernels associated with the reconstruction operators. Beside the data and the cut-off function they are the third essential part when calculating the approximation  $\tilde{\Lambda}_\gamma n$ .

The second subsection starts with a description of the used discretisation and the cut-off function. After that, we discuss how we generate data in case we have no measurements. In connection with this we argue what we expect to see in the numerical experiments based on the theoretical considerations of Chapter 3. Finally, we state information concerning the implementation.

In the last section, we show the numerical results. Here, we consider different cross sections and discuss the choice of certain parameters. Further, we experiment by generating data with an offset randomly distributed in an interval and by using a different offset for the data generation than for the reconstruction. It follows a discussion concerning the advantages and disadvantages of the different reconstruction operators we introduced in Chapter 3. Last, we present reconstructions we obtain with data generated from the wave equation.

### 5.1. Different reconstruction kernels

In this section, we define the different reconstruction kernels associated with the different reconstruction operators. We start with the reconstruction kernel for  $\Lambda$  which we describe in detail. Since the other reconstruction kernels are defined in an analogous way, we discuss them briefly afterwards.

#### 5.1.1. The reconstruction kernel for $\Lambda$

As already mentioned in Section 4.1 we approximate  $\Lambda n$  for  $n \in \mathcal{E}'(\mathbb{R}_+^3)$  evaluated at a point  $p \in \mathbb{R}_+^3$  with the help of a mollifier  $e_{p,\gamma}$  for some  $\gamma > 0$ . This approximation  $\Lambda_\gamma n$  is given by the relation

$$\Lambda_\gamma n(p) = \int_{S_0 \times (2\alpha, \infty)} \psi(s, t) F n(s, t) F \partial_3 \Delta e_{p,\gamma}(s, t) \, d(s, t) \quad (5.1)$$

which we calculated in (4.1). For the mollifier we choose the following function

$$e_{p,\gamma,k}(x) = \begin{cases} C_{\gamma,k}(\gamma^2 - |x - p|^2)^k, & |x - p| < \gamma, \\ 0, & |x - p| \geq \gamma, \end{cases}$$

for  $x \in \mathbb{R}_+^3$  with  $\gamma, k > 0$  and

$$C_{\gamma,k} = \left( \int_{B_\gamma(p)} (\gamma^2 - |x - p|^2)^k dx \right) = \left( 4\pi \int_0^\gamma (\gamma^2 - r^2)^k r^2 dr \right)^{-1} = \frac{\Gamma(k + 5/2)}{\pi^{3/2} \gamma^{2k+3} \Gamma(k + 1)}.$$

Here, in comparison to Section 4.1, the mollifier depends on a further parameter  $k$ . The parameter  $k$  determines the smoothness of  $e_{p,\gamma,k}$  for  $\gamma > 0$ . By the definition of  $e_{p,\gamma,k}$  and  $C_{\gamma,k}$  for  $\gamma, k > 0$ , we have  $\text{supp } e_{p,\gamma,k} = \overline{B_\gamma(p)}$  and  $\int_{\mathbb{R}^3} e_{p,\gamma,k}(x) dx = 1$ . Thus, it holds  $e_{p,\gamma,k} \rightarrow \delta(\cdot - p)$  for  $\gamma \rightarrow 0$  and  $e_{p,\gamma,k}$  is a mollifier.

This leads to the relation

$$\Lambda_\gamma n(p) = \langle \psi F n, F \partial_3 \Delta e_{p,\gamma,k} \rangle = \int_{S_0 \times (2\alpha, \infty)} \psi(s, t) F n(s, t) F \partial_3 \Delta e_{p,\gamma,k}(s, t) d(s, t) \quad (5.2)$$

for  $n \in \mathcal{E}'(\mathbb{R}_+^3)$ , where we inserted the just introduced mollifier in (5.1).

The reconstruction kernel  $r_{p,\gamma,k}$  for  $\Lambda$  is given by the right-hand side of the dual pairing in (5.2), that is

$$r_{p,\gamma,k}(s, t) := F \partial_3 \Delta e_{p,\gamma,k}(s, t)$$

for  $(s, t) \in S_0 \times (2\alpha, \infty)$ ,  $p \in \mathbb{R}_+^3$  and  $k > 0$ . It depends on the point  $p \in \mathbb{R}_+^3$ , in which we evaluate  $\Lambda n$  for  $n \in \mathcal{E}'(\mathbb{R}_+^3)$ , and the parameters  $\gamma, k > 0$ . Using this notation, we simplify

$$\Lambda_\gamma n(p) \approx \langle \Lambda n, e_{p,\gamma,k} \rangle = \langle \psi F n, r_{p,\gamma,k} \rangle$$

for  $n \in \mathcal{E}'(\mathbb{R}_+^3)$  and  $p \in \mathbb{R}_+^3$ . If we take a closer look at this identity, we notice that we only need the values of the cut-off function  $\psi$  and the data in addition to the reconstruction kernel to receive an approximation of  $\Lambda n$  evaluated at a point  $p \in \mathbb{R}_+^3$ .

This observation follows since the data  $y$  is given by  $y = F n$  according to (1.13). For this reason, the approximation simplifies to

$$\Lambda_\gamma n(p) \approx \langle \Lambda n, e_{p,\gamma,k} \rangle = \langle \psi y, r_{p,\gamma,k} \rangle$$

for  $n \in \mathcal{E}'(\mathbb{R}_+^3)$ . In this sense, the reconstruction kernel is a kind of inversion operator, which is independent of the data.

In the next lemma, we rewrite the reconstruction kernel using the operator  $F$ .

**5.1 Lemma.** *Let  $\gamma > 0$  and  $k \geq 3$  be given. Using the abbreviation*

$$\tilde{e}_{p,\gamma,k}(x) = \begin{cases} (\gamma^2 - |x - p|^2)^k, & \text{if } |x - p| < \gamma, \\ 0, & \text{if } |x - p| \geq \gamma, \end{cases}$$

we have

$$\Lambda_\gamma n(p) = \langle \Lambda n, e_{p,\gamma,k} \rangle = \langle \psi F n, r_{p,\gamma,k} \rangle$$

for  $n \in \mathcal{E}'(\mathbb{R}_+^3)$  with

$$\begin{aligned} r_{p,\gamma,k}(s,t) &= C_{\gamma,k} F \left( x \mapsto 20k(k-1)(x_3 - p_3) \tilde{e}_{p,\gamma,k-2}(x) \right. \\ &\quad \left. - 8k(k-1)(k-2)(x_3 - p_3)|x-p|^2 \tilde{e}_{p,\gamma,k-3}(x) \right) (s,t) \\ &= 4k(k-1) C_{\gamma,k} \left( 5F \left( x \mapsto (x_3 - p_3) \tilde{e}_{p,\gamma,k-2}(x) \right) \right. \\ &\quad \left. - 2(k-2)F \left( x \mapsto (x_3 - p_3)|x-p|^2 \tilde{e}_{p,\gamma,k-3}(x) \right) \right) (s,t) \end{aligned}$$

for  $(s,t) \in S_0 \times (2\alpha, \infty)$ .

*Proof.* By the definition of  $r_{p,\gamma,k}$ , we have to compute  $F\partial_3\Delta e_{p,\gamma,k}$ . Therefore, we calculate

$$\frac{\partial}{\partial x_i} \left( (\gamma^2 - |x-p|^2)^k \right) = -2k(x_i - p_i)(\gamma^2 - |x-p|^2)^{k-1}$$

and

$$\frac{\partial^2}{\partial x_i^2} \left( (\gamma^2 - |x-p|^2)^k \right) = -2k(\gamma^2 - |x-p|^2)^{k-1} + 4k(k-1)(x_i - p_i)^2(\gamma^2 - |x-p|^2)^{k-2}$$

for  $x \in \mathbb{R}_+^3$  and  $i \in \{1, 2, 3\}$ . This yields

$$\Delta \tilde{e}_{p,\gamma,k}(x) = -6k(\gamma^2 - |x-p|^2)^{k-1} + 4k(k-1)|x-p|^2(\gamma^2 - |x-p|^2)^{k-2} \chi_{B_\gamma(p)}(x)$$

for  $x \in \mathbb{R}_+^3$ . Further, by applying the derivative in third space direction we obtain

$$\begin{aligned} \partial_3 \Delta \tilde{e}_{p,\gamma,k}(x) &= \left( 12k(k-1)(x_3 - p_3)(\gamma^2 - |x-p|^2)^{k-2} + 8k(k-1)(x_3 - p_3)(\gamma^2 - |x-p|^2)^{k-2} \right. \\ &\quad \left. - 8k(k-1)(k-2)(x_3 - p_3)|x-p|^2(\gamma^2 - |x-p|^2)^{k-3} \right) \chi_{B_\gamma(p)}(x) \\ &= \left( 20k(k-1)(x_3 - p_3)(\gamma^2 - |x-p|^2)^{k-2} \right. \\ &\quad \left. - 8k(k-1)(k-2)(x_3 - p_3)|x-p|^2(\gamma^2 - |x-p|^2)^{k-3} \right) \chi_{B_\gamma(p)}(x). \end{aligned}$$

Together with the identity  $e_{p,\gamma,k} = C_{\gamma,k} \tilde{e}_{p,\gamma,k}$  this yields the claimed assertion.  $\square$

The reconstruction kernel contains two parameters we have not chosen up to now. For the smoothing parameter  $k$  we fix  $k = 3$ . Then  $\tilde{e}_{p,\gamma,k-3}$  is still smooth on the ball  $B_\gamma(p)$ . However, the scaling parameter  $\gamma$  will be chosen for each numerical experiment separately.

In Lemma 5.1 we expressed the reconstruction kernel by the operator  $F$ . However, for the numerical experiments this is not sufficient. In order to realise them, we need the explicit expression of the reconstruction kernel which we deduce in the following.

In the representation of  $C_{3,\gamma}$  two values of the  $\Gamma$ -function appear. With the identities  $\Gamma(1) = 1$ ,  $\Gamma(\frac{1}{2}) = \sqrt{\pi}$  and  $\Gamma(x+1) = x \cdot \Gamma(x)$  for  $x \in \mathbb{R}$  we deduce

$$\Gamma(4) = 3! \cdot \Gamma(1) = 6$$

and

$$\Gamma\left(3 + \frac{5}{2}\right) = \Gamma\left(\frac{9}{2} + 1\right) = \frac{9}{2} \cdot \frac{7}{2} \cdot \frac{5}{2} \cdot \frac{3}{2} \cdot \Gamma\left(\frac{1}{2}\right) = \frac{945\sqrt{\pi}}{32}.$$

By the definition of  $C_{\gamma,3}$ , we conclude

$$C_{\gamma,3} = \frac{\Gamma(3+5/2)}{\pi^{3/2}\gamma^{6+3}\Gamma(3+1)} = \frac{945\sqrt{\pi}}{\pi^{3/2} \cdot 32\gamma^9 \cdot 6} = \frac{315}{64\pi\gamma^9}.$$

Then, the reconstruction kernel  $r_{p,\gamma,3}$  is given by

$$\begin{aligned} r_{p,\gamma,3}(s,t) &= \frac{315}{64\pi\gamma^9} F\left(x \mapsto (120\gamma^2(x_3 - p_3) - 120(x_3 - p_3)|x - p|^2 - 48(x_3 - p_3)|x - p|^2) \right. \\ &\quad \left. \chi_{B_\gamma(p)}(x)\right)(s,t) \\ &= \frac{315}{64\pi\gamma^9} F\left(x \mapsto (120\gamma^2(x_3 - p_3) - 168(x_3 - p_3)|x - p|^2)\chi_{B_\gamma(p)}(x)\right)(s,t) \end{aligned} \quad (5.3)$$

for  $(s,t) \in S_0 \times (2\alpha, \infty)$  according to Lemma 5.1. By equation (4.11), we have to compute

$$Fn(s,t) = \frac{1}{2} \int_{\theta_{\min}}^{\theta_{\max}} \int_{\phi(\theta)_{\min}}^{\phi(\theta)_{\max}} \tilde{n}(R^{-1}x + (s_1, s_2, 0)^\top) \chi_{B_\gamma(p')}(x(t, \phi, \theta)) \sin(\phi) d\phi d\theta \quad (5.4)$$

with  $n = \tilde{n}\chi_{B_\gamma(p)}$  and the smooth function  $\tilde{n}(x) = 120\gamma^2(x_3 - p_3) - 168(x_3 - p_3)|x - p|^2$  for  $x \in \mathbb{R}^3$  in case of  $t \in (T_{\min}, T_{\max})$ . Furthermore, it holds  $Fn(s,t) = 0$  if  $t \leq T_{\min}$  or  $t \geq T_{\max}$  is satisfied for fixed  $s \in S_0$ . Here,  $p'$  is given by  $p' = R(p - (s_1, s_2, 0)^\top)$  as we observed in identity (4.2). Moreover, we have

$$x(t, \phi, \theta) = \begin{pmatrix} \sqrt{\frac{1}{4}t^2 - \alpha^2 \sin(\phi) \cos(\theta)} \\ \frac{1}{2}t \cos(\phi) \\ \sqrt{\frac{1}{4}t^2 - \alpha^2 \sin(\phi) \sin(\theta)} \end{pmatrix}$$

for  $t \in (T_{\min}, T_{\max})$ ,  $\phi \in [0, \pi)$  and  $\theta \in [0, 2\pi)$  by (1.14). With the relations in (4.4), we receive

$$R^{-1}x(t, \phi, \theta) + (s_1, s_2, 0)^\top = \begin{pmatrix} \sqrt{\frac{1}{4}t^2 - \alpha^2 \sin(\phi) (\cos(\beta) \cos(\theta) + \sin(\beta) \sin(\theta))} + s_1 \\ \frac{1}{2}t \cos(\phi) + s_2 \\ \sqrt{\frac{1}{4}t^2 - \alpha^2 \sin(\phi) (-\sin(\beta) \cos(\theta) + \cos(\beta) \sin(\theta))} \end{pmatrix} \quad (5.5)$$

with  $\beta = \arctan((p_1 - s_1)/p_3)$  as given in (4.3) and for  $t \in (T_{\min}, T_{\max})$ ,  $\phi \in [0, \pi)$  and  $\theta \in [0, 2\pi)$ . For further simplifications, we use the identity

$$|R^{-1}x(t, \phi, \theta) + (s_1, s_2, 0)^\top - p| = |x(t, \phi, \theta) - p'| \quad (5.6)$$

for  $t \in (T_{\min}, T_{\max})$ ,  $\phi \in [0, \pi)$  and  $\theta \in [0, 2\pi)$  verified in computation (4.6). In the following, we write  $[v]_3$  for the third component of an element  $v \in \mathbb{R}^3$ . Regarding all observations made above, we deduce

$$\begin{aligned} r_{p,\gamma,3}(s,t) &= \frac{315}{64\pi\gamma^9} \frac{1}{2} \int_{\theta_{\min}}^{\theta_{\max}} \int_{\phi(\theta)_{\min}}^{\phi(\theta)_{\max}} \left( 120\gamma^2 \left( [R^{-1}x(t, \phi, \theta) + (s_1, s_2, 0)^\top]_3 - p_3 \right) \right. \\ &\quad \left. - 168 \left( [R^{-1}x(t, \phi, \theta) + (s_1, s_2, 0)^\top]_3 - p_3 \right) |R^{-1}x(t, \phi, \theta) + (s_1, s_2, 0)^\top - p|^2 \right) \\ &\quad \chi_{B_\gamma(p')}(x(t, \phi, \theta)) \sin(\phi) d\phi d\theta \end{aligned}$$

$$\begin{aligned}
&= \frac{315}{64\pi\gamma^9} \frac{1}{2} \int_{\theta_{\min}}^{\theta_{\max}} \int_{\phi(\theta)_{\min}}^{\phi(\theta)_{\max}} \left( 120\gamma^2 \left( \sqrt{\frac{1}{4}t^2 - \alpha^2} \sin(\phi) (-\sin(\beta) \cos(\theta) + \cos(\beta) \sin(\theta)) - p_3 \right) \right. \\
&\quad \left. - 168 \left( \sqrt{\frac{1}{4}t^2 - \alpha^2} \sin(\phi) (-\sin(\beta) \cos(\theta) + \cos(\beta) \sin(\theta)) - p_3 \right) |x(t, \phi, \theta) - p'|^2 \right) \\
&\quad \chi_{B_\gamma(p')}(x(t, \phi, \theta)) \sin(\phi) \, d\phi \, d\theta \\
&= \frac{315}{64\pi\gamma^9} \frac{1}{2} \int_{\theta_{\min}}^{\theta_{\max}} \int_{\phi(\theta)_{\min}}^{\phi(\theta)_{\max}} \left( 120\gamma^2 \left( \sqrt{\frac{1}{4}t^2 - \alpha^2} \sin(\phi) (-\sin(\beta) \cos(\theta) + \cos(\beta) \sin(\theta)) - p_3 \right) \right. \\
&\quad \left. - 168 \left( \sqrt{\frac{1}{4}t^2 - \alpha^2} \sin(\phi) (-\sin(\beta) \cos(\theta) + \cos(\beta) \sin(\theta)) - p_3 \right) |x(t, \phi, \theta) - p'|^2 \right) \\
&\quad \chi_{B_\gamma(p')}(x(t, \phi, \theta)) \sin(\phi) \, d\phi \, d\theta \\
&= \frac{315}{64\pi\gamma^9} \frac{1}{2} \int_{\theta_{\min}}^{\theta_{\max}} \int_{\phi(\theta)_{\min}}^{\phi(\theta)_{\max}} \left( 120\gamma^2 (-\sin(\beta) \cos(\theta) + \cos(\beta) \sin(\theta)) \sqrt{\frac{1}{4}t^2 - \alpha^2} \sin^2(\phi) \right. \\
&\quad \left. - 120\gamma^2 p_3 \sin(\phi) \right. \\
&\quad \left. - 168 (-\sin(\beta) \cos(\theta) + \cos(\beta) \sin(\theta)) \sqrt{\frac{1}{4}t^2 - \alpha^2} |x(t, \phi, \theta) - p'|^2 \sin^2(\phi) \right. \\
&\quad \left. + 168 p_3 |x(t, \phi, \theta) - p'|^2 \sin(\phi) \right) \chi_{B_\gamma(p')}(x(t, \phi, \theta)) \, d\phi \, d\theta
\end{aligned} \tag{5.7}$$

for  $(s, t) \in S_0 \times (T_{\min}, T_{\max})$ . Further, we calculate

$$\begin{aligned}
&|x(t, \phi, \theta) - p'|^2 \\
&= \left| \begin{pmatrix} \sqrt{\frac{1}{4}t^2 - \alpha^2} \sin(\phi) \cos(\theta) \\ \frac{1}{2}t \cos(\phi) \\ \sqrt{\frac{1}{4}t^2 - \alpha^2} \sin(\phi) \sin(\theta) \end{pmatrix} - p' \right|^2 \\
&= \left( \sqrt{\frac{1}{4}t^2 - \alpha^2} \sin(\phi) \cos(\theta) - p'_1 \right)^2 + \left( \frac{1}{2}t \cos(\phi) - p'_2 \right)^2 + \left( \sqrt{\frac{1}{4}t^2 - \alpha^2} \sin(\phi) \sin(\theta) - p'_3 \right)^2 \\
&= (a + b \sin(\phi))^2 + (c + d \cos(\phi))^2 + (e + f \sin(\phi))^2
\end{aligned} \tag{5.8}$$

with the abbreviations

$$\begin{aligned}
a &= -p'_1 = 0, & b &= \sqrt{\frac{1}{4}t^2 - \alpha^2} \cos(\theta), & c &= -p'_2 = -p_2 + s_2, \\
d &= \frac{1}{2}t, & e &= -p'_3 = -\frac{p_3}{\cos\left(\arctan\left(\frac{p_1 - s_1}{p_3}\right)\right)}, & f &= \sqrt{\frac{1}{4}t^2 - \alpha^2} \sin(\theta)
\end{aligned}$$

for  $t \in (T_{\min}, T_{\max})$ ,  $\phi \in [0, \pi)$  and  $\theta \in [0, 2\pi)$ . Hence, in order to compute the reconstruction kernel  $r_{p,\gamma,3}$  stated in (5.7), we need the antiderivates of the following functions

$$\begin{aligned}
\phi &\mapsto \sin^2(\phi), & \phi &\mapsto (a + b \sin(\phi))^2 + (c + d \cos(\phi))^2 + (e + f \sin(\phi))^2 \sin^2(\phi), \\
\phi &\mapsto \sin(\phi), & \phi &\mapsto (a + b \sin(\phi))^2 + (c + d \cos(\phi))^2 + (e + f \sin(\phi))^2 \sin(\phi)
\end{aligned}$$

with  $b, c$  and  $d$  as above. Since these four functions are trigonometric polynomials in  $\phi$ , their antiderivates are analytically known. We calculate them using a computer algebra system and implement the calculation of the integrals by evaluating at the start and end point.

Altogether, we receive an expression for the reconstruction kernel  $r_{p,\gamma,3}$  at  $(s, t) \in S_0 \times (2\alpha, \infty)$  depending on the limits of the angles  $\theta$  and  $\phi = \phi(\theta)$  and  $T_{\min}$  and  $T_{\max}$ .

### 5.1.2. The reconstruction kernels for the modified operators

Before we compute the reconstruction kernels of the modified operators, we mentioned them once again. We have

$$\Lambda_{\text{mod},0} := -\Delta\partial_3 MF^*\psi F$$

and

$$\Lambda_{\text{mod},1} = -\Delta\partial_3(M + \alpha \text{Id})F^*\psi F \quad \text{and} \quad \Lambda_{\text{mod},2} = -\Delta\partial_3(M + \alpha^2 \text{Id})F^*\psi F$$

defined in Corollary 3.29 and Corollary 3.31, respectively. Analogously to the approach in Subsection 5.1.1, in case of  $\Lambda$  we approximate  $\Lambda_{\text{mod},i}$  for  $i \in \{0, 1, 2\}$  evaluated at  $p \in \mathbb{R}_+^3$  for  $n \in \mathcal{E}'(\mathbb{R}_+^3)$  by

$$\Lambda_{\text{mod},i,\gamma}n(p) := \langle \Lambda_{\text{mod},i}n, e_{p,\gamma,k} \rangle.$$

For this reason, we define analogue to  $r_{p,\gamma,k}$  the following reconstruction kernels

- (a)  $r_{p,\gamma,k,\text{mod},0}(s, t) := FM\partial_3\Delta e_{p,\gamma,k}(s, t),$
- (b)  $r_{p,\gamma,k,\text{mod},1}(s, t) := F(M + \alpha \text{Id})\partial_3\Delta e_{p,\gamma,k}(s, t),$
- (c)  $r_{p,\gamma,k,\text{mod},2}(s, t) := F(M + \alpha^2 \text{Id})\partial_3\Delta e_{p,\gamma,k}(s, t)$

for  $(s, t) \in S_0 \times (2\alpha, \infty)$ .

The next corollary yields representations of the above defined reconstruction kernels. It is a direct consequence of Lemma 5.1.

**5.2 Corollary.** *Let  $\gamma > 0$  and  $k \geq 3$  be given. With the abbreviation*

$$\tilde{e}_{p,\gamma,k}(x) = \begin{cases} (\gamma^2 - |x - p|^2)^k, & \text{if } |x - p| < \gamma, \\ 0, & \text{if } |x - p| \geq \gamma, \end{cases}$$

we have

$$\Lambda_{\text{mod},i,\gamma}n(p) = \langle \Lambda_{\text{mod},i}n, e_{p,\gamma,k} \rangle = \langle \psi F n, r_{p,\gamma,k,\text{mod},i} \rangle$$

for  $n \in \mathcal{E}'(\mathbb{R}_+^3)$  and  $i \in \{0, 1, 2\}$ . Here, depending on  $i \in \{0, 1, 2\}$  the reconstruction kernel  $r_{p,\gamma,i}$  is given in the following. We have

- (a)  $r_{p,\gamma,k,\text{mod},0}(s, t)$   
 $= 4k(k-1)C_{\gamma,k} \left( 5F \left( x \mapsto x_3^2(x_3 - p_3) \tilde{e}_{p,\gamma,k-2}(x) \right) \right.$   
 $\left. - 2(k-2)F \left( x \mapsto x_3^2(x_3 - p_3) |x - p|^2 \tilde{e}_{p,\gamma,k-3}(x) \right) \right) (s, t),$
- (b)  $r_{p,\gamma,k,\text{mod},1}(s, t)$   
 $= 4k(k-1)C_{\gamma,k} \left( 5F \left( x \mapsto x_3^2(x_3 - p_3) \tilde{e}_{p,\gamma,k-2}(x) \right) \right.$   
 $\left. - 2(k-2)F \left( x \mapsto x_3^2(x_3 - p_3) |x - p|^2 \tilde{e}_{p,\gamma,k-3}(x) \right) \right) (s, t)$   
 $+ \alpha 4k(k-1)C_{\gamma,k} \left( 5F \left( x \mapsto (x_3 - p_3) \tilde{e}_{p,\gamma,k-2}(x) \right) \right.$   
 $\left. - 2(k-2)F \left( x \mapsto (x_3 - p_3) |x - p|^2 \tilde{e}_{p,\gamma,k-3}(x) \right) \right) (s, t)$   
 $= r_{p,\gamma,k,\text{mod},0}(s, t) + \alpha r_{p,\gamma,k}(s, t),$

$$\begin{aligned}
(c) \quad & r_{p,\gamma,k,\text{mod},2}(s,t) \\
&= 4k(k-1)C_{\gamma,k} \left( 5F \left( x \mapsto x_3^2(x_3 - p_3) \tilde{e}_{p,\gamma,k-2}(x) \right) \right. \\
&\quad \left. - 2(k-2)F \left( x \mapsto x_3^2(x_3 - p_3) |x - p|^2 \tilde{e}_{p,\gamma,k-3}(x) \right) \right) (s,t) \\
&\quad + \alpha^2 4k(k-1)C_{\gamma,k} \left( 5F \left( x \mapsto (x_3 - p_3) \tilde{e}_{p,\gamma,k-2}(x) \right) \right. \\
&\quad \left. - 2(k-2)F \left( x \mapsto (x_3 - p_3) |x - p|^2 \tilde{e}_{p,\gamma,k-3}(x) \right) \right) (s,t) \\
&= r_{p,\gamma,k,\text{mod},0}(s,t) + \alpha^2 r_{p,\gamma,k}(s,t)
\end{aligned}$$

for  $(s,t) \in S_0 \times (2\alpha, \infty)$ .

According to the decompositions of the single reconstruction kernels in Corollary 5.2, we are able to represent all of them by  $r_{p,\gamma,k}$  and  $r_{p,\gamma,k,\text{mod},0}$ .

Since we calculated  $r_{p,\gamma,3}$  in Subsection 5.1.1, only the computation of  $r_{p,\gamma,3,\text{mod},0}$  is left to get an explicit expression for all reconstruction kernels mentioned in case of  $k = 3$ . When we compare  $r_{p,\gamma,3,\text{mod},0}$  with the representation of  $r_{p,\gamma,3}$  given in (5.3), we obtain

$$r_{p,\gamma,3,\text{mod},0}(s,t) = \frac{315}{64\pi\gamma^9} F \left( x \mapsto x_3^2(120\gamma^2(x_3 - p_3) - 168(x_3 - p_3)|x - p|^2) \chi_{B_\gamma(p)}(x) \right) (s,t)$$

for  $(s,t) \in S_0 \times (2\alpha, \infty)$ . As representation (5.4) in case of  $r_{p,\gamma,3}$  we get

$$Fn(s,t) = \frac{1}{2} \int_{\theta_{\min}}^{\theta_{\max}} \int_{\phi(\theta)_{\min}}^{\phi(\theta)_{\max}} \tilde{n}(R^{-1}x + (s_1, s_2, 0)^\top) \chi_{B_\gamma(p')}(x(t, \phi, \theta)) \sin(\phi) d\phi d\theta$$

by identity (4.11) with  $n = \tilde{n} \chi_{B_\gamma(p)}$  and the smooth function  $\tilde{n}(x) = x_3^2(120\gamma^2(x_3 - p_3) - 168(x_3 - p_3)|x - p|^2)$  for  $x \in \mathbb{R}^3$  in case of  $t \in (T_{\min}, T_{\max})$ . Furthermore, it holds  $Fn(s,t) = 0$  if  $t \leq T_{\min}$  or  $t \geq T_{\max}$  is satisfied for fixed  $s \in S_0$ . As before  $p'$  is given by  $p' = R(p - (s_1, s_2, 0)^\top)$  due to equation (4.2).

Since the square of the third component appears in the representation of  $r_{p,\gamma,3,\text{mod},0}$ , we simplify

$$([R^{-1}x(t, \phi, \theta) + (s_1, s_2, 0)]_3)^2 = \left(\frac{1}{4}t^2 - \alpha^2\right) \sin^2(\phi) (-\sin(\beta) \cos(\theta) + \cos(\beta) \sin(\theta))^2$$

for  $t \in (T_{\min}, T_{\max})$ ,  $\phi \in [0, \pi)$  and  $\theta \in [0, 2\pi)$ . Together with the simplifications (5.5) and (5.6) of the subsection before this yields

$$\begin{aligned}
& r_{p,\gamma,k,\text{mod},0}(s,t) \\
&= \frac{315}{64\pi\gamma^9} \frac{1}{2} \int_{\theta_{\min}}^{\theta_{\max}} \int_{\phi(\theta)_{\min}}^{\phi(\theta)_{\max}} \\
&\quad \left( 120\gamma^2 \left( [R^{-1}x(t, \phi, \theta) + (s_1, s_2, 0)^\top]_3 \right)^2 \left( [R^{-1}x(t, \phi, \theta) + (s_1, s_2, 0)^\top]_3 - p_3 \right) \right. \\
&\quad \left. - 168 \left( [R^{-1}x(t, \phi, \theta) + (s_1, s_2, 0)^\top]_3 \right)^2 \left( [R^{-1}x(t, \phi, \theta) + (s_1, s_2, 0)^\top]_3 - p_3 \right) \right. \\
&\quad \left. |R^{-1}x(t, \phi, \theta) + (s_1, s_2, 0)^\top - p|^2 \right) \\
&\quad \chi_{B_\gamma(p')}(x(t, \phi, \theta)) \sin(\phi) d\phi d\theta \\
&= \frac{315}{64\pi\gamma^9} \frac{1}{2} \int_{\theta_{\min}}^{\theta_{\max}} \int_{\phi(\theta)_{\min}}^{\phi(\theta)_{\max}} \left( 120\gamma^2 (-\sin(\beta) \cos(\theta) + \cos(\beta) \sin(\theta))^3 \left( \sqrt{\frac{1}{4}t^2 - \alpha^2} \right)^3 \sin^4(\phi) \right. \\
&\quad \left. - 120\gamma^2 p_3 (-\sin(\beta) \cos(\theta) + \cos(\beta) \sin(\theta))^2 \left( \sqrt{\frac{1}{4}t^2 - \alpha^2} \right)^2 \sin^3(\phi) \right)
\end{aligned}$$

$$\begin{aligned}
& -168(-\sin(\beta)\cos(\theta) + \cos(\beta)\sin(\theta))^3 \left(\sqrt{\frac{1}{4}t^2 - \alpha^2}\right)^3 |x(t, \phi, \theta) - p'|^2 \sin^4(\phi) \\
& + 168p_3(-\sin(\beta)\cos(\theta) + \cos(\beta)\sin(\theta))^2 \left(\sqrt{\frac{1}{4}t^2 - \alpha^2}\right)^2 |x(t, \phi, \theta) - p'|^2 \sin^3(\phi) \\
& \qquad \qquad \qquad \chi_{B_\gamma(p')}(x(t, \phi, \theta)) \, d\phi \, d\theta
\end{aligned} \tag{5.9}$$

for  $t \in (T_{\min}, T_{\max})$ . Analogue to the case of  $r_{p,\gamma,3}$  in the last subsection, we take advantage of

$$|x(t, \phi, \theta) - p'|^2 = (a + b \sin(\phi))^2 + (c + d \cos(\phi))^2 + (e + f \sin(\phi))^2$$

calculated in (5.8) with the given abbreviations there. This time we need the antiderivatives of

$$\begin{aligned}
\phi &\mapsto \sin^4(\phi), & \phi &\mapsto (a + b \sin(\phi))^2 + (c + d \cos(\phi))^2 + (e + f \sin(\phi))^2 \sin^4(\phi), \\
\phi &\mapsto \sin^3(\phi), & \phi &\mapsto (a + b \sin(\phi))^2 + (c + d \cos(\phi))^2 + (e + f \sin(\phi))^2 \sin^3(\phi)
\end{aligned}$$

with  $a, b, c$  and  $d$  as before for the computation of (5.9). As well as in the case of  $r_{p,\gamma,3}$  these are given analytically and we use again a computer algebra system for the calculation. The implementation is also done the same way. All in all, we receive in case of  $r_{p,\gamma,3,\text{mod},0}$  an explicit expression at a point  $(s, t) \in S_0 \times (2\alpha, \infty)$  depending on the limiting angles  $\theta_{\min}$ ,  $\theta_{\max}$ ,  $\phi_{\min}(\theta)$  and  $\phi_{\max}(\theta)$  and the travel times  $T_{\min}$  and  $T_{\max}$ .

Furthermore, we have

$$r_{p,\gamma,3,\text{mod},1} = r_{p,\gamma,3,\text{mod},0} + \alpha r_{p,\gamma,3}$$

and

$$r_{p,\gamma,3,\text{mod},2} = r_{p,\gamma,3,\text{mod},0} + \alpha^2 r_{p,\gamma,3}$$

according to Corollary 5.2. Thus, with the just established expression for  $r_{p,\gamma,3,\text{mod},0}$  and the representation of  $r_{p,\gamma,3}$ , we obtained in the last subsection, we receive expressions for the reconstruction kernels of the two modified reconstruction operators  $\Lambda_{\text{mod},1}$  and  $\Lambda_{\text{mod},2}$ .

## 5.2. Preparations for numerical experiments

In the following, we write  $\tilde{\Lambda}$  in place of one of the reconstruction operators  $\Lambda$ ,  $\Lambda_{\text{mod},0}$ ,  $\Lambda_{\text{mod},1}$ , and  $\Lambda_{\text{mod},2}$ . The notion  $\tilde{r}_{p,\gamma,3}$  denotes analogously the related reconstruction kernel each time, i.e. the respective reconstruction kernel of  $r_{p,\gamma,3}$ ,  $r_{p,\gamma,3,\text{mod},0}$ ,  $r_{p,\gamma,3,\text{mod},1}$  or  $r_{p,\gamma,3,\text{mod},2}$  associated with  $\tilde{\Lambda}$ . For the definitions of the reconstruction operators we refer to Theorem 3.17, Corollary 3.29 and Corollary 3.31. The reconstruction kernels are defined in the Subsections 5.1.1 and 5.1.2.

For the numerical examples we have to calculate

$$\tilde{\Lambda}_\gamma n(p) = \langle \psi y, \tilde{r}_{p,\gamma,3} \rangle = \int_{S_0 \times (2\alpha, \infty)} \psi(s, t) y(s, t) \tilde{r}_{p,\gamma,3}(s, t) \, d(s, t) \tag{5.10}$$

for  $p \in \mathbb{R}_+^3$ . Again, the given data is denoted by  $y$  and  $\tilde{r}_{p,\gamma,3}$  is one of the reconstruction kernels. Further, the function  $\psi \in C_c^\infty(S_0 \times (2\alpha, \infty))$  is the cut-off function we state now explicitly. We take the design of such a function from Section 5 in [QRS11]. Thus, given  $\bar{S} > 0$  and  $\underline{T}, \bar{T} > 0$  with  $\bar{T} > \underline{T} > 0$  we have

$$\psi(s, t) = \psi(s_1, s_2, t) = \Psi_1(s_1) \Psi_1(s_2) \Psi_2(t),$$

where

$$\Psi_1(s) = \begin{cases} 1, & \text{for } |s| < \bar{S}, \\ h(|s|, \bar{S}), & \text{for } \bar{S} \leq |s| \leq \bar{S} + 1, \\ 0, & \text{for } \bar{S} + 1 < |s|, \end{cases}$$

and

$$\Psi_2(t) = \begin{cases} 0, & \text{for } t \leq \underline{T}, \\ g(t, \underline{T}), & \text{for } \underline{T} < t < 2\underline{T}, \\ 1, & \text{for } 2\underline{T} \leq t \leq \bar{T}, \\ h(t, \bar{T}), & \text{for } \bar{T} < t < \bar{T} + 1, \\ 0, & \text{for } \bar{T} + 1 \leq t, \end{cases}$$

for  $(s, t) \in S_0 \times (2\alpha, \infty)$ . The appearing functions  $f, g$ , and  $h$  are defined as follows

$$f(r) = \begin{cases} \exp(-\frac{1}{r}), & \text{for } 0 < r, \\ 0, & \text{for } r \leq 0, \end{cases}$$

for  $r \in \mathbb{R}$  and

$$g(t, \underline{T}) = \frac{f(\frac{t}{\underline{T}} - 1)}{f(\frac{t}{\underline{T}} - 1) + f(2 - \frac{t}{\underline{T}})}$$

and

$$h(t, \bar{T}) = \frac{f(\bar{T} + 1 - t)}{f(\bar{T} + 1 - t) + f(t - \bar{T} - \frac{1}{2})}$$

for  $t \in \mathbb{R}$ . Then, it holds

$$\text{supp}(\psi) \subseteq [-\bar{S} - 1, \bar{S} + 1] \times [\underline{T}, \bar{T} + 1] \quad \text{and} \quad \psi|_{[-\bar{S}, \bar{S}] \times [2\underline{T}, \bar{T}]} = 1.$$

For the numerical experiments we have to compute identity (5.10) from discrete data. With  $s = (s_1, s_2)$  and given  $s_{\max} > 0$ ,  $t_{\min} > 2\alpha$  and  $t_{\max} > t_{\min}$  we consider

$$\begin{aligned} s_1^{(i)} &\in [-s_{\max}, s_{\max}] \text{ for } i \in \{1, \dots, N_s\}, \\ s_2^{(j)} &\in [-s_{\max}, s_{\max}] \text{ for } j \in \{1, \dots, N_s\}, \\ t^{(k)} &\in [t_{\min}, t_{\max}] \text{ for } k \in \{1, \dots, N_t\}, \end{aligned}$$

uniformly distributed with step sizes  $h_s$  and  $h_t$ , respectively, i.e.  $h_s = \frac{2s_{\max}}{N_s}$ ,  $h_t = \frac{t_{\max} - t_{\min}}{N_t}$ . Then, a simple approximation is given by

$$\tilde{\Lambda}_\gamma n(p) \approx h_t h_s^2 \sum_{i=1}^{N_s} \sum_{j=1}^{N_s} \sum_{k=1}^{N_t} \psi(s_1^{(i)}, s_2^{(j)}, t^{(k)}) y(s_1^{(i)}, s_2^{(j)}, t^{(k)}) \tilde{r}_{p, \gamma, 3}(s_1^{(i)}, s_2^{(j)}, t^{(k)})$$

for  $p \in \mathbb{R}_+^3$ . In order to reduce the computation time, we restrict the number  $N_t$ . We use the minimal and maximal travel time  $T_{\min}$  and  $T_{\max}$  such that the reconstruction kernel vanishes beyond the interval given by the two values. Since these two values depend on  $\gamma$ ,  $s_1^{(i)}$ ,  $s_2^{(j)}$  for fixed  $i \in \{1, \dots, N_s\}$  and  $j \in \{1, \dots, N_s\}$  and of course on the point  $p \in \mathbb{R}_+^3$ , we denote

them by  $T_{\min}(s_1^{(i)}, s_2^{(j)}, \gamma, p)$  and  $T_{\max}(s_1^{(i)}, s_2^{(j)}, \gamma, p)$ . Again, the integrals with respect to the outermost travel times vanish such that we consider the open interval

$$\mathcal{T}_{i,j}(\gamma, p) := \left( T_{\min}(s_1^{(i)}, s_2^{(j)}, \gamma), T_{\max}(s_1^{(i)}, s_2^{(j)}, \gamma) \right).$$

This yields

$$\tilde{\Lambda}_\gamma n(p) \approx h_t h_s^2 \sum_{i=1}^{N_s} \sum_{j=1}^{N_s} \sum_{t^{(k)} \in \mathcal{T}_{i,j}(\gamma, p)} \psi(s_1^{(i)}, s_2^{(j)}, t^{(k)}) y(s_1^{(i)}, s_2^{(j)}, t^{(k)}) \tilde{r}_{p,\gamma,3}(s_1^{(i)}, s_2^{(j)}, t^{(k)})$$

for  $p \in \mathbb{R}_+^3$ .

### 5.2.1. The considered data

In order to test our method, we use synthetic data which is not generated from the wave equation. We calculate the data  $y$  using

$$y = Fn$$

for a given  $n \in \mathcal{E}'(\mathbb{R}_+^3)$ . In most cases of the numerical experiments we choose  $n$  to be

$$n = \chi_{B_2(0,0,4)} - \chi_{B_1(0,0,4)} + \chi_{B_{1.5}(3,0,5)} + \chi_{\{x_3 \geq 6.5\}}.$$

An illustration is given in Figure 5.1. Whenever we change  $n$  in the following, for example

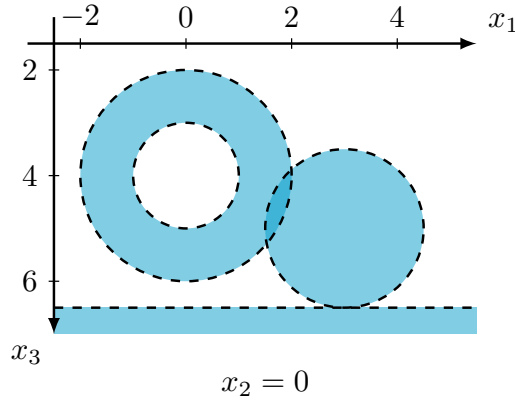


**Figure 5.1:** The function  $n$ . On the darker blue area where the two circles overlap  $n$  is equal to 2, on the light blue area to 1 and off the blue areas it is 0.

by not considering the characteristic function of the half-space, we mention it.

First, we discuss what we expect from the reconstructions  $\tilde{\Lambda}_\gamma n$ . Since all reconstruction operators we discussed in Chapter 3 have the same order and the same decisive microlocal properties, we are able to make the observations all at once.

According to Proposition 3.24, Corollary 3.29 and Corollary 3.31, all reconstruction operators are microlocally elliptic of order 1 at a point  $(x_*, \xi_*) \in \mathbb{R}_+^3 \times \mathbb{R}^3 \setminus \{0\}$  if  $\xi_* \in C(x_*)$  is satisfied with

$$C(x_*) = \{\xi \in \mathbb{R}^3 \mid \xi_3 \neq 0, \psi(s(x_*, \xi), \varphi(s(x_*, \xi), x_*)) > 0\}.$$

Hence, by Theorem 2.23 and Example 2.24 we obtain

$$(x_*, \xi_*) \in \text{WF}^{-1/2}(\tilde{\Lambda}n) \quad \text{for } (x_*, \xi_*) \in \text{WF}(n) = \text{WF}^{1/2}(n) \quad (5.11)$$

as we have already formulated in Corollary 3.26 in case of the reconstruction operator  $\Lambda$ . This means that if the third component of the corresponding direction to an element of the singular support does not vanish and the cut-off function  $\psi$  is strictly positive there, the related singularity is one degree less smooth in the Sobolev scale by applying  $\tilde{\Lambda}$ . More precisely, its smoothness decreases from  $H^{1/2}$  to  $H^{-1/2}$ . In order to analyse which singularities are emphasised by  $\tilde{\Lambda}$ , we take a look at the single components of  $n$ . We notice that we choose the cut-off function  $\psi$  for the reconstructions in such a way that it does not vanish at points we are interested in. For this reason, we neglect this condition on the set  $C(x)$  for  $x \in \mathbb{R}_+^3$  when we analyse whether a concerning singularity get strengthened by  $\tilde{\Lambda}$ . However, we recall that we have

$$\text{WF}(\tilde{\Lambda}n) \subseteq \text{WF}(F^*\psi F n)$$

by the pseudolocal property (see Theorem 2.17) and  $(x, \xi) \in \text{WF}(F^*\psi F n)$  if there exists  $s \in S_0$  and  $\omega \neq 0$  such that  $\xi = \omega \nabla_x \varphi(s, x)$  according to Theorem 3.15. Since the set  $S_0$  is finite in applications, there will be points  $(x, \xi)$  for which we do not find  $s \in S_0$  and  $\omega \neq 0$ . Then, the associated singularities will not be preserved.

We start with the characteristic function of a ball in  $\mathbb{R}_+^3$ . By Example 2.14 the singular support of such a function is its boundary. Hence, the singularities of this function are located at the boundary. For the decision whether the operator  $\tilde{\Lambda}$  emphasises them, we take a look

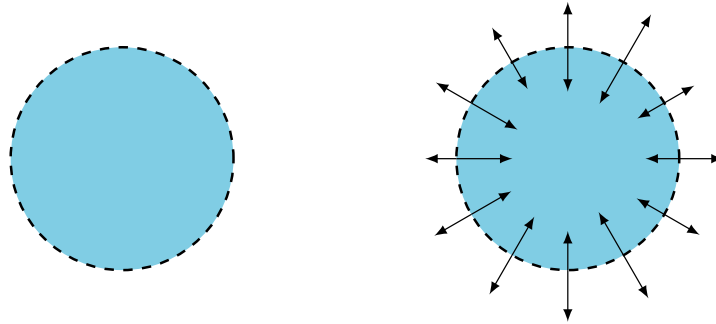


**Figure 5.2:** This figure shows a cross section of a characteristic function of a ball in  $\mathbb{R}_+^3$ , i.e. the value on the blue area is equal to 1 and the function is 0 off the blue area. The dashed lines in both pictures indicate the singular support of the function. In addition, on the right-hand side some directions contained in the wave front set are sketched. We recall that the directions are not normalised.

at the related directions. Again, by Example 2.14 the directions are perpendicular on its boundary. An illustration of the singular support and the wave front set is given in Figure 5.2. If we consider the cross section through the midpoint of the ball, there are two directions which are perpendicular and whose third component vanishes. Thus, these two directions are no elements of  $C(x)$  for any  $x \in \mathbb{R}_+^3$  and do not get emphasised by  $\tilde{\Lambda}$ . In Figure 5.3, we marked the regarding elements of the singular support and the associated directions whose third component vanishes. If we consider the whole space  $\mathbb{R}_+^3$  and not only this cross section, the singularities located at the “equator” of the ball do not get emphasised.

Next, we consider the characteristic function of the half-space  $\{x_3 \geq b\}$  for  $b > 0$ . Once again, by Example 2.14 (b) the singular support of this function is given by  $\{x \in \mathbb{R}_+^3 \mid x_3 = b\}$  and the related directions are perpendicular to this plane. Hence, there is no direction with

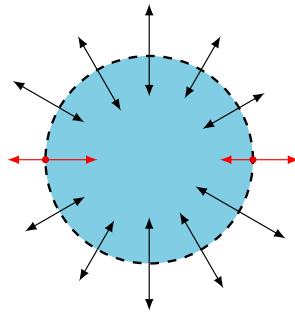


**Figure 5.3:** In this cross section the red marked singularities related to the red marked directions get not emphasised since the third component of the associated directions is zero.

vanishing third component and thus all singularities on the plane are emphasised by the reconstruction operator  $\tilde{\Lambda}$ . An illustration of a cross section is given in Figure 5.4.

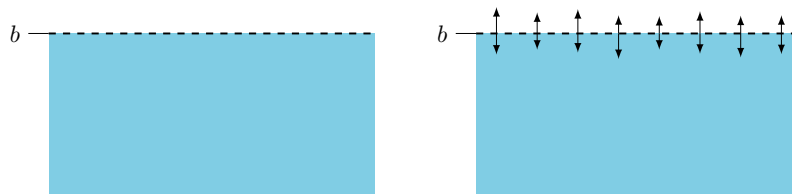


**Figure 5.4:** This is an illustration of parts of the wave front set of  $\chi_{\{x_3 \geq b\}}$  for  $b > 0$  in  $\mathbb{R}_+^3$ . Again, the value 1 is assigned to the blue area and it is otherwise zero. The dashed line indicates the singular support of the function in this cross section. Considering the whole space the singular support is given by the plane  $x_3 = a$ . The arrows are examples of the directions which are contained in the wave front set. Again, the directions associated with an element of the singular support are not normalised.

After we considered the single components, we combine the observations we made above and analyse what we expect concerning the function  $n$  we have chosen. In Figure 5.1, the dashed lines indicate the boundaries of the balls. Moreover, all the dashed lines together are the sum of the singular supports of all the characteristic functions and this is precisely the singular support of  $n$ . The dashed lines mark jumps between the values 0, 1 and 2.

The related directions are such that they are perpendicular to the boundary of a ball or the half-plane  $x_3 = b$  at the points of the singular support, i.e. in the cross section  $x_2 = 0$  there are six points  $x \in \mathbb{R}_+^3$  with a direction not contained in  $C(x)$ . In Figure 5.5, these points are marked. As mentioned in the discussion above, in  $\mathbb{R}_+^3$  this condition is satisfied by all points lying on the equator of one of the balls, so these are infinitely many.

Summarised, we expect that all elements of the singular support except the ones at an “equator” of a ball are reconstructed by  $\tilde{\Lambda}$ . The related singularities even get emphasised one order in the sense of assertion (5.11).

### 5.2.2. Implementation

The numerical experiments we present in the following section are implemented using the coding language Python. For the generation of the data from the wave equation in Subsection 5.3.5 we use Python 2.7.15, in all other cases Python 3.6.1. The process of data generation and the reconstruction is parallelised with the help of the “ProcessPoolExecuter”

interface provided by the “concurrent.futures” module. Since the values we have to compute are independent of each other, the parallelisation is simply performed.

We observe this by taking a look at the identity

$$\begin{aligned}\tilde{\Lambda}_\gamma n(p) &= \int_{S_0 \times (2\alpha, \infty)} \psi(s, t) F n(s, t) F \tilde{u}_{p, \gamma, 3}(s, t) \, d(s, t) \\ &= \int_{S_0 \times (2\alpha, \infty)} \psi(s, t) y(s, t) \tilde{r}_{p, \gamma, 3}(s, t) \, d(s, t)\end{aligned}$$

for  $p \in \mathbb{R}_+^3$ , which we have to compute according to (5.1). Here,  $\tilde{\Lambda}$  denotes one of the introduced reconstruction operators and  $\tilde{r}_{p, \gamma, 3} = F \tilde{u}_{p, \gamma, 3}$  the associated reconstruction kernel, where  $\tilde{u}_{p, \gamma, 3}$  is given by this identity for each reconstruction kernel separately.

When we generate the data  $y = F n$ , the value  $y(s_0, t_0) = F n(s_0, t_0)$  for fixed  $(s_0, t_0) \in S_0 \times (2\alpha, \infty)$  is independent of all other values  $F n(s, t)$  for  $(s, t) \in S_0 \times (2\alpha, \infty)$ . Hence, there is only one open half-ellipsoid determined by  $(s_0, t_0) \in S_0 \times (2\alpha, \infty)$  decisive to compute the elliptic Radon transform and we are able to calculate the single value  $F n(s, t)$  for each  $(s, t) \in S_0 \times (2\alpha, \infty)$  separately. This is precisely the situation for which the ProcessPoolExecuter is developed for, i.e. to evaluate a function at different points independent of each other.

The same is true if we consider the value of  $\tilde{\Lambda}_\gamma n$  for different values of  $p \in \mathbb{R}_+^3$ . For a fixed point  $p_0 \in \mathbb{R}_+^3$  the value of  $\tilde{\Lambda}_\gamma n(p_0)$  is independent of the values for other  $p \in \mathbb{R}_+^3$  around. Thus, we also compute  $\tilde{\Lambda}_\gamma n$  for each  $p \in \mathbb{R}_+^3$  separately. Further, each single value  $\tilde{r}_{p, \gamma, 3}(s_0, t_0) = F \tilde{u}_{p, \gamma, 3}(s_0, t_0)$  for fixed  $(s_0, t_0) \in S_0 \times (2\alpha, \infty)$  is independent of the others. We take advantage of this fact inside the application of the ProcessPoolExecuter interface for computing the values of  $\tilde{\Lambda}_\gamma n$  at a point  $p$ .

In order to distribute the single evaluations faster on the single cores, we divide the number of elements at which we want to evaluate by the number of cores and assign in this way to each core almost the same number of evaluations before applying the ProcessPoolExecuter interface.

In the last sections of Chapter 4, we presented a way to calculate the elliptic Radon transform  $F$  of functions supported in a closed ball and characteristic functions of half-spaces in theory. However, there are some parts in the calculation where there is no direct way to implement them because not everything is given explicitly. We close these remaining gaps by

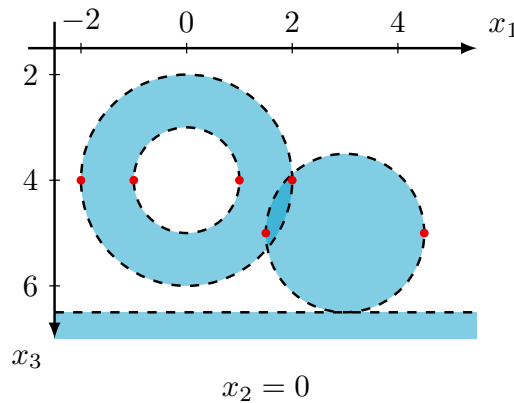


**Figure 5.5:** The red marked singularities get not emphasised since the third component of the related directions is zero.

explaining how we solve these parts numerically. Therefore, we consider the different cases separately.

### The case of Section 4.2

We described in Section 4.2 how to compute the integral given in (1.18) by

$$Fn(s, t) = \int_{\mathbb{R}_+^3} n(x)A(s, x)\delta(t - \varphi(s, x)) dx$$

for  $(s, t) \in S_0 \times (2\alpha, \infty)$  if  $n = \tilde{n}\chi_{B_r(P)}$  for  $\tilde{n} \in C^\infty(\mathbb{R}_+^3)$ . According to (4.11) we have to determine the value of the reformulation

$$Fn(s, t) = \frac{1}{2} \int_{\theta_{\min}}^{\theta_{\max}} \int_{\phi(\theta)_{\min}}^{\phi(\theta)_{\max}} \tilde{n}(R^{-1}x + (s_1, s_2, 0)^\top)\chi_{B_r(P')}(x(t, \phi, \theta)) \sin(\phi) d\phi d\theta$$

for  $s \in S_0$  and  $(T_{\min}, T_{\max})$  with  $P'$  as in identity (4.2).

In Subsection 4.2.3, we have presented how we calculate the limits for the angle  $\theta$  and depending on this, the limits for the angle  $\phi = \phi(\theta)$ . The limiting angles for  $\theta_{\min}$  and  $\theta_{\max}$  are given in (4.8) explicitly. We obtain the limits of the outer integral stated above without any approximation by

$$\theta_{\min} = \frac{\pi}{2} - \arccos\left(\frac{\sqrt{(p'_3)^2 - r^2}}{p'_3}\right)$$

and

$$\theta_{\max} = \frac{\pi}{2} + \arccos\left(\frac{\sqrt{(p'_3)^2 - r^2}}{p'_3}\right).$$

The limits of the inner integral depend on  $\theta$ . Hence, it is reasonable to use the trapezoidal rule for an approximation of the outer integral. Thus, for  $N_{\theta, \text{data}, 1} \in \mathbb{N}$  we consider  $N_{\theta, \text{data}, 1}$  steps given by  $\theta_i := \theta_{\min} + ih$  with step size  $h := \frac{\theta_{\max} - \theta_{\min}}{N_{\theta, \text{data}, 1}}$  for  $i \in \{0, \dots, N_{\theta, \text{data}, 1}\}$ . This yields

$$\begin{aligned} Fn(s, t) &= \frac{1}{2} \int_{\theta_{\min}}^{\theta_{\max}} \int_{\phi(\theta)_{\min}}^{\phi(\theta)_{\max}} \tilde{n}(R^{-1}x(t, \phi, \theta) + (s_1, s_2, 0)^\top)\chi_{B_r(P')}(x(t, \phi, \theta)) \sin(\phi) d\phi d\theta \\ &= \frac{h}{2} \left( \int_{\phi(\theta_{\min})_{\min}}^{\phi(\theta_{\min})_{\max}} \frac{1}{2} \tilde{n}(R^{-1}x(t, \phi, \theta_{\min}) + (s_1, s_2, 0)^\top)\chi_{B_r(P')}(x(t, \phi, \theta_{\min})) \sin(\phi) d\phi \right. \\ &\quad + \sum_{i=1}^{N_{\theta, \text{data}, 1} - 1} \int_{\phi(\theta_i)_{\min}}^{\phi(\theta_i)_{\max}} \tilde{n}(R^{-1}x(t, \phi, \theta_i) + (s_1, s_2, 0)^\top)\chi_{B_r(P')}(x(t, \phi, \theta_i)) \sin(\phi) d\phi \\ &\quad \left. + \int_{\phi(\theta_{\max})_{\min}}^{\phi(\theta_{\max})_{\max}} \frac{1}{2} \tilde{n}(R^{-1}x(t, \phi, \theta_{\max}) + (s_1, s_2, 0)^\top)\chi_{B_r(P')}(x(t, \phi, \theta_{\max})) \sin(\phi) d\phi \right) \end{aligned} \quad (5.12)$$

for  $(s, t) \in S_0 \times (2\alpha, \infty)$ . Further, the angles  $\phi(\theta_i)_{\min}$  and  $\phi(\theta_i)_{\max}$  to a fixed angle  $\theta_i$  for  $i \in \{1, \dots, N_{\theta, \text{data}, 1} - 1\}$  are given by

$$\phi(\theta_i)_{\min} = \arccos(z_1) \quad \text{and} \quad \phi(\theta_i)_{\max} = \arccos(z_2)$$

according to (4.9). Here,  $z_1$  and  $z_2$  are the two solutions to

$$c + bz + \alpha^2 z^2 = -d\sqrt{1 - z^2},$$

where

$$b = p'_2 t, \quad c = (p'_2)^2 + (p'_3)^2 + \frac{1}{4}t^2 - \alpha^2 - r^2 \quad \text{and} \quad d = -p'_3 \sqrt{t^2 - 4\alpha^2} \sin(\theta).$$

In order to determine these two solutions numerically, we use Newton's method. Since the two solutions are between  $-1$  and  $1$ , we use the start values  $-0.9999$  and  $0.9999$ . As mentioned before, in case of  $\theta_{\min}$  and  $\theta_{\max}$  we only obtain one solution. Hence, the corresponding integrals stated in (5.12) vanish. Using this we deduce

$$Fn(s, t) = \frac{h}{2} \sum_{i=1}^{N_{\theta, \text{data}, 1} - 1} \int_{\phi(\theta_i)_{\min}}^{\phi(\theta_i)_{\max}} \tilde{n}(R^{-1}x(t, \phi, \theta_i) + (s_1, s_2, 0)^\top) \chi_{B_r(P')} (x(t, \phi, \theta_i)) \sin(\phi) \, d\phi$$

for  $(s, t) \in S_0 \times (2\alpha, \infty)$ .

There is another simplification left, which we have already seen in Section 4.2. For  $t \in (2\alpha, \infty)$  with  $t \notin (T_{\min}, T_{\max})$  the value of  $Fn(s, t)$  for  $s \in S_0$  vanishes. By identity (4.10), the limits of the interval are

$$T_{\min} = \min_{x \in C} \left( |(0, -\alpha, 0)^\top - x| + |x - (0, \alpha, 0)^\top| \right)$$

and

$$T_{\max} = \max_{x \in C} \left( |(0, -\alpha, 0)^\top - x| + |x - (0, \alpha, 0)^\top| \right),$$

where

$$C = \left\{ x \in \mathbb{R}^3 \mid x = \begin{pmatrix} R \sin(\theta) \sin(\tau) + \frac{\lambda_1 + \lambda_2}{2} p'_3 \tan(\theta) \\ p'_2 + R \cos(\tau) \\ R \cos(\theta) \sin(\tau) + \frac{\lambda_1 + \lambda_2}{2} p'_3 \end{pmatrix} \text{ for } 0 \leq \tau \leq 2\pi \right\}$$

with  $R = \frac{(\lambda_1 - \lambda_2)p'_3}{2 \cos(\theta)}$ . Since the searched values of  $T_{\min}$  and  $T_{\max}$  are clearly separated, we determine these approximately by Newton's method. As start values we choose  $0.5\pi$  and  $0.5\pi + 1.1$ .

### The case of Section 4.3

In Section 4.3, we presented how to determine the value of the integral

$$Fn(s, t) = \int_{\mathbb{R}_+^3} n(x) A(s, x) \delta(t - \varphi(s, x)) \, dx$$

for  $(s, t) \in S_0 \times (2\alpha, \infty)$  given in (1.18) if  $n = \chi_{\{x_3 \geq l\}}$  for some  $l > 0$ . According to (4.15), we have to compute

$$Fn(s, t) = \frac{1}{2} \int_{\theta_{\min}}^{\theta_{\max}} \int_{\phi(\theta)_{\min}}^{\phi(\theta)_{\max}} \sin(\phi) \, d\phi \, d\theta$$

for  $s \in S_0$  and  $t > T_{\min}$ . The limits for the angle  $\theta$  are explicitly given by

$$\theta_{\min} = \arcsin \left( \frac{l}{\sqrt{\frac{1}{4}t^2 - \alpha^2}} \right) \quad \text{and} \quad \theta_{\max} = \pi - \arcsin \left( \frac{l}{\sqrt{\frac{1}{4}t^2 - \alpha^2}} \right)$$

as stated in (4.13). The angle  $\phi = \phi(\theta)$  depends on  $\theta$ . Hence, we use, as in the case of a function supported in a ball, the trapezoidal rule to compute the outer integral. This works

exactly the same as in the case before. The only difference is that we use  $N_{\theta,\text{data},2}$  steps for angles  $\theta$  in the trapezoidal rule this time.

For fixed  $\theta$  we obtain the limits for the angle  $\phi = \phi(\theta)$  by identity (4.14). These are the following

$$\phi(\theta)_{\min} = \arcsin\left(\frac{l}{\sqrt{\frac{1}{4}t^2 - \alpha^2 \sin(\theta)}}\right) \quad \text{and} \quad \phi(\theta)_{\max} = \pi - \arcsin\left(\frac{l}{\sqrt{\frac{1}{4}t^2 - \alpha^2 \sin(\theta)}}\right).$$

These two angles are also given explicitly. Hence, we do not approximate anything here.

The minimal travel time is explicit given by  $T_{\min} = 2\sqrt{\alpha^2 + l^2}$ . There is no maximal travel time as every travel time  $t$  with  $t > T_{\min}$  generates an open half-ellipsoid which intersects the half-space.

In a nutshell, in the case of the characteristic function of a half-space we only approximate once when we use the trapezoidal rule.

### The case of a reconstruction kernel

At the beginning of this section we argued that we are able to treat the reconstruction kernels as described in Section 4.2 since they are supported in a closed ball and smooth on the open ball. For this reason, we apply the same methods as described above in “The case of Section 4.2” to compute the reconstruction kernel semi-analytically with  $N_{\theta,\text{recon}}$  steps for angles  $\theta$  in the trapezoidal rule.

## 5.3. Numerical results

Before we present the reconstructions we achieve with the presented approach, we state and discuss the choice of some parameters. First, we mention the parameters we choose for the cut-off function  $\psi$ . These are  $\bar{S} := s_{\max} - 1$ ,  $\bar{T} := t_{\max} - 1$  and  $\underline{T} := 0.01$ . The values of  $s_{\max}$ ,  $t_{\max}$  and  $t_{\min}$  depend on the individual case of the assembly of each experiment. In Subsection 5.3.5, we use a different cut-off function.

We consider different distances from source to receiver, i.e. different offsets  $\alpha$ . Also the function  $n$  and thus the cuboid we reconstruct changes from time to time. The parameter  $\gamma$  of the mollifier in the reconstruction kernel varies as well a few times in this section depending on each single setting. The choice of  $\gamma$  is related to the offset  $\alpha$ , to the number of measurements and consequently to the discretisation step size of  $s_1$ ,  $s_2$  and  $t$ . For a large offset  $\alpha$  we choose a larger parameter  $\gamma$  than for a small one. Further, the higher the number of points for  $s_1$ ,  $s_2$  and  $t$ , the smaller the value of  $\gamma$ . In order to explain these rules of thumb for the choice of  $\gamma$ , we recall that the support of the mollifier  $e_{p,\gamma,3}$  is given by  $\text{supp}(e_{p,\gamma,3}) = \overline{B_\gamma(p)}$  for a point  $p \in \mathbb{R}_+^3$ . Hence, the parameter  $\gamma$  determines the radius of the neighbourhood of the point  $p$  in which we regularise. For large  $\alpha$  numerical instabilities occur if  $\text{supp}(n)$  is near to the surface (“near” relates to  $\alpha$ ). These errors are compensated by regularising in a larger neighbourhood of  $p$ , i.e. the choice of a larger value of  $\gamma$ . In the same way we adjust an appearing lack of data points.

Beside these, there are the three numbers of steps denoted by  $N_{\theta,\text{data},1}$ ,  $N_{\theta,\text{data},2}$  and  $N_{\theta,\text{recon}}$  with uniformly step size in the trapezoidal rule. The first one  $N_{\theta,\text{data},1}$  appears during the data generation in case of the characteristic function of a ball and analogue the second one  $N_{\theta,\text{data},2}$  in case of the characteristic function of a half-space. These two parameters and the number of discretisation points  $N_{s_1}$ ,  $N_{s_2}$  and  $N_t$  decide about the quality and the sharpness of the reconstructions. Nevertheless, the numbers  $N_{s_1}$ ,  $N_{s_2}$  and  $N_t$  have a greater

impact. In case of the parameters  $N_{\theta, \text{data}, 1}$  and  $N_{\theta, \text{data}, 2}$  there is some limit beyond which there is no more change in the numerical reconstructions, which is visible for the naked eye.

Last,  $N_{\theta, \text{recon}}$  counts the steps of the angle  $\theta$  in computing the reconstruction kernel. Many times we work with a low number for  $N_{\theta, \text{recon}}$ . As a consequence, we obtain not the best reconstructions but the difference is only in quantity and not in quality. A higher quality is not worth the additional computation time. A more precise discussion on how the parameter  $N_{\theta, \text{recon}}$  influences the reconstructions follows later in context of Figure 5.7.

### 5.3.1. Reconstructions with the reconstruction operator $\Lambda$

Actually, we consider a three dimensional setting. We compute the elliptic Radon transform integrating over open half-ellipsoids in  $\mathbb{R}_+^3$  with foci  $\mathbf{x}_s = (s_1, s_2 - \alpha, 0)^\top$  and  $\mathbf{x}_r = (s_1, s_2 + \alpha, 0)^\top$ . Nevertheless, the computation of  $\Lambda_\gamma(p)$  for a fixed  $\gamma > 0$  and a point  $p$  in the given cuboid is independent from the other points in the cuboid. Hence, it is no problem to calculate cross sections in one direction. Here and in the following, we compute cross sections in  $x_2$ -direction.

In a first experiment, we consider the function  $n = \chi_{B_2(0,0,4)} - \chi_{B_1(0,0,4)} + \chi_{B_{1.5}(3,0,5)} + \chi_{\{x_3 \geq 6.5\}}$  and approximate  $\Lambda n$  for the two different offsets  $\alpha = 1$  and  $\alpha = 10$ .

For the scaling parameter  $\gamma$ , we choose  $\gamma = 0.2$  for  $\alpha = 1$  and we set  $\gamma = 0.3$  for  $\alpha = 10$ . We compute  $\Lambda_\gamma n$  at points  $p$  in  $[-2.5, 5] \times \{0\} \times [1.5, 7]$  uniformly discretised by  $N_{x_1} = 135$ ,  $N_{x_2} = 1$  and  $N_{x_3} = 99$  discretisation points. Further, we restrict the travel time  $t$  to  $t_{\min} = 2\alpha + 0.1$  and  $t_{\max} = t_{\min} + 17$  depending on the offset  $\alpha$ . The elements  $s_1$  and  $s_2$  determining source and receiver are in the interval  $[-10.0, 10.0]$ , i.e.  $s_{\max} = 10.0$ . For each of these three parameters  $s_1, s_2$  and  $t$  we use 600 discretisation points. Hence, we compute integrals over  $600^3 = 216\,000\,000$  open half-ellipsoids given by  $Fn(s_1, s_2, t)$  to generate the data.

In Figure 5.6 both results for the two values of the offset  $\alpha$  are presented. These results confirm our expectations from Subsection 5.2.1 concerning what we observe in the reconstructions. In both cross sections the singular support of  $n$ , i.e. the boundaries of the single balls are visible. Only at the outermost points, for example at  $(-2, 0, 4)^\top$  and  $(2, 0, 4)^\top$ , there is a gap since they are not imaged. This is exactly what we predicted in Subsection 5.2.1 and illustrated in Figure 5.3 using the red colour.

Nevertheless, in case of  $\alpha = 1$  the strength of the reconstructed singularities depends strongly on their locations. The singularities closer to the surface are more emphasised than the ones further away. This differs from the case  $\alpha = 10$ . Here, the intensity of the singularities is nearly independent of the distance to the surface.

In case of  $\alpha = 10$  we get two additional artifacts. There is a horizontal line between  $x_3 = 3.5$  and  $x_3 = 4.0$  and at the right bottom an oblique line from the outermost right point of the right ball to the bottom. However, these artifacts have no relation to the ball. We convinced ourselves that both artifacts appear in the reconstruction of the singularities of the half-space  $\{x_3 \geq 6.5\}$  since they also occur when we choose  $n = \chi_{\{x_3 \geq 6.5\}}$ . The horizontal line probably arises by a summation of weak artifacts caused by the cut-off function and the numerical scheme. Concerning the other appearing artifact we argue with a result given in [FQ15]. The authors of this publication show that the characteristic function of a half-space causes two artifacts due to limited data. In Figure 3 of their publication they consider the same setting in case of  $\alpha = 0$ . Thus, we adapt the results mentioned there. We deduce that the oblique line is one of the two artifacts related to the half-space. The second artifact is not visible in the figure since it is on the left-hand side beyond the area we reconstructed. In our case, the two artifacts are mirrored at the line  $x_1 = x_2 = 0$  since the values we choose for  $s_1$

and  $s_2$  are symmetric to zero.

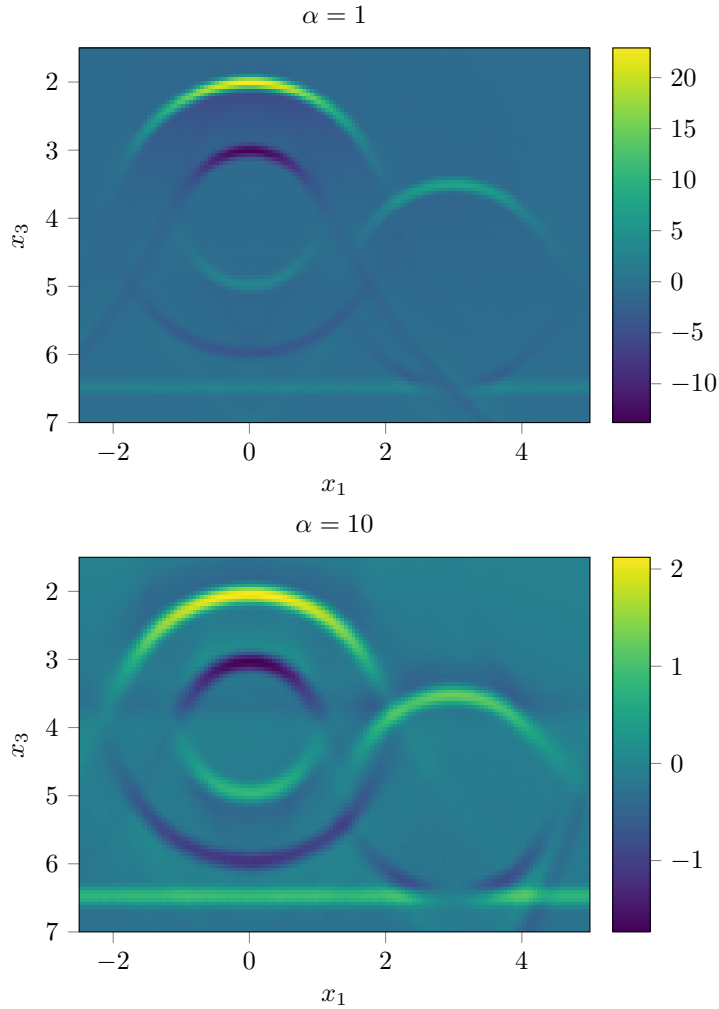
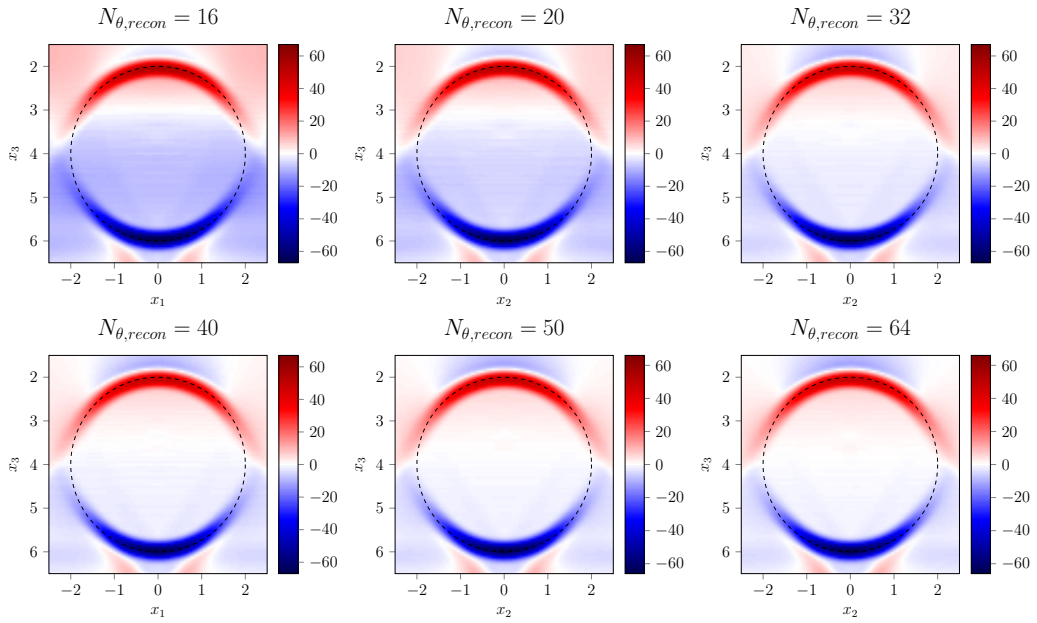


**Figure 5.6:** Two reconstructions  $\Lambda_\gamma n$  obtained with the reconstruction operator  $\Lambda$ . The only difference is the offset  $\alpha$  and the regularisation parameter  $\gamma$  which depends on the offset. In case of  $\alpha = 1$  we have  $\gamma = 0.2$ , for  $\alpha = 10$  it is  $\gamma = 0.3$ .

We notice that the values of the reconstructions inside and outside the circles are not zero. Hence, the intensity is not displayed in relation to zero. The reason for this are too few chosen angles for  $\theta$  in the trapezoidal rule for computing the reconstruction kernel.

In Figure 5.7 we present cross sections in  $x_2 = 0$  for different choices of the parameter  $N_{\theta, \text{recon}}$ , i.e. the number of angles for  $\theta$ , for  $n = \chi_{B_2(0,0,4)}$ . We remark that the more angles we choose, the more the value of  $\Lambda_\gamma n$  vanishes inside and outside the circle we see in the cross sections. There is virtually no difference between the reconstructions with  $N_{\theta, \text{recon}} = 50$  and  $N_{\theta, \text{recon}} = 64$ , which is visible to the naked eye. However, in all images there is no real difference in the visibility of the singularities. As a consequence, we choose  $N_{\theta, \text{recon}} = 16$  in many experiments and save computation time. The computation time for  $N_{\theta, \text{recon}} = 50$  increases by a factor of about three in comparison to  $N_{\theta, \text{recon}} = 16$ .

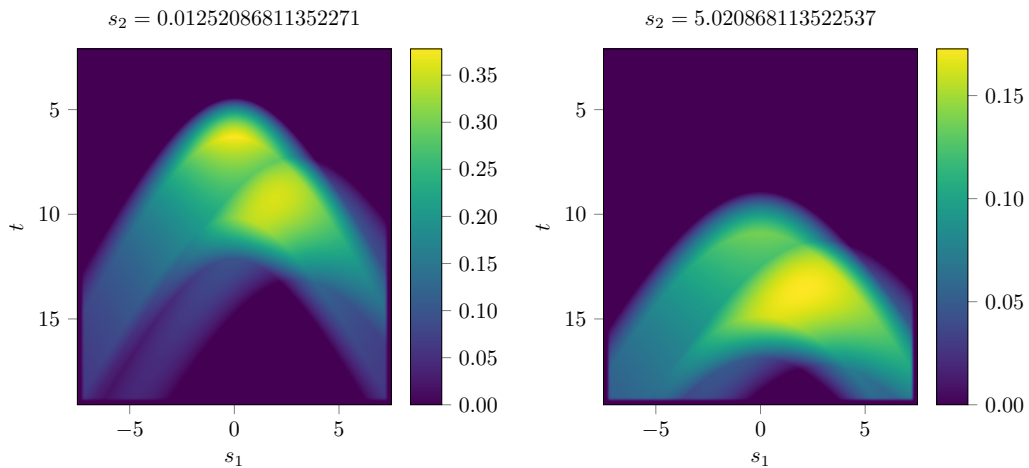
According to identity (5.10), the approximation  $\Lambda_\gamma n$  consists out of two independent parts before integration. The first one involves the generation of the data  $y = Fn$  modified



**Figure 5.7:** The same reconstruction using a different value of  $N_{\theta, recon}$ , which determines the number of angles  $\theta$  in the reconstruction procedure.

with the cut-off function  $\psi$ . The computation of the reconstruction kernel  $r_{p,\gamma,3}$  is the second one.

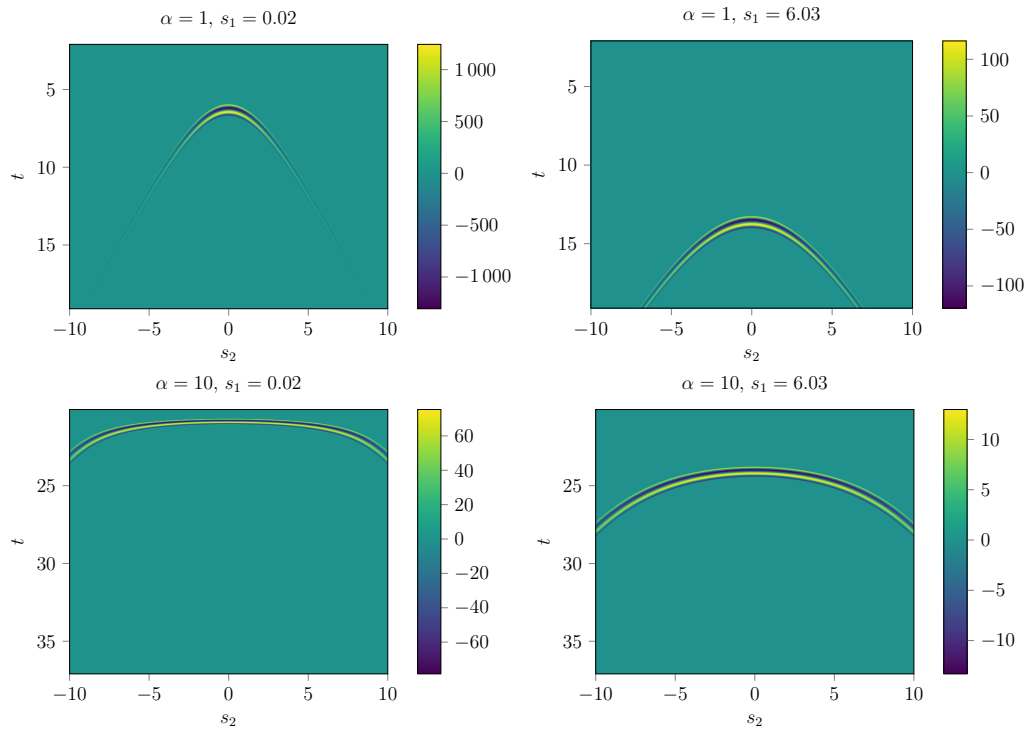
In Figure 5.8 two cross sections of the modified data  $\psi Fn$  for  $n = \chi_{B_2(0,0,4)} - \chi_{B_1(0,0,4)} + \chi_{B_{1.5}(3,0,5)}$  are plotted. In comparison to the data, which we used for the generation of the left cross section in Figure 5.6 with offset  $\alpha = 1$ , the only difference is that the characteristic function of the half-space  $\{x_3 \geq 6.5\}$  is missing in the definition of  $n$ . All other parameters have the same value as in the first experiment presented in Figure 5.6. We notice the frame around the images caused by the cut-off function  $\psi$ .



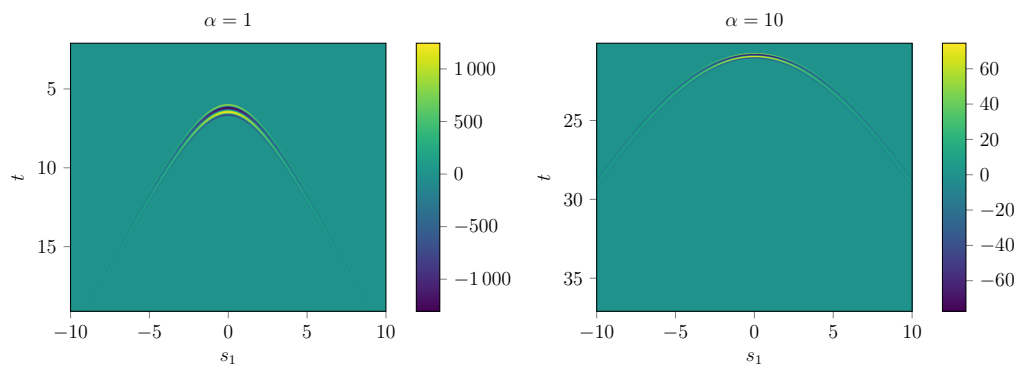
**Figure 5.8:** Two cross sections in  $s_2$  of the modified data  $\psi Fn$ .

Figure 5.9 shows some cross sections of reconstruction kernels. Here, we use the same parameters as for the two cross sections in Figure 5.6 before. For convenience, we repeat the

most important one. As it is readable at the axis, we consider  $s_1, s_2 \in [-10.0, 10.0]$ . Moreover, we use  $\alpha = 1$  and  $\gamma = 0.2$  for the two pictures in the top and  $\alpha = 10$  and  $\gamma = 0.3$  for the two in the bottom. All four images show the reconstruction kernel  $r_{p,\gamma,3}$  at the point  $p = (0, 0, 3)^\top$ . In these cross sections in  $s_2$  we notice that the visible arc is more flat in case of  $\alpha = 10$  than in case of  $\alpha = 1$ . This effect is directly related to the value of  $\alpha$  and can also be observed in the data. However, if we take a look at the cross sections in  $s_1$ , so in the first space direction, this effect is not so pronounced. The reason is that source and receiver are positioned on an axis parallel to the  $x_2$ -axis. These cross sections are presented in Figure 5.10.



**Figure 5.9:** Different cross sections of the reconstruction kernel  $r_{(0,0,3)^\top, \gamma, 3}$  for two cases of offsets  $\alpha$  evaluated at the same point  $p = (0, 0, 3)^\top$ .



**Figure 5.10:** The reconstruction kernel  $r_{(0,0,3)^T, \gamma, 3}$  in the cross section  $s_2 = 0.02$  for two different values of  $\alpha$ .

Last, in Figure 5.11 we additionally consider the reconstruction kernel  $r_{p,\gamma,3}$  at  $p = (0, 0, 5)^\top$ . This is presented in the right image. If we compare this with the left image where we have  $p = (0, 0, 3)^\top$  as before, we see that the first value of a travel time  $t$  where the reconstruction kernel  $r_{(0,0,5)^\top,\gamma,3}$  does not vanish is significant higher than for  $r_{(0,0,3)^\top,\gamma,3}$ . This is due to the fact that the point  $p = (0, 0, 5)^\top$  is further away from the surface than  $p = (0, 0, 3)^\top$ .

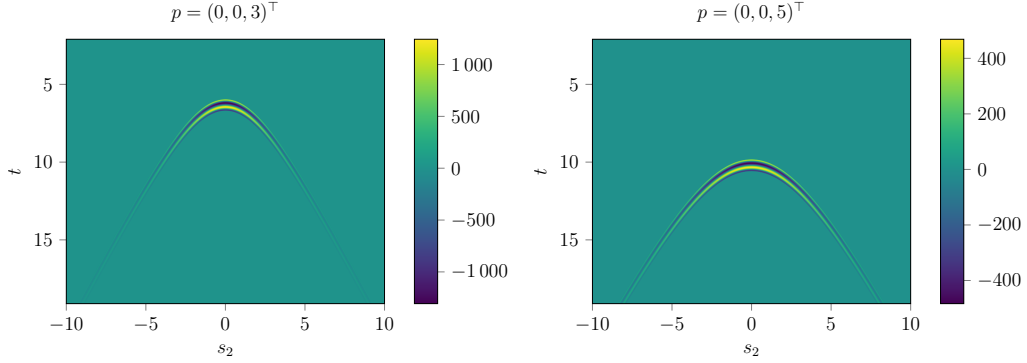


**Figure 5.11:** Two cross sections of the reconstruction kernel  $r_{p,\gamma,3}$  in  $s_1 = 0.02$  for offset  $\alpha = 1$  evaluated at two different points  $p$ .

### 5.3.2. Experiments concerning the offset $\alpha$

In this subsection, we consider two experiments related to the stability of the data and the reconstructions concerning the offset  $\alpha$ . In a first experiment, we simulate errors in the arrangement of the sources and receivers while generating the data. A second experiment shows what happens when we use an offset  $\alpha_{\text{recon}}$  in the reconstruction procedure different from the offset  $\alpha_{\text{data}}$ , which we use for the data generation.

For both experiments we choose  $n = \chi_{B_2(0,0,4)} - \chi_{B_1(0,0,4)} + \chi_{B_{1.5}(3,0,5)} + \chi_{\{x_3 \geq 6.5\}}$  as described in Subsection 5.2.1. We work in the cross section  $[-2, 5, 5] \times \{0\} \times [1.5, 7]$  of a cuboid which we discretise uniformly using  $N_{x_2} = 1$  and  $N_{x_1} = N_{x_3} = 99$  points. Moreover, we consider travel times  $t$  between  $t_{\min} = 2\alpha + 0.1 = 4.1$  and  $t_{\max} = t_{\min} + 17 = 21.1$  with sources  $\mathbf{x}_s(s)$  and receivers  $\mathbf{x}_r(s)$  determined by  $s_{\max} = 7.5$ , i.e.  $s_1, s_2 \in [-7.5, 7.5]$ . For the three parameters  $s_1, s_2$  and  $t$  we use  $N_s = N_t = 300$  discretisation points. These are half as many as before for each variable. We will see that the more open half-ellipsoids determined by  $s_1, s_2$  and  $t$  we regard, the sharper the reconstructions become. Nevertheless, in order to recognise the appearing effects 300 discretisation points for each of those variables are sufficient. Last, we choose  $N_{\theta,\text{data},1} = 201$ ,  $N_{\theta,\text{data},2} = 33$  and  $N_{\theta,\text{recon}} = 16$ .

Now, we generate the data using the offset  $\alpha_{\text{data},\text{random}}$ . This offset is uniformly distributed in an interval  $[2 - \beta, 2 + \beta]$  for  $\beta > 0$ . It simulates positioning errors while arranging sources and receivers. For the reconstruction we do not vary the offset  $\alpha$  since we are able to set  $\alpha$  to one fixed value in the code which permits no mistakes. Here, we use  $\alpha = 2$  which is suitable to the choice of  $\alpha_{\text{data},\text{random}}$ . The results are presented in Figure 5.13. A reference, in order to compare with a reconstruction of data generated with  $\alpha_{\text{data}} = 2$ , is given in Figure 5.12. In the top image of Figure 5.13, we vary  $\alpha_{\text{data},\text{random}}$  between 1.9 and 2.1. In this case, there are no big changes in comparison to  $\alpha_{\text{data}} = 2$ . For  $\alpha_{\text{data},\text{random}} \in [1.75, 2.25]$  the reconstructions are a bit more blurry as we see in the middle image. However, the singular support is still visible. If we are further away from the surface, the reconstructions get more distinct and

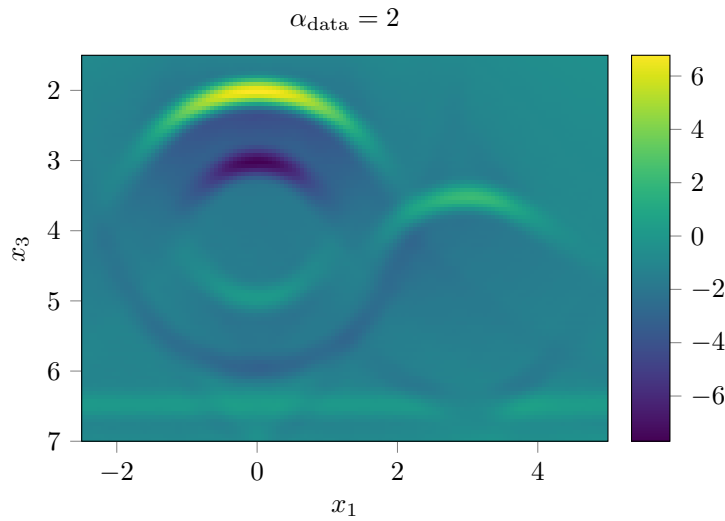


**Figure 5.12:** The reference image for Figure 5.13 with constant  $\alpha_{\text{data}} = 2$ .

the singularities are stronger noticeable than in case of  $\alpha_{\text{data}} = 2$ . Last, we use  $\alpha_{\text{data,random}}$  between 1.5 and 2.5. Here, the boundaries of the balls near to the surface are very blurry. Nevertheless, we obtain an area in which the singular support of  $n$  is contained. The elements far away from the surface are more strongly reconstructed than in the aforementioned cases and also than in our reference using  $\alpha_{\text{data}} = 2$ .

One possible explanation for the stronger reconstructions of singularities far away from the surface is that we consider in  $\alpha_{\text{data,random}}$  also higher values than 2. Later on, we will see that for larger values of  $\alpha$  the singularities further away from the surface get more emphasised by  $\Lambda$ .

The fact that the effects, appearing when we use randomly distributed values of  $\alpha_{\text{data}}$ , are more pronounced near to the surface is a phenomena which also appears in the next experiment. For an explanation we refer to the lines below.

In Figure 5.14 we plotted the generated data of the reference case  $\alpha_{\text{data}} = 2$  and the last case with  $\alpha_{\text{data,random}} \in [1.5, 2.5]$ . We see that the contours of the data in the right image are very blurry. Nevertheless, the shape we obtain by the plotted data in the left image is also still recognisable in the right one.

Altogether, we summarise that deviations up to 5% in the position of sources and receivers while generating data do not really affect the reconstructions. Whereas deviations of about 25% are noticeable in the reconstructions.

In a second experiment, we generate the data with a fixed offset  $\alpha_{\text{data}}$  and reconstruct with a different offset  $\alpha_{\text{recon}}$ . This means we use a wrong offset in the reconstruction kernel  $r_{p,\gamma,3}$ . We consider two different cases. In the first one, we choose  $\alpha_{\text{data}} = 2$  and reconstruct with  $\alpha_{\text{recon}} = 1.5$  and  $\alpha_{\text{recon}} = 2.5$ . This is presented in Figure 5.15. As reference image the top image is a reconstruction with  $\alpha_{\text{recon}} = \alpha_{\text{data}} = 2$ . Concerning the second one, we use  $\alpha_{\text{data}} = 5$  and as a consequence, we reconstruct with  $\alpha_{\text{recon}} = 4.5$  and  $\alpha_{\text{recon}} = 5.5$ . Also here, the top image in Figure 5.16 is thought as reference with  $\alpha_{\text{recon}} = \alpha_{\text{data}} = 5$ .

We explain the appearing phenomenas in both cases using the example of  $\alpha_{\text{data}} = 2$  presented in Figure 5.15. Afterwards we explain which role the size of  $\alpha_{\text{data}}$  plays.

By looking at the images in Figure 5.15, we observe that for  $\alpha_{\text{recon}} < \alpha_{\text{data}}$  the recon-

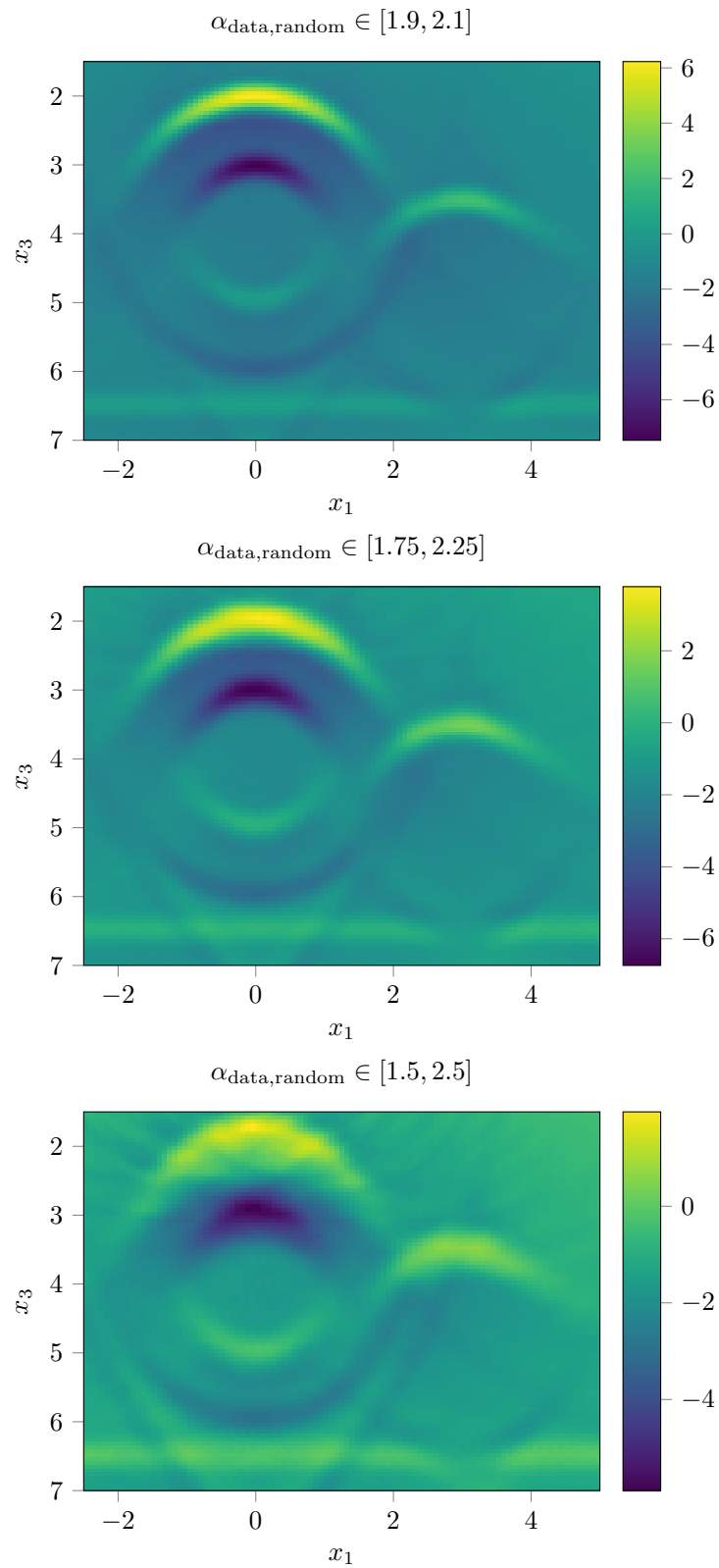


**Figure 5.13:** The reconstructions  $\Lambda_\gamma n$  for an offset  $\alpha_{\text{data,random}}$  randomly distributed in different intervals.

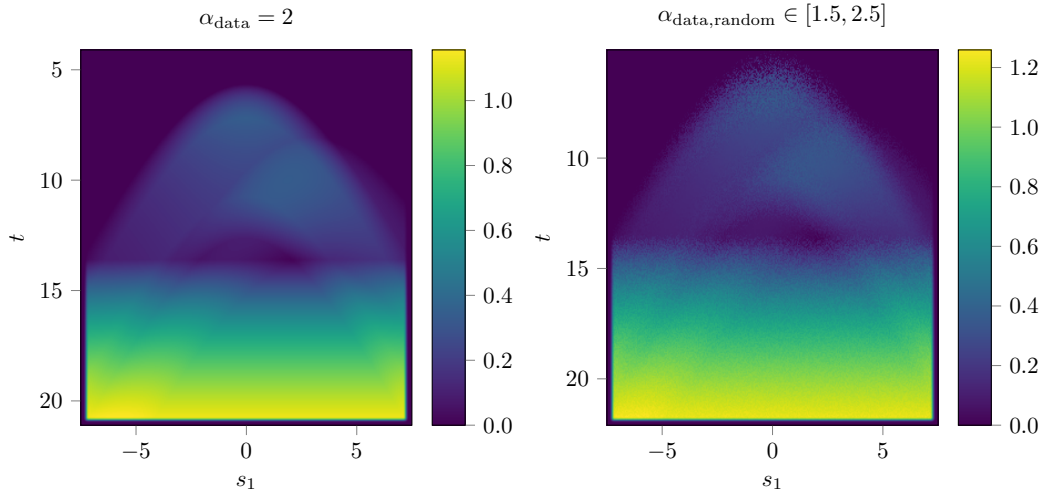


**Figure 5.14:** The modified data  $\psi F n$  in case of  $\alpha_{\text{data}} = 2$  displayed on the left-hand side and randomly distributed in  $[1.5, 2.5]$  presented on the right-hand side.

structed singularities appear further down than by choosing the right offset for the reconstructions, i.e.  $\alpha_{\text{recon}} = \alpha_{\text{data}}$ . In case of  $\alpha_{\text{recon}} > \alpha_{\text{data}}$ , it is the other way round. Here, the reconstructed singularities appear closer to the surface than with  $\alpha_{\text{recon}} = \alpha_{\text{data}}$ . We further remark that only the vertical position of the singularities is changed and not the horizontal one. This can be recognised by the imaged horizontal line, the singular support of the characteristic function of the half-space  $\{x_3 \geq 6.5\}$ .

We verify these observations by reference to the representation of an ellipsoid. According to Lemma 3.1, the open half-ellipsoid for the data generation for fixed  $(s, t) \in S_0 \times (2\alpha, \infty)$  is given by

$$\frac{(x_1 - s_1)^2}{\frac{1}{4}t^2 - \alpha^2} + \frac{(x_2 - s_2)^2}{\frac{1}{4}t^2} + \frac{x_3^2}{\frac{1}{4}t^2 - \alpha^2} = 1$$

for  $x = (x_1, x_2, x_3)^\top \in \mathbb{R}_+^3$ . If we consider now  $\alpha_{\text{recon}} > \alpha_{\text{data}}$ , the value of  $\frac{1}{4}t^2 - \alpha_{\text{recon}}^2$  is smaller than  $\frac{1}{4}t^2 - \alpha_{\text{data}}^2$ , where we choose  $t$  large enough such that the square root is defined. Thus, the minor half-axis of the open half-ellipsoid in the reconstruction procedure given by  $\frac{1}{4}t^2 - \alpha_{\text{recon}}^2$  is smaller than the minor half-axis during the data generation  $\frac{1}{4}t^2 - \alpha_{\text{data}}^2$ . We deduce that the radius of the half-circle, which we obtain by making a cross section through the open half-ellipsoid parallel to the  $x_1$ -axis, decreases. As a consequence, the difference  $x_1 - s_1$  and the value of  $x_3$  get smaller in the equation above. The latter yields that the singularity at a fixed point  $p$  appears closer to the surface. The effect regarding  $x_1 - s_1$  is not really visible in the reconstructions. It is averaged since we consider many positive and negative values for  $s_1$ . In case we have  $\alpha_{\text{recon}} < \alpha_{\text{data}}$ , it is the other way round.

For fixed  $(s, t) \in S_0 \times (2\alpha, \infty)$  this phenomena is easy to understand by looking at the point  $p = (s_1, s_2, \sqrt{\frac{1}{4}t^2 - \alpha_{\text{data}}^2})^\top$ . The distance of  $p$  to the surface is exactly  $\sqrt{\frac{1}{4}t^2 - \alpha_{\text{data}}^2}$ , i.e. the radius of the aforementioned circle. For  $\alpha_{\text{recon}} > \alpha_{\text{data}}$  the distance decreases and for  $\alpha_{\text{recon}} < \alpha_{\text{data}}$  it increases. In these ways, the related singularity changes the distance to the surface.

Near to the surface this effect is more visible. The open half-ellipsoids going through points there have a smaller travel time  $t$  than the open half-ellipsoids going through the

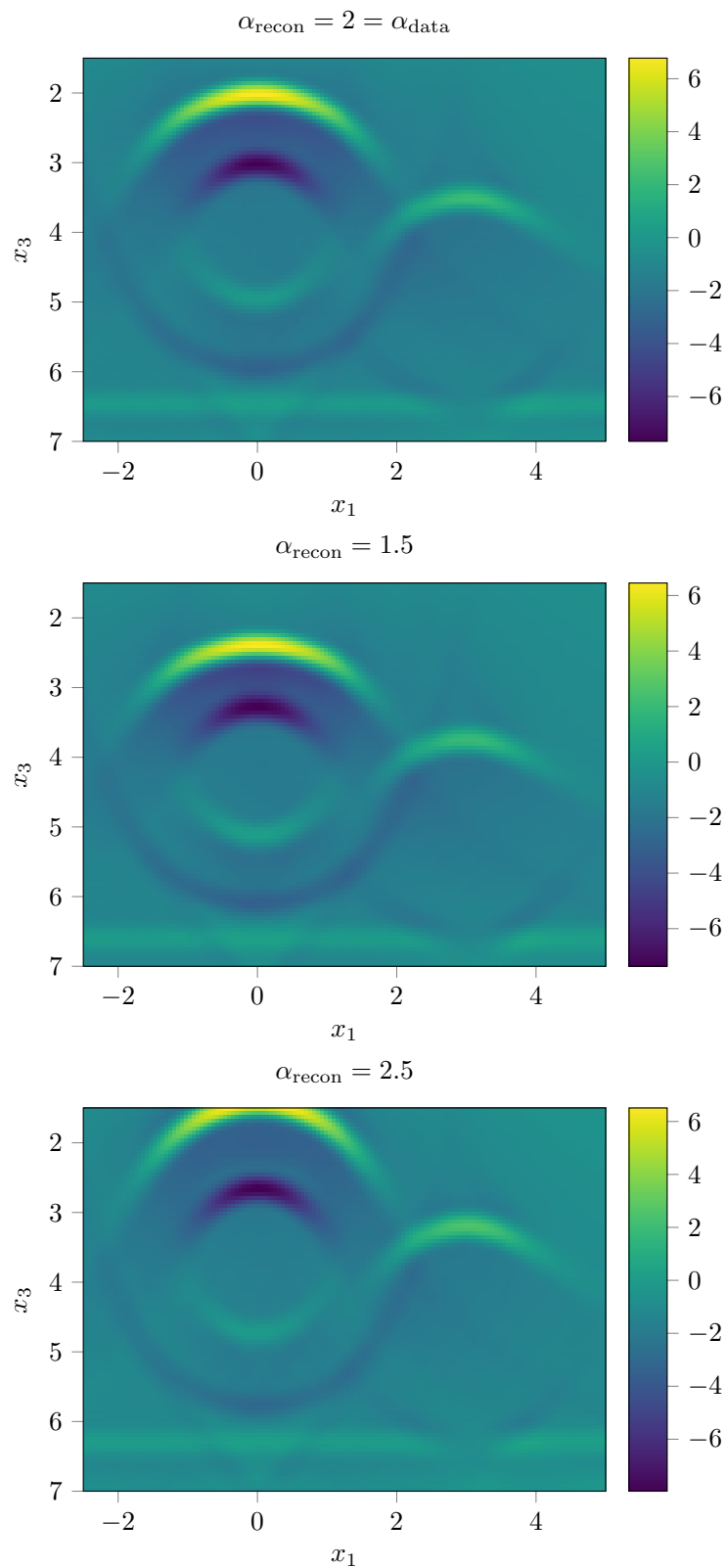


**Figure 5.15:** Cross sections of  $\Lambda_\gamma n$  in  $x_2 = 0$ . In all three images we use  $\alpha_{\text{data}} = 2$  for the generation of the data, whereas the offset  $\alpha_{\text{recon}}$  in the reconstruction procedure is different.

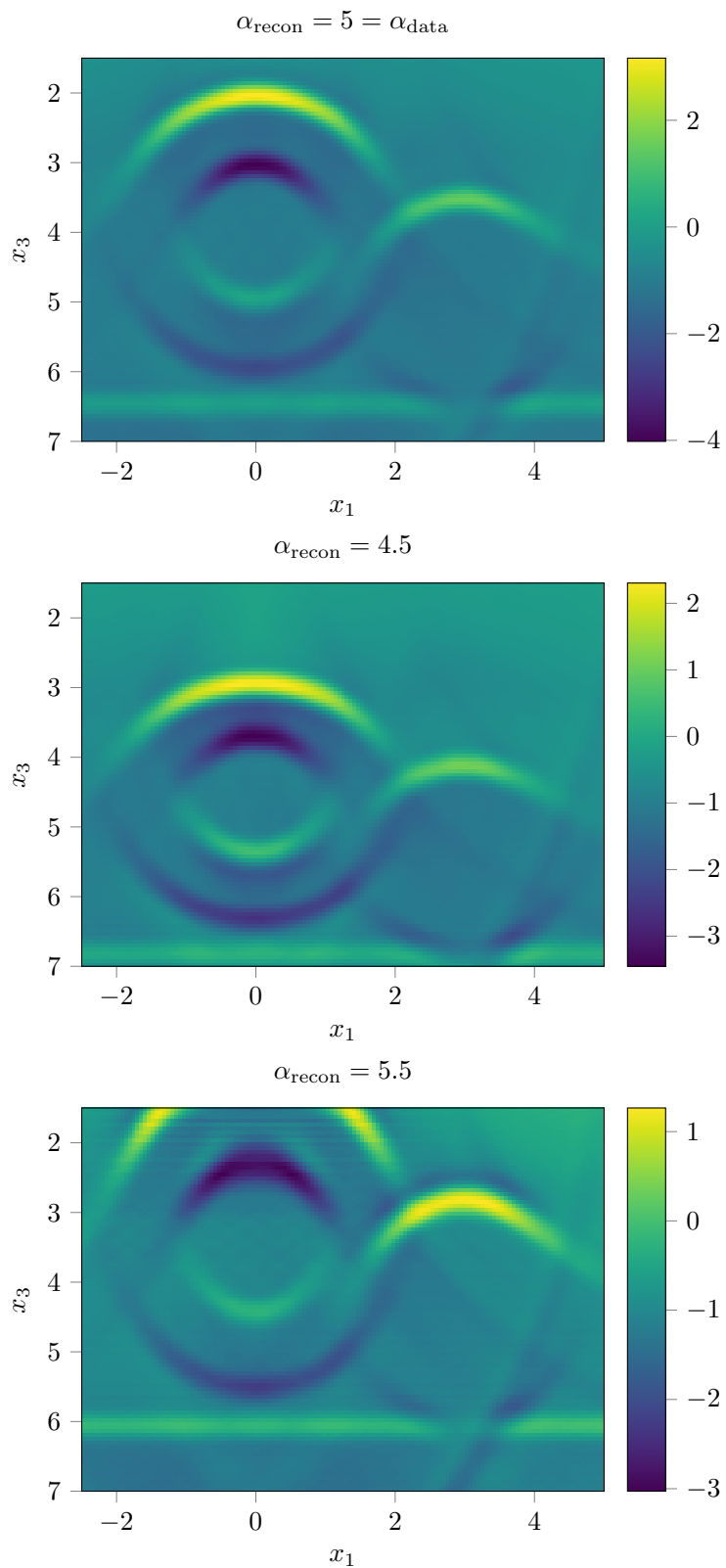


**Figure 5.16:** These cross sections of  $\Lambda_{\gamma n}$  in  $x_2 = 0$  are generated with  $\alpha_{\text{data}} = 5$  and three different values of  $\alpha_{\text{recon}}$ .

points further away from the surface. Thus, the difference of the radius  $\sqrt{\frac{1}{4}t^2 - \alpha_{\text{data}}^2}$  to  $\sqrt{\frac{1}{4}t^2 - \alpha_{\text{recon}}^2}$  is greater for small values of  $t$  than in case of larger ones.

Last, we compare the images in Figure 5.15 and in Figure 5.16. We notice that the effects described above are more pronounced for higher values of  $\alpha_{\text{data}}$  provided the difference between  $\alpha_{\text{data}}$  and  $\alpha_{\text{recon}}$  is the same. In order to verify this, we consider  $\alpha_{\text{recon}} = \alpha_{\text{data}} + \Delta\alpha$  with  $\Delta\alpha > 0$  or  $\Delta\alpha < 0$ . For the difference of the radius related to the data and to the reconstruction we obtain

$$\sqrt{\frac{1}{4}t^2 - \alpha_{\text{data}}^2} - \sqrt{\frac{1}{4}t^2 - \alpha_{\text{recon}}^2} = \frac{\Delta\alpha(2\alpha_{\text{data}} + \Delta\alpha)}{\sqrt{\frac{1}{4}t^2 - \alpha_{\text{data}}^2} + \sqrt{\frac{1}{4}t^2 - (\alpha_{\text{data}} + \Delta\alpha)^2}}.$$

This difference increases with  $\alpha_{\text{data}}$ . Hence, the effect is more visible for large values of  $\alpha_{\text{data}}$  than for small ones.

Details concerning the appearing artifacts are given in the subsections before and after this one.

### 5.3.3. Comparison of the different reconstruction operators

In this subsection, we compare the different reconstruction operators introduced in Subsection 3.3.1 and Subsection 3.3.3, respectively. Up to now, we have only seen reconstructions generated with the reconstruction kernel  $r_{p,\gamma,3}$  computed in Subsection 5.1.1. However, we introduced the modified reconstruction operators and calculated their reconstruction kernels in Subsection 5.1.2 to improve the reconstructions concerning the independence of  $\alpha$  and the distance to the surface. Now, we analyse whether these modified operators lead to the predicted improvements.

In order to compare the different operators, we consider the same setting as in Subsection 5.3.1 for the reconstruction operator  $\Lambda$ . We use the two different offsets  $\alpha = 1$  and  $\alpha = 10$  but this time combined with each of the three reconstruction operators  $\Lambda_{\text{mod},0}$ ,  $\Lambda_{\text{mod},1}$  and  $\Lambda_{\text{mod},2}$ . Again, we choose the function  $n = \chi_{B_2(0,0,4)} - \chi_{B_1(0,0,4)} + \chi_{B_{1.5}(3,0,5)} + \chi_{\{x_3 \geq 6.5\}}$  as described in Subsection 5.2.1. Further, we restrict the travel time  $t$  to  $t_{\text{min}} = 2\alpha + 0.1$  and  $t_{\text{max}} = t_{\text{min}} + 17$  depending on the offset  $\alpha$ . The elements  $s_1$  and  $s_2$  determining source and receiver are in  $[-10.0, 10.0]$ , i.e.  $s_{\text{max}} = 10.0$ . For each of these parameters we use 600 discretisation points such that we compute 216 000 000 elliptic Radon transforms  $F_n$  to generate the data. Moreover, we consider again the cross section given by  $[-2.5, 5] \times \{0\} \times [1.5, 7]$  and discretised by  $N_{x_1} = 135$ ,  $N_{x_2} = 1$  and  $N_{x_3} = 99$ . Last, we choose the three different numbers of angles for  $\theta$  in the trapezoidal rule as  $N_{\theta,\text{data},1} = 201$ ,  $N_{\theta,\text{data},2} = 16$  and  $N_{\theta,\text{recon}} = 50$ .

In Corollary 3.28, we analysed how the top order symbol of  $\Lambda$  looks like for  $\alpha = 0$ . As a consequence, we defined the first modified reconstruction operator  $\Lambda_{\text{mod},0}$  and investigate its microlocal properties in Corollary 3.29. The idea behind was to highlight singularities for small values of the offset  $\alpha$ . If we apply  $\Lambda_{\text{mod},0}$  and the associated reconstruction kernel considering the same setting as before, we obtain the reconstructions  $\Lambda_{\text{mod},0,\gamma}n$  presented in Figure 5.17. Also in this case the predictions made in Subsection 5.2.1 are visible.

A comparison with Figure 5.6 yields that the intensity of the singularities for  $\alpha = 1$  is now significantly more uniform and more independent of the location than before. Nevertheless, for the choice  $\alpha = 10$  the strength of the reconstructed singularities is less uniform than with the reconstruction operator  $\Lambda$ . These observations confirm the intention we had by introducing the modified reconstruction operator  $\Lambda_{\text{mod},0}$ .

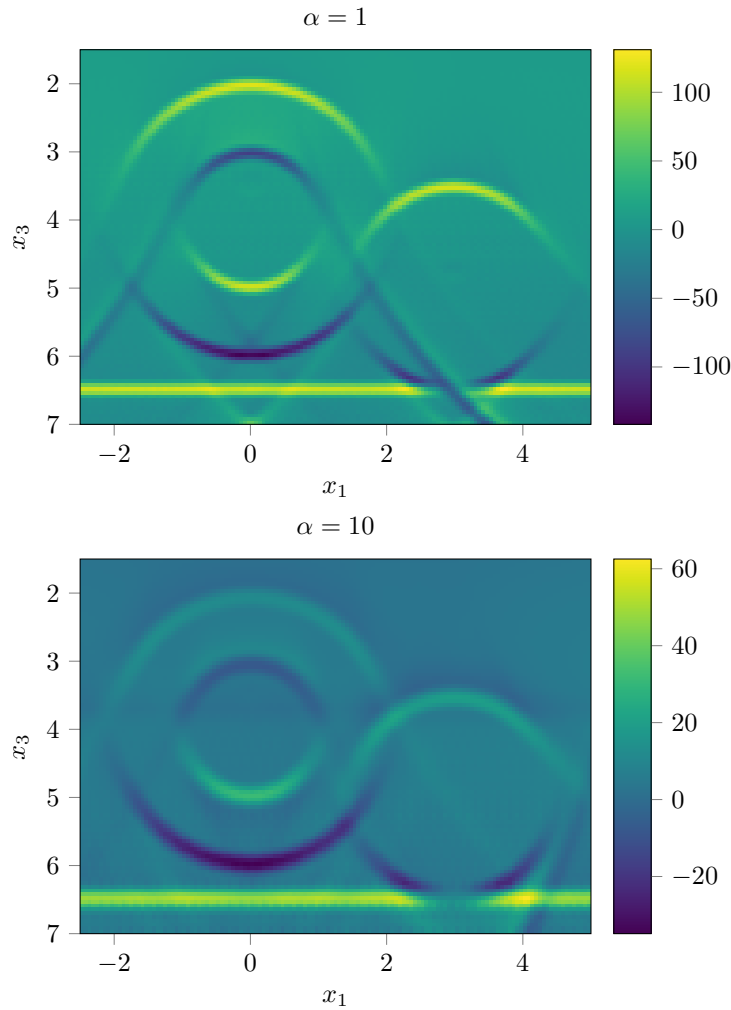


**Figure 5.17:** Two reconstructions  $\Lambda_{\text{mod},0,\gamma}n$  obtained with the reconstruction operator  $\Lambda_{\text{mod},0}$ . In the above image we have  $\alpha = 1$  and  $\gamma = 0.2$ , in the one below  $\alpha = 10$  and  $\gamma = 0.3$ .

In the theoretical considerations in Chapter 3, we continued the analysis of the operator  $\Lambda$  further. In a second investigation, we analysed how the top order symbol of  $\Lambda$  behaves for  $\alpha$  going to infinity. The result is stated in Corollary 3.30. Based on this we defined two other modified reconstruction operators  $\Lambda_{\text{mod},1}$  and  $\Lambda_{\text{mod},2}$  and presented their microlocal properties in Corollary 3.31. This time we introduced two operators since the top order symbol of  $\Lambda$  behaves differently depending on the directions related to the singularities. In the following, we present reconstructions using both operators. But before we repeat the two definitions. We have

$$\Lambda_{\text{mod},1} = \Lambda_{\text{mod},0} + \alpha\Lambda$$

and

$$\Lambda_{\text{mod},2} = \Lambda_{\text{mod},0} + \alpha^2\Lambda.$$

Further, we recall that we defined them in such a way that the first operator  $\Lambda_{\text{mod},0}$  of the sum dominates for small values of  $\alpha$  in comparison to the distance to the surface. The second

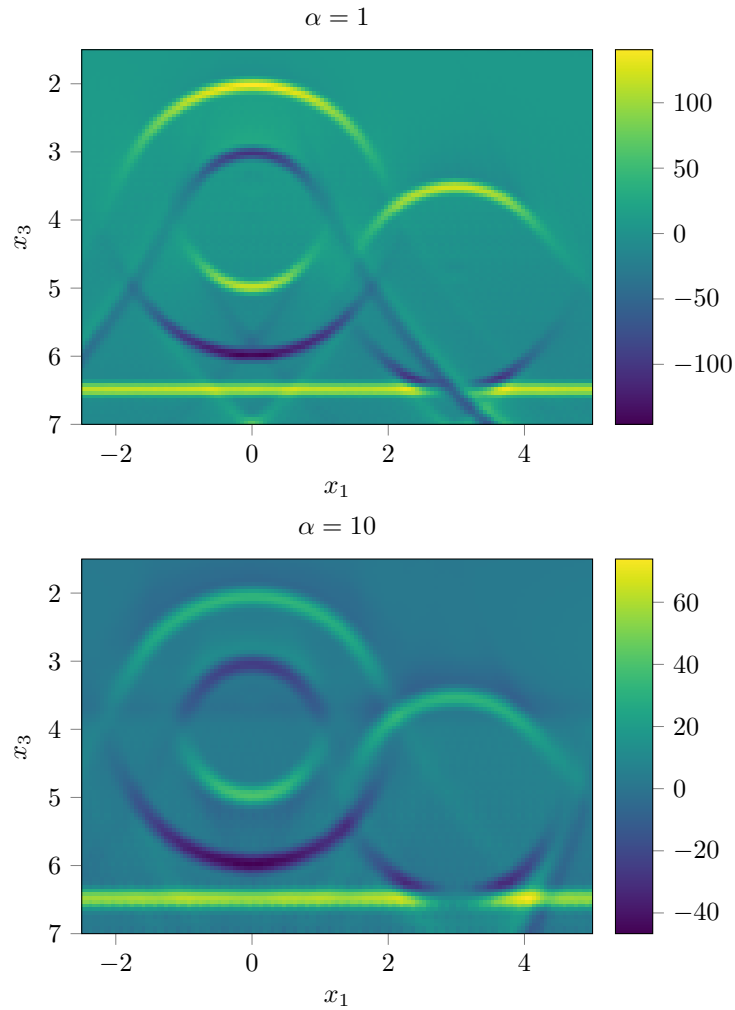


**Figure 5.18:** The reconstructions  $\Lambda_{\text{mod},1,\gamma}n$  associated with the reconstruction operator  $\Lambda_{\text{mod},1}$ . The images differ in the offsets. The above image is reconstructed with  $\alpha = 1$  and  $\gamma = 0.2$ , the bottom image with  $\alpha = 10$  and  $\gamma = 0.3$ .

one is decisive for large values of  $\alpha$  compared with the distance to the surface.

We start with the first reconstruction operator  $\Lambda_{\text{mod},1}$ . Again, we recover the singularities predicted in Subsection 5.2.1. The associated approximations  $\Lambda_{\text{mod},1,\gamma}n$  are given in Figure 5.18. For  $\alpha = 1$  the changes compared to the reconstructions with  $\Lambda_{\text{mod},0,\gamma}$  are marginal since the absolute values of  $\Lambda_{\gamma}n$  are too small in comparison to  $\Lambda_{\text{mod},0,\gamma}n$ . In case of  $\alpha = 10$ , the modification changes the reconstructions a bit more but not much. The imaged singularities near to the surface are reconstructed a bit stronger as the lower image in Figure 5.18 shows. However, the reconstruction for  $\alpha = 10$  is not as good as the one in Figure 5.6.

Last, we consider the reconstruction operator  $\Lambda_{\text{mod},2}$ . We notice that in case of  $\alpha = 1$  we have  $\Lambda_{\text{mod},1} = \Lambda_{\text{mod},2}$ . Thus, also the approximation  $\Lambda_{\text{mod},2,\gamma}$  is equal to  $\Lambda_{\text{mod},1,\gamma}$ . But for  $\alpha = 10$  there is a difference. The corresponding results are presented in Figure 5.19. Once again, we recognise the predictions concerning the singularities made in Subsection 5.2.1. We remark that the factor  $\alpha^2$  in front of  $\Lambda$  for  $\alpha = 10$  yields a higher value of  $\Lambda_{\gamma}n$  than the factor  $\alpha$ . Thus, adding the operator  $\alpha^2\Lambda$  to  $\Lambda_{\text{mod},0,\gamma}n$  provides a noticeable difference

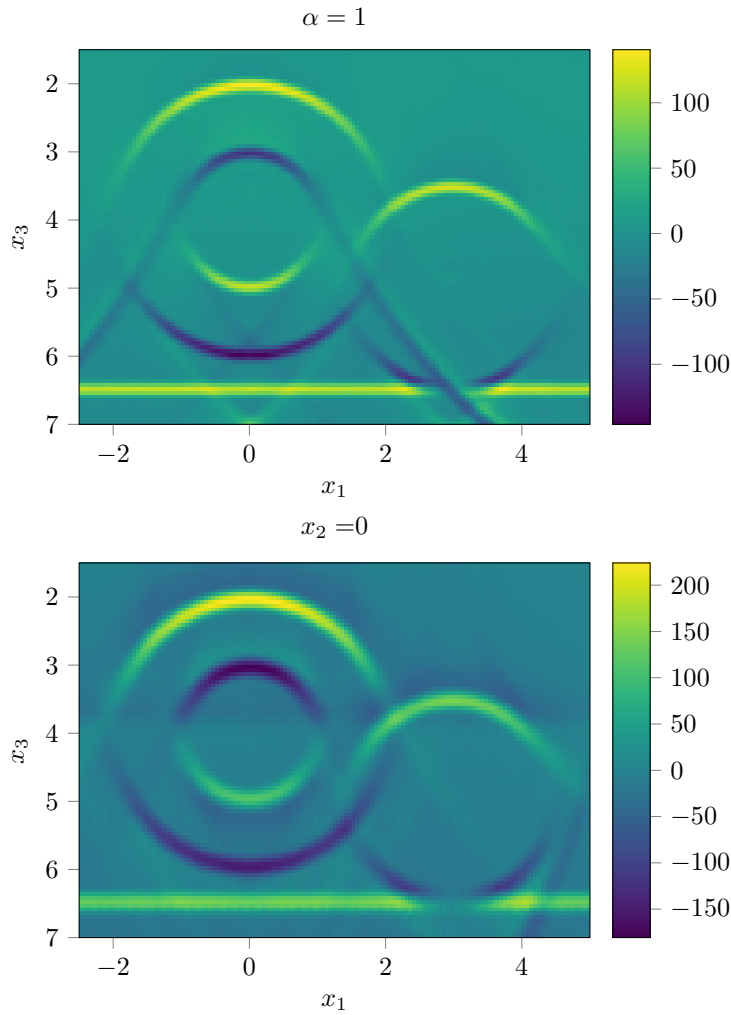


**Figure 5.19:** These images show  $\Lambda_{\gamma, \text{mod}, 2}$  in two cases of offsets  $\alpha$ . First, we have  $\alpha = 1$  and  $\gamma = 0.2$  and in the second image  $\alpha = 10$  and  $\gamma = 0.3$ .

compared to using only  $\Lambda_{\text{mod}, 0, \gamma} n$ .

In Subsection 5.2.1 we explained that the directions are perpendicular to the boundary of the balls. Thus, the corresponding directions in the  $x_2 = 0$  cross section are zero in the second component since the midpoints of all three balls are in the  $x_2 = 0$ -plane. By the theoretical considerations in Subsection 3.3.3 this yields that the top order symbol of  $\Lambda$  behaves like  $\frac{1}{\alpha}$  for  $\alpha$  going to infinity. Hence, according to the theory  $\Lambda_{\text{mod}, 1}$  would be the most suitable reconstruction operator. In contrast to this argumentation, the results are better when we choose the reconstruction operator  $\Lambda_{\text{mod}, 2}$ .

We conclude, that in the end, the behaviour of the top order symbol of  $\Lambda$  for  $\alpha$  going to infinity recommends us to increase the value of  $\Lambda_{\text{mod}, 0, \gamma}$  by a factor  $\alpha$  or  $\alpha^2$ . Depending on the absolute values one of these two might be more suitable. In practical use this is easy to realise by saving the data of  $r_{p, \gamma, 3}$  separately. Multiplication with  $\alpha$  or  $\alpha^2$  and adding  $r_{p, \gamma, 3, \text{mod}, 0}$  yields the reconstruction kernels  $r_{p, \gamma, 3, \text{mod}, 1}$  and  $r_{p, \gamma, 3, \text{mod}, 2}$ . Thus, it is simple to try both options. Altogether, by using one of the operators  $\Lambda_{\text{mod}, 1}$  or  $\Lambda_{\text{mod}, 2}$  we achieve quite good and more or less depth independent approximations of the reconstruction using

the same reconstruction operator for both values of  $\alpha$ .

We close the comparison with some remarks concerning the reconstruction kernels associated with the modified reconstruction operators. The three reconstruction kernels  $r_{p,\gamma,3,\text{mod},0}$ ,  $r_{p,\gamma,3,\text{mod},1}$  and  $r_{p,\gamma,3,\text{mod},2}$  behave qualitatively like the reconstruction kernel  $r_{p,\gamma,3}$ , which is illustrated in the Figures 5.9-5.11. The reason for this is that these figures show  $r_{p,\gamma,3}$  in a certain point  $p$ . Since the reconstruction kernel  $r_{p,\gamma,3,\text{mod},0}$  differs from  $r_{p,\gamma,3}$  only in a factor of  $x_3^2$  and we consider only points in a ball with a small radius  $\gamma$  around the fixed point  $p$ , there is no qualitative difference. The same is valid in case of  $\alpha r_{p,\gamma,3,\text{mod},0}$  or  $\alpha^2 r_{p,\gamma,3,\text{mod},0}$  and consequently in case of  $r_{p,\gamma,3,\text{mod},1}$  and  $r_{p,\gamma,3,\text{mod},2}$ .

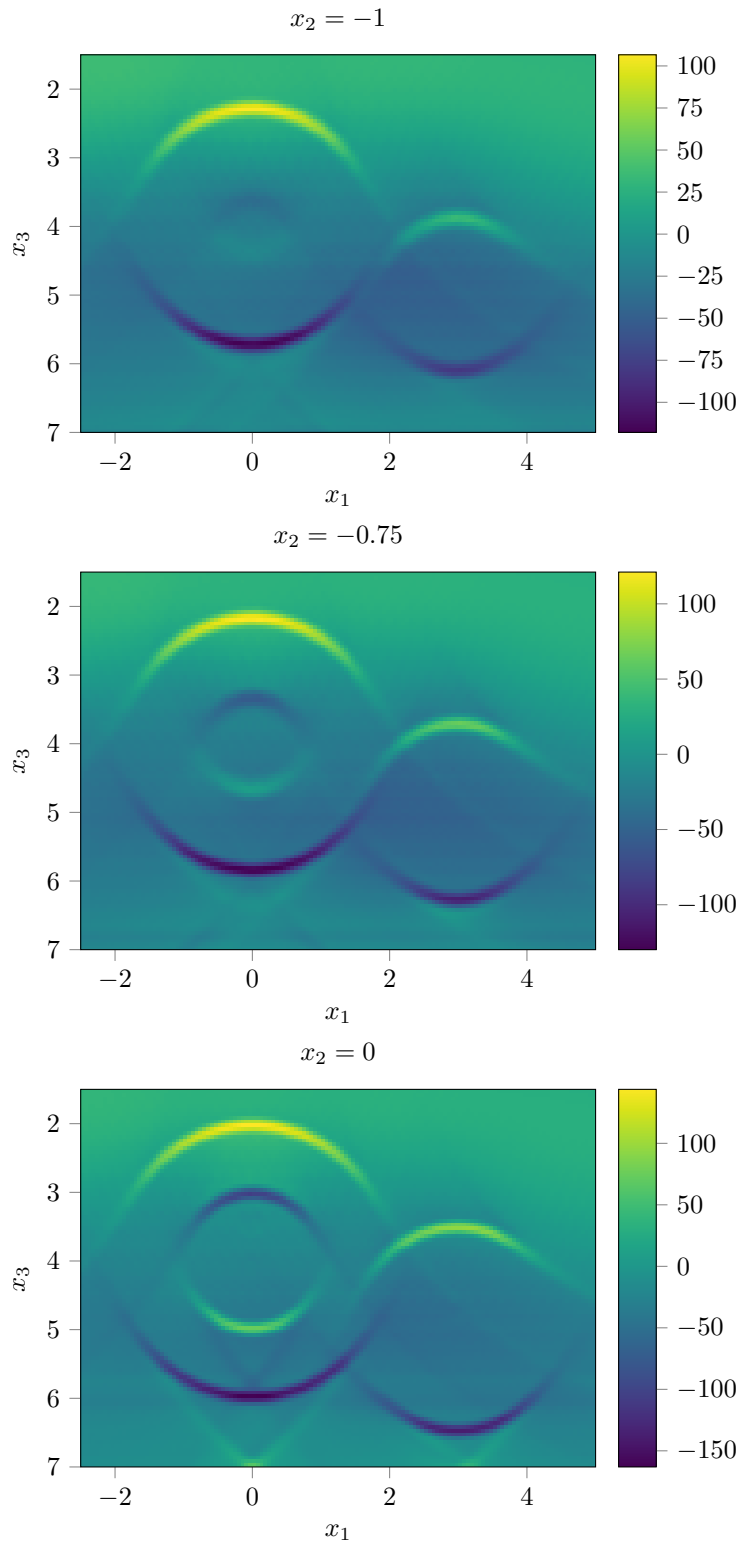
### 5.3.4. Reconstructions of different planes

In a last experiment using data computed via  $y = Fn$ , we aim to visualise the three dimensional setting. For this reason, we consider five cross sections of the cuboid given by  $[-2.5, 5] \times [-2.5, 2.5] \times [1.5, 7]$ . This time we consider the function  $n = \chi_{B_2(0,0,4)} - \chi_{B_1(0,0,4)} + \chi_{B_{1.5}(3,0,5)}$ . In comparison to the function described in Subsection 5.2.1, we do not take the characteristic function of the half-space  $\{x_3 \geq 6.5\}$  into account. For the offset  $\alpha$ , we choose  $\alpha = 1$  and so we use the reconstruction operator  $\Lambda_{\text{mod},0,\gamma}$ , which fits to small values of  $\alpha$  in comparison to  $x_3$  by Subsection 5.3.3. In the reconstruction kernel we use the scaling parameter  $\gamma = 0.2$ . Further, we set  $t_{\min} = 2\alpha + 0.1 = 2.1$ ,  $t_{\max} = t_{\min} + 17 = 19.1$  and  $s_{\max} = 7.5$ , i.e. we have  $s_1, s_2 \in [-7.5, 7.5]$ . Since we use  $N_s = N_t = 600$  uniformly distributed discretisation points, we compute the reconstructions from integrals over 216 000 000 open half-ellipsoids. For the generation of the data we consider  $N_{\theta,\text{data},1} = 201$  angles for  $\theta$  and in the reconstruction kernel  $N_{\theta,\text{recon}} = 16$  angles for  $\theta$ .

The five cross sections through the cuboid are shown in Figure 5.20. Each cross section of  $\Lambda_{\text{mod},0,\gamma}n$  is in  $x_2$ -direction and partitioned uniformly with  $N_{x_1} = 135$ ,  $N_{x_2} = 1$  and  $N_{x_3} = 99$  discretisation points.

If we compare the cross section in  $x_2 = -1$  with  $x_2 = 1$  or the one in  $x_2 = -0.75$  with  $x_2 = 0.75$ , we notice the symmetry. It is ensured by the fact that we consider the same choices concerning the parameters  $s_1$  and  $s_2$  and the symmetry of the function  $n$ . This is obvious apparent in the reconstructions. Moreover, the cross sections confirm our expectations from Subsection 5.2.1 concerning what we observe in the reconstructions. In all five cross sections the parts of the singular support of  $n$  we expected to see are clearly visible. In the cross sections in  $x_2 = -1$  and  $x_2 = 1$ , we notice that the ball with midpoint  $(0, 0, 4)^\top$  and radius 1 is almost not to see. There is only a little shadow left.

The weaker not so distinct lines in comparison to the singularities of  $n$  are artifacts. In general these are caused by the limited data, the numerical scheme and the cut-off function  $\psi$ . According to [FQ15] the few artifacts appearing in Figure 5.20 and having the form of a curved letter “v” are due to limited data. In the publication [FQ15] the authors analyse which singularities are added because the data is limited. The example they study in Section 4.2 is taken from the publication [QRS11], in which our setting with  $\alpha = 0$  is considered. In relation to Figure 3 in [FQ15] the authors argue that the added singularities are just the ones they predicted. As the image there also shows a reconstruction generated using a similar sum of characteristic functions like  $n$ , this is applicable to our reconstructions. We conclude that the aforementioned artifacts are caused by limited data.



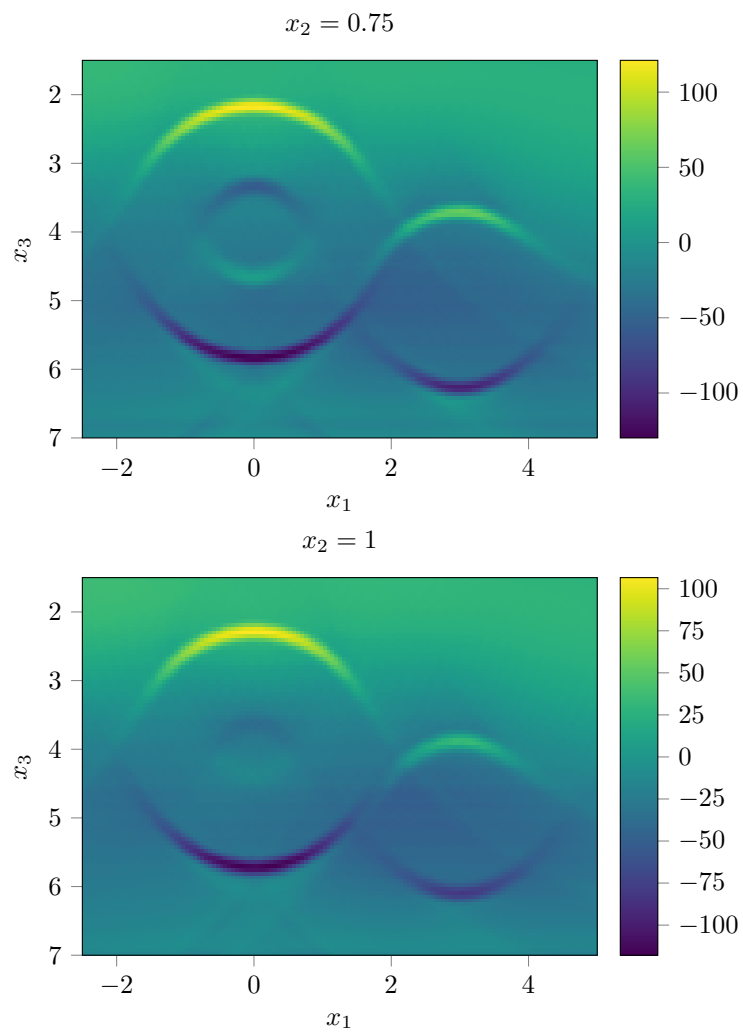


**Figure 5.20:** Different cross sections of  $\Lambda_{\text{mod},0,\gamma} n$  in  $x_2$ -direction.

### 5.3.5. Reconstructions using data from the wave equation

Up to now, we generated the data via the identity  $y = Fn$  with the same implementation for  $F$  as we use it in the different reconstruction kernels  $\tilde{r}_{p,\gamma,3}$ . This is a situation where inverse crime occurs, i.e. we use the same theoretical model to generate the synthetic data and to obtain properties of the data in our reconstructions. In other words, we identify reality with our model and consequently with our approximation of it. So, we assume the model and the way we approximate it to be perfect. According to [CK13], such situations have to be avoided since they yield too optimistic results.

For this reason, we present a last example in which we generate data from the wave equation and not by using data which is in the range of the elliptic Radon transform.

By solving the acoustic wave equation numerically we get an approximation of the data. In order to obtain this approximation, we use PySIT which is an open source toolbox for Python considering aspects of seismic imaging and inversion. For further information we refer to [Py13]. We rely on PySIT for the solutions of the two acoustic wave equations, we need to generate data and also for the measurements at the receivers.

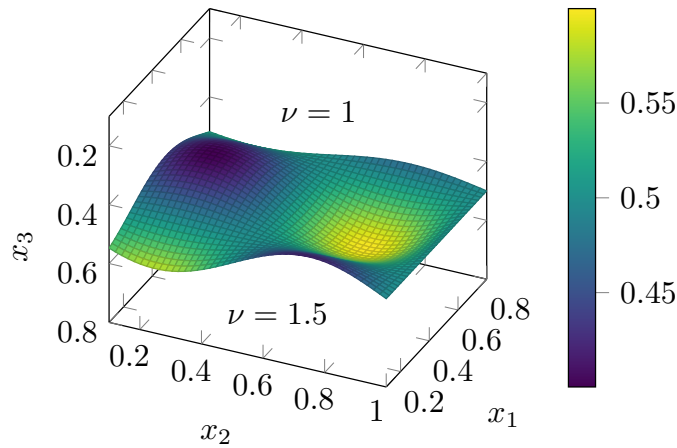


Figure 5.21: An illustration of the speed of sound  $\nu$ .

We consider a situation in the cuboid  $[0.1, 0.8] \times [0.1, 1.0] \times [0.1, 0.8]$  with absorbing boundary conditions using a perfectly matched layer. The perfectly matched layer is implemented in the toolbox PySIT and ensures that outgoing waves are absorbed almost without reflections at the boundaries. Hence, it is used to simulate problems with open boundaries as in the situation we consider. Further, we discretise the cuboid with a step size of 0.01. At the surface of the cuboid we choose  $13 \times 35$  source and receiver pairs. Their positions are given by  $\mathbf{x}_s(s) = (s_1, s_2 - \alpha, 0.1)^\top$  and  $\mathbf{x}_r(s) = (s_1, s_2 + \alpha, 0.1)^\top$  with  $s_1 \in \{0.15 + 0.05i \mid i \in \{0, \dots, 12\}\}$  and  $s_2 \in \{0.125 + 0.025j \mid j \in \{0, \dots, 35\}\}$ . For the travel time  $t$  we take 1709 points between  $t_{\min} = 0.1$  and  $t_{\max} = 2$  into account. The offset  $\alpha$  is given by  $\alpha = 0.025$ . We notice that the third component of sources and receivers is not equal to zero here. However, this does not matter since we are able to shift the setting.

As mentioned before we use PySIT to solve the two acoustic wave equations

$$\frac{1}{\nu^2(x)} \partial_t^2 u(t, x; \mathbf{x}_s(s)) - \Delta u(t, x; \mathbf{x}_s(s)) = \delta(x - \mathbf{x}_s(s)) \delta(t) \quad \text{for } t \geq 0, x \in \mathbb{R}^3, \quad (5.13)$$

and

$$\partial_t^2 \tilde{u}(t, x; \mathbf{x}_s(s)) - \Delta \tilde{u}(t, x; \mathbf{x}_s(s)) = \delta(x - \mathbf{x}_s(s))\delta(t) \quad \text{for } t \geq 0, x \in \mathbb{R}^3, \quad (5.14)$$

where we use a scaled and truncated Gaussian to model the temporal impulse at time  $t = 0$ . In the second equation (5.14), we inserted the speed of sound  $c$  equal to 1 as assumed throughout this thesis. More details are given in Section 1.2. In equation (5.13), we choose the speed of sound  $\nu$  in the following way

$$\nu(x) = \begin{cases} 1, & \text{if } x_3 \leq 0.1 \sin(2\pi x_2) \cos(2\pi x_1) + 0.5, \\ 1.5, & \text{if } x_3 > 0.1 \sin(2\pi x_2) \cos(2\pi x_1) + 0.5, \end{cases}$$

for  $x \in \mathbb{R}^3$ . This choice of  $\nu$  simulates two different material layers. An illustration of  $\nu$  on the considered cuboid is given in Figure 5.21. The value of  $\nu$  is equal to 1 above the surface plotted in this Figure and to 1.5 below.

Further, we implement the common offset geometry in the PySIT toolbox and use the provided routines to record the reflections of the solutions to the two wave equations at the receiver points  $\mathbf{x}_r(s)$ . With these measurements we compute the data

$$y(s, t) = -16\pi^2 \int_0^t (t - \tau)(u - \tilde{u})(\tau, \mathbf{x}_r(s); \mathbf{x}_s(s)) d\tau$$

for points  $(s, t)$  as mentioned before.

This time we choose a slightly different cut-off function than introduced in Section 5.2. We consider

$$\psi(s, t) = \psi(s_1, s_2, t) = \tilde{\Psi}(s_1)\tilde{\Psi}(s_2)\tilde{\Psi}(t)$$

for the points  $(s, t)$ , where

$$\tilde{\Psi}(r) = \begin{cases} 0, & \text{for } r \leq a - d_1, \\ \frac{f(r - (a - d_1))}{f(r - (a - d_1)) + f(a - r)}, & \text{for } a - d_1 < r < a, \\ 1, & \text{for } a \leq r \leq b, \\ \frac{f(b + d_2 - r)}{f(r - b) + f(b + d_2 - r)}, & \text{for } b < r < b + d_2, \\ 0, & \text{for } b + d_2 \leq r, \end{cases}$$

for  $r \in \mathbb{R}$ . The appearing function  $f$  is defined as in Section 5.2, i.e.

$$f(r) = \begin{cases} \exp(-\frac{1}{r}), & \text{for } 0 < r, \\ 0, & \text{for } r \leq 0, \end{cases}$$

for  $r \in \mathbb{R}$ . Then, we have  $\text{supp}(\tilde{\Psi}) \subseteq [a - d_1, b + d_2]$  and  $\tilde{\Psi}|_{[a, b]} = 1$ .

Here, we consider two different choices of parameters. In a first example, we choose in case of  $s_1$  the parameters  $a = 0.225, b = 0.675$  and  $d_1 = d_2 = 0.2$ , in case of  $s_2$  we have  $a = 0.175, b = 0.925$  and  $d_1 = d_2 = 0.2$ . For a second one we make the choices  $a = 0.4, b = 0.5$  and  $d_1 = d_2 = 0.5$  for  $s_1$  and  $a = 0.5, b = 0.6$  and  $d_1 = d_2 = 0.55$  for  $s_2$ . We use in both cases the parameters  $a = 0.15, d_1 = 0.05$  and  $b = 1.7, d_2 = 0.3$  for the travel time  $t$ . In Figure 5.22 the cross sections in  $s_1 = 0.5$  of the two different cut-off functions applied to the

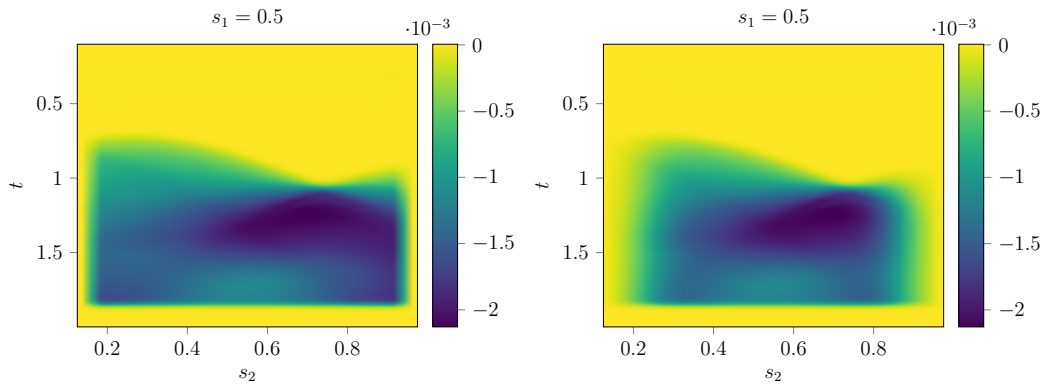


**Figure 5.22:** The data  $\psi y$  generated by using the seismic imaging toolbox PySIT for two different choices of the cut-off function  $\psi$ . As it can be observed in the images, the truncation of the data caused by  $\psi$  is less hard in the right image than in the left one. The exact parameters chosen for  $\psi$  are given in the text.

data  $y$  are plotted. The left image corresponds to the choice where the cut-off function  $\psi$  is equal to 1 for  $s_2$  between  $a = 0.225$  and  $b = 0.925$ . In the right image the cut-off function  $\psi$  is equal to 1 in case of  $s_2$  between  $a = 0.5$  and  $b = 0.6$ . As a consequence, the truncation in the right image is less hard than in the left image. We remark that the discontinuities in both images are due to the small number of data points for  $s_2$ . Moreover, we choose the regularisation parameter  $\gamma = 0.07$  in the reconstruction kernel.

In Figure 5.23 we present four cross sections of  $\Lambda_\gamma n$ , where we used the hard truncated data presented in the left image of Figure 5.22. The left images in Figure 5.23 show the structure of the material layers we reconstruct. According to the theory, actually all related directions to the appearing singularities have a non-vanishing third component. Thus, we expect to reconstruct all singularities in the considered cuboid.

In all reconstructed cross sections, the singular support which corresponds to the boundary between the two different material layers is reconstructed as a relatively thick curve. From the experience we got from the reconstructions without using data from the wave equation, we know that this effect comes from a lack of data. In the reconstructed images presented in the subsection before, the visible lines in the images are much more distinct and thinner when we used  $N_s = N_t = 600$  instead of  $N_s = N_t = 300$  for the numbers of steps of  $s_1, s_2$  and  $t$ . Thus, we compare the lower limitation of the blue visible curve, which appears where the jumps between negative and positive values occur, with the original situation.

Now, we take a closer look at Figure 5.23. We notice that in all four reconstructions the singularities at the left boundaries of the images are less visible than the ones near to the right boundaries. The reason is that we start positioning sources on the left-hand side at  $x_2 = 0.125$  with the first receiver at  $x_2 = 0.15$  whereas we end on the right-hand side of the images with a receiver. By this means, the data concerning the area near to the left boundary is not recorded.

We start with a comparison of the two cross sections in  $x_1 = 0.1$  and  $x_1 = 0.5$ . In the latter one, the reconstructed singularities have nearly all the same intensity and the curve, which is formed by them, is clearly recognisable. This observation goes back to the location of the cross sections inside the cuboid. The cross section in  $x_1 = 0.1$  is a part of the boundary of the considered cuboid. Thus, there are only sources and receivers positioned behind the cross

section for  $0.1 < x_1 \leq 0.8$  and not in front of, i.e. for values  $x_1 < 0.1$ . In contrast, regarding the cross section  $x_1 = 0.5$  there are sources and receivers in front of and behind since it is taken from the middle of the cuboid. Although the cross sections in  $x_1 = 0.3$  and  $x_1 = 0.7$  are both from the middle of the cuboid, the reconstructed singularities are a bit more consistent in intensity and sharpness in the one which is further away from the boundary, i.e.  $x_1 = 0.3$ .

In all four cross sections, we see that the strength of the singularities at the boundaries depends on how the curve of the reconstructed singularities hits the boundary. The reason is that by Theorem 3.15 and the pseudolocal property (see Theorem 2.17 and Corollary 3.26) the reconstruction operator  $\Lambda$  preserves a singularity of  $n$  if there is an open half-ellipsoid going through the location of this singularity such that the related direction is perpendicular to the open half-ellipsoid (see also Subsection 5.2.1). So, if there is no open half-ellipsoid in the data set going through the location of a singularity in this way the related singularity will not be detected.

Further, we notice artifacts induced by the numerical scheme, the limited data and the cut-off function in all four reconstructions. The two most noticeable artifacts, the oblique lines looking like a curved letter “v”, are caused by limited data. In the cross sections in  $x_1$ -direction these two artifacts are symmetric with respect to the line  $x_2 = 0.55$ . The reason is that the values we use for  $s_2$  are arranged symmetrically with respect to  $x_2 = 0.55$ . In [FQ15] the authors mention that such artifacts are due to hard truncation. Although we used a smooth truncation, we are able to improve our numerical results by using a cut-off function which decays slower.

In order to realise such a soft truncation, we use the data presented in the right image of Figure 5.22. The results are illustrated in Figure 5.24. We notice that the singularities appearing in the original situation shown in the left images are reconstructed as well as in Figure 5.23. The great difference between the reconstructions presented in Figure 5.23 and Figure 5.24 is in the artifacts. Using the cut-off function with slower decay reduces the artifacts enormously and does not change the quality of the existing singularities noticeably. Since limited data causes artifacts, it is quite intuitively that smooth truncation reduces them. However, according to [FQ15] this has not yet been mathematically justified. Considering a softer truncation is intuitively one step further. In contrast, hard truncation does not change the data much. Especially, when we have not much data, there is no great difference between a hard truncation and no truncation, i.e. only considering raw limited data. This can be seen in the left image of Figure 5.22.

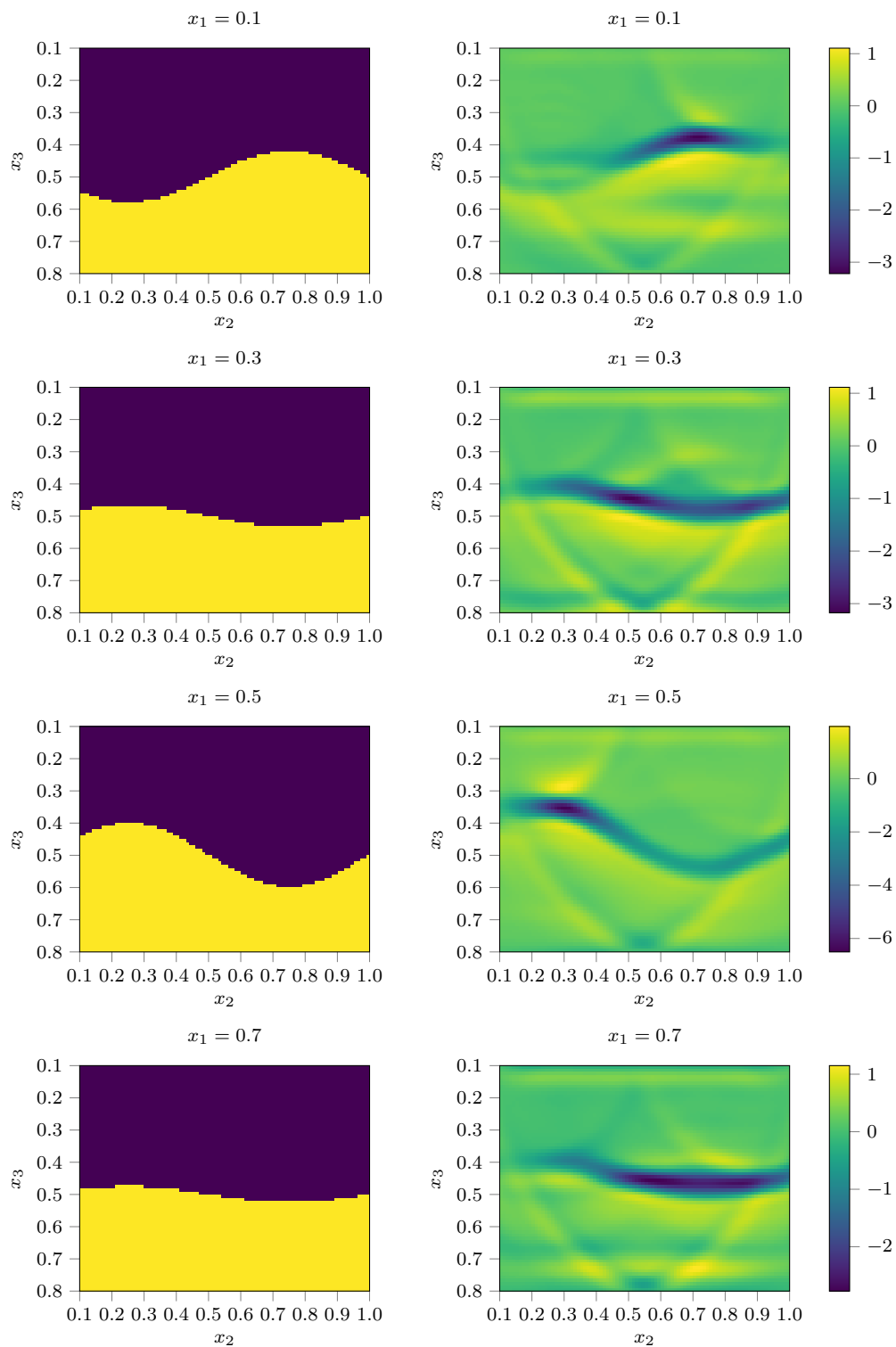


**Figure 5.23:** The given situation with speed of sound  $\nu = 1$  in the blue and  $\nu = 1.5$  in the yellow area and the corresponding reconstructions  $\Lambda_{\gamma} n$  generated from the hard truncated data, which is illustrated in the left image of Figure 5.22.

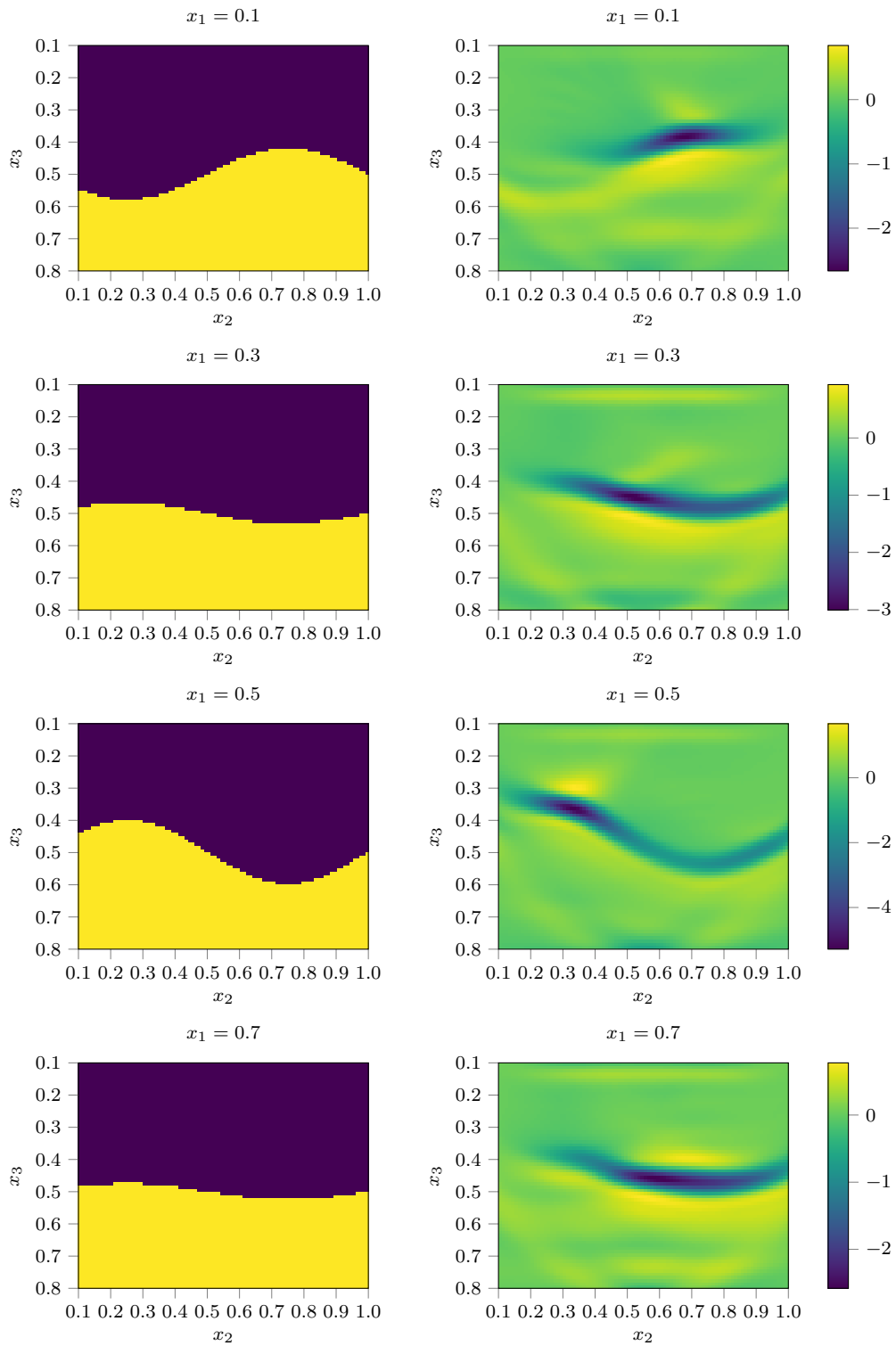


**Figure 5.24:** The given situation with speed of sound  $\nu = 1$  in the blue and  $\nu = 1.5$  in the yellow area and the corresponding reconstructions  $\Lambda_{\gamma}^n$  generated from the soft truncated data, which is illustrated in the right image of Figure 5.22.



---

## Various calculations

---

### A.1. The explicit expression of the Beylkin determinant $B$

As in other parts in this thesis, we use the abbreviations

$$D = |\mathbf{x}_s(s) - x| = \sqrt{(s_1 - x_1)^2 + ((s_2 - \alpha) - x_2)^2 + x_3^2}$$

and

$$E = |x - \mathbf{x}_r(s)| = \sqrt{(x_1 - s_1)^2 + (x_2 - (s_2 + \alpha))^2 + x_3^2}$$

for  $s \in S_0$  and  $x \in \mathbb{R}_+^3$ . For  $\varphi(s, x) = |\mathbf{x}_s(s) - x| + |x - \mathbf{x}_r(s)|$  we calculate

$$\nabla_x \varphi(s, x) = \left( \begin{array}{c} \frac{x_1 - s_1}{|\mathbf{x}_s(s) - x|} + \frac{x_1 - s_1}{|x - \mathbf{x}_r(s)|} \\ \frac{x_2 - (s_2 - \alpha)}{|\mathbf{x}_s(s) - x|} + \frac{x_2 - (s_2 + \alpha)}{|x - \mathbf{x}_r(s)|} \\ \frac{x_3}{|\mathbf{x}_s(s) - x|} + \frac{x_3}{|x - \mathbf{x}_r(s)|} \end{array} \right), \quad (\text{A.1})$$

$$\partial_{s_1} \nabla_x \varphi(s, x) = \left( \begin{array}{c} -\frac{(x_2 - (s_2 - \alpha))^2 + x_3^2}{|\mathbf{x}_s(s) - x|^3} - \frac{(x_2 - (s_2 + \alpha))^2 + x_3^2}{|x - \mathbf{x}_r(s)|^3} \\ \frac{(x_1 - s_1)(x_2 - (s_2 - \alpha))}{|\mathbf{x}_s(s) - x|^3} + \frac{(x_1 - s_1)(x_2 - (s_2 + \alpha))}{|x - \mathbf{x}_r(s)|^3} \\ \frac{x_3(x_1 - s_1)}{|\mathbf{x}_s(s) - x|^3} + \frac{x_3(x_1 - s_1)}{|x - \mathbf{x}_r(s)|^3} \end{array} \right),$$

$$\partial_{s_2} \nabla_x \varphi(s, x) = \left( \begin{array}{c} \frac{(x_1 - s_1)(x_2 - (s_2 - \alpha))}{|\mathbf{x}_s(s) - x|^3} + \frac{(x_1 - s_1)(x_2 - (s_2 + \alpha))}{|x - \mathbf{x}_r(s)|^3} \\ -\frac{(x_1 - s_1)^2 + x_3^2}{|\mathbf{x}_s(s) - x|^3} - \frac{(x_1 - s_1)^2 + x_3^2}{|x - \mathbf{x}_r(s)|^3} \\ \frac{x_3(x_2 - (s_2 - \alpha))}{|\mathbf{x}_s(s) - x|^3} + \frac{x_3(x_2 - (s_2 + \alpha))}{|x - \mathbf{x}_r(s)|^3} \end{array} \right)$$

each for  $s \in S_0$  and  $x \in \mathbb{R}_+^3$ . Further, we write  $c := x_1 - s_1$  and  $d := x_2 - s_2$ . By the definition of  $B$  given in (3.23), we obtain

$$\begin{aligned}
B(s, x) &= \det \begin{pmatrix} \nabla_x \varphi(s, x)^\top \\ \partial_{s_1} \nabla_x \varphi(s, x)^\top \\ \partial_{s_2} \nabla_x \varphi(s, x)^\top \end{pmatrix} \\
&= \det \begin{pmatrix} c \left( \frac{1}{D} + \frac{1}{E} \right) & \frac{d + \alpha}{D} + \frac{d - \alpha}{E} & x_3 \left( \frac{1}{D} + \frac{1}{E} \right) \\ \frac{-(d + \alpha)^2 - x_3^2}{D^3} + \frac{-(d - \alpha)^2 - x_3^2}{E^3} & c \left( \frac{d + \alpha}{D^3} + \frac{d - \alpha}{E^3} \right) & x_3 c \left( \frac{1}{D^3} + \frac{1}{E^3} \right) \\ c \left( \frac{d + \alpha}{D^3} + \frac{d - \alpha}{E^3} \right) & (-c^2 - x_3^2) \left( \frac{1}{D^3} + \frac{1}{E^3} \right) & x_3 \left( \frac{d + \alpha}{D^3} + \frac{d - \alpha}{E^3} \right) \end{pmatrix} \\
&= x_3 c^2 \left( \frac{1}{D} + \frac{1}{E} \right) \left( \frac{d + \alpha}{D^3} + \frac{d - \alpha}{E^3} \right)^2 - x_3 c^2 \left( \frac{1}{D} + \frac{1}{E} \right) \left( \frac{d + \alpha}{D^3} + \frac{d - \alpha}{E^3} \right)^2 \\
&\quad + x_3 \left( \frac{1}{D} + \frac{1}{E} \right) \left( \frac{1}{D^3} + \frac{1}{E^3} \right) (-c^2 - x_3^2) \left( \frac{-(d + \alpha)^2 - x_3^2}{D^3} + \frac{-(d - \alpha)^2 - x_3^2}{E^3} \right) \\
&\quad + c^2 x_3 \left( \frac{1}{D^3} + \frac{1}{E^3} \right) \left( \frac{d + \alpha}{D} + \frac{d - \alpha}{E} \right) \left( \frac{d + \alpha}{D^3} + \frac{d - \alpha}{E^3} \right) \\
&\quad - x_3 c^2 \left( \frac{1}{D} + \frac{1}{E} \right) \left( -c^2 - x_3^2 \right) \left( \frac{1}{D^3} + \frac{1}{E^3} \right)^2 \\
&\quad - x_3 \left( \frac{d + \alpha}{D^3} + \frac{d - \alpha}{E^3} \right) \left( \frac{d + \alpha}{D} + \frac{d - \alpha}{E} \right) \left( \frac{-(d + \alpha)^2 - x_3^2}{D^3} + \frac{-(d - \alpha)^2 - x_3^2}{E^3} \right) \\
&= x_3 \left( \frac{1}{D} + \frac{1}{E} \right) \left( \frac{1}{D^3} + \frac{1}{E^3} \right) (c^2 + x_3^2) \left( \frac{(d + \alpha)^2 + x_3^2}{D^3} + \frac{(d - \alpha)^2 + x_3^2}{E^3} + \frac{c^2}{D^3} + \frac{c^2}{E^3} \right) \\
&\quad + x_3 \left( \frac{d + \alpha}{D} + \frac{d - \alpha}{E} \right) \left( \frac{d + \alpha}{D^3} + \frac{d - \alpha}{E^3} \right) \left( \frac{c^2}{D^3} + \frac{c^2}{E^3} + \frac{(d + \alpha)^2 + x_3^2}{D^3} + \frac{(d - \alpha)^2 + x_3^2}{E^3} \right) \\
&= x_3 \left( \frac{1}{D} + \frac{1}{E} \right) \left( \frac{1}{D^3} + \frac{1}{E^3} \right) (c^2 + x_3^2) \left( \frac{c^2 + (d + \alpha)^2 + x_3^2}{D^3} + \frac{c^2 + (d - \alpha)^2 + x_3^2}{E^3} \right) \\
&\quad + x_3 \left( \frac{d + \alpha}{D} + \frac{d - \alpha}{E} \right) \left( \frac{d + \alpha}{D^3} + \frac{d - \alpha}{E^3} \right) \left( \frac{c^2 + (d + \alpha)^2 + x_3^2}{D^3} + \frac{c^2 + (d - \alpha)^2 + x_3^2}{E^3} \right) \\
&= x_3 \left( \frac{1}{D} + \frac{1}{E} \right)^2 \left( \frac{1}{D^3} + \frac{1}{E^3} \right) (c^2 + x_3^2) + x_3 \left( \frac{d + \alpha}{D} + \frac{d - \alpha}{E} \right) \left( \frac{d + \alpha}{D^3} + \frac{d - \alpha}{E^3} \right) \left( \frac{1}{D} + \frac{1}{E} \right) \\
&= x_3 \left( \frac{1}{D} + \frac{1}{E} \right) \left( \frac{1}{D^4} + \frac{1}{D^3 E} + \frac{1}{D E^3} + \frac{1}{E^4} \right) (c^2 + x_3^2) \\
&\quad + x_3 \left( \frac{1}{D} + \frac{1}{E} \right) \left( \frac{(d + \alpha)^2}{D^4} + \frac{(d + \alpha)(d - \alpha)}{D^3 E} + \frac{(d + \alpha)(d - \alpha)}{D E^3} + \frac{(d - \alpha)^2}{E^4} \right) \\
&= x_3 \left( \frac{1}{D} + \frac{1}{E} \right) \left( \frac{c^2 + (d + \alpha)^2 + x_3^2}{D^4} + \frac{c^2 + (d + \alpha)(d - \alpha) + x_3^2}{D^3 E} \right. \\
&\quad \left. + \frac{c^2 + (d + \alpha)(d - \alpha) + x_3^2}{D E^3} + \frac{c^2 + (d - \alpha)^2 + x_3^2}{E^4} \right) \\
&= x_3 \left( \frac{1}{D} + \frac{1}{E} \right) \left( \frac{1}{D^2} + \frac{1}{E^2} + \left( \frac{1}{D^2} + \frac{1}{E^2} \right) \frac{c^2 + (d + \alpha)(d - \alpha) + x_3^2}{D E} \right) \\
&= x_3 \left( \frac{1}{D} + \frac{1}{E} \right) \left( \frac{1}{D^2} + \frac{1}{E^2} \right) \left( 1 + \frac{c^2 + (d + \alpha)(d - \alpha) + x_3^2}{D E} \right) \\
&= x_3 \left( \frac{1}{D} + \frac{1}{E} \right) \left( \frac{1}{D^2} + \frac{1}{E^2} \right) \left( 1 + \frac{(x_1 - s_1)^2 + (x_2 - (s_2 - \alpha))(x_2 - (s_2 + \alpha)) + x_3^2}{D E} \right) \\
&= x_3 \left( \frac{1}{D} + \frac{1}{E} \right) \left( \frac{1}{D^2} + \frac{1}{E^2} \right) \left( 1 + \frac{x - \mathbf{x}_s(s)}{D} \cdot \frac{x - \mathbf{x}_r(s)}{E} \right)
\end{aligned}$$

for  $s \in S_0$  and  $x \in \mathbb{R}_+^3$ .

## A.2. The proof of Lemma 3.22

First, we introduce the abbreviations  $p = p(\xi) = \frac{\xi_1}{\xi_3}$  and  $q = q(\xi) = \frac{\xi_2}{\xi_3}$  and recall the transformation  $\xi = \omega \nabla_x \varphi(s, x)$  which yields to each  $(x, \xi) \in \mathbb{R}_+^3 \times \mathbb{R}^3$  with  $\xi_3 \neq 0$  unique  $s \in S_0$  and  $w \in \mathbb{R} \setminus \{0\}$ . The representation of  $s = (s_1, s_2)$  is explicitly given in Lemma 3.13 and Remark 3.14.

Further, the support of the cut-off function  $\psi$  in  $S_0 \times (2\alpha, \infty)$  is compact. Thus, we assume

$$\text{supp}(\psi) \subseteq [-s_{\max}, s_{\max}] \times [-s_{\max}, s_{\max}] \times [t_{\min}, t_{\max}] \subseteq S_0 \times (2\alpha, \infty)$$

for  $s_{\max} > 0$  and  $t_{\min}, t_{\max} \in (2\alpha, \infty)$  with  $t_{\min} < t_{\max}$ . If we are able to show that  $|s_1(x, \xi)|$  or  $|s_2(x, \xi)|$  is larger than  $s_{\max}$  for  $x \in K$  and  $p = |\frac{\xi_1}{\xi_3}|$  or  $q = |\frac{\xi_2}{\xi_3}|$  large enough, we obtain

$$\psi(s(x, \xi), \varphi(s(x, \xi), x)) = 0.$$

We start with  $M_{1,\delta}$  and define  $M_{1,\delta} := \frac{s_{\max} + \max_{x \in K} |x|}{\delta} > 0$ . For  $|p| \geq M_{1,\delta}$  we have

$$|s_1| = |s_1(x, \xi)| \geq |px_3| - |x_1| \geq |p| \min_{x \in K} |x_3| - \max_{x \in K} |x| \geq \frac{s_{\max} + \max_{x \in K} |x|}{\delta} \delta - \max_{x \in K} |x| = s_{\max}.$$

Before we can define  $M_{2,\delta}$ , we need to show that there exists a constant  $C > 0$  such that

$$\left| \frac{2 \frac{\alpha^2}{x_3} q}{\sqrt{(p^2 + q^2 + 1)^2 + 4 \frac{\alpha^2}{x_3^2} q^2 + p^2 + 1}} \right| \leq C.$$

Note, that we have

$$\frac{2 \frac{\alpha^2}{x_3} q}{\sqrt{(p^2 + q^2 + 1)^2 + 4 \frac{\alpha^2}{x_3^2} q^2 + p^2 + 1}} = \frac{2 \frac{\alpha^2}{x_3 q}}{\sqrt{1 + \frac{2}{q^2} + \frac{1}{q^4} + 4 \frac{\alpha^2}{x_3^2 q^2} + \frac{1}{q^2}}} \rightarrow \frac{0}{\sqrt{1 + 0 + 0 + 0 + 0}}$$

for  $q \rightarrow \pm\infty$ . Together with the fact that the function

$$q \mapsto \frac{2 \frac{\alpha^2}{x_3} q}{\sqrt{(p^2 + q^2 + 1)^2 + 4 \frac{\alpha^2}{x_3^2} q^2 + p^2 + 1}}$$

is continuous and hence bounded yields the existence of  $C > 0$ .

Now, we can define  $M_{2,\delta} := 2 \frac{s_{\max} + \max_{x \in K} |x| + C}{\delta} > 0$ . Let  $|q| \geq M_{2,\delta}$ . The representation we use for  $s_2$  is stated in Remark 3.14. Then, we have

$$\begin{aligned} |s_2| = |s_2(x, \xi)| &= \left| x_2 - x_3 \left( \frac{1}{2} q + \frac{\frac{1}{2} q^3 + q(p^2 + 1) + 2 \frac{\alpha^2}{x_3^2} q}{\sqrt{(p^2 + q^2 + 1)^2 + 4 \frac{\alpha^2}{x_3^2} q^2 + p^2 + 1}} \right) \right| \\ &\geq \left| \frac{1}{2} q + \frac{\frac{1}{2} q^3}{\sqrt{(p^2 + q^2 + 1)^2 + 4 \frac{\alpha^2}{x_3^2} q^2 + p^2 + 1}} + \frac{q(p^2 + 1)}{\sqrt{(p^2 + q^2 + 1)^2 + 4 \frac{\alpha^2}{x_3^2} q^2 + p^2 + 1}} \right| |x_3| \\ &\quad - |x_2| - \left| \frac{2 \frac{\alpha^2}{x_3} q}{\sqrt{(p^2 + q^2 + 1)^2 + 4 \frac{\alpha^2}{x_3^2} q^2 + p^2 + 1}} \right| \\ &\geq \frac{1}{2} |q| |x_3| - |x_2| - \left| \frac{2 \frac{\alpha^2}{x_3} q}{\sqrt{(p^2 + q^2 + 1)^2 + 4 \frac{\alpha^2}{x_3^2} q^2 + p^2 + 1}} \right|, \end{aligned}$$

where we used that all summands in the first absolute value of the second line have the same sign due to the factors  $q$  and  $q^3$ . Finally, we get

$$\begin{aligned} |s_2| &\geq \frac{1}{2} |q| \min_{x \in K} |x_3| - \max_{x \in K} |x| - C \geq \frac{1}{2} 2 \frac{s_{\max} + \max_{x \in K} |x| + C}{\delta} \delta - \max_{x \in K} |x| - C \\ &= s_{\max}. \end{aligned}$$

According to the above considerations, we obtain

$$\psi(s(x, \xi), \varphi(s(x, \xi), x)) = 0$$

for  $x \in K$  if  $\left| \frac{\xi_1}{\xi_3} \right| \geq M_{1,\delta}$  or  $\left| \frac{\xi_2}{\xi_3} \right| \geq M_{2,\delta}$  is satisfied.

In order to show the second assertion, we define  $M := \max\{M_{1,\delta}, M_{2,\delta}\}$  and assume  $\left| \frac{\xi_1^2}{\xi_3^2} \right| < M$  or  $\left| \frac{\xi_2^2}{\xi_3^2} \right| < M$ . Then, we have

$$\sqrt{\frac{\xi_1^2}{\xi_3^2} + \frac{\xi_2^2}{\xi_3^2}} < \sqrt{2}M < 2M.$$

According to this we deduce  $\left| \frac{\xi_1^2}{\xi_3^2} \right| \geq M$  or  $\left| \frac{\xi_2^2}{\xi_3^2} \right| \geq M$  if  $\sqrt{\frac{\xi_1^2}{\xi_3^2} + \frac{\xi_2^2}{\xi_3^2}} \geq 2M$  is satisfied. As a consequence, we conclude

$$\psi(s(x, \xi), \varphi(s(x, \xi), x)) = 0$$

for  $x \in K$  if  $\sqrt{\frac{\xi_1^2}{\xi_3^2} + \frac{\xi_2^2}{\xi_3^2}} \geq 2M$  holds. □

### A.3. Calculations of limits associated with the top order symbol $\sigma(\Lambda)$

In order to analyse the behaviour of the top order symbol  $\sigma(\Lambda)$  of  $\Lambda$  for  $\alpha \rightarrow \infty$ , we calculate some limits in different cases. As we want to express these in terms of  $x$  and  $\xi$ , we repeat the definitions of the abbreviations introduced in Remark 3.23. We have

$$p := p(\xi) = \frac{\xi_1}{\xi_3} \quad \text{and} \quad q := q(\xi) = \frac{\xi_2}{\xi_3}$$

for  $\xi \in \mathbb{R}^3$  with  $\xi_3 \neq 0$  and

$$Q(p, q, \lambda) = \begin{cases} \frac{1}{2q} \left( q^2 - p^2 - 1 + \sqrt{(p^2 + q^2 + 1)^2 + 4\lambda^2 q^2} \right), & \text{for } q \neq 0, \\ 0, & \text{for } q = 0, \end{cases}$$

for  $p, q$  as above and  $\lambda > 0$ . We consider two different cases.

(a) Let  $\xi_2 > 0$  and  $\xi_3 > 0$  or  $\xi_2 < 0$  and  $\xi_3 < 0$ , so we have  $q > 0$  and thus

$$Q(p, q, \lambda) \longrightarrow \infty \tag{A.2}$$

for  $\lambda \rightarrow \infty$ . But we obtain

$$\begin{aligned} Q(p, q, \lambda) - \lambda &= \frac{1}{2q} (q^2 - p^2 - 1) + \sqrt{\frac{(p^2 + q^2 + 1)^2}{4q^2} + \lambda^2} - \lambda \\ &= \frac{1}{2q} (q^2 - p^2 - 1) + \frac{\frac{(p^2 + q^2 + 1)^2}{4q^2} + \lambda^2 - \lambda^2}{\sqrt{\frac{(p^2 + q^2 + 1)^2}{4q^2} + \lambda^2} + \lambda} \\ &\longrightarrow \frac{1}{2q} (q^2 - p^2 - 1) = \frac{1}{2\xi_2 \xi_3} (\xi_2^2 - \xi_1^2 - \xi_3^2) \end{aligned} \tag{A.3}$$

for  $\lambda \rightarrow \infty$ . Further, we get the limit

$$\frac{1}{\lambda}Q(p, q, \lambda) = \frac{1}{2\lambda q}(q^2 - p^2 - 1) + \sqrt{\frac{(p^2+q^2+1)^2}{4\lambda^2 q^2} + 1} \rightarrow 0 + \sqrt{0+1} = 1 \quad (\text{A.4})$$

again for  $\lambda \rightarrow \infty$ . Using the expressions for  $D$  and  $E$  introduced in Remark 3.23, we have

$$D = x_3 \sqrt{\left(Q(p, q, \frac{\alpha}{x_3}) + \frac{\alpha}{x_3}\right)^2 + p^2 + 1} \rightarrow \infty$$

for  $\alpha \rightarrow \infty$  by (A.2). However, with the limit (A.3) we get

$$\begin{aligned} E &= x_3 \sqrt{\left(Q(p, q, \frac{\alpha}{x_3}) - \frac{\alpha}{x_3}\right)^2 + p^2 + 1} \rightarrow x_3 \sqrt{\left(\frac{1}{2q}(q^2 - p^2 - 1)\right)^2 + p^2 + 1} \\ &= \frac{x_3}{2q}(q^2 + p^2 + 1) \\ &= \frac{x_3}{2\xi_2\xi_3}|\xi|^2 \end{aligned}$$

for  $\alpha \rightarrow \infty$ . So, one of the distances to the foci converges for  $\alpha \rightarrow \infty$ . The limit of the other one does not exist. Nevertheless, we obtain limits for the relation of  $D$  with  $\alpha$  and  $x_2 - s_2(p, q, x)$ . We recall that we have  $s_2(p, q, x) = x_2 - x_3Q(p, q, \frac{\alpha}{x_3})$  according to Remark 3.23. These limits are

$$\begin{aligned} \frac{\alpha}{D} &= \frac{\alpha}{x_3 \sqrt{\left(Q(p, q, \frac{\alpha}{x_3}) + \frac{\alpha}{x_3}\right)^2 + p^2 + 1}} \\ &= \frac{1}{\left(\frac{x_3}{\alpha}Q(p, q, \frac{\alpha}{x_3}) + 1\right)^2 + \frac{p^2 x_3^2}{\alpha^2} + \frac{x_3^2}{\alpha^2}} \rightarrow \frac{1}{\sqrt{(1+1)^2 + 0 + 0}} = \frac{1}{2} \end{aligned}$$

for  $\alpha \rightarrow \infty$  and

$$\begin{aligned} \frac{x_2 - s_2(p, q, x)}{D} &= \frac{x_3Q(p, q, \frac{\alpha}{x_3})}{x_3 \sqrt{\left(Q(p, q, \frac{\alpha}{x_3}) + \frac{\alpha}{x_3}\right)^2 + p^2 + 1}} \\ &= \frac{x_3Q(p, q, \frac{\alpha}{x_3})}{\alpha \sqrt{\left(\frac{x_3}{\alpha}Q(p, q, \frac{\alpha}{x_3}) + 1\right)^2 + \frac{p^2 x_3^2}{\alpha^2} + \frac{x_3^2}{\alpha^2}}} \rightarrow \frac{1}{\sqrt{(1+1)^2 + 0 + 0}} = \frac{1}{2} \end{aligned}$$

for  $\alpha \rightarrow \infty$  using the limit (A.4) for  $\alpha \rightarrow \infty$ . Again, with calculation (A.3) we obtain

$$x_2 - s_2(p, q, x) - \alpha = x_3\left(Q(p, q, \frac{\alpha}{x_3}) - \frac{\alpha}{x_3}\right) \rightarrow \frac{x_3}{2q}(q^2 - p^2 - 1) = \frac{x_3}{2\xi_2\xi_3}(\xi_2^2 - \xi_1^2 - \xi_3^2)$$

for  $\alpha \rightarrow \infty$  and

$$\frac{\alpha}{x_2 - s_2(p, q, x)} = \frac{\alpha}{x_3Q(p, q, \frac{\alpha}{x_3})} = \frac{1}{\frac{x_3}{\alpha}Q(p, q, \frac{\alpha}{x_3})} \rightarrow 1$$

for  $\alpha \rightarrow \infty$ .

- (b) Second, we consider the analogous limits for  $\xi_2 > 0$  and  $\xi_3 < 0$  or  $\xi_2 < 0$  and  $\xi_3 > 0$ , so  $q < 0$ . Then, we obtain

$$Q(p, q, \lambda) \rightarrow -\infty \quad (\text{A.5})$$

for  $\lambda \rightarrow \infty$ . This time, we get a limit by adding  $\lambda$ . This is

$$\begin{aligned} Q(p, q, \lambda) + \lambda &= \frac{1}{2q}(q^2 - p^2 - 1) - \sqrt{\frac{(p^2+q^2+1)^2}{4q^2} + \lambda^2} + \lambda \\ &= \frac{1}{2q}(q^2 - p^2 - 1) + \frac{\lambda^2 - \frac{(p^2+q^2+1)^2}{4q^2} - \lambda^2}{\lambda + \sqrt{\frac{(p^2+q^2+1)^2}{4q^2} + \lambda^2}} \\ &\rightarrow \frac{1}{2q}(q^2 - p^2 - 1) = \frac{1}{2\xi_2\xi_3}(\xi_2^2 - \xi_1^2 - \xi_3^2) \end{aligned} \quad (\text{A.6})$$

for  $\lambda \rightarrow \infty$ . Multiplying  $Q$  by  $\frac{1}{\lambda}$  yields now the negative limit in comparison to case (a). We have

$$\frac{1}{\lambda}Q(p, q, \lambda) = \frac{1}{2\lambda q}(q^2 - p^2 - 1) - \sqrt{\frac{(p^2 + q^2 + 1)^2}{4\lambda^2 q^2} + 1} \rightarrow 0 - \sqrt{0 + 1} = -1 \quad (\text{A.7})$$

for  $\lambda \rightarrow \infty$ . Next, we consider the limits of  $D$  and  $E$ , the distances from a point to the two foci. For the distance  $D$  we obtain

$$\begin{aligned} D &= x_3 \sqrt{\left(Q(p, q, \frac{\alpha}{x_3}) + \frac{\alpha}{x_3}\right)^2 + p^2 + 1} \rightarrow x_3 \sqrt{\left(\frac{1}{2q}(q^2 - p^2 - 1)\right)^2 + p^2 + 1} \\ &= -\frac{x_3}{2q}(q^2 + p^2 + 1) = -\frac{x_3}{2\xi_2\xi_3}|\xi|^2 \end{aligned}$$

for  $\alpha \rightarrow \infty$  using the limit (A.6) and that  $q < 0$  holds. Further, for the distance  $E$  it follows

$$E = x_q \sqrt{\left(Q(p, q, \frac{\alpha}{x_3}) - \frac{\alpha}{x_3}\right)^2 + p^2 + 1} \rightarrow \infty$$

for  $\alpha \rightarrow \infty$  using (A.5). So, in this case the limit of the distance  $D$  exists and the distance  $E$  does not converge for  $\alpha \rightarrow \infty$ . Hence, we consider the relations of  $E$  with  $\alpha$  and  $x_2 - s_2$ . We deduce

$$\begin{aligned} \frac{\alpha}{E} &= \frac{\alpha}{x_3 \sqrt{\left(Q(p, q, \frac{\alpha}{x_3}) - \frac{\alpha}{x_3}\right)^2 + p^2 + 1}} \\ &= \frac{1}{\left(\frac{x_3}{\alpha}Q(p, q, \frac{\alpha}{x_3}) - 1\right)^2 + \frac{p^2 x_3^2}{\alpha^2} + \frac{x_3^2}{\alpha^2}} \rightarrow \frac{1}{\sqrt{(-1 - 1)^2 + 0 + 0}} = \frac{1}{2} \end{aligned}$$

for  $\alpha \rightarrow \infty$  and

$$\begin{aligned} \frac{x_2 - s_2(p, q, x)}{E} &= \frac{x_3 Q(p, q, \frac{\alpha}{x_3})}{x_3 \sqrt{\left(Q(p, q, \frac{\alpha}{x_3}) - \frac{\alpha}{x_3}\right)^2 + p^2 + 1}} \\ &= \frac{x_3 Q(p, q, \frac{\alpha}{x_3})}{\alpha \sqrt{\left(\frac{x_3}{\alpha}Q(p, q, \frac{\alpha}{x_3}) - 1\right)^2 + \frac{p^2 x_3^2}{\alpha^2} + \frac{x_3^2}{\alpha^2}}} \rightarrow \frac{-1}{\sqrt{(-1 - 1)^2 + 0 + 0}} = -\frac{1}{2} \end{aligned}$$

for  $\alpha \rightarrow \infty$  according to calculation (A.7). Last, we get

$$x_2 - s_2 + \alpha = x_3 \left(Q(p, q, \frac{\alpha}{x_3}) + \frac{\alpha}{x_3}\right) \rightarrow \frac{x_3}{2q}(q^2 - p^2 - 1) = \frac{x_3}{2\xi_2\xi_3}(\xi_2^2 - \xi_1^2 - \xi_3^2)$$

with the limit (A.6) for  $\alpha \rightarrow \infty$  and

$$\frac{\alpha}{x_2 - s_2(p, q, x)} = \frac{\alpha}{x_3 Q(p, q, \frac{\alpha}{x_3})} = \frac{1}{\frac{x_3}{\alpha} Q(p, q, \frac{\alpha}{x_3})} \rightarrow -1$$

for  $\alpha \rightarrow \infty$  using the result (A.7).

#### A.4. The transformation theorem and the $\delta$ -distribution

In Chapter 4, we transform the elliptic Radon transform ignoring the fact that we work with the  $\delta$ -distribution. This calculation justifies that this is possible. We consider the set  $S = \{x \in \mathbb{R}^3 \mid \varphi(s, x) = t\}$  on the whole space  $\mathbb{R}^3$  for fixed  $s \in S_0$  and  $t \in (2\alpha, \infty)$ . Also in this case,  $\nabla_x \varphi$  given in identity (A.1) does not vanish on  $S$ . The first component of  $\nabla_x \varphi$  vanishes if and only if  $x_1 = s_1$ , the second one if and only if  $x_2 = s_2$  and the third one if and only if

$x_3 = 0$ . However, the point  $(s_1, s_2, 0)^\top$  is no element of  $S$ . Thus, with  $\Phi(s, t, x) = t - \varphi(s, x)$  for  $x \in \mathbb{R}_+^3$  and fixed  $s \in S_0$  and  $t \in (2\alpha, \infty)$  we obtain that  $\nabla_x \Phi(s, t, \cdot)$  does not vanish on  $S$ . Then, the second point of Section XI.3.1.2 in [Ste95] yields

$$\begin{aligned} \int_{\mathbb{R}^3} f(x) \delta(t - \varphi(s, x)) \, dx &= \lim_{\varepsilon \rightarrow 0} \frac{1}{2\varepsilon} \int_{\{x \in \mathbb{R}^3 \mid t - \varepsilon < \varphi(s, x) < t + \varepsilon\}} f(x) \, dx \\ &= \lim_{\varepsilon \rightarrow 0} \frac{1}{2\varepsilon} \int_{\{y \in \mathbb{R}^3 \mid t - \varepsilon < \varphi(s, T^{-1}(y)) < t + \varepsilon\}} f(T^{-1}(y)) |\det T^{-1}(y)| \, dy \\ &= \int_{\mathbb{R}^3} f(T^{-1}(y)) \delta(t - \varphi(s, T^{-1}(y))) |\det(T^{-1}(y))| \, dy \end{aligned}$$

for a transformation  $T: \mathbb{R}^3 \rightarrow \mathbb{R}^3$  and  $f \in C_c^\infty(\mathbb{R}^3)$ .



---

## Danksagung

---

Bei meinem Betreuer, Prof. Dr. Andreas Rieder, bedanke ich mich für die hilfreiche Unterstützung und das entgegengebrachte Vertrauen während meiner Promotion. Vielen Dank auch dafür, dass Sie mir die Möglichkeit gegeben haben, nach Leiden zu gehen! Und wenn uns nicht öfter das Fortune gefehlt hätte, hätten wir sicherlich häufiger am Tischkicker gewonnen, denn überzeugt haben wir ja immer.

Meinem zweiten Betreuer, PD Dr. Peer Christian Kunstmann, danke ich dafür, dass er seinen Tisch immer für mich freigeräumt hat, wenn ich mal wieder unangemeldet bei ihm vorbeikam. Peer hat die unglaubliche Fähigkeit, selbst von den theoretischsten Begriffen immer noch eine genaue Anschauung zu haben.

Meine bisherigen Abschlussarbeiten habe ich unter der Betreuung von Prof. Dr. Roland Schnaubelt verfasst. Roland hat mir gezeigt, wie wichtig es ist, Mathematik gut und präzise aufzuschreiben. Seine herzliche Art gab mir auch nach meiner Abwanderung in die Angewandte Mathematik stets das Gefühl, willkommen zu sein. Es hat mich sehr gefreut, dass er eines der Korreferate dieser Arbeit übernommen hat.

Die Zusammenarbeit mit Prof. Eric Todd Quinto hat diese Arbeit sehr vorangebracht. Es war mir eine große Freude, mit ihm über Mathematik zu sprechen und über seine Einladung nach Oberwolfach habe ich mich sehr gefreut. Die Woche, in der ich viele andere Doktoranden kennen lernen durfte, war ein tolles Erlebnis.

Auch im Rahmen des durch die Deutsche Forschungsgemeinschaft (DFG) finanzierten Sonderforschungsbereiches 1173, in dem ich promovieren durfte, war es leicht, Kontakt zu anderen Doktoranden zu knüpfen.

Auch wenn Lydia und Martin den Fortschritt dieser Arbeit in den letzten Monate außerhalb des Mathematikgebäudes verfolgt haben, sind sie wohl diejenigen, die die Zeit meiner Promotion am längsten und stärksten geprägt haben.

Mit Lydia habe ich tagtäglich die schönen und traurigen Seiten des Lebens erörtert. Unvergessen sind die zahlreichen Stunden, in denen wir an diversen Whiteboards über Randbedingungen philosophierten und die verschiedensten geometrischen Objekte geschnitten haben. Selbst als TikZ wahllos Pfeile rot färbte, ließen wir uns nicht aus dem Konzept bringen.

Mit Martin und mir als Bundestrainer wären wir jetzt sicherlich noch Weltmeister. Auch hätten wir Spieler der älteren Generation, wie etwa Martin, nie aus dem Kader gestrichen. Abseits des Fußballs hatte Martin stets ein offenes Ohr für meine mathematischen Erlebnisse und brachte neue Sichtweisen ein. Selbst kuchentechnisch konnte ich mich immer auf ihn verlassen, denn Wettschulden sind ja bekanntlich Ehrenschulden.

Danke Euch beiden für zahlreiche schöne Stunden inner- und außerhalb des Mathematikgebäudes und die aufbauenden Worte, wenn ich von allem genervt war!

In meiner Arbeitsgruppe am Institut für Angewandte und Numerische Mathematik habe ich mich von Beginn an wohlfühlt. Die Zeit hier wird mir immer als etwas Besonderes in

Erinnerung bleiben. Unermüdliche Diskussionen über Politik, Umwelt und die kleinen Probleme des Alltags, Spiele- und Fußballabende, ausartende Hut-Bastelaktionen, Klebezettel-Nachmittage und unzählige Stunden am Tischkicker stellen nur einen kleinen Bruchteil dessen dar, was wir gemeinsam erlebt haben.

Nicht unerwähnt bleiben dürfen die gemeinsamen Grillabende. Hierfür bedanke ich mich herzlich für die Gastfreundschaft von Prof. Dr. Christian Wieners.

Wenn es darauf ankam, konnte ich mich auf die Treue von Prof. Dr. Tobias Jahnke zu seinem Verein verlassen. Danke für die gewonnene Wette und die zahlreichen Diskussionen über Fußball, Tobias!

Daniel hat von Beginn an daran geglaubt, dass wir beim Kickern keine zehn Gegentore in Folge kassieren. Es tut mir heute noch leid, dass wir doch einmal kriechen mussten. Seine aufmunternden Worte in den letzten Wochen vor der Abgabe dieser Arbeit haben mir sehr geholfen.

Ich danke Benny dafür, dass ich auf seine Unterstützung in all den Jahren immer zählen konnte. Christian und ich kannten uns bereits aus dem Studium. Umso schöner fand ich es, als er Teil unserer Arbeitsgruppe wurde. Danke dafür, dass Deine Bürotür immer offen ist, Christian! Julian, dem Schauspieler, bin ich dankbar dafür, dass er immer für einen Spaß zu haben ist. Auf meinen Büronachbarn Julian war selbst Verlass, als es darum ging, frühmorgens meinen Büroschrank zu verschieben. Nicht unerwähnt bleiben darf mein ehemaliger Kollege Johannes. Er hat mich bei meinen ersten Schritten mit Python unterstützt und mit Hilfe seiner Idee, Teile meines Codes in Maschinencode übersetzen zu lassen, wurde das Programm um ein Vielfaches schneller. Außerdem haben Daniel, Daniele, Jonathan, Katharina, Laura, Nathalie, Niklas, Philip, Sonja und meine ehemaligen Kollegen Marcel, Patrick, Ramin, Robert und Simon auf vielfältige Art und Weise zu einem stets angenehmen Arbeitsklima beigetragen.

Neben meiner eigentlichen Arbeitsgruppe war mir das Glück einer „Zweitarbeitungsgruppe“ vergönnt. Die Gespräche dienstags in der Mittagspause mit den Funktionalanalytikern Andreas, Johannes, Konstantin und Lucrezia über Teigtaschenfabriken, österreichische Schnitzel und neuerdings die deutsche Sprache sind immer ein Erlebnis. Auch die anschließende „Kaffeerunde“ mit Dorothee, Lutz, Peer und Roland ist ein schönes Zusammentreffen.

Fabian, Michael und Samuel haben mich auf meinem mathematischen Weg seit Beginn des Studiums begleitet. Vielen Dank für etliche Diskussionen über Vorlesungsinhalte und Übungsaufgaben!

Besonders danke ich meiner Mutter dafür, dass sie stets daran geglaubt hat, dass ich „das“ kann und mir dies auch vermittelt hat. Bei meiner Schwester Susanne bedanke ich mich dafür, dass sie immer mindestens 100 Prozent gibt. Dies hat mir schon oft geholfen und einiges erleichtert. Heidi und Jens waren immer für uns drei da. Ich bin sehr froh darüber, Teil einer solchen Familie zu sein.

Abschließend möchte ich mich bei Luca bedanken. Luca hat mich die letzten Jahre darin unterstützt, „den Wagen zu ziehen“ und immer wieder ermutigt, am Ball zu bleiben. Über all die Jahre sind wir – in und abseits der Mathematik – zu einem eingespielten Team zusammengewachsen.

Christine Grathwohl  
*Karlsruhe, im Oktober 2019*

*„Zuviel Gelehrsamkeit kann selbst den Gesundesten kaputtmachen.“*

Pippi Langstrumpf



---

## Bibliography

---

- [Beyl84] G. Beylkin, *The inversion problem and applications of the generalized Radon transform*. Communications on Pure and Applied Mathematics **37** (1984), 579–599.
- [Beyl85] G. Beylkin, *Imaging of discontinuities in the inverse scattering problem by inversion of a causal generalized Radon transform*. Journal of Mathematical Physics **26** (1985), 99–108.
- [BC77] N. Bleistein and J. K. Cohen, *An inverse method for determining small variations in propagation speed*. SIAM Journal on Applied Mathematics **32** (1977), 784–799.
- [BC79] N. Bleistein and J. K. Cohen, *Velocity inversion procedure for acoustic waves*. Geophysics **44** (1979), 1077–1085.
- [BCS01] N. Bleistein, J. K. Cohen and J. W. Stockwell, Jr., *Mathematics of multidimensional seismic imaging, migration, and inversion*. Springer-Verlag, 2001.
- [BDM18] L. Borcea, V. Druskin and A. Mamonov, *Untangling the nonlinearity in inverse scattering with data-driven reduced order models*, Inverse Problems **34** (2018), 065008.
- [BDH14] C. Brouder, N. V. Dang and F. H elein, *A smooth introduction to the wavefront set*. Journal of Physics. A. Mathematical and Theoretical **47** (2014), 443001.
- [Bro99] R. Brown, *Birth of the seismic-reflection method*. Oklahoma Geological Survey Special Publication 99 **1**, 6–9.
- [CK13] D. Colton and R. Kress, *Inverse Acoustic and Electromagnetic Scattering Theory*. Third edition, Springer-Verlag, 2013.
- [Dem15] L. Demanet, *Waves and Imaging, Class Notes*. Lecture notes, 2015.
- [Py13] L. Demanet, R. J. Hewett and the PySIT Team, *PySIT: Python Seismic Imaging Toolbox v0.5*. <http://www.pysit.org>, 2013.
- [El11] J. Elstrodt, *Ma - und Integrationstheorie*. Siebte, korrigierte und aktualisierte Auflage, Springer-Verlag, 2011.
- [FR12] D. Faraco and K. M. Rogers, *The Sobolev norm of characteristic functions with applications to the Calder on inverse problem*. The Quarterly Journal of Mathematics **64** (2012), 133–147.
- [FRS92] A. Faridani, E. Ritman and K. Smith, *Local tomography*. SIAM Journal on Applied Mathematics, **52** (1992), 459–484.

- [FG10] R. Felea and A. Greenleaf, *Fourier integral operators with open umbrellas and seismic inversion for cusp caustics*. *Mathematical Research Letters* **17** (2010), 867–886.
- [FKNQ16] R. Felea, V. P. Krishnan, C. J. Nolan and E. T. Quinto, *Common midpoint versus common offset acquisition geometry in seismic imaging*. *Inverse Problems & Imaging* **10** (2016), 87–102.
- [FQ15] J. Frikel and E. T. Quinto, *Artifacts in incomplete data tomography with applications to photoacoustic tomography and sonar*. *SIAM Journal on Applied Mathematics*, **75** (2015), 703–725.
- [GKQR18a] C. Grathwohl, P. C. Kunstmann, E. T. Quinto and A. Rieder, *Approximate inverse for the common offset acquisition geometry in 2D seismic imaging*. *Inverse Problems* **34** (2018), 014002.
- [GKQR18b] C. Grathwohl, P. C. Kunstmann, E. T. Quinto and A. Rieder, *Microlocal analysis of imaging operators for effective common offset seismic reconstruction*. *Inverse Problems* **34** (2018), 114001.
- [GS77] V. Guillemin and S. Sternberg, *Geometric asymptotics*. *Mathematical Surveys* **14** (1977), American Mathematical Society.
- [Hör65] L. Hörmander, *Pseudodifferential operators*. *Communications on Pure and Applied Mathematics* **18** (1965), 501–517.
- [Hör70] L. Hörmander, *Linear differential operators*. *Actes du Congrès International des Mathématiciens* **1** (1970), 121–133.
- [Hör71] L. Hörmander, *Fourier integral operators. I*. *Acta Mathematica* **127** (1971), 79–183.
- [Hör90] L. Hörmander, *The Analysis of Linear Partial Differential Operators I*. Second edition, Springer-Verlag, 1990.
- [Kar29] J. C. Karcher, *Determination of subsurface formations*. US Patent no. 1,843,725, Application filed May 1, 1929 and patented February 2, 1932.
- [Klei04] J. Klein, *Mathematical problems in synthetic aperture radar*. PhD Thesis Westfälische Wilhelms-Universität, Mathematisches Institut, Münster, Germany, 2004.
- [KLQ12] V. P. Krishnan, H. Levinson and E. T. Quinto, *Microlocal analysis of elliptical Radon transforms with foci on a line*. *The mathematical legacy of Leon Ehrenpreis*, Springer Proceedings in Mathematics **16** (2012), 163–182.
- [KQ11] V. P. Krishnan and E. T. Quinto, *Microlocal aspects of common offset synthetic aperture radar imaging*. *Inverse Problems & Imaging* **5** (2011), 659–674.
- [KQ15] V. P. Krishnan and E. T. Quinto, *Microlocal analysis in tomography*. *Handbook of Mathematical Methods in Imaging*, Springer-Verlag (2015), 847–902.
- [Lind87] A. Lindgren, *Pippi Langstrumpf*. Gesamtausgabe, printed 1995, Oettinger Verlag, 1987.

- [Lou96] A. K. Louis, *Approximate inverse for linear and some nonlinear problems*. Inverse Problems **12** (1996), 175–190.
- [LM90] A. K. Louis and P. Maaß, *A mollifier method for linear operator equations of the first kind*. Inverse Problems **6** (1990), 427–440.
- [NS97] C. J. Nolan and W. W. Symes, *Global solution of a linearized inverse problem for the wave equation*. Communications in Partial Differential Equations **22** (1997), 919–952.
- [Pet83] B. E. Petersen, *Introduction to the Fourier transform and pseudo-differential operators*. Pitman, Boston, 1983.
- [Quin80] E. T. Quinto, *The dependence of the generalized Radon transform on defining measures*. Transactions of the American Mathematical Society **257** (1980), 331–346.
- [Quin93] E. T. Quinto, *Singularities of the X-ray transform and limited data tomography in  $\mathbb{R}^2$  and  $\mathbb{R}^3$* . SIAM Journal on Mathematical Analysis **24** (1993), 1215–1225.
- [QRS11] E. T. Quinto, A. Rieder and T. Schuster, *Local inversion of the sonar transform regularized by the approximate inverse*. Inverse Problems **27** (2011), 035006.
- [Ra17] J. Radon, *Über die Bestimmung von Funktionen durch ihre Integralwerte längs gewisser Mannigfaltigkeiten*. Berichte über die Verhandlungen der Königlich-Sächsischen Gesellschaft der Wissenschaften zu Leipzig. Mathematisch-Physische Klasse **69** (1917), 262–277.
- [Scha07] P. Schapira, *Mikio Sato, a visionary of mathematics*. Notices of the American Mathematical Society, **54** (2007), 243–245.
- [Shu87] M. A. Shubin, *Pseudodifferential Operators and Spectral Theory*. Translated from the Russian by S. I. Andersson, Springer-Verlag, 1987.
- [Sjö00] J. Sjöstrand, *Microlocal analysis*. Development of mathematics 1950–2000, Birkhäuser, Basel, 2000, 967–991.
- [Ste95] E. M. Stein, *Harmonic Analysis: Real-variable Methods, Orthogonality, and Oscillatory Integrals*. Second printing, with corrections and additions, Princeton University Press, Princeton New Jersey, 1995.
- [Sym98] W. W. Symes, *Mathematics of reflection seismology*. Technical report, The Rice Inversion Project, Rice University, Houston, 1998.
- [Sym09] W. W. Symes, *The seismic reflection inverse problem*, Inverse Problems, **25** (2009), 123008.
- [Tre801] F. Trèves, *Introduction to Pseudodifferential and Fourier Integral Operators. Volume 1: Pseudodifferential Operators*. Plenum Press, New York-London, 1980.
- [Tre802] F. Trèves, *Introduction to Pseudodifferential and Fourier Integral Operators. Volume 2: Fourier Integral Operators*. Plenum Press, New York-London, 1980.